Università degli studi di Torino

PhD: Medicine and Experimental Therapy

Academic discipline: BIO/09 Physiology

PhD Thesis - XXXIII Cycle

The venous side of cardiovascular haemodynamics

Tutor:
Prof. Silvestro Roatta

Candidate:
Dr. Leonardo Ermini

Doctoral coordinator:
Prof. Pasquale Pagliaro

Academic years 2017/2021

It was in love I was created

and in love it's how I hope I die

Paolo Nutini

Contents

Original Papers

This Thesis is founded on the original papers listed below. In the following text these papers will be referred to by their Roman numerals:

I. **Ermini L**, Ferraresi C, De Benedictis C, Roatta S* *"Objective Assessment of Venous Pulse Wave Velocity in Healthy Humans"* Ultrasound in Medicine & Biology, 2020; 46(3):849-854.

II. **Ermini L**, Chiarello NE, De Benedictis C, Ferraresi C, Roatta S* *"Venous Pulse Wave Velocity variation in response to a simulated fluid challenge in healthy subjects"* Biomedical Signal Processing and Control, 2021; 63(102177):1-7.

III. Ferraresi C, Franco W, Maffiodo D, De Benedictis C*, Paterna M, Quiñones P D, **Ermini L**, Roatta S *"Applications of intermittent pneumatic compression for diagnostic and therapeutic purposes"* Proceedings of I4SDG Workshop 2021, Mechanisms and Machine Science, 2022; 108(1):209-218.

IV. Barbagini A, **Ermini L***, Pertusio R, Roatta S *"A portable device for the measurement of venous Pulse Wave Velocity"* Applied Sciences, 2022; *under review.*

V. **Ermini L***, Seddone S, Policastro P, Mesin L, Pasquero P, Roatta S *"The cardiac caval index. Improving non-invasive assessment of cardiac preload"* Journal of Ultrasound in Medicine, 2021; 9999:1-12, *Epub ahead of print.*

VI. Seddone S, **Ermini L**, Policastro P, Mesin L, Roatta S* *"Evidence that large vessels do affect near infrared spectroscopy"* Scientific Reports, 2022; 12(2155):1-12.

VII. Mesin L*, Albani S, Pasquero P, Porta M, Policastro P, Leonardi G, Albera C, Scacciatella P, Melchiorri C, Pellicori P, Stolfo D, Fabris B, Grillo A, Bini R, Giannoni A, Pepe A, **Ermini L**, Seddone S, Sinagra G, Antonini-Canterin F, Roatta S *"Assessment of phasic changes of vascular size by automated edge tracking - State of the art and clinical perspectives"* Frontiers in Cardiovascular Medicine, 2022; 8(775635):1-9.

* Corresponding Author

Summary of the Thesis

Cardiovascular (CV) diseases are, so far, the leading cause of death in the more technologically advanced countries (one third of the total in 2017). Therefore, studies about cardiovascular physiology have been, and still are, paramount. For decades the research has focused on the cardiac pump and the arterial district but in recent years, the formerly neglected capillary and venous sides of the circulation have gained increasing attention. Particularly the veins, as they are the biggest blood reservoir of our body and the way they can accommodate blood transfusions or redistribute the circulating blood volume among the organs, has become increasingly important for the clinical management of the so-called fluid therapy. Indeed, the issue of whether and in what amount fluids need to be administered to a haemodynamically unstable patient, is a key clinical question, also given the lack of a gold standard technique to rely on and being the overzealous fluid administration hazardous in about half of those patients. Moreover, such clinical question can be framed in a more general debate about basic CV physiology that regards the 1950's Guyton studies about venous return and in particular about the role of Central Venous Pressure (CVP) as independent variable affecting the heart pumping function. This point of view about CVP, has likely contributed to its unjustified use as the single haemodynamic parameter to guide the management of the fluid therapy, which fortunately has been abandoned in the recent years in favour of other, non-static (i.e., dynamic), haemodynamic parameters. The persisting lack of consensus on these basic cardiovascular questions may be also due to the difficulty of assessing and monitoring either central and peripheral venous pressures or the extent of "vascular filling", in simple and non-invasive ways.

In this respect, the main aim of this thesis was to explore the potential of a new approach (actually a reconsideration of an old idea) to the assessment of vascular filling (otherwise termed volaemic status): the measurement of the pulse wave velocity in the veins (vPWV). Although PWV has been widely studied in the arteries, to the point that nowadays arterial PWV is the gold standard for the evaluation of the arterial stiffness (a CV disease marker), it was measured in the veins only in a handful of dated studies. The reason for this paucity of investigations about vPWV is based essentially on its inherent measurement difficulty: given the lack of a natural pulsatility in the venous flow, the artificial generation of reliable Pulse Waves (PWs) is mandatory, as well as the synchronization with the main mechanisms that are known to modulate the venous flow, such as respiratory and cardiac activity. In a first study, I tested whether the technique was able to detect moderate changes in leg venous

pressure, produced by raising the trunk at two different levels (paper I). Then, in a second study, I verified whether the measurement of vPWV in the arms was sensitive enough to detect the blood volume changes simulated by a well-known postural manoeuvre, the Passive Leg Raising (PLR) (paper II). Given the positive outcome of these studies, this methodology was included in a narrative review of clinical applications of pneumatic compression (paper III). Then, the aim was to the develop a portable device capable of performing the vPWV measurement outside the laboratory, as a necessary step to start a clinical trial. The design of this device was based on a Raspberry Pi (i.e., a small single-board computer) equipped with an analog-to-digital converter, an ECG module, a respiratory sensor, and a pneumatic actuator for the artificial generation of the PWs (paper IV).

In parallel, the attention was focused on another common approach to the non-invasive assessment of the volaemic status: the echographic assessment of the Inferior Vena Cava (IVC) pulsatility. This technique is easy and fast to perform but is also affected by the operator experience and the variability of the patient respiratory effort, thus resulting in an attractive but moderately reliable technique. Thanks to an automatic edge-tracking algorithm, developed by our collaborators, it was possible to demonstrate that, once the respirophasic oscillations of the IVC size were removed and the cardiac related oscillations averaged within each respiratory cycle, a more stable (in time) index of IVC collapsibility is obtained (paper V). This new IVC collapsibility index was termed averaged Cardiac Caval Index (aCCI). Furthermore, it was demonstrated that the information carried by aCCI is complementary and not antithetical to the classical IVC collapsibility index, based on their performance during a simulated fluid challenge (a PLR manoeuvre).

Finally, in order to develop a subject specific computational model, i.e., an *in silico* model, of the propagation of a venous PW, both to validate our *in vivo* measurements and to explore the possibility to derive information from them, it was necessary to calibrate the model on single vessels measurements, particularly in terms of compliance, which may greatly differ among subjects and among different vessels in the same subject. In this respect, I was engaged in developing methodologies for the non-invasive assessment of volume-pressure curves of large limb veins, based on NIRS and US measurements. The results have contributed to other two manuscripts, one describing to what extent large veins may actually affect the NIRS measurement (paper VI), and the other presenting a narrative review about the usefulness of edge tracking algorithms applied to US imaging to track phasic changes of vessels size (paper VII).

List of Abbreviations

ABF Arterial Blood Flow.

ABP Arterial Blood Pressure.

aCCI averaged Cardiac Caval Index.

ACS Abdominal Compartment Syndrome.

ANOVA analysis of variance.

ARDS Acute Respiratory Distress Syndrome.

BL Beer-Lambert.

BV Basilic Vein.

CARS Cardio Abdominal Renal Syndrome.

CCI Cardiac Caval Index.

CI Caval Index.

CO Cardiac Output.

COPD Chronic Obstructive Pulmonary Disease.

CoV Coefficient of Variation.

CPAP Continuous Positive Airway Pressure.

CRT Capillary Refill Time.

CV Cardiovascular.

CVP Central Venous Pressure.

CW Continuous Wave.

ECG Electrocardiogram.

ECMO Extracorporeal Membrane Oxygenation.

EDV end diastolic volume.

EEOT End-Expiratory Occlusion Test.

EIOT End-Inspiratory Occlusion Test.

FC Fluid Challenge.

FD Frequency-Domain.

FN False Negative.

FO Fluid Overload.

FP False Positive.

FR Fluid Responsiveness.

GUI Graphical User Interface.

Hb Haemoglobin.

HDT Head Down Tilt.

HF Heart Failure.

HHb Deoxyhaemoglobin.

HMb Deoxymyoglobin.

HR Heart Rate.

IAH intra-abdominal hypertension.

IAP intra-abdominal pressure.

ICC intra-class correlation coefficients.

ICH intra-cranial hypertension.

ICS Intra-cranial Compartment Syndrome.

ICU Intensive Care Unit.

IPC Intermittent Pneumatic Compression.

ITP intra-thoracic pressure.

IV Intravenous.

IVC Inferior Vena Cava.

IVCc Inferior Vena Cava *collapsibility*.

IVCd Inferior Vena Cava diameter.

IVCd Inferior Vena Cava *distensibility*.

LRM Lung Recruitment Manoeuvre.

MANOVA multivariate analysis of variance.

MAP Mean Arterial Pressure.

Mb Myoglobin.

NIR Near Infrared.

NIRS Near Infrared Spectroscopy.

NIV non-Invasive ventilation.

O_2Hb Oxyhaemoglobin.

O_2Mb Oxymyoglobin.

OCS Ocular Compartment Syndrome.

PAC Pulmonary Artery Catheter.

PCS Pulse Contour System.

PEEP Positive End Expiratory Pressure.

PI Perfusion Index.

PLR Passive Leg Raising.

Pms Mean Systemic Pressure.

PP Pulse Pressure.

PPV Pulse Pressure Variation.

PSV Pressure Support Ventilation.

PVP Peripheral Venous Pressure.

PW Pulse Wave.

PWV Pulse Wave Velocity.

RAP Right Atrial Pressure.

RCI Respiratory Caval Index.

RCT Randomized Controlled Trial.

RV right ventricle.

RvR Resistance to venous Return.

SB Spontaneous Breathing.

SRS Spatially-Resolved Spectroscopy.

SV Stroke Volume.

SVC Superior Vena Cava.

SVR Systemic Vascular Resistance.

SVV Stroke Volume Variation.

TD Time-Domain.

tHb Total Haemoglobin.

THI Tissue Haemoglobin Index.

TOI Tissue Oxygenation Index.

TR tricuspid regurgitation.

TV Tidal Volume.

TVC Tidal Volume Challenge.

US Ultrasound.

vPWV venous Pulse Wave Velocity.

VR Venous Return.

VTI Velocity Time Integral.

List of Figures

Chapter 1

Introduction

1.1 General background

Among the principal constituents of the Cardiovascular (CV) system, the venous compartment is one of the most overlooked with regard to its relevance for the maintenance of system homeostasis (Wardhan et al., 2009; Gelman and Bigatello, 2018b). Although its main characteristics have been acknowledged since the renaissance (Scultetus et al., 2001), functional *in vivo* studies have been always very challenging due to the low pressure and low flow velocity of the venous circulation, limiting the investigation to the big central veins, e.g. the Venae Cavae (Koeppen et al., 2017; Hall et al., 2020).

Given these constraints, the field of vascular physiology has been characterized by an imbalance of attention towards the arterial compartment, that brought to the first non-invasive technique for measuring the arterial pressure back in 1905 by Nikolai Sergeyevich Korotkoff (Korotkoff, 1905), who exploited the sounds (which later took his name) originating from the turbulent blood flow regime in the arteries compressed by the pneumatic cuff. Relating the appearance of these sounds with the cuff pressure allowed for reliable detection of systolic and diastolic blood pressure levels (Shlyakhto et al., 2005). This technique tremendously affected the clinical practice to the point that it is still nowadays the gold standard for the non-invasive assessment of the maximum and minimum level of Arterial Blood Pressure (ABP), i.e., systolic and diastolic level, respectively. This assessment is paramount in the field of CV physiology because Arterial Blood Pressure (ABP) can be considered, in a first approximation, about equal across all arteries and therefore it is a very good indicator of the whole body perfusion. Instead, something similar cannot be achieved in the venous compartment.

Venous pressure is so low that it is easily affected by changes in posture, as well as by the activity of muscles and/or respiration or, perhaps more critically, by local changes in the vessels tone (i.e., changes in the tension developed by smooth muscle cells). The latter characteristic can cause a change in venous pressure also indirectly: indeed, a venoconstriction, i.e., an increase in venous tone, can results in a local increase of venous pressure but can also cause, as side effect, a shift of blood volume

from that compartment to other compartments, rising venous pressure elsewhere. The ability to mobilize blood volumes is pertinent particularly to high compliant compartments, e.g., the splanchnic venous compartment, and it accounts for a relevant fraction of physiological venous pressures changes in several body venous compartments (Pang, 2001; Rothe, 2011). For those reasons, it makes no sense considering a mean venous pressure, as analogue to the mean arterial pressure. Instead, a physician should be interested in the small and distributed pressure gradients that may develop within the venous system (George L. Brengelmann, 2019).

Historically, the first region of interest for a non-invasive assessment of venous pressure was nearby of the right atrium, specifically in the jugular vein. Indeed, the jugular veins is one of the most superficial and visible veins among the big central ones, that's maybe why it was the first region of interest. Such pressure, characterizing jugular vein as well as all the big central veins, is called Central Venous Pressure (CVP) and it is relevant particularly because it determines the passive filling of the heart, i.e., the heart *preload*. The technique, presented only in the 1930 (Lewis, 1930), exploited the jugular vein as a fluid filled manometer, looking for its collapse point during a semi-recumbent position in order to measure the height of the blood with respect to a reference point specifically chosen nearby the right atrium. Such methodology was the first to describe how to assess non-invasively the CVP but till then, no valuable improvements regarding the measurement accuracy have been made, although other methodologies have been explored (Uthoff et al., 2012; Beigel et al., 2013; Rizkallah et al., 2014; Sathish et al., 2016), leaving room for further research.

Moving from the heart towards the periphery of the circulation, the non-invasive assessment of Peripheral Venous Pressure (PVP), despite the widespread use of venous catheters in intraoperative patients, has been neglected for long time. This happened likely because of its undefined role in clinical practice (Charalambous et al., 2003; Wardhan et al., 2009; Kinsky et al., 2016), which oriented the preference towards CVP. For sure, CVP is a key indicator of the heart pumping function, as formalized by the Frank-Starling curve. This curve links the cardiomyocytes contractility, whereof Cardiac Output (CO) is a proxy, to the pressure stretching the ventricles right before the systole onset, namely the Right Atrial Pressure (RAP), whereof CVP is a good estimate (Beigel et al., 2013). Thus, through the analysis of the CVP waveform, a physician can detect dysfunctions in the major components of the right heart, i.e., atrium, ventricle and tricuspid valve (Sheldon Magder, 2017). On the other hand, CVP alone is not informative about the amount of blood that returns to the heart in a given time unit, defined as Venous Return (VR), which, it is worth to point out, at steady state matches the CO (this is straightforward if one thinks that the CV system is a closed loop). Being VR a flow, it is inevitably driven by a pressure gradient, that is ultimately produced by heart activity but, since the interest is focused only in the venous compartment, the latter can be modelled as the difference between a virtual Peripheral Venous Pressure (PVP) (whose location is not unequivocally defined but can be assumed at the level of venules) and CVP. Unfortunately, since PVP cannot be unequivocally assessed, CVP has been commonly used to get an indication about VR but, as it has

been pointed out by several authors, the measurement of CVP has no utility for this purpose, if used without measuring the corresponding CO (P. E. Marik, Baram, et al., 2008; Sheldon Magder, 2015; Gelman and Bigatello, 2018b; Shah et al., 2021).

1.2 The Guyton's venous return curve debate

Concerning the determinants of the VR, the 21th century has seen the awakening of a heated debate (Tyberg, 2002; George L. Brengelmann, 2003; G L Brengelmann, 2006; Magder, 2006; Curran-Everett, 2007; Gelman, 2008; Henderson et al., 2010; Sheldon Magder, 2012; Sunagawa, 2017; George L. Brengelmann, 2019; Gelman and Bigatello, 2018b; Werner-Moller et al., 2020), which dates back to the 1960s and 1970s (Grodins et al., 1960; Levy, 1979), challenging the classical view about RAP (or, alternatively, CVP) and VR, as well as the usefulness of Mean Systemic Pressure (Pms) as haemodynamic parameter, along with the assumptions underlying the famous 1950s Guyton's (and co-workers) studies (A. C. Guyton, 1955; A. C. Guyton, Lindsey, et al., 1957; A. C. Guyton, Abernathy, et al., 1959). This review about the Guyton's (and co-workers) studies will be discussed with a special attention to the clinical field of Fluid Responsiveness (FR) prediction, in which, the author believes, the debate has a direct but subtle connection.

1.2.1 Systemic flow and central venous pressure: a causal relationship?

In the 1955 study (A. C. Guyton, 1955), Sir Guyton first described what he termed the "Venous Return curve" and put it in a graphical way that gave the birth to the so-called "Guyton's curves" (A C Guyton et al., 1973; Hall et al., 2020). He put the Frank-Starling curve together on the same plot with the aforementioned "Venous Return curve". The Frank-Starling curve (Figure 1.9), otherwise termed "Cardiac response curve" describes, as stated above, how the heart adapts its output (i.e., the CO), by changing its contractility, following changes in its input (i.e., CVP, otherwise termed *preload*). The "Venous Return curve", instead, describes how the CO behaves when CVP is artificially varied across a range of values, under the assumption that CVP independently drives VR, which was one of the most critical points of the debate. It is worth to mention that in this graphical analysis, as per experimental design, the CV system is in a steady state: namely, CO equals VR, so it makes no difference considering VR or CO and perhaps it is clearer calling it systemic flow (F).

The point of intersection between those two curves (Figure 1.2), that is exactly the equalization of VR and CO, is said to be the working point of the CV system. Therefore, in those studies but also in the following, CO and VR, besides being allowed to equalize at successive steady states, were considered to be dependent upon the CVP, which was then represented on the *abscissa* and treated as the independent variable. It is now worth to mention that, here and hereafter, the pulmonary circulation is, and will be, treated as a pure resistive element that therefore cannot accommodate blood volume; it is an unrealistic assumption but it serves the purpose of simplicity in order to better

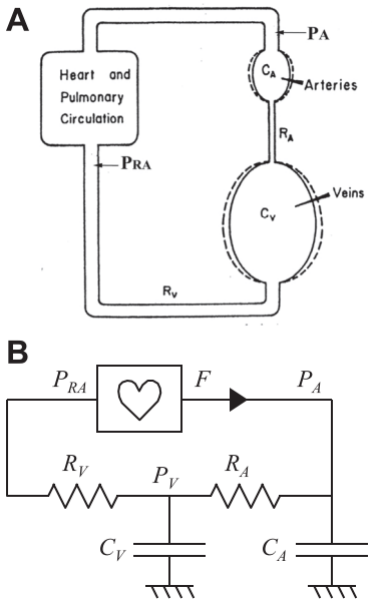

Figure 1.1: **Cardiovascular (CV) systemic flow (toy) model.** A two compartment lumped parameters model of CV system, first presented by Guyton (A. C. Guyton, Abernathy, et al., 1959) (A), and its electrical circuit analogy (B). Resistances are resistive elements (Ra is arterial resistance and Rv venous resistance) and compliances are capacitive elements (Ca is arterial compliance and Cv is venous compliance). Reprint from (Beard et al., 2011).

focus on the systemic circulation.

Assuming the systemic flow F dependent upon RAP, thus CVP, was the most critical point of the debate. Indeed, in the Guyton's experimental set-up for the construction of the VR curve (A. C. Guyton, 1955), the independence of CVP from CO was ambiguous: for each incremental step of CVP (obtained varying the height of a *starling resistor*) the output of the pump replacing the heart, which in this case drives F, was accordingly adjusted. Such ambiguity was resolved by Grodins and co-workers (Grodins et al., 1960) by means of an analogue experimental set-up, except that the starling resistor was not present, resulting in the same CO-CVP relationship as Guyton and co-workers (A. C. Guyton, 1955), therefore showing the dependency of CVP upon changes in CO.

This finding was further confirmed by Levy (Levy, 1979) who proposed the name of "Vascular Function curve" instead of "Venous Return curve" in order to be more clear that such curve does not belong only to the venous side of the circulation but instead it is produced by the interaction of both sides of circulation (i.e., arterial and venous) or, in other terms, by the circuit that connects the heart output to its input (Tyberg, 2002). In order to support this interpretation, that is CO to change CVP by shifting blood volume among venous and arterial compartments, Levy (Levy, 1979) plotted CVP and MAP values against CO, all simultaneously recorded during his 1979 experiment (Figure 1.3).

With this regard, the connection between arterial circulation and peripheral veins was one of the points of debate (G L Brengelmann, 2006; Dalmau, 2018; Gelman and Bigatello, 2018b), particularly the role of MAP in altering any arbitrary PVP, since it is somehow neglected by authors supporting the Guyton's interpretation and it is an implicit assumption of the bathtub model (Magder, 2006; Magder, 2016).

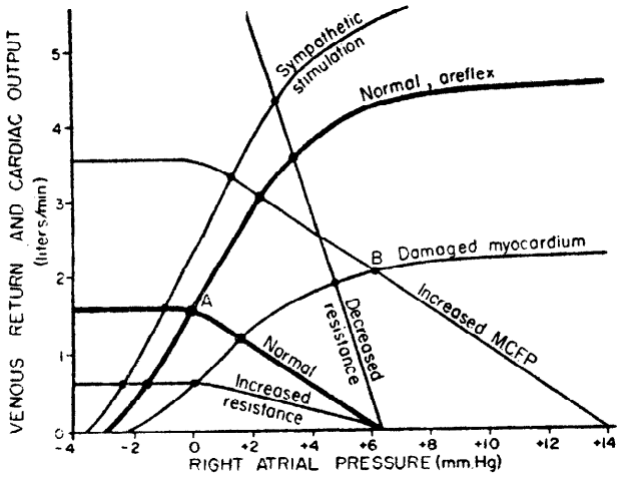

Figure 1.2: **Guyton curves.** Equilibration of various venous return curves with different cardiac response curves. Reprint from (A. C. Guyton, 1955).

1.2.2 Unstressed and stressed volume (and mean systemic filling pressure)

With this regard, another critical point of controversy about Guyton's interpretation was related to the pressure gradient that drives the VR but before going further in the explanation, Mean Systemic Pressure (Pms) needs to be introduced. This pressure is precisely the pressure value at which the whole CV equilibrates once the heart is stopped and the systemic flow F is zero: Pms is then function only of the total blood volume and of arterial and venous compliances and resistances.

More precisely, total blood volume can be divided into *stressed* and *unstressed* volume. Stressed volume is based merely on the compliance of the system, defined as the variation in volume following a variation in pressure, or the slope of the pressure-volume curve, measured in mL/mmHg. The unstressed volume is based on the vessel volume at zero pressure level, that is the maximum volume that can be filled before starting developing tension along the vessels wall (Figure 1.4).

This concept is nicely explained by Brengelmann (George L. Brengelmann, 2019) and reprinted in Figure 1.4 for the sake of clarity and convenience; of note, in Figure 1.4 unstressed volume is termed resting volume (Vr) and stressed volume is termed distending volume (Vd). The dashed line represents a leftward shift of the pressure volume relationship, that is a decrease of unstressed volume accompanied with no alteration in the compliance of the vessel, that is the inverse of the slope. This shift can be produced by a constriction of the smooth muscle cells that surround vessels walls, that in case of veins is termed venoconstriction. It is worth to mention that it is still not clear whether vessels constriction, aside of reducing the unstressed volume, might also alter significantly vessels compliance (Magder, 2016; George L. Brengelmann, 2019; Gelman and Bigatello, 2018b).

From a physiological point of view, a reduction in the fraction of the unstressed volume usually happens either in response to a blood volume loss or in response to an increased demand of systemic flow, as in case of physical activity. In the first case the total blood volume is depleted and the consequence of a venoconstriction is to maintain Pms constant, as precisely represented by the dashed line in Figure 1.4, by mobilizing a fraction of unstressed volume, while the fraction of stressed volume

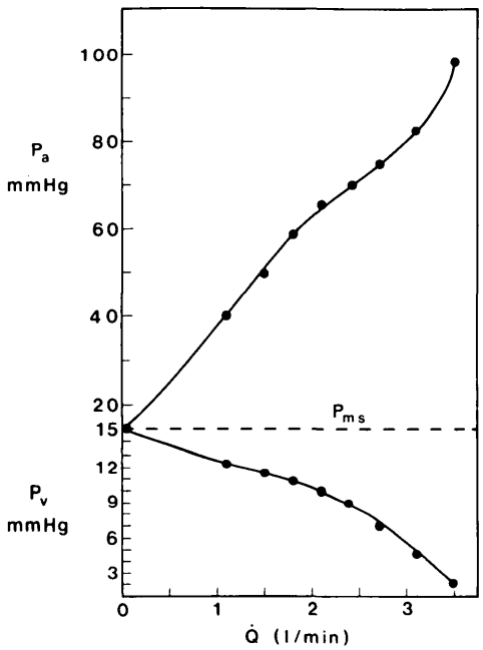

Figure 1.3: **Levy's contribution.** Mean arterial pressure (Pa) and central venous pressure (Pv) as functions of the systemic flow (here termed Q), in a canine right-heart bypass preparation. Reprint from (Levy, 1979).

is kept fixed. This is what happens for example during an haemorrhage to counteract hypotension, in which a large fraction of blood is mobilized from the venous reservoir, in particular from the splanchnic bed, in order to accommodate the tissues perfusion demand on the arterial side (Rothe, 1983; Pang, 2001). Instead, in case of physical activity, total blood volume is in principle preserved and the consequence of venoconstriction is to increase Pms and Venous Return, namely the systemic flow. This scenario is not depicted in Figure 1.4 but the higher value of Pms can be find by projecting the dashed line till the preserved Vt value. Another theoretical scenario is depicted in Figure 1.4 by the dotted line: here the slope of the line is diminished, meaning that the compliance is increased. An increased compliance allows to recruit the mobilized fraction of unstressed volume into the fraction of stressed volume. In this case, the increased compliance may be due to a pathological state, which would result in a decreasing of Pms and systemic flow if not counteracted by a venoconstriction response. Such pathological scenario happens, for example, in patients which suffer of sympathetic dysfunction at venous level, such as those with paraplegia: in those patients the Pms inherent of legs cannot be increased to support SV in case of orthostatic stress or exercise. Anyway, beyond the explanation about the determinants of Pms, the debate remains about its usefulness as clinical parameter (Maas, Pinsky, Aarts, et al., 2012; Hollmann D Aya et al., 2015; George L Brengelmann, 2016; Berger et al., 2016; Gelman and Bigatello, 2018b; Dalmau, 2019), since it is a quantity measured only with no flow (indeed it was originally defined as the intercept of the VR curve with the *abscissa*, see Figure 1.2) and that does not have unequivocal location in the venous compartment. The Pms is then a virtual quantity during normal circulation, but since it is defined as the ratio of stressed volume and total compliance, and being the arterial compliance far smaller than venous compliance, it

has been assumed to represent a proxy of peripheral venous pressure (PVP) that drives the return of the venous blood to the heart (Maas, Geerts, et al., 2009). Thus, the gradient for VR was defined as the difference among Pms and Right Atrial Pressure (RAP). However, as elegantly demonstrated by Brengelmann in 2003 (George L. Brengelmann, 2003) and resumed by others (Curran-Everett, 2007; Beard et al., 2011), this definition implies that the Resistance to venous Return (RvR) is in fact not dependent only by venous circulation but it is composed by both resistances and compliances of both arterial and venous circulation ($RvR = Rv + RaCa/(Ca + Cv)$, see Figure 1.1 for model information).

It is now clear that the "Venous Return curve", as measured by Guyton, is not driven only by the venous subsystem but by the whole circulatory loop, so it is in principle wrong to tune the slope of the VR curve in Figure 1.2 referring only to changes in the veins properties, given also the fact that the arterial and venous constriction, under some circumstances, have a common determinant in the sympathetic system. This complex relationship can be observed easily from the non linear trend shown in Figure 1.3 by arterial and venous pressure as CO increases. Finally, the use of Pms as representing an upstream pressure to define venous return complicates with no reason the equation of the underlying two compartment model that would instead be simple: the difference MAP-CVP is the pressure gradient for systemic flow and the Systemic Vascular Resistance (SVR) is the sum of arterial and venous resistances across which pressure gradient and flow are developed (George L. Brengelmann, 2019).

1.2.3 The steady state constraints of the model

It is likely that the Guyton's interpretation about CVP driving CO, is based upon a Frank-Starling mechanism's point-of-view, in which effectively CO depends upon *preload*, but the superimposition of the two curves (Figure 1.2) forces them to share the same axes and that is what confuses so much: those two curves depict the behaviour of two different subsystems in a scenario where they are studied alone, i.e., disconnected from each other. Instead, heart and circulation are two interconnected subsystems that reciprocally interact with negative feedbacks, thus the superimposition of the two curves makes one or another plotted backwards, i.e., with the independent variable on the y-axis (George L. Brengelmann, 2003; Beard et al., 2011).

Another important drawback of using the Guyton approach (Figure 1.2) as a tool to interpret and upon which to teach the CV system behaviour, is that it is limited to a steady state description and therefore it is inadequate to describe dynamic changes in the system (Rothe, 2006) indeed, it is not a state space; instead, it can only serve the purpose of describing what happens once variables are changed one at a time while holding other factors constant (Beard et al., 2011). However, this approach appears inadequate to describe how changing one of the variables affects the other: indeed, prior knowledge about the complex underlying interconnection is mandatory to manipulate those curves in order to describe multiple realistic states (Sheldon Magder, 2012; Magder, 2016; Sunagawa,

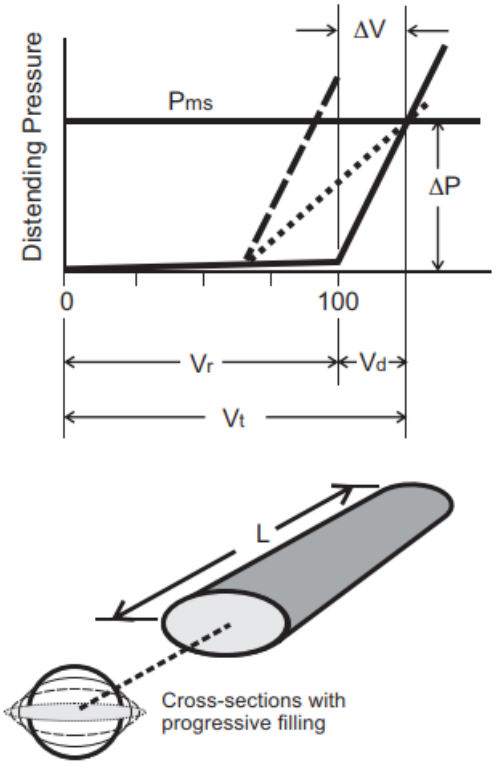

Figure 1.4: **Pressure volume relationship of a vein.** On the top graph is a schematic representation of a pressure-volume relationship: Vt is total blood volume within the vessel, Vr the volume needed to round the vessel and start to develop tension in its wall (i.e., unstressed volume or resting volume), Vd the volume that effectively develops tension (i.e., stressed volume or distending volume). Of note: in real life pressure-volume relationship for veins is not linear and it is also frequency dependent, e.g., because of the stress-relaxation mechanism (Hall et al., 2020). The image on the bottom shows what happens to the vessel's cross sectional area at progressively increasing volume. Reprint from (George L. Brengelmann, 2019).

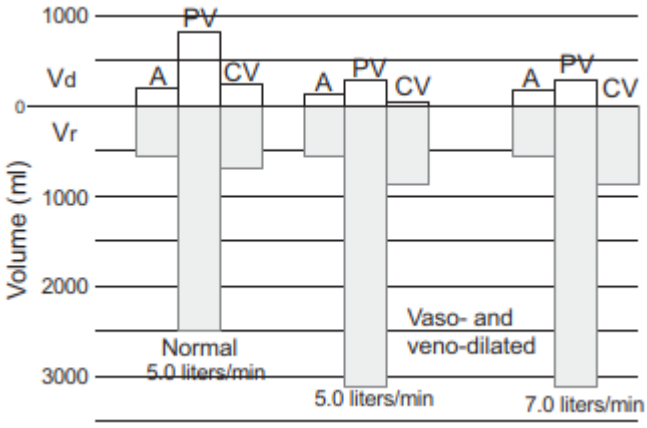

Figure 1.5: **Unstressed and stressed volume distribution in a three compartment model.** The model used here is composed by an arterial element (A), a peripheral venous element (PV) and a central venous element (CV). Three situations depicted: normal flow with normal vessel tone (left), normal flow with low vessel tone (center) and high flow with high vessel tone (center). Reprint from (George L. Brengelmann, 2019).

2017). In summary, not only the heart but the entire CV system has proven to have a strongly dynamic and non-linear behaviour. Therefore, mathematical approaches that take those features into consideration and that can deal with them, are of course a better choice to interpret and model a such complex system (Skinner et al., 1990; Nayak et al., 2018; Stepanyan et al., 2020).

Following the Guyton interpretation, other misconceptions were born. The first was considering CVP as a "back-pressure" (Beard et al., 2011) that impedes VR, instead of the product of the interaction between metabolic demands, total blood volume, compliances and cardiac response. The consequence of this interpretation was the promotion of targeting CVP value to guide CV therapeutic interventions (P. E. Marik, Baram, et al., 2008). In addition to that, another peculiar idea took place about veins: they were supposed to actively promote the return of blood to the heart, by their elastic recoil, instead of being simple passive elements. This turned out to be a misconception since each elastic structure can only exchange (i.e., absorb and release) energy and cannot be considered a source of energy, when its contribution is averaged over large intervals (or over an integer number of cycles) (Beard et al., 2011). However, some hypothesis of active work on circulation by peripheral veins still appears in the literature (Kenny, 2021).

1.2.4 Modelling perspectives

In conclusion, whether the model is designed to describe steady state or not, it is obvious that the complex real-life redistribution of blood volume between the venous compartments, which are characterized by different fraction of stressed and unstressed volume (Figure 1.5) and which respond differently to vasoactive/vasopressor drugs, e.g., due to the difference distribution of adrenergic receptors (Gelman and Bigatello, 2018b), is poorly represented by a two compartment model, as already acknowledged more than 100 years ago (Krogh, 1912).

It would be preferable for clinical decision making, to characterize the venous district as detailed

as possible about its segmental pressures and volumes distribution (Truijen et al., 2010; Magder, 2016; Gelman and Bigatello, 2018b; Gelman and Bigatello, 2018a; George L. Brengelmann, 2019; Werner-Moller et al., 2020). Nevertheless, modelling the entire CV system, despite some valuable efforts (Stiles et al., 2021) and advances in the field (Quarteroni et al., 2016), is seriously affected by the difficulties of acquiring high quality data in a non-invasive way (Veneziani et al., 2013), given the high variability of what is usually called the physiological range. With this regard, techniques aimed at a non-invasive characterization of the vessels properties, like, for instance, the venous compliance (Hollmann D Aya et al., 2015; Gelman and Bigatello, 2018b), are increasingly relevant for the appropriate tailoring of both mathematical models and therapeutic strategies (Quarteroni et al., 2016). This is one of the reasons why, during this Doctoral project, I engaged myself in the assessment of venous compliance first by means of venous Pulse Wave Velocity (vPWV), developing and patenting (Ermini et al., 2019) a novel measurement technique (paper I, II, III, IV), and also by means of Near Infrared Spectroscopy (NIRS), resulting in the first description of a subtle and overlooked confounding factor (paper VI).

1.3 Fluid therapy management

The question about who is (or which are) the leading variable(s), among the many that make up the CV system, assumes an important role particularly when what is treated as a constant, for instance total blood volume, is altered (Gelman and Bigatello, 2018b). This is one of the most widespread scenario in clinical routine: there are several pathological states that cause either a loss or an accumulation of body fluids, therefore changing the definition of *euvolaemia*, alternatively *normovolaemia* (Truijen et al., 2010). In those cases, understanding how the body handles blood and redistributes it among the main compartments of the circulation is paramount for choosing the right therapeutic approach, which could be either a fluid therapy, a drug (vasoactive/vasopressor) therapy, or a combination of them (Figure 1.6).

Despite the long history of Intravenous (IV) fluids administration and its widespread use in the clinical settings (Finfer et al., 2018), only in the recent years it has been reported that, as well as being ineffective, the overzealous fluids administration can be also detrimental, resulting in Fluid Overload (FO) consequences (Figure 1.7) (Silva et al., 2013; Malbrain et al., 2014; Kelm et al., 2015; W. L. Miller, 2016; Sakr et al., 2017; Nieto et al., 2021). On this basis, a careful evaluation of the patient haemodynamics is recommended in order to being able to predict, as precise as possible, its response to a fluid infusion before administering it (Bentzer et al., 2016; Monnet, P. E. Marik, et al., 2016; Monnet and J. L. Teboul, 2018). This evaluation is called Fluid Responsiveness (FR), upon which patients are divided into two categories: responders and non-responders, namely a binary classification (Figure 1.6).

A FR prediction could be necessary virtually in each clinical department but it becomes critical in the operating room, intensive care unit, emergency room, nephrology and cardiology. In those hospital

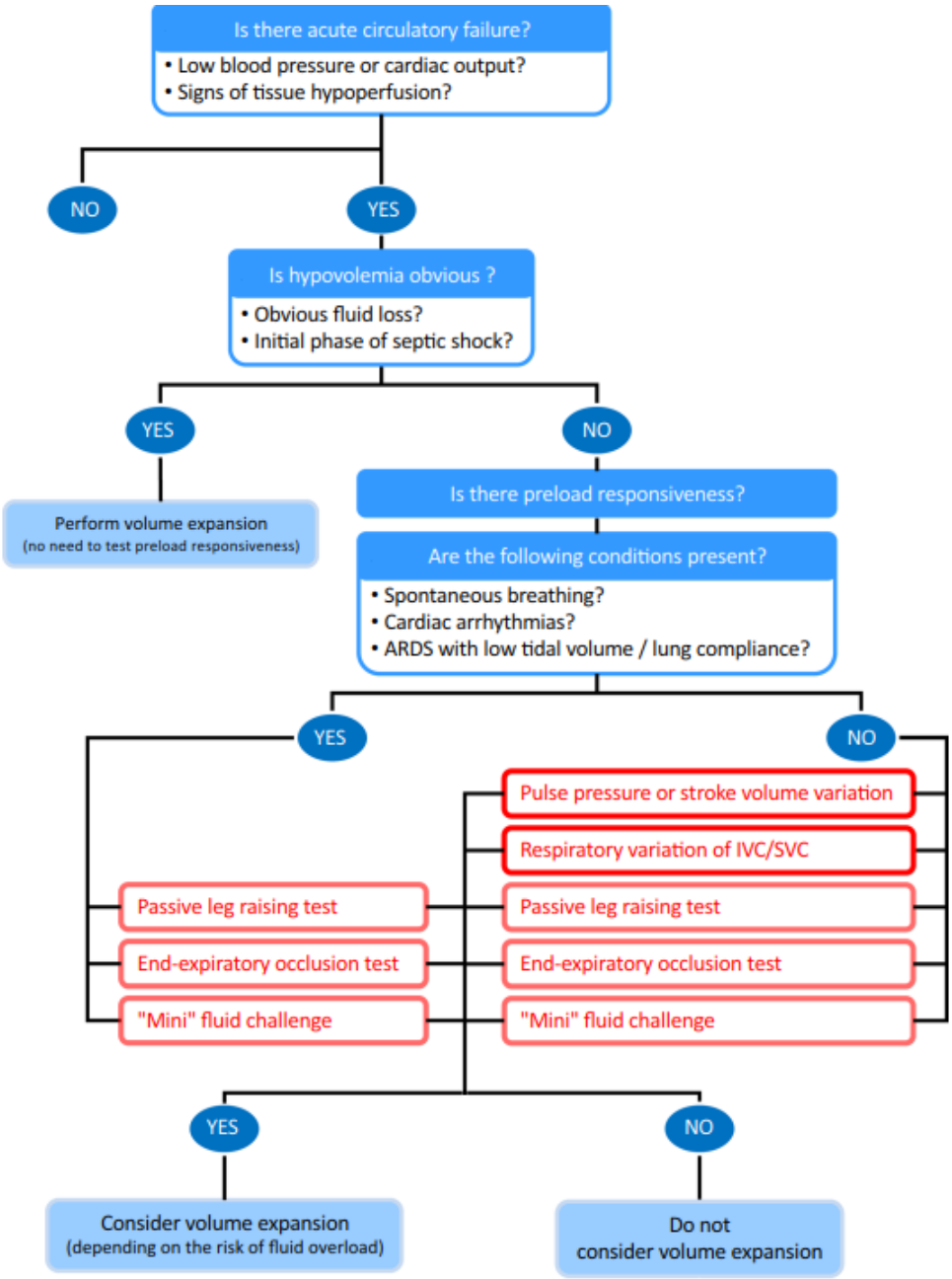

Figure 1.6: **An example of fluid therapy management.** The presented strategy is not official but it is a good example of clinical reasoning when dealing with an acute circulatory failure. Acute Respiratory Distress Syndrome (ARDS); Inferior Vena Cava (IVC); Superior Vena Cava (SVC). Reprint from (Monnet, P. E. Marik, et al., 2016).

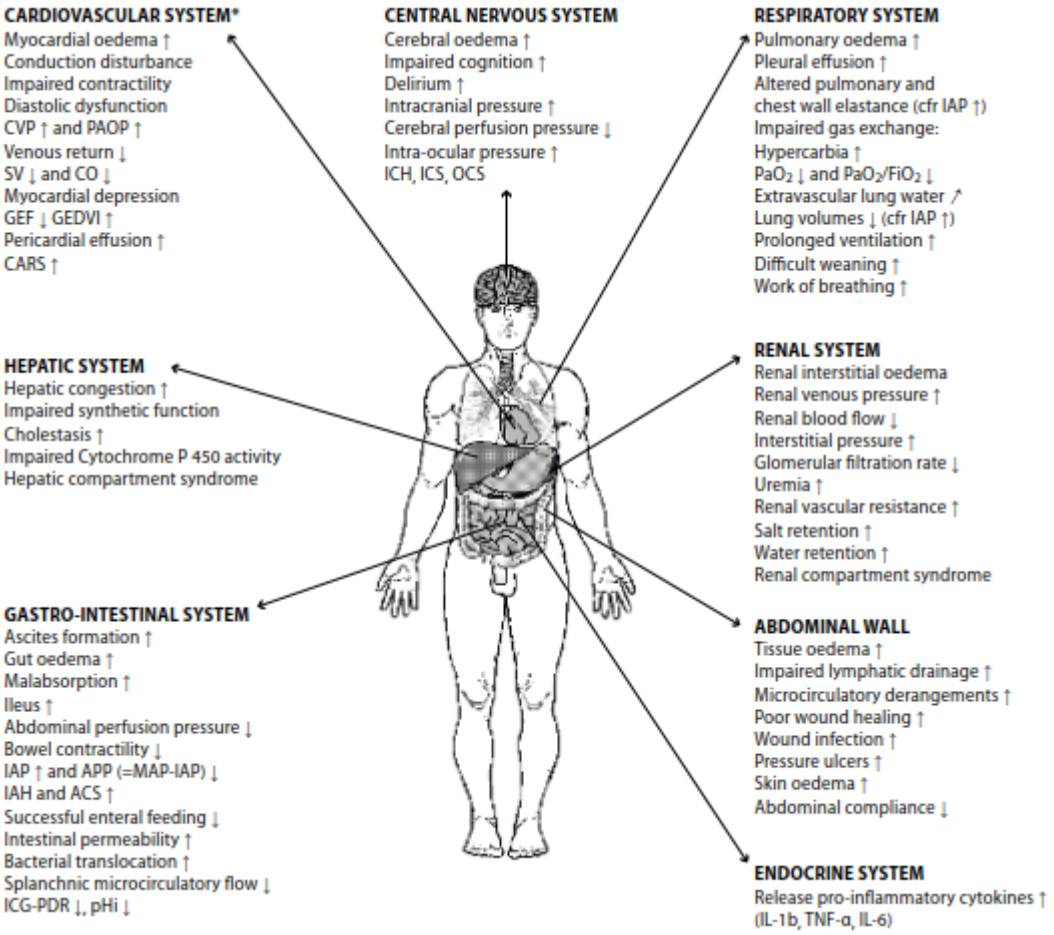

Figure 1.7: **Pathophysiologic effects of fluid overload on end-organ function.** See text for explanation. intra-abdominal pressure (IAP), intra-abdominal hypertension (IAH), Abdominal Compartment Syndrome (ACS), intra-cranial hypertension (ICH), Intra-cranial Compartment Syndrome (ICS), Ocular Compartment Syndrome (OCS), Cardio Abdominal Renal Syndrome (CARS). Reprint from (Malbrain et al., 2014).

wards, the question about the correct volaemic status of a patient, i.e., the amount of blood volume that is more appropriate to the clinical condition of the patient, is central and strictly related to the patient haemodynamics stability. Indeed, it is demonstrated, and widely accepted, that a patient, who presents symptoms of haemodynamics instability, needs an Intravenous (IV) fluid administration in only half of the cases (Bentzer et al., 2016). Thus, a careful evaluation is mandatory.

Unfortunately, still nowadays, a gold standard for FR prediction is missing and the reference methodology is basically the assessment of the response to a test infusion of 250-500 mL of fluids (Monnet, P. E. Marik, et al., 2016), termed Fluid Challenge (FC). This methodology obviously risks to harm the patient and secondly, it poses an ethical constraint to the experimental design used to test novel techniques, i.e., only patients that really need fluids can be included in the study, thereby leading to a sampling bias that is difficult to evaluate.

It is particularly in this regard that the debate about the determinants of VR and about the role of CVP with respect to CO becomes meaningful (Section 1.2.1 and 1.2.2). With the "Guyton's curves" in mind a clinician has been taught that VR is driven by CVP, which means that systemic flow depends upon the CVP value; the consequence is that, as long as CVP remains confined within "safe values", i.e. those who are supposed to correspond to the linear slope of the Frank-Starling curve (Figure 1.9), the heart should have the right amount of blood to pump in order to guarantee a correct tissues perfusion, with no need of blood infusion or removal; in fact, the hypothetical pressure gradient that drives VR is assured. This hypothesis is clearly unharmful, as long as the clinicians can directly monitor a representative parameter of tissues perfusion, for instance cardiac output, but reality is that CO is rarely measured (Cecconi, Hofer, et al., 2015).

In clinical practice, it is common to get an indication of the patient haemodynamic status simply looking at CVP or its surrogates (as discussed in Section 1.1) to see if it falls within some theoretically "safe values", other than looking at physical signs of tissues perfusion; however, within those safe values there is a large grey area of operation of this parameter (De Backer et al., 2018) indeed, in the recent international guidelines for management of sepsis and septic shock this approach is deprecated (Rhodes et al., 2017). In a more comprehensive view, several factors can contribute to establish a certain CVP value, such as heart *afterload* and heart *preload* responsiveness, myocardial stiffening (resulting in diastolic dysfunction), as well as blood volume redistribution or net variation, intra-abdominal hypertension (IAH), impairment of muscle pump, pulmonary hypertension, and so on (Gelman, 2008; Sheldon Magder, 2015; Via et al., 2016). All those factors, although in a first approximation they can be neglected, in real life they are likely to play a big role in the closed loop of circulation. In fact, CVP has been demonstrated to have a poor predictive value about FR (the same as flipping a coin) (P. E. Marik, Baram, et al., 2008; P. E. Marik and Cavallazzi, 2013; Cecconi and Hollman D Aya, 2014; Eskesen et al., 2016; De Backer et al., 2018), even though in 2015 it was still the most common worldwide haemodynamic parameter to guide the fluid therapy (Cecconi, Hofer, et al., 2015).

Fluid responsiveness tests	Available haemodynamic techniques	Main advantages	Main drawbacks
PLR test	Pulse contour analysis (*CO*) Echocardiography (VTI) Oesophageal Doppler (ABF) Bioreactance (*CO*) Pulse oximeter (PI)	Applicable in ventilated and nonventilated patients	Requires real-time haemodynamic assessment Unreliable in cases of IAH
PPV	Arterial catheter	Continuous monitoring No need for *CO* monitoring	Unreliable in cases of SB, cardiac arrhythmias and IAH False negatives in cases of low V_T and low lung compliance
SVV	Pulse contour analysis	Continuous monitoring	Unreliable in cases of SB, cardiac arrhythmias and IAH False negatives in cases of low V_T and low lung compliance
EEO test	Pulse contour analysis	Easy to perform	Requires precise and real-time measurement of *CO* Impossible to perform in cases of intense SB activity
EEO + EIO tests	Echocardiography Oesophageal Doppler	Less invasive assessment	Requires precise and real-time measurement of *CO* Impossible to perform in cases of intense SB activity Cumbersome procedure
ΔIVCd	Transthoracic echocardiography	No need for *CO* monitoring	Requires experienced operator Limited value in cases of IAH Questions exist regarding its reliability in ventilated patients even in cases of normal V_T Its value in nonintubated patients able to sustain deep inspiration needs confirmation
SVC collapsibility index	Transoesophageal echocardiography	No need for *CO* monitoring	Requires experienced operator Impossible to perform in nonventilated patients Doubts on its reliability even in cases of normal V_T
TVC	Arterial catheter	Reliable in low V_T ventilation No need for *CO* monitoring	Applicability to specific conditions (mechanical ventilation with SB, severe ARDS and IAH) needs confirmation Reliability during prone position needs further investigation
Mini-fluid challenge	Pulse contour analysis (Echocardiography?)	Applicable even when the other tests are not available Limited risk of fluid overload	Its low cut-off value (5%) requires a very precise measurement
LRM	Pulse contour analysis	Quite easy to perform	Risk of misinterpretation as LRM can also increase the right ventricular afterload Reliability and applicability require further confirmation
Sigh manoeuvre	Arterial catheter	Applicable during PSV No need for *CO* monitoring	Requires automatization to be routinely applicable Risk of misinterpretation as sign manoeuvre can also increase the right ventricular afterload Reliability and applicability require further confirmation
PEEP test	Pulse contour analysis	Easy to perform	Requires real-time measurement of CO

Figure 1.8: **Summary of dynamic tests used for Fluid Responsiveness (FR) prediction with available monitoring techniques, main advantages and drawbacks.** Inferior Vena Cava diameter (IVCd); descending Arterial Blood Flow (ABF); Cardiac Output (CO); End-Expiratory Occlusion Test (EEOT); End-Inspiratory Occlusion Test (EIOT); intra-abdominal hypertension (IAH); Lung Recruitment Manoeuvre (LRM); Positive End Expiratory Pressure (PEEP); Perfusion Index (PI); Passive Leg Raising (PLR); Pulse Pressure Variation (PPV); PSV; Spontaneous Breathing (SB); Superior Vena Cava (SVC); Tidal Volume Challenge (TVC); Tidal Volume (TV); Velocity Time Integral (VTI). Reprint from (Shi et al., 2020).

1.3.1 From static to dynamic parameters

Over the last ten years the field of FR has grown a lot and the paradigm about the techniques to employ is evolved, moving from static haemodynamic parameters (e.g., CVP) to dynamic ones, namely the variation of an haemodynamic parameter in response to a perturbation (Ansari et al., 2016), termed also dynamic test. Such perturbation can came from different types of stimuli, based on the patient status (e.g., if mechanically ventilated or not) and the availability of dedicated devices and invasive lines for arterial/venous pressure measurements (Monnet, P. E. Marik, et al., 2016). Indeed, it is obvious that an invasive measurement results in a better accuracy to record the dynamics of the response to the perturbation. In the table of Figure 1.8 all the most commonly used dynamic tests to predict FR are listed, along with relative monitoring techniques, advantages and drawbacks: for a comprehensive and detailed review see (Shi et al., 2020).

Among dynamic tests listed in Figure 1.8, few are the ones that can be both recorded by completely non-invasive techniques and performed on Spontaneous Breathing (SB) patients (Vistisen et al., 2017; Monnet and J. L. Teboul, 2018; Shi et al., 2020). The first is the analysis of pressure variations within central veins (venae cavae) due to respiration, which can be assessed by Ultrasound (US) imaging and will be addressed in details in Section 1.3.4. The second is the *preload* challenge induced by postural manoeuvres, among which Passive Leg Raising (PLR) is the most used, assessed by accurately monitoring CO (see Section 1.3.2), as well as by the recently proposed Perfusion Index (PI) and Capillary Refill Time (CRT) techniques (Shi et al., 2020). The third is the classical Fluid Challenge (FC) that is usually assessed by accurately monitoring CO.

In case the patient is intubated or has an arterial/venous line for accurate pressure measurements, the possibility became more, including: functional haemodynamic tests, like End-Expiratory Occlusion Test (EEOT), Pulse Pressure Variation (PPV), Stroke Volume Variation (SVV) or mini FC (100mL) (Messina et al., 2019; Lee et al., 2020), and surrogate measures of Pms (Maas, Geerts, et al., 2009; Schulz et al., 2021). Indeed, invasive arterial/venous lines are exploited by some commercial devices to better estimate the necessary haemodynamic parameters, particularly SV and CO (see Section 1.3.2). With this regard, clinical trials about surrogates of Mean Systemic Pressure have been investigated (Maas, Pinsky, Aarts, et al., 2012; Maas, Pinsky, Geerts, et al., 2012; Schulz et al., 2021), also in combination with PLR, reporting encouraging results (Monnet and Pinsky, 2015; Cooke et al., 2018). However, surrogates of Pms are derived directly from invasive arterial pressure measurements, casting shadows about the name of this quantity. Indeed, in order to validate the utility of Mean Systemic Pressure, as a concept, to guide FR (Repessé et al., 2015), beyond the utility of its surrogate measures (Schulz et al., 2021), a technique to estimate Pms which doesn't need an estimate of CO, or an arterial line, would be more appropriate.

In conclusion, despite this continuing evolution and increase of the methodologies used to assess FR, a gold standard technique is still missing: the best classification method, in terms of sensitivity

and specificity, is an the increase of CO above 10% after a PLR manoeuvre (when possible), even though the technique is dependent upon the accuracy of the CO monitoring technique employed (Monnet, P. E. Marik, et al., 2016; Shi et al., 2020); however, given the risk associated with invasive measurements and the costs of modern sophisticated instruments for non-invasive o minimally-invasive CO monitoring (see Section 1.3.2), there is a compelling need for reliable (hopefully low-cost) non-invasive methodologies to assess FR (Cecconi, Hofer, et al., 2015; Vistisen et al., 2017; Monnet and J. L. Teboul, 2018) which, in a near future, will allow to personalize the haemodynamic management (Saugel, Vincent, et al., 2017; Lin Wang, 2019) and likely to overcome the classical dichotomous approach to FR in favour to a continuous quantification of fluids imbalance (Ansari et al., 2016; Cooke et al., 2018).

1.3.2 Real-time Cardiac Output monitoring

The role of a real-time CO monitoring was shown to be critical in the last years, given the fact that is employed in almost half of the recently reported dynamic tests to predict FR, as reported in Figure 1.8. The gold standard technique for measuring CO is Pulmonary Artery Catheter (PAC), which is thermodilution-based: it is both invasive and time consuming, thus unsuitable for real-time monitoring and affected by several limitations and risks associated to its inherent invasiveness (Pugsley et al., 2010; Sangkum et al., 2016).

On the contrary, the modern non-invasive or minimally-invasive techniques, theoretically suitable for real-time monitoring of dynamic tests, are rarely available, as reported by an observational study conducted in Intensive Care Unit (ICU) around the world (Cecconi, Hofer, et al., 2015). Moreover, at this stage of development, devices based on a completely non-invasive methodology to estimate CO (e.g., CNAP®, ClearSight®, Nexfin®) seems to have poor accuracy, particularly regarding the ability to follow time trends (Critchley et al., 2010), even though the heterogeneity among studies is high (Lakhal, M. Martin, et al., 2016; Wagner et al., 2018; Saugel, Hoppe, et al., 2020).

On the other hand, the minimally-invasive methodologies still require an arterial pressure catheter to estimate CO (e.g., PiCCO®, LIDCO®, NiCCO®, FloTrac®), thereby reaching a higher accuracy (P. E. Marik, 2013; Sangkum et al., 2016; Grensemann, 2018), even though apparently it is still not sufficient to be interchangeable with the PAC thermodilution technique, in terms of both accuracy and precision (Clement et al., 2017). Nevertheless, minimally-invasive devices as well as Oesophageal Doppler and Velocity Time Integral (VTI) (assessed by means of transthoracic Echocardiography) when used to monitor PLR response in order to predict FR, resulted in an overall high accuracy, if compared to other techniques (Monnet, P. E. Marik, et al., 2016; Mesquida et al., 2017; Monnet and J. L. Teboul, 2018).

Of note, in the recent years, two novel methodologies that are not based on an estimate of CO, have demonstrated to correctly detect indirectly the effect of PLR on CO (Shi et al., 2020), despite

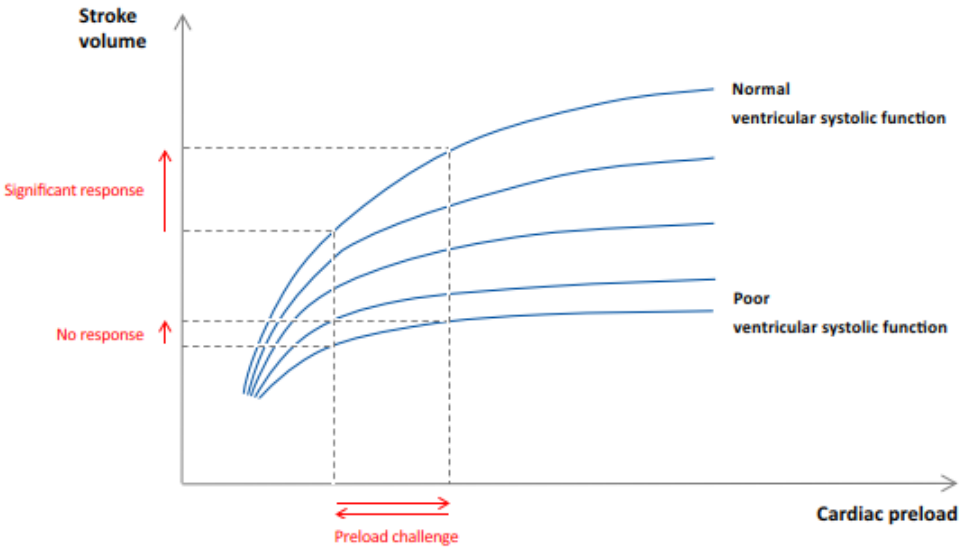

Figure 1.9: **Frank–Starling curve representing the ventricular systolic function.** One given level of cardiac *preload* does not help in predicting fluid responsiveness. By contrast, dynamic tests include a *preload* challenge, either spontaneous (e.g., respiration) or induced (e.g., passive leg raising or "mini" fluid infusion). Observing the resulting effects either on stroke volume or cardiac output allows for the detection of *preload* responsiveness. Reprint from (Monnet, P. E. Marik, et al., 2016).

some precedent conflicting results (Monnet, P. E. Marik, et al., 2016; Monnet and J. L. Teboul, 2018). The first is the Perfusion Index (PI) computed from a pulse oximetry signal (plethysmography) while the second is Capillary Refill Time (CRT), assessed by an external camera (Shi et al., 2020). Finally, a last methodology to estimate CO is worth to be mentioned: bioreactance, used to estimate CO from the analysis of blood flow dependent changes in phase shifts of an electrical current applied across the thorax (Jones et al., 2015). This methodology has the advantage of being completely non-invasive but until recently its results, when evaluating FR were conflicting, casting shadows on its reliability; however, those conflicting results were likely related to technical limits, for instance a too low time resolution (one measurement every 30s), which now seems solved (reduced to 8s), as suggested by a novel encouraging evidence (Shi et al., 2020).

1.3.3 Passive Leg Raising

Postural manoeuvres, like Passive Leg Raising (PLR), allow to instantly mobilize the blood volumes accumulated into distal venous compartments (Figure 1.10), therefore effectively simulating the effects of a Fluid Challenge (FC): for this reason, PLR is sometimes termed "simulated fluid challenge". PLR is a really useful tool in the field of FR, fundamentally because it is a safe way to challenge the heart *preload* responsiveness and therefore to assess on which portion of the Frank-Starling curve the heart is actually working (Figure 1.9). On this basis, the effect has to be evaluated by monitoring CO, or at least Stroke Volume (SV), and FR can be predicted according to the peak response observed within the first minute. So, the general indication is that an increase in CO of at least 10% is necessary to classify a patient as responder and to proceed the therapy with fluid administration (Pugsley et al., 2010; Mesquida et al., 2017).

As already discussed in previous section (Section 1.3.2), the techniques to evaluate PLR response based on either a direct or indirect CO measurement have repeatedly exhibited good performance when used to predict FR, while the more recent alternatives, namely pulse oximetry, bioreactance and CRT, need more investigations, despite some promising results (Shi et al., 2020).

The mobilization of blood volumes from venous compartment obtained with PLR has been estimated to be around 300mL if starting the manoeuvre from a semi-recumbent position (Monnet and J.-L. Teboul, 2015) as depicted in Figure 1.10; however, if the manoeuvre is performed starting from a supine position the results may be inconsistent (Lakhal, Ehrmann, Runge, et al., 2010; Monnet and J.-L. Teboul, 2015), likely because the fraction of blood mobilized from the legs venous compartments is smaller (Jabot et al., 2008; Cherpanath et al., 2016). Nevertheless, from a recent meta-analysis, no significant differences were observed depending on the starting position (semi-recumbent vs. supine) (Cherpanath et al., 2016), even though the heterogeneity of the studies was high.

Furthermore, in order to properly capture the transient effect of PLR, the CO monitoring technique should be fast and accurate, suitable to capture real-time variations, which is why modern continuous non-invasive techniques are appealing (Mesquida et al., 2017; Saugel, Hoppe, et al., 2020). The effect of PLR is supposed to vanish quickly (Wong et al., 1988; Monnet and J.-L. Teboul, 2015), even though the 1-min time window, as derived by old studies performed with slow (i.e., low temporal resolution) techniques, has been recently questioned and considered to be of longer duration (Lakhal, Ehrmann, and Boulain, 2016). For sure, the time course of the haemodynamic response to PLR is poorly described in literature and it deserves further studies: indeed, the majority of the investigations report only a single measurement and only recently some authors have started reporting the time course (Elwan et al., 2018).

The doubts concerning the duration of the response to PLR are also related to the correct functioning of the physiological adaptation mechanisms involved (e.g., baroreceptor reflex, myogenic effect on arteriolar resistances, preserved vessels compliance, heart *preload* responsiveness, etc.), given the fact that many studies were conducted on patients but very few on healthy subjects, in which all those mechanisms are supposed to be intact (Godfrey et al., 2014; J. Miller et al., 2016; Elwan et al., 2018; Chopra et al., 2019). Fortunately nowadays, thanks to novel non-invasive haemodynamic monitoring techniques, this gap is going to be filled (Chaves et al., 2018; Shi et al., 2020).

In summary, despite PLR is inapplicable in some clinical situations where the patient cannot be mobilized (e.g., during surgery) or in the presence of an elevated intra-abdominal pressure (IAP) (a not so uncommon clinical symptom) (Mahjoub et al., 2010), it can be operated in most clinical conditions and it is the most recommended test for FR prediction, its reliability being supported by several reviews and meta-analysis (Cherpanath et al., 2016; Monnet, P. Marik, et al., 2016; Mesquida et al., 2017; Pickett et al., 2017; Cooke et al., 2018). However, it is worth to mention here that in a recent meta-analysis of RCTs no difference in mortality has been found by using a PLR-guided resuscitation protocol (Azadian et al., 2021), suggesting that a comprehensive knowledge about this

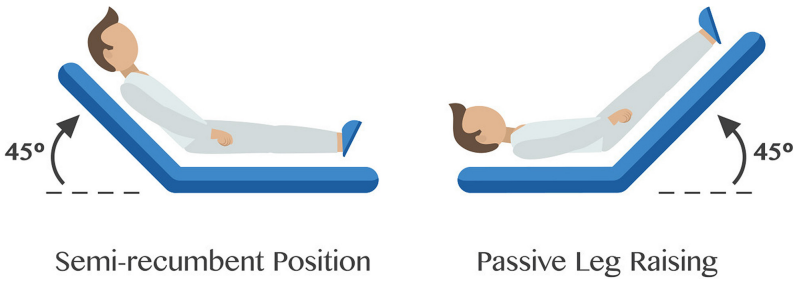

Figure 1.10: **Passive Leg Raising (PLR) manoeuvre.** PLR is usually performed starting from a semi-recumbent position and after a reasonable time (minutes at least) switching to the PLR position. An automated clinical bed is highly recommended in order to avoid any discomfort of the patient which might affects the response to the manoeuvre. Reprint from (Toppen et al., 2018).

manoeuvre and how to integrate it in a standardized protocol is still missing.

Anyway, given the notable advantages of PLR as simulated FC and adding the fact that is easily implemented even in the absence of special mechanical beds, unlike the Trendelenburg position or Head Down Tilt (HDT) (J. T. Martin, 1995), during this Doctoral project Passive Leg Raising (PLR) has been used as a model to evaluate the sensitivity of the haemodynamic parameters under investigation to mild blood volume increase. In particular, PLR was employed in two experimental series: first to test vPWV measured on upper limbs (paper II) and then to test IVC pulsatility indexes (paper V).

1.3.4 Inferior Vena Cava pulsatility indexes

Among all the methodologies reported in Figure 1.8 to assess FR, respiratory variation of Inferior Vena Cava diameter (IVCd) as assessed by US imaging is one of the most simple and versatile (Millington, 2019; Shi et al., 2020). The filling status of IVC is directly dependent upon CVP, in case of physiological IAP values, and it reflects what can be called central volume status. However, the absolute value of IVCd has no clinical usefulness, given the high inter-subject variability of IVC size and shape, that's why the respiratory variation of IVCd is exploited.

The respiratory activity acts as a small perturbation (but the magnitude depends strongly upon the respiratory effort) affecting IVC *transmural* pressure; by measuring the corresponding IVCd variation it is possible to have an estimate about the *relative* filling of the vessel, i.e., with respect to its capacity limit. In other words, since the compliance of the vessel decreases proportionally with the vessel *transmural* pressure, the respiratory IVCd variation is as small as the IVC filling volume is large; however, the respiratory variation of IVCd is still dependent upon IVC size. Thus, it becomes more clinically useful once it is described by means of the so-called Inferior Vena Cava *collapsibility* (IVCc), also termed Caval Index (CI), which conveniently normalizes the respiratory (or respirophasic) variation of IVCd ($d_{max} - d_{min}$) to d_{max}, thus accounting for individual differences in IVC size, with d_{max} and d_{min} being the maximum and minimum diameters, respectively, observed within a respiratory cycle (Via et al., 2016).

Beyond its working principle, this methodology to predict FR has two main advantages: first it

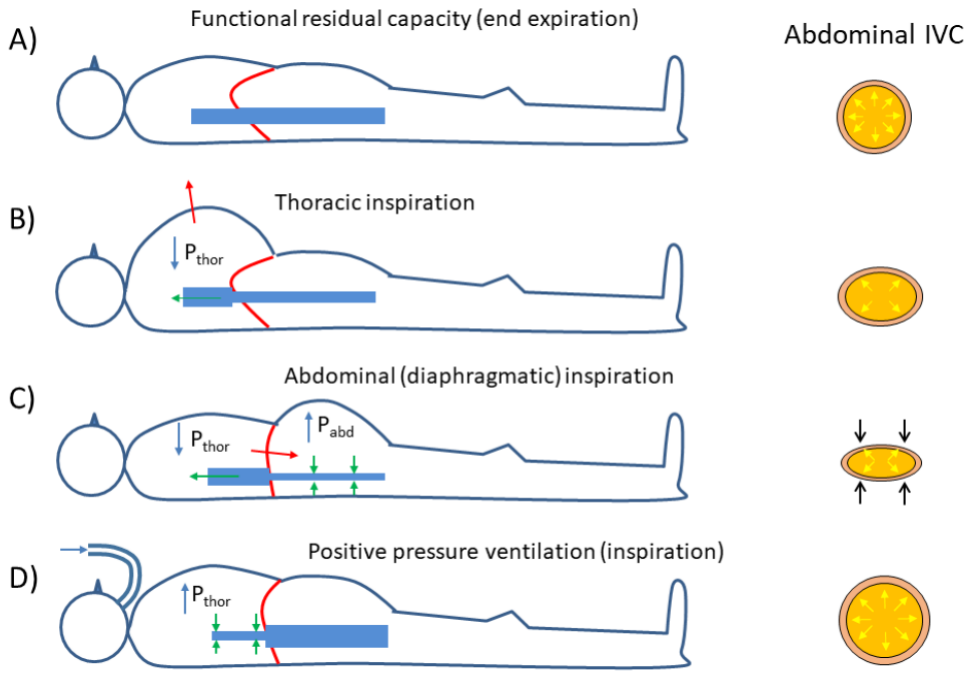

Figure 1.11: **Respirophasic variations in abdominal Inferior Vena Cava (IVC).** Three representative situations of spontaneous breathing (A,B,C) and one situation of mechanical ventilation (D), performed by positive pressure ventilation. P_{thor} is intra-thoracic pressure (ITP) and P_{abd} is intra-abdominal pressure (IAP). A) End of expiratory phase: pressures of abdomen and thorax are equals and the abdominal Inferior Vena Cava diameter (IVCd) is at its maximum. B) Mainly thoracic inspiratory effort: P_{abd} is unaffected but P_{thor} decreases and this increase the drainage of blood from abdominal IVC. C) Mainly diaphragmatic inspiratory effort: P_{abd} increases and this squeezes the abdominal IVC and P_{thor} decreases, thus increasing the drainage of blood from abdominal IVC which now is at its minimum. D) Mechanical ventilation during inspiratory phase: P_{abd} is unaffected but P_{thor} increases, squeezing the thoracic IVC and thus decreasing the drainage of blood from abdominal IVC which is now at its maximum. Reprint from (paper VII).

exploits a device that is widespread in several clinical settings, i.e., the echograph, whose usage is affordable by many physician, even though proper training is needed, as the accuracy is strongly operator-dependent and it is particularly affected by the experience (Corl et al., 2020); second, it can be applied both to SB patients and mechanically ventilated patients so, its use can span across almost all the hospital wards in which a FR prediction is needed.

As mentioned, variation of IVCd is considered primarily due to respiratory activity but, before introducing the underlying mechanism, a consideration is mandatory: the US assessment of IVCd is usually performed by a *sub-xiphoid* approach (Finnerty et al., 2017; Millington, 2019), which means that only the abdominal portion of the IVC is considered. This fact is relevant because respiration differently affects the pressures in the abdomen and in the thorax. Moreover, inspiration is in general a combination of thoracic and diaphragmatic movements, with a ratio among them highly variable, both from an inter- and an intra-subject point of view (Tobin et al., 1988; Kimura et al., 2011; Gignon et al., 2016; Folino et al., 2017). So, in order to clarify how those two inspiratory mechanisms affect differently abdomen and thorax, they are going to be addressed separately in the following explanation.

Let's start with a mainly thoracic inspiration: during that, intra-thoracic pressure (ITP) becomes progressively more negative and in turn it causes an increase in the *transmural* pressure of thoracic

IVC, therefore distending that portion of the vessel (i.e., thoracic IVCd increases) and, on the same time, this increases the drainage of the abdominal portion of IVC (Figure 1.11B).

On the contrary, if the inspiration is mainly diaphragmatic, ITP again decreases, but the intra-abdominal pressure (IAP) this time is increased, due to the downward displacement of the diaphragm, therefore the abdominal portion of IVC is essentially squeezed, i.e., its *transmural* pressure is decreased, leading the abdominal IVCd to its minimum (Figure 1.11C). Finally, during SB, at the end of expiration (Figure 1.11A) the abdominal IVCd is at its maximum, being its *transmural* pressure at its maximum due to the minimum in IAP.

A different situation occurs if patients are mechanically ventilated, by means of positive pressure ventilation, which basically consists of inflating the lungs to achieve inspiration and then deflating them to achieve expiration. Briefly, with a positive pressure ventilation, while abdomen pressure is approximately unaffected, during inspiration ITP increases and this, as well as decreasing the *transmural* pressure of the thoracic IVC, diminishes the drainage of the abdominal IVC, whose diameter then increases.

In summary, if patient is mechanically ventilated, its IVCd during inspiration increases, instead if it is SB its IVCd during inspiration is decreased (to a bigger extent if respiration is mainly diaphragmatic). This is the reason why, sometimes, in case the IVCd methodology is applied to a cohort of patients mechanically ventilated, the index take the name of *distensibility* index (Barbier et al., 2004), instead of *collapsibility*, referring explicitly to the characteristic of the abdominal IVC to distend during a mechanical inspiration, instead of collapsing, as during spontaneous inspiration.

Notwithstanding the above mentioned advantages of this methodology to predict FR, its performances, when compared to other methodologies (Figure 1.8), are mediocre, as already confirmed by several meta-analysis (Zhang et al., 2014; Long et al., 2017; Das et al., 2018; Orso et al., 2020; Unal Akoglu et al., 2021). Moreover, regarding its applicability, although first evidences reported a better diagnostic accuracy for FR in mechanically ventilated patients respect to SB patients (Zhang et al., 2014; Long et al., 2017), as one would expect giving the more standardized and reliable ITP variation with mechanical ventilation, more recent meta-analysis indicates the contrary (Das et al., 2018; Orso et al., 2020; Unal Akoglu et al., 2021), even though the authors reported a high heterogeneity among the included studies, casting doubts about the reliability of the pooled results. One hypothesis, to explain those inconsistent findings, might be related to the low overall stimulus (i.e., ITP variation) associated with positive pressure ventilation (Suehiro, 2020) as compared to SB, which makes the relative errors in the measurements of IVCd bigger and therefore relevant for the FR diagnostic accuracy. With this regard, a recent meta-analysis focusing only on mechanically ventilated patients reported a lower accuracy in those ventilated with low Tidal Volume (TV) as compared to those ventilated with normal TV (Si et al., 2018).

In addition to these problems concerning mechanically ventilated patients, CI has also poor performances when applied to SB patients. The major source of variability in CI measurements is the

variability in amplitude and frequency of the spontaneous inspiratory effort (Tobin et al., 1988), considering also the variable diaphragmatic activation, as explained above, that results in an overall poor repeatability of the measurements (Kimura et al., 2011; Gignon et al., 2016): this causal relationship between inspiratory effort and CI (Folino et al., 2017) has been exploited recently by a pilot study, in which the authors, through a standardized deep inspiratory effort, obtained a better diagnostic accuracy in terms of FR (Bortolotti et al., 2018); however, this approach has likely limited applicability in clinical settings due to the general weakness of patients who cannot reproduce the desired inspiratory effort.

In addition to all the aforementioned limitations related to the respiratory activity (both spontaneous and assisted), the IVCd methodology for FR prediction is affected by other confounding factors introduced by different pathological states (Via et al., 2016): indeed, there are pathologies that can alter either IAP or ITP, as well as directly diminish VR by decreasing cardiac function or by obstructing central veins, as thoroughly summarized in Figure 1.12.

Unfortunately, besides the pathophysiological constraints explained above, the US assessment of respirophasic variation of IVCd suffers of other more technical limitations, which all together contribute to the overall modest performances of CI to predict FR (Millington, 2019; Orso et al., 2020). First, this methodology is not standardized (Wallace et al., 2010; Finnerty et al., 2017): it can be performed either in long (Barbier et al., 2004) or short axis (Blehar, Dickman, et al., 2009) and either in B-mode or M-mode, even though the best approach seems to be *sub-xiphoid* transabdominal long axis in B-mode (Finnerty et al., 2017). Second, concerning the US assessment itself, the most common technical problems that makes this methodology highly operator-dependent (Mesin, Pasquero, and Roatta, 2019) and susceptible to measurement errors (Townsend et al., 2015) are, on one hand, related to displacements, deformations and rotations of IVC during respiratory activity (Blehar, Resop, et al., 2012), which make difficult to keep track of the central axis (i.e., the real diameter). On the other hand, they are related to the high irregularity of the IVC shape, which makes difficult, if not impossible, the extraction of a single representative diameter (Pasquero et al., 2015; Mesin, Pasquero, Albani, et al., 2015). Those are likely the reasons why such methodology, despite its advantages, it is not among the top suggestions when speaking of FR (Monnet and J. L. Teboul, 2018; Shi et al., 2020) and its accuracy in estimating CVP or RAP is only modest (Uthoff et al., 2012; Bouzat et al., 2014; Magnino et al., 2017).

Nevertheless, some attempts were made to circumvent such limitations. For instance, two semi-automatic edge tracking algorithms were recently developed that work on continuous B-mode US video recordings, delineating IVC edges and tracking vein displacements and deformations: the first algorithm was designed to work on long axis acquisition and, by tracking *anteroposterior* displacements of IVC, to assist the operator to choose the best M-line (Mesin, Pasquero, Albani, et al., 2015); the other, was designed more recently and it is instead dedicated only to short axis acquisitions (Mesin, Pasquero, and Roatta, 2020). The long axis algorithm was subsequently improved to compute

Physiological determinant	Condition affecting IVC ultrasound reliability for FR	Cause of inaccuracy for FR	Type of inaccuracy for FR
Ventilator settings	1. Mechanical ventilation with high PEEP and/or low tidal volumes	Larger IVC size, potentially with systemic venous congestion and low respiratory variations, but coexisting with FR	FN
Patient's inspiratory efforts	2. Assisted ventilation modalities, NIV, CPAP	Spontaneous breathing activity makes IVC variation unpredictable	FP and FN
	3. Varying respiratory pattern in spontaneous breathing	Significant inspiratory effort, producing markedly negative intrathoracic pressures may induce IVCc in absence of FR	FP
		Shallow breathing, with small intrathoracic pressure changes, may induce absence of IVCc in presence of FR	FN
Lung hyperinflation	4. Asthma/COPD exacerbation	Lung hyperinflation and auto-PEEP simultaneously reduce venous return and induce IVC distension: this may mimic absence of FR	FN
		Forced expiration ("abdominal breathing" causing expiratory collapse) may mimic IVCc	FP
Cardiac conditions impeding venous return	5. Chronic RV dysfunction, severe TR	Chronic enlargement of IVC and reduced IVCc may erroneously rule out FR	FN
	6. RV myocardial infarction	RV dilatation and systemic venous congestion (large IVC) may be associated with FR	FN
	7. Cardiac tamponade	Marked venous return hindrance: fluid challenge may be a beneficial haemodynamic intervention despite IVC plethora	FN
Increased abdominal pressure	8. Intra-abdominal hypertension	Smaller IVC size, IVCd or IVCc abolition (depending on type respiration/ventilation mode)	FP and FN
Other factors	9. Local mechanical factors	Venous return hindrance, IVC dilatation (stenosis, thrombosis)	FN
		IVC compression (masses)	FP
		Hindrance to IVC size change (ECMO cannulae, cava filters)	FN
	10. Patients with pronounced IVC inspiratory lateral displacement	Migration of IVC imaging plane, false inspiratory size reduction	FP

Figure 1.12: **Pathological conditions affecting Inferior Vena Cava diameter (IVCd) reliability to predict Fluid Responsiveness (FR).** The pathophysiological determinants are listed along with the cause of inaccuracy for FR prediction and the type of error they lead to. False Negative (FN); False Positive (FP); right ventricle (RV); Positive End Expiratory Pressure (PEEP); non-Invasive ventilation (NIV); Continuous Positive Airway Pressure (CPAP); Inferior Vena Cava *collapsibility* (IVCc); Inferior Vena Cava *distensibility* (IVCd); Chronic Obstructive Pulmonary Disease (COPD); tricuspid regurgitation (TR); Extracorporeal Membrane Oxygenation (ECMO). Reprint from (Via et al., 2016).

the diameter of different sections orthogonal to the vein and to provide an estimation of pulsatility which is averaged across sections and respiratory cycles (Mesin, Pasquero, and Roatta, 2019): these advances made the semi-automatic estimate of CI more repeatable than those obtained manually by M-mode, in terms of different respiratory cycles, different sections along the longitudinal axis, different experimental sessions and different operators (Mesin, Giovinazzo, et al., 2019). Moreover, the method was also successfully applied to estimate RAP (Mesin, Albani, et al., 2019; Albani et al., 2020) and to automatically classify patients based on their volaemic status (Mesin, Roatta, et al., 2020), in other words predicting their FR.

Clearly, semi-automatic or automatic edge tracking algorithms made a step towards the standardization of US assessment of respirophasic variation of IVCd but still they need to be integrated in the software of US machines in order to start collecting more evidence of their performance, a necessary step before being included in clinical practice.

Concerning semi-automatic image segmentation algorithms applied to US B-mode video recordings of IVC, as the ones just described above, a pioneer work from Nakamura and co-workers (Nakamura et al., 2013) is worth to be mentioned (Nakamura et al., 2013; Folino et al., 2017): they reported, for the first time, that oscillations of IVCd are not only due to respiratory activity but also include faster, superimposed oscillations due to cardiac activity (Nakamura et al., 2013), likely too small to be exploited by manual tracking. They developed a raw, but valid algorithm, based on Snakes, to delineate and track the edge of IVC in continuous short-axis B-mode video recordings, and to analyse it approximating by an ellipse: this allowed them to isolate the *cardiac* pulsatility of IVCd from the *respiratory* pulsatility (i.e., respirophasic variation), given their different frequency content and to suggest that *cardiac* pulsatility of IVCd could be more reliable than the *respiratory* one (Nakamura et al., 2013; Folino et al., 2017), given the inherent high variability of SB respiratory effort (described previously in this Section) and the hypothesis that the effect of the heartbeat is about constant. The authors therefore proposed a novel index based on the cardiac pulsatility of IVCd, termed Cardiac Caval Index (CCI), and subsequently tested its accuracy to classify patients, based on their volaemic status, with encouraging results (Sonoo et al., 2015).

The two investigations from Nakamura and co-workers (Nakamura et al., 2013; Sonoo et al., 2015) paved the way for the decomposition of oscillations of IVCd time series into its two main components: respiratory and cardiac, both described by their respective *collapsibility* index, namely Respiratory Caval Index (RCI) and Cardiac Caval Index (CCI) (Sonoo et al., 2015). As mentioned, these indexes, together with CI, were isolated and then analysed, also by means of the more recent semi-automatic edge tracking algorithms, developed by Mesin and co-workers (Mesin, Pasquero, Albani, et al., 2015; Mesin, Pasquero, and Roatta, 2019; Mesin, Giovinazzo, et al., 2019; Mesin, Roatta, et al., 2020). In particular, in the study focused on repeatability (Mesin, Giovinazzo, et al., 2019), aside of comparing semi-automatic CI with manual CI, the authors included in the comparison also RCI and CCI, reporting, as expected, a lower variability among experimental sessions, in terms of Coefficient

of Variation (CoV) and of CCI compared to RCI but, surprisingly, not to semi-automatic CI; two reasons may explain this result: first, only the variability over different subjects and measurement sessions were studied, while the actual CCI variability over time has never been evaluated, second, the *cardiac* pulsatility may still be affected by a respiratory modulation, as apparent from published recordings (Mesin, Giovinazzo, et al., 2019; Mesin, Roatta, et al., 2020) and confirmed in preliminary observations.

Finally, in a later study by Mesin and co-workers (Mesin, Roatta, et al., 2020), several classifiers of FR using several combinations of CI, RCI and CCI were tested: the most accurate classifier turned out to be one in which CCI was a fundamental parameter, supporting further investigations aimed at delineating the significance and clinical role of CCI, particularly in the field of FR (Nakamura et al., 2013; Sonoo et al., 2015).

On this basis, during the last part of this Doctoral project, I aimed at investigating the potential of the aforementioned IVCd indexes derived by semi-automatic algorithm (Mesin, Pasquero, and Roatta, 2019), in particular addressing the intra-subject (i.e., in time) variability of CI, RCI and CCI and their response to a simulated fluid challenge, as obtained by means of PLR. Indeed, I hypothesized that by improving the signal processing it would be possible to reduce the respiratory modulation of CCI and that CCI and RCI could exhibit a different time course in resting condition and a different response to PLR (paper V).

1.4 Pulse Wave Velocity

During the last two decades, the arterial compartment has been characterized non-invasively also in terms of stiffness. In particular, the propagation velocity of the Pulse Wave (PW), as produced with each heartbeat, was used to get indirect indications about arterial stiffness. Indeed, with each systole, the heart pumps a volume of blood, called Stroke Volume (SV), into the circulation and this creates a pulse (namely a pressure pulse) wave that propagates along arteries with an average speed, called Pulse Wave Velocity (PWV), proportional to the vessel stiffness (Chirinos et al., 2019).

Despite the complex interplay between the fluid dynamic properties of blood and the mechanical properties of vessels, that establishes the propagation velocity of the PWs, a simple mathematical model of such interplay has been developed already at the end of the 19th century by Moens and Koertweg, who proposed what is now called the Moens-Koertweg equation (Tijsseling et al., 2012), linking the square of PWV directly to the Young's elastic modulus (E) and thickness (h) of the tube wall and inversely to the tube inner radius (r) and blood density (ρ):

$$PWV^2 = \frac{Eh}{2r\rho}$$

Later on, Bramwell and Hill (Bramwell et al., 1922) applied this model to arterial physiology and reported the relationship in terms of the ratio between relative change in volume ($\frac{\Delta V}{V}$) and pressure

(ΔP):

$$PWV = \sqrt{\frac{V\Delta P}{\rho \Delta V}} = \sqrt{\frac{1}{\rho D}} = \sqrt{\frac{V}{\rho C}}$$

linking in a more elegant formulation PWV and vessel stiffness, which is simply the inverse of the distensibility (D) which in turn can be considered like a "relative compliance", being defined as $D = \frac{C}{V}$.

During the last decades, central arterial stiffening has been fully recognized as an important consequence of aging, whose side effect is an increase in arterial Pulse Pressure (PP), due to an increasing "reflected wave" phenomena, which can cause primarily systolic hypertension but secondarily also diastolic hypotension, both distinct factors of particular relevance for CV risk (Shirwany et al., 2010); moreover, arterial stiffening has been demonstrated to have also a crucial role in essential and chronic hypertension, as a viscoelastic remodelling process inherent of stressed vessels (Safar, 2018). For these reasons, it has been widely demonstrated that arterial stiffness, either measured by PWV or PP, is an *independent* predictor of CV risk (Safar, 2018; Sequí-Domínguez et al., 2020). Indeed, arterial PWV is attracting a lot of attention from the medical community and several dedicated commercial devices have been already developed (Boutouyrie et al., 2009; Pereira et al., 2015; Milan et al., 2019). All of them are based on the measurement of two quantities: the pulse transit time (Δt) and the pulse transit distance (Δx), whose ratio gives the pulse propagation velocity:

$$PWV = \frac{\Delta x}{\Delta t}$$

Notwithstanding those possibilities to measure non-invasively and with a sufficient accuracy both arterial blood pressure and arterial stiffness, CV diseases are still the world leading cause of deaths accounting alone for about one third of deaths in 2017 (Ritchie et al., 2018), a fact that itself suggests that we are still far away from a comprehensive characterization of the CV system. Indeed, still nowadays clinical exams about CV system health are mostly focused on heart and arterial compartment while venous side remains little considered. As a consequence, this leads to under-sample the high amount of different and complex situations in which the heart, or the whole body from an holistic point-of-view, finds itself working, limiting the probabilities to identify the underlying pathological states. It is in this regard that the characterization of the entire vascular bed becomes relevant: in addition to the arterial compartment the venous compartment needs to be investigated and, to this purpose, better non invasive techniques need to be developed (Gelman, 2008; Funk et al., 2013; Hollmann D Aya et al., 2015; George L. Brengelmann, 2019).

1.4.1 Venous Pulse Wave Velocity

Considering this operational framework, it was the time to blow the dust off an old idea: the venous Pulse Wave Velocity (vPWV). Nowadays we are aware that the arterial PWV turned out to be a gold standard when evaluating arterial stiffness (Section 1.4). At the same time, FR is a growing field in which novel non-invasive techniques are strongly welcomed (Section 1.3). The link among

those two facts comes from few studies, dated back between 1960's and 1970's, in which the authors reported the first measurements of PWV in veins (Mackay et al., 1967; Anliker et al., 1969; Felix Jr. et al., 1971; Nippa et al., 1971; Minten et al., 1983), documenting an almost linear dependence upon venous pressure (Mackay et al., 1967; Anliker et al., 1969; Nippa et al., 1971; Minten et al., 1983) and indicating it as possible early marker of haemorrhage (Felix Jr. et al., 1971).

In support of the use of vPWV as indicator of volaemic status, it is worth remembering that veins host about 70% of the total blood volume (Rothe, 2011). Moreover, PWV depends upon vessel distensibility (Equation 1.4), which in turn depends upon vessel filling with a relationship based on vessel's compliance curve (Figure 1.13). On this basis, it is intuitive to understand that, the higher the volume status, the higher the venous distention (i.e., filling), the higher the venous stiffness and the higher the vPWV. On this basis, vPWV is an haemodynamic parameter theoretically able to reflect the volaemic status of a patient, thus able to predict its FR. Moreover, additional information could be obtained by using vPWV in combination with a dynamic test (Section 1.3.1), e.g., PLR or mini-fluid challenge.

However, after these aforementioned dated studies, vPWV was subsequently abandoned, probably due to the inherent difficulties of the measurement. In fact, vPWV measurement requires that a Pulse Wave must be externally generated in the veins (that is a big difference from arteries!) because a natural pressure pulsatility is missing and when it is present, back propagating from the right atrium, it is often weak and unreliable (Minten et al., 1983). Furthermore, venous pressure is so low that it is significantly affected by variations induced by both respiratory and cardiac activity (Nippa et al., 1971; Minten et al., 1983). All together, these complications produced a relatively high variability of vPWV measures, with a CoV of 14% (Nippa et al., 1971), which is large enough to make the measurement almost useless. Indeed, only two out of five previously mentioned studies have investigated vPWV in humans: one was conducted only on superficial prominent veins, suitable to be digitally compressed/decompressed (Mackay et al., 1967) and the other based on the small back propagated pulsation of the venous flow detected by echo-Doppler at the level of subclavian and femoral veins (Nippa et al., 1971).

Based on this considerations, the first aim of my Doctoral project was to develop a novel non-invasive technique for the accurate measurement of vPWV in humans (patent). To this aim the Pulse Wave was artificially generated by rapid compression of the limb extremity (foot in this case) and detected at a more proximal site at the level of the femoral vein by means of Doppler US. The PW generation was synchronized with respiration, assuring that the PW was propagating during the end of the expiratory phase, which gives the most reproducible ITP level (Section 1.3.4), which in turn, in terms of lungs volume, is referred as functional residual capacity (Folino et al., 2017).

In the first investigation (paper I), three different venous pressure levels at the legs were obtained, by raising the subject trunk, and the corresponding vPWV values were measured. After that study, the experimental set-up was improved by adding the ECG recording, which was exploited for the

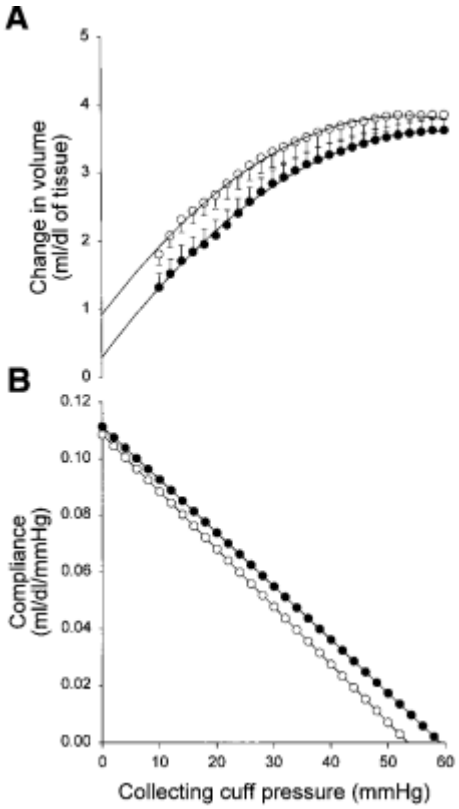

Figure 1.13: **Pressure-Volume and Compliance curves of calf and forearm veins.** Black filled circles represent calf data while empty circles represent forearm data. Solid lines are the second order polynomial regression lines. A) Volume as function of pressure. B) Compliance (first derivative of the curves depicted in A) as function of pressure. Reprint from (Halliwill et al., 1999).

synchronization of the PW generation with the cardiac activity, in order to avoid any confounding effect due to the possible presence of a cardiac pulsatility in the venous blood flow, which can drastically affect the exact identification of the PW passage.

Then, vPWV was investigated also on the upper limb (paper II), therefore compressing the hand and detecting the PW passage at the level of the Basilic Vein (BV), aiming to primarily assess whether and to what extent vPWV responds to a simulated fluid challenge, as obtained by PLR and, secondly, to get an indication about its reproducibility in terms of response to a subsequent second PLR. The relevant results obtained in these first two studies were included in a review about applications to clinical settings of Intermittent Pneumatic Compression (IPC) devices, like the one exploited for the generation of venous PWs.

Finally, the focus moved to the design of an experimental clinical trial to test vPWV potential. However, before doing that it was mandatory to develop a portable, preferably embedded, compulsory electrically safe, measurement system: the solution was to exploit the potentialities offered by the single board computer Raspberry Pi and to integrate all the necessary hardware into a small custom-made box, exploiting compressed air line, widespread in clinical settings, to generate the compression. Finally, this innovative device was validated by performing a small experimental series (four subjects) and comparing the results with those obtained by the previously used bench instrumentation (paper IV).

Chapter 2

Technical notes on haemodynamic measurements

Ultrasound (US)s have been, and still, are, widely used in literature to investigate central and peripheral haemodynamics, in particular for the evaluation of both vessels size, by means of either B-mode or M-mode imaging, and blood flow, by means of Doppler. Such US based techniques, aside of being a research tool, are extremely widespread in clinical settings (Aldrich, 2007) thus, any improvement or novel application related to them can profoundly affect clinical practice (Golemati et al., 2022). In this Doctoral project, US techniques were exploited first to measure non-invasively the vPWV, by means of Doppler US, and subsequently to assess IVCd respirophasic variations, by means of B-mode imaging. Therefore, an overview about the working principles of such US based techniques is summarized in the next paragraphs.

A different way to look non-invasively at the tissue haemodynamics is using NIRS: such measurement, unlike the US, allows to investigate solely a small sample volume, about few cubic centimetres, and gives a quantification of the whole sample volume oxygenation, quantifying the oxygenated and de-oxygenated haemoglobin + myoglobin content (NIRS doesn't distinguish between haemoglobin and myoglobin) (Barstow, 2019), Oxyhaemoglobin (O_2Hb) + Oxymyoglobin (O_2Mb) and Deoxyhaemoglobin (HHb) + Deoxymyoglobin (HMb), respectively. On this basis, NIRS has been extensively used in literature to investigate muscle haemodynamics both at rest and during exercises (Barstow, 2019). In general the NIRS signals have always been considered unaffected by large vessels, in particular large veins. However, this statement, after its theoretical postulation in 1994 by Mancini and collegues (Mancini et al., 1994), has surprisingly never been tested *in vivo*; therefore, in this Doctoral project, NIRS and Doppler were employed together in order to evaluate whether or not the NIRS signal can be affected by large veins. As done for the US based technique, an overview of the NIRS functional principles is briefly summarized in paragraphs.

2.1 Ultrasound (US)

US waves are generated by applying alternating current to piezoelectric crystals embedded in the probe, which works as transducer. The result is a mechanical wave (otherwise termed pressure wave) which is transmitted to the skin and then into the body. US waves propagate through tissue and are scattered by variations in acoustic impedance, and absorbed. The scattered waves propagate back and are detected by the transducer, i.e., the probe. Taken together, absorption and scattering result in gradual attenuation of the signal as it travels to deeper layers of tissue.

2.1.1 US imaging

A representation of the spatial distribution of the structures over which the US has been reflected is performed by analysing the amplitude of the echoed waves, thus getting information about anatomical distances and size of the underlying tissues and organs. More technical details about US beamforming techniques, related decodification methods, and probes design (Demi, 2018) are beyond the scope of this manuscript and are not strictly needed to understand the implications related to the different US-based methodology employed in this Doctoral thesis. It is enough to know that an US probe is composed by a linear array (i.e., 1D) of piezoelectric elements, which work both as emitters and as sensors. With this regard, one dimension of the B-mode US image (width, for instance) corresponds to the linear array of piezoelectric elements and the time delay with which the US pulses return to the probe, through reflection, corresponds to the second image dimension (depth, for instance). Finally, the grey level of pixels is proportional to the intensity of the reflected US pulse.

2.1.2 Doppler US velocimetry

The quantification of blood flow velocity is possible exploiting a secondary effect of US elastic collision, the Doppler effect: it is a notorious effect that is often explained with the common situation of a moving car equipped with a siren, whose sound frequency is perceived differently by listeners depending on the mutual velocity of the car with respect to the listeners. Indeed, a big difference is perceived if trivially the velocity sign changes, i.e., if the car is approaching or moving away. This relationship between frequency and movement can be exploited by medical US where blood is moving and the listener is the US probe (which in this case plays also the role of USs generator). Of note, among the blood constituents, red blood cells and their clumps (i.e., rouleaoux), play a major role in reflecting US waves. In this way it is possible to compute the blood flow velocity from which, once the vessel size is measured, it is easily computed the blood flow, that is a volumetric flow rate:

$$\text{Blood flow } (cm^3/s) = \text{vessel area } (cm^2) * \text{mean blood velocity } (cm/s)$$

For the purpose of this project, the quantification of blood flow was never necessary. Indeed, to measure vPWV it was sufficient to record the mean velocity profile of the blood. To measure blood

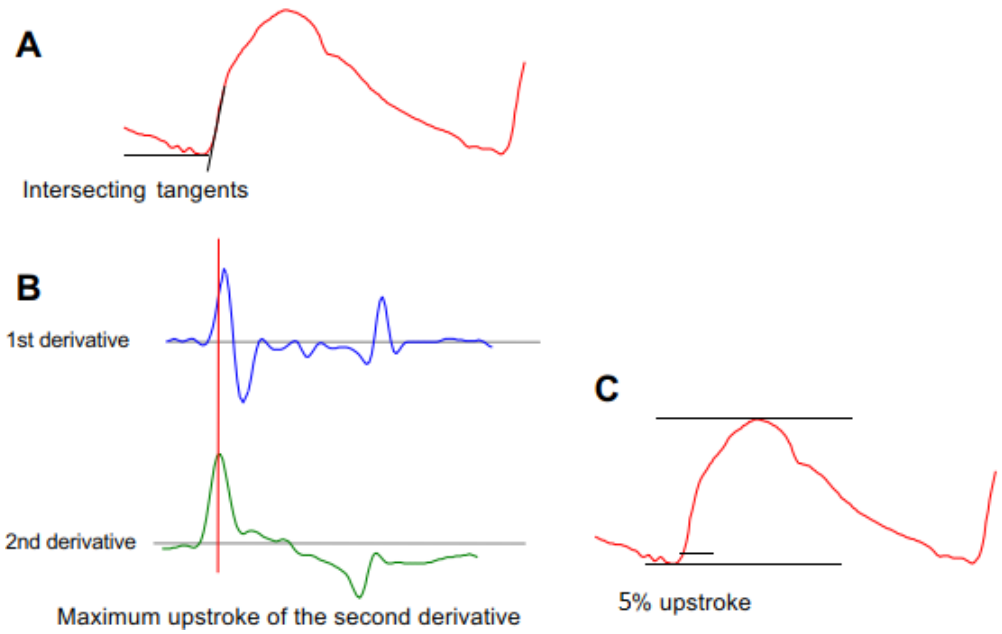

Figure 2.1: **Algorithm for identifying the footprint of the Pulse Wave (PW).** Three different approaches are represented. A) The footprint is identified as the intersecting point among the two lines, one tangent to baseline and the other tangent to the rasing edge. B) The footprint is identified as the maximum of the second derivative of the PW. C) The footprint is identified as the point, on the raising edge, at which the PW cross an arbitrary threshold, usually expressed as percentage of the difference between peak and baseline values. Reprinted from (Boutouyrie et al., 2009).

velocity the Doppler technique analyses the frequency shift of back scattered US waves, which is dependent on the velocity of the moving reflectors (i.e., red blood cells) within the vessel, as stated by the Doppler equation:

$$f_d = \frac{2F_o v \cos(\theta)}{c}$$

Where: (f_d) Doppler shift; (F_o) transmitted frequency; (v) reflector velocity; (θ) insonation angle between US beam and velocity vector, that is usually approximated by the angle of the probe relative to the skin; (c) velocity of US in tissue (≈ 1540 m/s). In US imaging, the blood is moving relative to the US transducer, so when an US wave is transmitted into the body, it is back scattered with a change in its frequency by all the moving cells in the insonated area. The received signal represents a spectrum of velocities, being the sum of contributions and therefore it is analysed in the frequency domain by means of a Time-Frequency representation. Of note, during the time-frequency transformation the Doppler shift signal is windowed and the resulting sampling interval in the time-frequency plane is therefore decreased, by a fraction equals to the window length: this obviously affects the time resolution of the mean velocity profile computed on the time-frequency representation, which in turn affects the time resolution of the footprint identification on the mean velocity profile. Concerning specifically the footprint identification on the mean velocity waveform of a venous PW, three methods have been tested on experimental data, during this Doctoral project, but only one was found to be suitable for being applied to the velocimetric waveforms recorded from the venous blood stream. In Figure 2.1 the three most common methods used in literature for footprint identification (on arterial

PW waveforms) are depicted, along with their corresponding explanation. Once dealing with venous flow, the signal-to-noise ratio of Doppler-shift can be sometimes really low, mostly due to the low signal amplitude from the venous flow rather than due to an high noise amplitude, which in turn causes a low signal-to-noise ratio in the corresponding mean velocity waveform. This made the application of the derivative method (Figure 2.1B) unreliable, since the operation of derivative tends to amplify the noise. Moreover, the venous flow is characterized by a high inter-subject variability, to the point that it can be either pulsatile or about constant. Again, this characteristic drastically affects the footprint identification, in particular the tangents method (Figure 2.1A), since the line tangent to baseline can have different orientations depending on basal flow, particularly on the time of arrival of the exogenous PW with respect to basal flow, thereby affecting the footprint identification. On this basis, the threshold method, although it doesn't take into account the shape of the PW, is more robust again these sources of variability and for this reason it was the elective choice when dealing with footprint identification on venous PW, as necessary for vPWV measurements.

2.2 Near Infrared Spectroscopy (NIRS)

NIRS is a quite recent technology, which allows to measure haemodynamic changes of muscle, brain, and other tissues (Wolf et al., 2007; Yu et al., 2018; Grassi et al., 2016; Barstow, 2019) in a non-invasive way. Two physical principles are the basis of NIRS measurement: (1) substances and molecules have a characteristic absorbance spectrum; and (2) biological tissues are relatively transparent to light in the near infrared region of the spectrum.

2.2.1 Tissue oxygenation

In the NIR spectrum there are absorbers whose concentration is fixed over time (e.g. skin melanin), and absorbers whose concentration varies with time or with oxygenation status. Three biological compounds show oxygen-dependent absorption spectra in the NIR range of light: Haemoglobin (Hb), Myoglobin (Mb) and cytochrome c oxidase (Grassi et al., 2016; Barstow, 2019). The measurement of these latter compounds provides information on tissue haemodynamic and oxygenation status. The relation between the attenuation of light and the proprieties of the medium through which the light is travelling is described by the Beer-Lambert (BL) law, stating that there is a linear relationship between absorbance and concentration of an absorber of the light. However when light travels through a tissue there are multiple collisions between photons and non-absorbing substances that cause the change of photon direction (scattering effect). The effect of scattering is a net increase of the attenuation measured at a single point, higher than what related to absorption alone. To take into account both phenomena occurring into tissues, the classical Beer-Lambert law is modified as follows (the modified Beer-Lambert law):

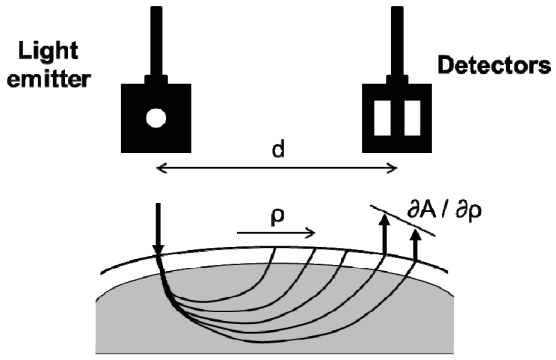

Figure 2.2: **Spatially-Resolved Spectroscopy (SRS)** measures the attenuation of NIR light (A) as a function of the distance between emitter and detectors (d).

$$ln\left[\frac{I_o}{I}\right] = \alpha c d x + K$$

Where: (I_o) light emitted by the emitter; (I) light detected by the detector; (α) extinction coefficient; (c) concentration of light absorber; (d) distance between emitter and detector; (x) differential path-length factor, which increases the distance travelled by photons due to scattering; (K) coefficient for the signal loss due to scattering. Thus by using different wavelengths (typically 3-6), NIRS systems allow to estimate the changes of HHb and O_2Hb in tissues (Wolf et al., 2007; Grassi et al., 2016). However, since the absorption spectra of Hb and Mb are substantially overlapped in the NIR interval of light, measures actually refer to the sum of both of them. Three are the techniques available for NIRS systems, each characterized by how the tissue is illuminated (Wolf et al., 2007):

1. the Continuous Wave (CW), based on constant illumination of the tissue, measures the attenuation of light through the tissues

2. the Frequency-Domain (FD), illuminating the tissue with intensity modulated light, measure both the attenuation and the phase shift of the emerging light

3. the Time-Domain (TD), illuminating the tissue with short pulses of light, detects the amount of time for the propagation of photons through the tissues synchronizing emission and detection windows

When muscle oxygenation is the main focus of the measurement, the fact that the NIR light has to cross the skin and subcutaneous fat in order to reach the target tissue (i.e. underlying skeletal muscle) causes a sensitivity problem that can be particularly noteworthy in conditions in which skin blood flow changes significantly, e.g. during exercise for thermoregulation. A solution to this is represented by the Spatially-Resolved Spectroscopy (SRS) (Suzuki et al., 1999; Messere et al., 2013). SRS is a CW system realized with several (2 or more) detectors located at different distances from the light emitter, that measures the attenuation of light as a function of the source-detector distance (Fig 1) (Suzuki et al., 1999). By analysing the differential signal collected by detectors, SRS is more sensitive

to the changes occurring in deeper tissues, being the contribution of superficial layers a common signal to the detectors and therefore rejected.

The CW NIRS system utilized in this work was a NIRO 200NX (Hamamatsu Photonics, Hamamatsu City, Japan), which simultaneously implements BL and SRS methods. In particular, it provides the following measurements:

1. BL provides a measure of concentration changes, with respect to an arbitrary initial value, in O_2Hb, HHb and Total Haemoglobin (tHb), being the latter the sum of the first two (i.e., tHb = O_2Hb + HHb); these parameters are expressed in μMcm.

2. SRS provides a measure of haemoglobin contents, by the Tissue Haemoglobin Index (THI), and oxygenation, by the Tissue Oxygenation Index (TOI), in the tissue. THI is expressed in arbitrary units and may be reported in relative terms, e.g., as percentage of the initial value. Instead, TOI is expressed in percentage and represents the percentage ratio of O_2Hb to tHb.

Tissue oxygenation can therefore be estimated by O_2Hb, taking into account all the sample volume, cutaneous circulation included, or alternatively by TOI, resulting in a relative measurement of oxygenation but focusing specifically on the deepest portion of the sample volume.

2.2.2 Tissue compliance

The NIRS variables reflecting blood volume are derived either from BL or SRS measurements. The Beer-Lambert blood volume variable provided by our CW NIRS system, i.e., tHb, is no more than the sum of the concentrations of oxy- and deoxy- haemoglobin+myoglobin and it is also affected by changes in the cutaneous circulation. Instead, the SRS blood volume index, i.e., THI, neglects the superficial circulation but expresses only the blood volume variation relative to the initial value.

For both tHb and THI it is possible to build a compliance curve, e.g., recording the corresponding blood volume changes during venous occlusions at different pressure levels. Indeed, reporting the pressure value on one axis and the volume value on the other axis, it is possible to first build a pressure-volume curve (except for an unknown offset affecting volume values) and then, by computing its first derivative, to obtain the compliance curve. It is worth to notice than any offset, related to volume measurements, vanishes with the derivative operation. In general, the measured compliance results from the sum of the compliances of the different tissues and organs included in the NIRS sample volume, but, considering that veins have a much bigger compliance than other vessels or other tissues in general, it is reasonable to approximate the measured compliance to the local venous compliance.

Finally, it is worth to remember that NIRS signals, and therefore the derived compliance, have always been considered to be dependent only on changes in microcirculation and small vessels, since the large amount of blood contained in large vessels would completely absorb the NIR light and prevent back-scattering (Mancini et al., 1994); however, the recordings collected in our investigation

challenge this dogma, evidencing that the presence of a large vein within the NIRS sample volume can profoundly affect the measurement (paper VI).

Chapter 3

Aims of the Thesis

3.1 General aims

My PhD activity was oriented to the investigation of the venous function. In particular, the attention was oriented to the veins mechanical characteristics and behavior as a mean to non-invasively infer about the volaemic status of a patient, addressing in particular:

I. the development of a novel non-invasive technique for the measurement of Pulse Wave Velocity in human veins (patent) and its following characterization in response to changes in venous pressure (paper I);

II. the sensitivity of venous Pulse Wave Velocity in response to a mild blood volume increase induced by Passive Leg Raising (paper II);

III. the revision of the scientific literature about the therapeutic and diagnostic applications of intermittent mechanical pressure stimuli on a person's body, like the one used to generate the venous Pulse Wave (paper III);

IV. the development of a compact and portable device for the measurement of venous Pulse Wave Velocity in hospital wards (paper IV);

V. the study of Inferior Vena Cava (IVC) pulsatility by edge tracking, in particular about its inherent cardiac component, with the aim to improve the Cardiac Caval Index (CCI) and to characterize its potential usefulness as marker of FR (paper V);

VI. the investigation of the actual influence of large veins on Near infrared spectroscopy assessment of local haemodynamic (paper VI).

VII. the revision of the scientific literature about automated edge tracking methods applied to US medical imaging, for the detection of phasic changes in vessels size (paper VII).

3.2 Summary of papers

Paper I: Objective assessment of vPWV in healthy humans

Central or peripheral venous pressure and volume status are relevant parameters for the characterization of a patient's haemodynamic condition; however, their invasive assessment is affected by various risks while non-invasive approaches provide limited and subjective indications. Here we reconsidered the feasibility of a neglected methodology: the possibility to assess vPWV as a possible indicator of venous pressure.

Approach: In eight healthy volunteers (7 M, 1 F, age 31 ± 9 yr), Pulse Waves were generated in the leg veins by rapid compression of the foot (t_0), synchronously with end-expiratory phase; the PWs were detected at the level of the superficial femoral vein with Doppler US and once footprints (time t_1) of PWs were identified in the Doppler shift signal, vPWV was easily calculated as $\Delta x/(t_1 - t_0)$, with Δx being the distance among generation site and US probe. Changes in leg venous pressure were obtained by raising the trunk from the initial supine position by 30° and 60° and measured as hydrostatic loads.

Results: vPWV was correctly measured in all subjects, with an intra-subjects variability, as expressed by Coefficient of Variation (CoV), of 5.6 ± 2.5 %. On average, vPWV increased from 1.78 ± 0.06 m/s (supine) to 2.26 ± 0.19 m/s (60°) ($p < 0.01$) and exhibited an overall linear relationship with venous pressure, confirming previous findings. Thus, here we provided a proof-of-concept for a new methodology for the non-invasive assessment of vPWV in humans.

Paper II: vPWV variation in response to a simulated fluid challenge in healthy subjects

The vPWV measurement technique was further improved, adding the synchronization of PW generation with cardiac activity (ECG), in addition to respiration, in order to avoid the confounding effect caused by the cardiac pulsatile component in the venous flow, if present. After that, a study about vPWV sensitivity to detect the effect of PLR was performed.

Approach: In fifteen healthy volunteers (7 M, 8 F, age 26 ± 3 yr) venous PWs were elicited by pneumatic compression of the left hand and detected by Doppler US at a proximal site on the Basilic Vein (BV). We also non-invasively measured BV cross-sectional perimeter and Peripheral Venous Pressure (PVP). PLR was performed twice to evaluate reliability of the assessment.

Results: PLR had an overall statistically significant effect on the entire set of variables (MANOVA, $p < 0.05$): vPWV increased from 2.11 ± 0.46 to 2.30 ± 0.47 m/s ($p = 0.01$; average increase: 10 %). This effect was transient and dropped below 5 % after about 3 min. A significant increase was also exhibited by BV size and PVP. In consecutive measurements vPWV showed little intra-subject variability (CoV = 8 %) and good reliability (ICC = 0.87). Finally, the vPWV responses to the two PLRs exhibited good agreement (paired T-test, $p = 0.96$), and moderate reliability (ICC = 0.57). These results demonstrated that vPWV can be non-invasively, objectively and

reliably measured in healthy subjects and that it is adequate to detect small pressure/volume variations, as induced by PLR-from-supine. These characteristics make it suitable for clinical applications, even though possible confounding factors deserve further investigations.

Paper III: Applications of intermittent pneumatic compression for diagnostic and therapeutic purposes

The pneumatic equipment for generating PWs in veins, employed in the first two works, is a direct evolution of a special category of Intermittent Pneumatic Compression (IPC) systems, which enable the full customization of the compressive patterns and a high dynamic response. Indeed, commercial IPC devices are usually designed for single purpose and lack of flexibility, despite their potentialities. In this paper, the results of the research on IPC devices produced in collaboration with Politecnico di Torino (Turin, Italy) are presented. In particular, applications regarding the treatment of the EDV reduction, the investigation of vascular phenomena as *hyperemia*, and the assessment of vPWV are discussed. The outcomes of the research demonstrate that IPC technology can lead to the creation of widely used diagnostic, therapeutic and rehabilitative devices.

Paper IV: A portable device for the measurement of venous Pulse Wave Velocity

In order to start designing clinical trials to test venous Pulse Wave Velocity (vPWV) usefulness as diagnostic haemodynamic parameter, a portable and electrically safe device was necessary. Indeed, bench instrumentation employed in the previous investigations is not suitable for hospital wards. Unfortunately, no device currently exists to serve this purpose. Thus, a portable prototype for the assessment of vPWV is here presented.

Approach: The vPWV portable device is based on the single-board PC Raspberry PI, equipped with A/D acquisition board. It acquires the respiratory and ECG signal as well as the Doppler shift from the US machine, it drives the pneumatic cuff inflation and returns multiple measurements of vPWV, allowing visualization of time-trend and storage of patients data. The device was tested in four healthy volunteers (2M, 2F, age 33 ± 13 yr) during supine position and PLR.

Results: Measurement of vPWV in the Basilic Vein (BV) exhibited a low Coefficient of Variation (3.6 ± 1.1 %) and a significant increase in response to PLR in all subjects, consistent with previous investigations. This compact device makes it possible to carry-out investigations in hospital wards on different patient populations, as necessary to assess the actual clinical potential of vPWV.

Paper V: The Cardiac Caval Index. Improving non-invasive assessment of cardiac *preload*

Regarding volume status assessment, the big central Inferior Vena Cava (IVC) plays a critical role in clinical practice. Indeed, IVC offers a good estimates about cardiac *preload*, particularly

regarding its pulsatility which, in first approximation, can be decomposed in two main components:the respiratory and the cardiac component. The aim of this study was to test whether the IVC cardiac oscillatory component, through its index, i.e., Cardiac Caval Index (CCI), could provide a more stable indicator of FR compared to CI or Respiratory Caval Index (RCI).

Approach: Nine healthy volunteers (7 M, 2 F, age 34 ± 9 yr) underwent long-term monitoring in supine position of IVC, followed by 3 minutes passive leg raising (PLR). CI, RCI, and CCI were extracted from video recordings thanks to semi-automatic edge-tracking and CCI was averaged over each respiratory cycle (aCCI), obtaining a single value for each respiratory cycle, as CI. Cardiac output (CO), mean arterial pressure (MAP) and heart rate (HR) were also recorded during baseline (1 minutes prior to PLR) and PLR (first minute).

Results: In response to PLR, all IVC indices decreased ($p < 0.01$), CO increased by 4 ± 4 % ($p = 0.055$) while HR and MAP did not vary. The Coefficient of Variation (CoV) of aCCI (13 ± 5 %) was lower than that of CI (17 ± 5 %, $p < .01$), RCI (26 ± 7 %, $p < 0.001$) and CCI (25 ± 7%, $P < 0.001$). The mutual correlations in time of the indices were 0.81 (CI-RCI), 0.49 (CI-aCCI) and 0.2 (RCI-aCCI). This study concerning long-term IVC monitoring by automated edge-tracking allowed us to evidence that 1) respiratory and averaged cardiac pulsatility components are uncorrelated and thus carry different information and 2) the new index aCCI, exhibiting the lowest CoV while maintaining good sensitivity to blood volume changes, may overcome the poor reliability of CI and RCI.

Paper VI: Evidence that large vessels do affect Near Infrared Spectroscopy

Among the few non-invasive techniques used to characterize vascular compliance *in vivo*, there is Near Infrared Spectroscopy (NIRS), which allow a relative quantification of blood volume changes through a quantification of the absorbed NIR light by oxy- and deoxy- haemoglobin. Usually, the influence of large vessels on Near Infrared Spectroscopy (NIRS) measurement is considered negligible but this statement was never demonstrated *in vivo*. Aim of this study is to test the hypothesis that changes in the vessel size, by varying the amount of absorbed NIR light, could profoundly affect NIRS blood volume indexes.

Approach: Changes in Total Haemoglobin (tHb) and in Tissue Haemoglobin Index (THI) were monitored over the Basilic Vein (BV) and over the biceps muscle belly, in 11 subjects (7 M, 4 F, age 31 ± 8 yr) with simultaneous ultrasound monitoring of BV size. The arm was subjected to venous occlusion, according to two pressure profiles: slow (from 0 to 60 mmHg in 135 s) and rapid (0 to 40 mmHg maintained for 30s). Results: Both tHb and THI detected a larger blood volume increase (1.7 to 4-fold; $p < 0.01$) and exhibited a faster increase and a greater convexity on the BV than on the muscle. In addition, signals from BV exhibited higher correlation with changes in BV size than from muscle ($r = 0.91$ vs 0.55, $p < 0.001$ for THI). A collection of individual relevant recordings, in different experimental scenarios, was also included. These

results challenge the long-standing belief that the NIRS measurement is unaffected by large vessels and support the concept that large veins may be a major determinant of blood volume changes in multiple experimental conditions.

Paper VII: Assessment of phasic changes of vascular size by automated edge tracking - State of the art and clinical perspectives

Assessment of vascular size and of its phasic changes by US is important for the management of many clinical conditions, aside of studying their physiological determinants. However, lack of standardization and sub-optimal intra- and inter- operator reproducibility limit the use of these techniques. To overcome these limitations, semi-automatic edge tracking algorithms, or more generally image-processing algorithms. were developed in order to quantify phasic vascular deformation and displacement, by tracking wall movements, either in long or in short axis. In this paper, present and future clinical applications are discussed, while prospective studies will define the utility of these methods in different settings, vessels and clinical conditions.

Chapter 4

Discussion

4.1 Venous Pulse Wave Velocity

The beginning of my PhD activity regarded the development of a measurement set-up for vPWV, which, afterwards, was employed to measure vPWV in the femoral vein and to characterized its response to changes in local venous pressure, as obtained by raising the trunk from supine position (0°) to two different levels (30° and 60°) (paper I). The results substantially confirmed previous observations, which reported i) a strong linear correlation of vPWV with venous pressure (Mackay et al., 1967; Anliker et al., 1969; Minten et al., 1983), ii) vPWV values in the range of 1-3 m/s (Anliker et al., 1969; Nippa et al., 1971; Felix Jr. et al., 1971; Minten et al., 1983).

Among the few aforementioned previous studies, only two were conducted on humans (Mackay et al., 1967; Nippa et al., 1971), limiting the chances to make a comparison with our results. In particular, one study reported only vPWV measurements during venous occlusion on superficial veins (Mackay et al., 1967), therefore obtaining high venous pressures (20-80 mmHg) and high vPWV values (5-15 m/s), which obviously have a limited meaning when compared to our results. The other study, instead, reported an average vPWV value of 2.05 ± 0.49 m/s on various arm's veins during supine position (Nippa et al., 1971), slightly higher but still in line with our findings, since our values were measured on leg's veins. The only investigation conducted on femoral vein was instead on anaesthetised dogs, reporting an average value of 1.3 m/s (Felix Jr. et al., 1971), slightly lower than ours.

Of note, our measurement technique, being based on the time elapsed between the generation of PW and the detection of its passage, it is inherently affected by an unknown time delay between the trigger used to inflate the cuff, which essentially marks the moment of generation of the electric signal used to activate the relay of the inflation valve, and the generation of PW, i.e., the actual inflation of the cuff. This delay was supposed to be constant both in intra- and inter-subject measurements, with the consequence that it can be neglected when considering vPWV variations following a stimulus, but it cannot be overlooked when dealing with absolute values of vPWV. Indeed, a measurement technique

based on a differential detection of the passage of PW would be more accurate in measuring the *true* quantity. However, it would also be more cumbersome and affected by other side effects, one above all, the increased relative errors in the measurements of both transit time (Δt) and transit distance (Δx), from which PWV is computed.

In addition to this, it is worth to remember that vPWV as measured by the present methodology could be slightly overestimated, given that the PW travels over a flowing blood: indeed, it was suggested to correct the measured vPWV value by subtracting the mean blood flow velocity (Nippa et al., 1971); nonetheless, this correction seems to not affect the validity of the results (Boutouyrie et al., 2009; Sequí-Domínguez et al., 2020). On the other hand, regarding specifically the technique employed in our investigations to detect the PW passage, namely the Doppler US, it has been shown that its agreement with applanation tonometry is excellent, therefore the two detection techniques can be considered equally precise and consequently interchangeable (Calabia et al., 2011; Jiang et al., 2008). In the end, our measurement set-up, maximizing the travelling distance of PW and being synchronized with the respiratory activity that significantly affects venous pressure and consequently vPWV (Nippa et al., 1971; Minten et al., 1983), reached a good repeatability of the measurements, as expressed by a low CoV, about 6 %, which is less than half of the one obtained previously (14 %) by Nippa and co-workers, in humans with a similar approach (Nippa et al., 1971).

Having proven that vPWV is roughly proportional to venous pressure in a quite large venous pressure range, the next aim was to assess the sensitivity of the measurement to the more clinically relevant situation of a volume challenge. The rationale of this further investigation was supported by one of the previously mentioned studies about vPWV, in which the authors suggested vPWV as a possible early marker of blood loss (Felix Jr. et al., 1971). Moreover, the response to Fluid Overload (FO), i.e., the opposite of blood loss, was also investigated in one previous study, where authors reported a higher vPWV value compared to baseline, suggesting that the technique could be adequate to detect volume changes (Minten et al., 1983). Thus, in order to non-invasively assess the response of vPWV to a variation of blood volume, a standardized postural manoeuvre was exploited, i.e., Passive Leg Raising (already explained in Section 1.3.3), while measuring vPWV on the upper limb, in particular on the Basilic Vein (BV). The PLR manoeuvre was performed starting from the supine position, instead of starting from semirecumbent, because of technical constrains due to vPWV measurements involving the upper limb. For this reason, the amount of simulated FC is supposed to be smaller than the theoretical 300 mL (Monnet and J.-L. Teboul, 2015), a fact supported also by the decreased accuracy to predict FR (Monnet, P. Marik, et al., 2016; Lakhal, Ehrmann, Runge, et al., 2010). In spite of the low amount of displaced volume, vPWV varied significantly from 2.1 m/s (supine) to 2.3 m/s (PLR) and ten subjects out of fifteen shown at least a 5 % increase. The repeatability of the vPWV measurements was confirmed to be good by a low CoV (8 %) and by a high ICC (0.87), as expected.

A secondary outcome of this study (paper II) concerned the physiological response to PLR. In

particular, based on experimental results, it has been hypothesized the presence of a possible inhibition of the sympathetically mediated venoconstriction, triggered by PLR. This hypothesis was based on the observation of a diminished vPWV and PVP mean baseline values after PLR compared to the ones before PLR. Instead, BV cross-sectional perimeter was unchanged, suggesting that the volume displacement caused by the manoeuvre was completely reverted. Regarding the vPWV response to the second PLR, it is worth to notice that the percentage increment (i.e., ΔvPWV) was of the same intensity, on average, irrespective of the baseline value and a relevant response (i.e., ΔvPWV > 5 %) was preserved in 8 out of 10 subjects. Finally, more significantly, vPWV increase during PLR remained above 5 % for 3 minutes (on average), resulting in an apparent much slower decrease compared to that declared for CO, whose response to PLR is supposed to last 1 minute. Thus, the vPWV measurement appears to be a useful tool to describe the time course of PVP during volume challenges and it candidates for relevant clinical applications such as dialysis.

Although the measurement set-up employed in the second study about vPWV (paper II) seems similar to the one presented before (paper I), the methodological improvement was significant: besides the cardiac synchronization, a novel algorithm was developed for the automatic identification of PW's footprint, obtaining a totally operator-free technique; in addition, it is computationally less expensive compared to the previous one, since it analyses the Doppler-shift signal in time domain, instead of frequency domain. Concerning the cardiac synchronization, it is worth to mention that it is not always useful, but in case of a strong natural pulsatility in the venous flow, the identification of the footprint can be drastically affected and disturbed by this pulsatility of venous blood flow. This was also observed in the first set-up, in which an arbitrary delay before the delivery of the PW was sometimes manually inserted in order to attenuate this confounding effect (paper I). Similarly, in the actual set-up the delay is set with respect to the heartbeat, as identified by R-wave in the ECG recording. For these reasons, the developed techniques for vPWV assessment allowed a *quasi* real-time and operator-free measurement, except for probe positioning and distance measurement, increasing significantly the objectivity of the assessment. As merit, the present technique was included in a recent review about IPC devices (paper III).

At this stage, it was necessary to start thinking to embed the whole experimental set-up in a single device to perform vPWV measurements in hospital wards. As a first step, the automatic detection of the end of expiratory phase was implemented, by means of a chest band equipped with strain gauge, designed to works within the respiratory frequency band. Regarding the device components, the choice was oriented towards less expensive electronics, integrated in a single board computer, i.e., Raspberry Pi, used as both control unit and storage system, which can be easily managed by a GUI hosted on a separate personal computer, through wireless connection. Moreover, the device is powered by a battery, thereby it is floating and electrically safe. After proper testing, the device was validated by measuring vPWV on the arm of 4 subjects, during supine position and in response to PLR. Results confirmed the good repeatability of vPWV measurements and the potential clinical applicability of

the present device which is finally ready to be employed in patients (paper IV).

4.2 Inferior Vena Cava pulsatility

In parallel, in order to explore different possibilities to assess the volaemic status of patients and to deepen the knowledge about the physiological response to PLR, a common US-based technique for Fluid Responsiveness (FR) prediction was studied, namely the Inferior Vena Cava diameter (IVCd) respirophasic variation (paper V). This study included a long-term continuous monitoring of IVCd and exploited an innovative semi-automatic edge-tracking algorithm that allowed to extract Inferior Vena Cava *collapsibility* (IVCc) indexes as time-series.

The major outcome of the study concerned the cardiac oscillatory component of IVC pulsatility, in particular the optimization of its corresponding index, i.e., Cardiac Caval Index (CCI), which was averaged over single respiratory cycles in order to diminish its inherent respiratory modulation. The resulting index, termed averaged Cardiac Caval Index (aCCI), exhibited the lowest variability over time compared to the other IVCc indexes, while its response to PLR was still significant and sharp. Thanks to this investigation it was possible to implement a more reliable IVCc index that, being based on cardiac pulsatility instead of respiratory pulsatility, is no longer affected by the inherent variability of the respiratory effort (see Section 1.3.4).

A secondary outcome of this study was the description of the IVCc index based only on the respiratory variation of IVCd, i.e., Respiratory Caval Index (RCI). It was demonstrated that those two indexes, i.e., aCCI and RCI, account each one for about half of the commonly used IVCc index, i.e., the CI, thereby suggesting that the cardiac oscillatory component of IVC pulsatility weights more than previously thought in the total variation exhibited by IVCd during a respiratory cycle. Moreover, RCI and aCCI were uncorrelated, both during baseline and in response to PLR, suggesting that they carry different information, with CCI possibly revealing also specific changes in cardiac function (e.g. inotropism, valve efficiency, etc.).

It is worth to mention that, although both IVCd variations and vPWV are techniques useful to assess FR, they are not mutually exclusive but can be used alternatively depending on the clinical needs. In fact, IVCd monitoring can be achieved rapidly, since it only requires an US machine, thereby being suitable for situations in which time is important. Alternatively, vPWV can be more suitable in those situations that require a long-term monitoring, in which IVCd monitoring can be inadequate. Moreover, vPWV gives information about peripheral venous compartments while IVC gives information about the central venous compartment: in principle, a combined use of these two techniques can offer a more complete description of the venous district than if used singularly. With this regard, further investigations comparing the outcome of these two technique in response to PLR and/or in classifying patient volaemic status, deserve to be carried out. In particular, CCI potentialities remain entirely to be explored.

4.3 Physiological response to Passive Leg Raising

Finally, a brief comment about the physiological response to PLR. In the present study of IVC, a volume-clamp based photoplethysmography device to monitor non-invasively CO, MAP and HR was employed. In this way, it was possible to assess the response of these haemodynamic parameters to PLR, showing a transient increase of CO that vanished in about 1 minute from the beginning of PLR, in line with recent guidelines (see Section 1.3.3). However, if the PLR would involve only the Frank-Starling mechanism, the return of CO should be a consequence of returned *preload* to control level (before the end of PLR). Instead, recordings of IVCd and IVCc indexes indicate that the increase in CVP is maintained for the whole duration of PLR (paper V).

Of note, the observed vPWV increase with PLR (paper II) and its slow decrease during the entire duration of the manoeuvre, supports the hypothesis that heart *preload* remained higher (with respect to the baseline value) much longer than 1 minute. Besides the MAP and HR which in the present analysis did not reveal any significant effect, the transient response of CO may be due to a late (more than 30 sec after the beginning of PLR) inhibition of the sympathetically mediated *inotropism* of the heart. This inhibition would explain the decrease of CO in spite of unchanged *preload* during PLR. Basically, a reduced *inotropism* of the heart corresponds to a rightward shift of the cardiac response curve, i.e., towards higher *preload* values (see Section 1.2.1), and it is in line with what hypothesized concerning vPWV response to PLR (paper II).

Further study on healthy subjects will help to fully understand the mechanisms underlying the response to PLR, allowing for a more aware use of this, as trivial as powerful, manoeuvre.

4.4 Non invasive assessment of venous compliance

A third approach to the non-invasive characterization of the venous compartment has been the assessment of venous compliance. This information is particularly relevant when attempting to develop mathematical models of the venous circulation (I supervised two master thesis in biomedical engineering on this topic). Two methodologies were considered for the construction of the volume-pressure curve of individual veins: the US B-mode monitoring of the vessel size (with automatic edge-tracking) and the NIRS monitoring of blood volume changes, whereby local changes in venous pressure can be achieved by proximal venous occlusion at incremental (controlled) cuff pressure levels.

Regarding the latter methodology, the compliance estimated by NIRS represents the summation of the compliance of the different tissues included in the sample volume: with this regard, since arterial compliance is far smaller than venous compliance, and big veins are considered in the literature to not contribute to NIRS signal, their contribution can be neglected so, in first approximation, the measured compliance can be attributed only to small veins, i.e., veins whose diameter is smaller than 1 mm (Mancini et al., 1994), as already explained in Section 2.2. When this measurement of compliance by

means of NIRS was performed simultaneously on two different regions of the arm, for instance one above the muscle belly and one precisely over the BV, the effect of the presence of a large vein within the sample volume of NIRS was evident.

With this regard, a study was conducted to investigate this effect, adding to the present set-up the monitoring of BV cross-sectional area by means of an adapted version of the semi-automatic edge-tracking algorithm employed in previous work on IVC. In this way it was possible to correlate the BV size variation with the blood volume variation measured at both sites, highlighting the influence of BV size on the compliance measured over its path, with respect to the compliance measured over the muscle belly (paper VI). This evidence demonstrated that, contrary to what is usually reported in literature, a careful placement of the NIRS optodes is mandatory to minimize the influence of big vessels, particularly when studying muscles oxygenation and secondarily when estimating venous compliance.

The edge tracking methodology is proving to be very advantageous to automatize and objectively perform measurements that have been carried out manually for a long time. This feature has been exploited in this thesis for the purpose of extracting the cardiac pulsatility of the IVC and for the P-V characterization of limb veins, but the potential applications extend to other regions of the CV system (e.g. arteries) and have implications in many clinical areas, as was briefly presented in a review article (paper VII).

4.5 Conclusions

Through this doctoral project I was able to explore three different approaches to investigate and characterize the condition of the venous compartment: a key player in the setting of the Cardiovascular system. In each of them innovative features were implemented or relevant implications disclosed.

1. A promising index of vascular filling, the venous Pulse Wave Velocity, was reconsidered with substantial methodological improvements, achieving excellent repeatability and sensitivity to blood volume changes.

2. The traditional Ultrasound assessment of the collapsibility of the Inferior Vena Cava was for the first time employed in a long term monitoring and a new formulation of a collapsibility index was proposed to improve repeatability.

3. Working at the non invasive assessment of the capacitance curve of specific venous segments, abundant evidences against a consolidated dogma of NIRS methodology were collected; this dogma, namely that large veins would not affect the NIRS measurement, has been acritically accepted in the literature for more than 20 years.

Each one of these approaches to the investigation of the venous compartment has its own pros and cons, for this reason they all deserve to be better investigated, particularly because little research

has been conducted in patients, as yet. With this regard, the first prototype of a portable device for the venous Pulse Wave Velocity measurement has been developed and validated, which will allow to test the clinical usefulness of this novel haemodynamic parameter in different hospital wards, e.g., in nephrology to monitor the patient volaemic status during dialysis or in ICU to get indications about Fluid Responsiveness. Moreover, thanks to this device it will also be possible to compare the venous Pulse Wave Velocity with the new formulation of Inferior Vena Cava collapsibility index in estimating the patient volaemic status and Fluid Responsiveness.

Finally, future developments will also be directed towards the building of mathematical models of the venous compartment, as accurate as possible, by collecting *in vivo* data about specific venous segments exploiting either NIRS, vPWV or edge-tracking methodologies applied to US imaging.

Acknowledgments

Here we are. I always found acknowledgements pretty foregone (this is trivial to notice, too, sorry) and that's why I used to skip them. However, this time I will try to address all the emotions that came from thinking about whom I owe this achievement. I must recognize that if you can thank your family first and foremost, it means that your life has already been lucky. And of course my life has been. Furthermore, I believe that luck is a big part of anyone's success: so, to you who are still on this earth and to other whose spirit flew away, thank you for being my family! I am sure that this honour (namely, being loved) was not a matter of merits but rather a matter of luck. Definitely, I always felt that this acknowledgment should be extended to cover my whole life: it would sounds trivial, but my existence would have never been possible without your efforts, even though I know that sometimes I used this consideration as a subtle blame. But hey, honestly, who can assert that life's achievements are only joy and satisfaction? Who can intimately affirm to not regret any mistakes made along the path, exalting the notorious commonplace that "mistakes are useful to learn"? I admit, I've never been sure about important choices in my life. I strongly believe that many of them are not even understandable, least of all recognizable as correct or wrong. But for sure, they do have consequences. It's the same in science: I believe I did several mistakes that I not even recognized. This was the major limit, because I deeply know that mistakes identification is the first and most critical step along the way of learning. However, as I said, success is more about being lucky that being smart, or rather learning from our choices. Therefore, I have to admit to myself that this freedom to made mistakes, choosing randomly from a big repository of opportunities, despite it frightened me, it was, and still it is, a gift that keeps on giving and for which I definitely must acknowledge the deterministic role that other people near me, in addition to my family, have played by my side. For this reason, I want to explicitly thank my supervisor Silvestro, who gave me a big opportunity, and whose patience and stoicism will be always inspiring for me. Then, people from the lab, among which Raffaele and Stefano deserves a special mention: for their company and invaluable help that, if not solved the problem, at least mitigated the consequences. Finally, I take this opportunity to spend few words about the last two years. For most of the human being they will be unequivocally associated with COVID-19 pandemic emergency, whose consequences included strong limits to our freedom, of course relevant for my PhD, too. However, about me, these two years will be equally and unequivocally associated with the only important choice in my life that I had never to think about, that is love. And it is precisely in

the name of love that I wish my life keeps on moving, taking care of that intimate corner, where logic is pointless and instinct releases you from the weight of consequences. As my grandmother said once - Leo, only in your mind you are completely free - and now I deeply acknowledge that this freedom is far better when shared with you, my dear Arianna.

In the end, thank you everyone for not leaving me alone, especially during this challenging period of my life.

Bibliography

Albani, Stefano, Bruno Pinamonti, Tatiana Giovinazzo, Marco de Scordilli, Enrico Fabris, Davide Stolfo, Andrea Perkan, Caterina Gregorio, Giulia Barbati, Pietro Geri, Marco Confalonieri, Francesco Lo Giudice, Giovanni D Aquaro, Paolo Pasquero, Massimo Porta, Gianfranco Sinagra, and Luca Mesin (2020). "Accuracy of right atrial pressure estimation using a multi-parameter approach derived from inferior vena cava semi-automated edge-tracking echocardiography: a pilot study in patients with cardiovascular disorders". In: *The International Journal of Cardiovascular Imaging* 36.7, pp. 1213–1225.

Aldrich, John E (2007). "Basic physics of ultrasound imaging". In: *Critical care medicine* 35.5, S131–S137.

Anliker, Max, Michael K Wells, and Eric Ogden (1969). "The Transmission Characteristics of Large and Small Pressure Waves in the Abdominal Vena Cava". In: *IEEE Transactions on Biomedical Engineering* BME-16.4, pp. 262–273.

Ansari, B M, V Zochios, F Falter, and A A Klein (2016). "Physiological controversies and methods used to determine fluid responsiveness: a qualitative systematic review". In: *Anaesthesia* 71.1, pp. 94–105.

Aya, Hollmann D and Maurizio Cecconi (2015). "Can (and should) the venous tone be monitored at the bedside?" In: *Current Opinion in Critical Care* 21.3, pp. 240–244.

Azadian, Moosa, Suyee Win, Amir Abdipour, Carolyn Krystal Kim, and H Bryant Nguyen (2021). "Mortality Benefit From the Passive Leg Raise Maneuver in Guiding Resuscitation of Septic Shock Patients: A Systematic Review and Meta-Analysis of Randomized Trials." eng. In: *Journal of intensive care medicine*, p. 8850666211019713.

Barbier, Christophe, Yann Loubières, Christophe Schmit, Jan Hayon, Jean-Louis Ricôme, François Jardin, and Antoine Vieillard-Baron (2004). "Respiratory changes in inferior vena cava diameter are helpful in predicting fluid responsiveness in ventilated septic patients." eng. In: *Intensive care medicine* 30.9, pp. 1740–1746.

Barstow, Thomas J (2019). "Understanding near infrared spectroscopy and its application to skeletal muscle research." eng. In: *Journal of Applied Physiology* 126.5, pp. 1360–1376.

Beard, Daniel A. and Eric O. Feigl (2011). "Understanding Guyton's venous return curves". In: *American Journal of Physiology - Heart and Circulatory Physiology* 301.3, p. 2007.

Beigel, Roy, Bojan Cercek, Huai Luo, and Robert J Siegel (2013). "Noninvasive Evaluation of Right Atrial Pressure". In: *Journal of the American Society of Echocardiography* 26.9, pp. 1033–1042.

Bentzer, Peter, Donald E. Griesdale, John Boyd, Kelly MacLean, Demetrios Sirounis, and Najib T. Ayas (2016). "Will This Hemodynamically Unstable Patient Respond to a Bolus of Intravenous Fluids?" In: *JAMA* 316.12, pp. 1298–1309.

Berger, David, Per W Moller, Alberto Weber, Andreas Bloch, Stefan Bloechlinger, Matthias Haenggi, Soren Sondergaard, Stephan M Jakob, Sheldon Magder, and Jukka Takala (2016). "Effect of PEEP, blood volume, and inspiratory hold maneuvers on venous return." eng. In: *American journal of physiology. Heart and circulatory physiology* 311.3, H794–806.

Blehar, David J, Eitan Dickman, and Romolo Gaspari (2009). "Identification of congestive heart failure via respiratory variation of inferior vena cava diameter." eng. In: *The American journal of emergency medicine* 27.1, pp. 71–75.

Blehar, David J, Dana Resop, Benjamin Chin, Matthew Dayno, and Romolo Gaspari (2012). "Inferior vena cava displacement during respirophasic ultrasound imaging." eng. In: *Critical ultrasound journal* 4.1, p. 18.

Bortolotti, Perrine, Delphine Colling, Vincent Colas, Benoit Voisin, Florent Dewavrin, Julien Poissy, Patrick Girardie, Maeva Kyheng, Fabienne Saulnier, Raphael Favory, and Sebastien Preau (2018). "Respiratory changes of the inferior vena cava diameter predict fluid responsiveness in spontaneously breathing patients with cardiac arrhythmias". In: *Annals of Intensive Care* 8.1, p. 79.

Boutouyrie, Pierre, Marie Briet, Sebastian Vermeersch, and Bruno Pannier (2009). "Assessment of pulse wave velocity". In: *Artery research* 3.1, pp. 3–8.

Bouzat, Pierre, Guillaume Walther, Thomas Rupp, Patrick Levy, and Samuel Vergès (2014). "Inferior vena cava diameter may be misleading in detecting central venous pressure elevation induced by acute pulmonary hypertension." eng. In: *American journal of respiratory and critical care medicine* 190.2, pp. 233–235.

Bramwell, J Crighton and A V Hill (1922). "Velocity of transmission of the pulse-wave: and elasticity of arteries". In: *The Lancet* 199.5149, pp. 891–892.

Brengelmann, G L (2006). "Counterpoint: The classical Guyton view that mean systemic pressure, right atrial pressure, and venous resistance govern venous return is not correct". In: *Journal of Applied Physiology* 101.5, pp. 1525–1526.

Brengelmann, George L (2016). "Letter to the editor: Why persist in the fallacy that mean systemic pressure drives venous return?" eng. In: *American journal of physiology. Heart and circulatory physiology* 311.5, H1333–H1335.

Brengelmann, George L. (2003). "A critical analysis of the view that right atrial pressure determines venous return". In: *Journal of Applied Physiology* 94.3, pp. 849–859.

Brengelmann, George L. (2019). "Venous return and the physical connection between distribution of segmental pressures and volumes". In: *American Journal of Physiology - Heart and Circulatory Physiology* 317.5, H939–H953.

Calabia, Jordi, Pere Torguet, Maria Garcia, Isabel Garcia, Nadia Martin, Bernat Guasch, Diana Faur, and Martí Vallés (2011). "Doppler ultrasound in the measurement of pulse wave velocity: agreement with the Complior method". eng. In: *Cardiovascular ultrasound* 9.1, p. 13.

Cecconi, Maurizio and Hollman D Aya (2014). "Central venous pressure cannot predict fluid-responsiveness". In: *Evidence Based Medicine* 19.2, 63 LP –63.

Cecconi, Maurizio, Christoph Hofer, Jean-Louis Teboul, Ville Pettila, Erika Wilkman, Zsolt Molnar, Giorgio Della Rocca, Cesar Aldecoa, Antonio Artigas, Sameer Jog, Michael Sander, Claudia Spies, Jean-Yves Lefrant, and Daniel De Backer (2015). "Fluid challenges in intensive care: the FENICE study: A global inception cohort study." eng. In: *Intensive care medicine* 41.9, pp. 1529–1537.

Charalambous, C, T A Barkers, C S Zipitis, I Siddique, R Swindell, R Jackson, and J Benson (2003). "Comparison of peripheral and central venous pressures in critically ill patients". In: *Anaesthesia and Intensive Care* 31.1, pp. 34–39.

Chaves, Renato Carneiro de Freitas, Thiago Domingos Corrêa, Ary Serpa Neto, Bruno de Arruda Bravim, Ricardo Luiz Cordioli, Fabio Tanzillo Moreira, Karina Tavares Timenetsky, and Murillo Santucci Cesar de Assunção (2018). "Assessment of fluid responsiveness in spontaneously breathing patients: a systematic review of literature". In: *Annals of Intensive Care* 8.1, p. 21.

Cherpanath, Thomas G.V., Alexander Hirsch, Bart F. Geerts, Wim K. Lagrand, Mariska M. Leeflang, Marcus J. Schultz, and A. B.Johan Groeneveld (2016). "Predicting fluid responsiveness by passive leg raising: A systematic review and meta-analysis of 23 clinical trials". In: *Critical Care Medicine* 44.5, pp. 981–991.

Chirinos, Julio A., Patrick Segers, Timothy Hughes, and Raymond Townsend (2019). "Large-Artery Stiffness in Health and Disease: JACC State-of-the-Art Review". In: *Journal of the American College of Cardiology* 74.9, pp. 1237–1263.

Chopra, Sahil, Jordan Thompson, Shahab Shahangian, Suman Thapamagar, Dafne Moretta, Chris Gasho, Avi Cohen, H Bryant, and Nguyen Id (2019). "Precision and consistency of the passive leg raising maneuver for determining fluid responsiveness with bioreactance non-invasive cardiac output monitoring in critically ill patients and healthy volunteers". In: 14.9, pp. 1–10.

Clement, R P, J J Vos, and T W L Scheeren (2017). "Minimally invasive cardiac output technologies in the ICU: Putting it all together". In: *Current Opinion in Critical Care* 23.4, pp. 302–309.

Cooke, K., R. Sharvill, S. Sondergaard, and A. Aneman (2018). "Volume responsiveness assessed by passive leg raising and a fluid challenge: a critical review focused on mean systemic filling pressure". In: *Anaesthesia* 73.3, pp. 313–322.

Corl, Keith A., Nader Azab, Mohammed Nayeemuddin, Alexandra Schick, Thomas Lopardo, Fatima Zeba, Gary Phillips, Grayson Baird, Roland C. Merchant, Mitchell M. Levy, Michael Blaivas, and

Adeel Abbasi (2020). "Performance of a 25 percent Inferior Vena Cava Collapsibility in Detecting Fluid Responsiveness When Assessed by Novice Versus Expert Physician Sonologists". In: *Journal of Intensive Care Medicine* 35.12, pp. 1520–1528.

Critchley, Lester A, Anna Lee, and Anthony M.-H. Ho (2010). "A Critical Review of the Ability of Continuous Cardiac Output Monitors to Measure Trends in Cardiac Output". In: *Anesthesia and Analgesia* 111.5.

Curran-Everett, Douglas (2007). "A classic learning opportunity from Arthur Guyton and colleagues (1955): circuit analysis of venous return." eng. In: *Advances in physiology education* 31.2, pp. 129–135.

Dalmau, Rafael (2018). "The "stressed blood volume" revisited". In: *Canadian Journal of Anesthesia/Journal canadien d'anesthésie* 65.9, pp. 1070–1071.

Dalmau, Rafael (2019). "Venous return: a fresh start". In: *American Journal of Physiology-Heart and Circulatory Physiology* 317.5, H1102–H1104.

Das, Saurabh K, Nang S Choupoo, Debasis Pradhan, Priyam Saikia, and Xavier Monnet (2018). "Diagnostic accuracy of inferior vena caval respiratory variation in detecting fluid unresponsiveness: a systematic review and meta-analysis". In: *European Journal of Anaesthesiology* 35.11, pp. 831–839.

De Backer, Daniel and Jean-Louis Vincent (2018). "Should we measure the central venous pressure to guide fluid management? Ten answers to 10 questions." eng. In: *Critical care* 22.1, p. 43.

Demi, Libertario (2018). "Practical Guide to Ultrasound Beam Forming: Beam Pattern and Image Reconstruction Analysis". In: *Applied Sciences* 8.9, p. 1544.

Elwan, Mohammed H, Ashraf Roshdy, Joseph A Reynolds, Eman M Elsharkawy, Salah M Eltahan, and Timothy J Coats (2018). "What is the normal haemodynamic response to passive leg raise? A study of healthy volunteers". In: *Emergency Medicine Journal* 35.9, pp. 544–549.

Ermini, Leonardo, Raffaele Pertusio, Franco Walter, Maffiodo Daniela, De Benedictis Carlo, Ferraresi Carlo, Mesin Luca, Paolo Pasquero, Massimo Porta, and Silvestro Roatta (2019). *Apparato per la misurazione della velocità di un'onda pressoria propagantesi nel distretto venoso di un individuo e procedimento corrispondente.*

Eskesen, T G, M Wetterslev, and A Perner (2016). "Systematic review including re-analyses of 1148 individual data sets of central venous pressure as a predictor of fluid responsiveness". In: *Intensive Care Medicine* 42.3, pp. 324–332.

Felix Jr., W Robert, Bernard Sigel, Karl V Amatneek, and Marshall H Chrablow (1971). "Venous Pulse Wave Propagation Velocity in Hemorrhage". In: *Archives of Surgery* 102.1, pp. 53–56.

Finfer, Simon, John Myburgh, and Rinaldo Bellomo (2018). "Intravenous fluid therapy in critically ill adults". In: *Nature Reviews Nephrology* 14.9, pp. 541–557.

Finnerty, Nathan M., Ashish R. Panchal, Creagh Boulger, Amar Vira, Jason J. Bischof, Christopher Amick, David P. Way, and David P. Bahner (2017). "Inferior Vena Cava Measurement with Ul-

trasound: What Is the Best View and Best Mode?" In: *Western Journal of Emergency Medicine* 18.3, p. 496.

Folino, Anna, Marco Benzo, Paolo Pasquero, Andrea Laguzzi, Luca Mesin, Alessandro Messere, Massimo Porta, and Silvestro Roatta (2017). "Vena Cava Responsiveness to Controlled Isovolumetric Respiratory Efforts". In: *Journal of Ultrasound in Medicine* 36.10, pp. 2113–2123.

Funk, Duane J, Eric Jacobsohn, and Anand Kumar (2013). "The role of venous return in critical illness and shock-Part I: Physiology". In: *Critical Care Medicine* 41.1, pp. 255–262.

Gelman, Simon (2008). "Venous Function and Central Venous Pressure". In: *Anesthesiology* 108.4, pp. 735–748.

Gelman, Simon and Luca Bigatello (2018a). "In reply: Why goal-directed hemodynamic therapy is often ineffective and how can we try to improve the results". In: *Canadian Journal of Anesthesia/Journal canadien d'anesthésie* 65.9, pp. 1076–1077.

Gelman, Simon and Luca Bigatello (2018b). "The physiologic basis for goal-directed hemodynamic and fluid therapy: the pivotal role of the venous circulation". In: *Canadian Journal of Anesthesia/Journal canadien d'anesthésie* 65.3, pp. 294–308.

Gignon, Lucile, Claire Roger, Sophie Bastide, Sandrine Alonso, Laurent Zieleskiewicz, Hervé Quintard, Lana Zoric, Xavier Bobbia, Mathieu Raux, Marc Leone, Jean-Yves Lefrant, and Laurent Muller (2016). "Influence of Diaphragmatic Motion on Inferior Vena Cava Diameter Respiratory Variations in Healthy Volunteers". In: *Anesthesiology* 124.6, pp. 1338–1346.

Godfrey, G. E.P., S. W. Dubrey, and J. M. Handy (2014). "A prospective observational study of stroke volume responsiveness to a passive leg raise manoeuvre in healthy non-starved volunteers as assessed by transthoracic echocardiography". In: *Anaesthesia* 69.4, pp. 306–313.

Golemati, Spyretta and Demosthenes D Cokkinos (2022). "Recent advances in vascular ultrasound imaging technology and their clinical implications". In: *Ultrasonics* 119, p. 106599.

Grassi, Bruno and Valentina Quaresima (2016). "Near-infrared spectroscopy and skeletal muscle oxidative function in vivo in health and disease: a review from an exercise physiology perspective." eng. In: *Journal of biomedical optics* 21.9, p. 91313.

Grensemann, Jörn (2018). "Cardiac Output Monitoring by Pulse Contour Analysis, the Technical Basics of Less-Invasive Techniques". In: *Frontiers in Medicine* 5, p. 64.

Grodins, F S, W H Stuart, and R L Veenstra (1960). "Performance characteristics of the right heart bypass preparation." eng. In: *The American journal of physiology* 198, pp. 552–560.

Guyton, A C and C E Jones (1973). "Central venous pressure: physiological significance and clinical implications." eng. In: *American heart journal* 86.4, pp. 431–437.

Guyton, A. C. (1955). "Determination of Cardiac Output By Equating Venous Return Curves With Cardiac Response Curves". In: *Physiological Reviews* 35.1, pp. 123–129.

Guyton, A. C., B. Abernathy, J. B. Langston, B. N. Kaufmann, and H. M. Fairchild (1959). "Relative importance of venous and arterial resistances in controlling venous return and cardiac output". In: *American Journal of Physiology* 196.5, pp. 1008–1014.

Guyton, A. C., A. W. Lindsey, B. Abernathy, and T. Richardson (1957). "Venous Return at Various Right Atrial Pressures and the Normal Venous Return Curve". In: *American Journal of Physiology* 189.3, pp. 609–615.

Hall, John E and Michael E Hall (2020). *Guyton and Hall textbook of medical physiology e-Book*. Elsevier Health Sciences.

Halliwill, John R, Christopher T Minson, and Michael J Joyner (1999). "Measurement of limb venous compliance in humans: technical considerations and physiological findings". In: *Journal of Applied Physiology* 87.4, pp. 1555–1563.

Henderson, William R, Donald E G Griesdale, Keith R Walley, and A William Sheel (2010). "Clinical review: Guyton–the role of mean circulatory filling pressure and right atrial pressure in controlling cardiac output." eng. In: *Critical care* 14.6, p. 243.

Jabot, Julien, Jean-Louis Teboul, Christian Richard, and Xavier Monnet (2008). "Passive leg raising for predicting fluid responsiveness: importance of the postural change". In: *Intensive Care Medicine* 35.1, p. 85.

Jiang, Benyu, Baoming Liu, Karen L McNeill, and Philip J Chowienczyk (2008). "Measurement of Pulse Wave Velocity Using Pulse Wave Doppler Ultrasound: Comparison with Arterial Tonometry". In: *Ultrasound in Medicine & Biology* 34.3, pp. 509–512.

Jones, T W, D Houghton, S Cassidy, G A MacGowan, M I Trenell, and D G Jakovljevic (2015). "Bioreactance is a reliable method for estimating cardiac output at rest and during exercise". In: *British Journal of Anaesthesia* 115.3, pp. 386–391.

Kelm, Diana J, Jared T Perrin, Rodrigo Cartin-Ceba, Ognjen Gajic, Louis Schenck, and Cassie C Kennedy (2015). "Fluid Overload in Patients With Severe Sepsis and Septic Shock Treated With Early Goal-Directed Therapy Is Associated With Increased Acute Need for Fluid-Related Medical Interventions and Hospital Death". In: *Shock* 43.1, pp. 68–73.

Kenny, Jon-Emile S (2021). "Letter to the editor: The venous circulation actively alters flow: a brief evolutionary perspective." eng. In: *American journal of physiology. Heart and circulatory physiology* 320.1, H469–H470.

Kimura, Bruce J, Randy Dalugdugan, Glynn W Gilcrease III, James N Phan, Brian K Showalter, and Tanya Wolfson (2011). "The effect of breathing manner on inferior vena caval diameter†". In: *European Journal of Echocardiography* 12.2, pp. 120–123.

Kinsky, Michael, Nicole Ribeiro, Maxime Cannesson, Donald Deyo, George Kramer, Michael Salter, Muzna Khan, Hyunsu Ju, and William E Johnston (2016). "Peripheral Venous Pressure as an Indicator of Preload Responsiveness During Volume Resuscitation from Hemorrhage". In: *Anesthesia and Analgesia* 123.1.

Koeppen, Bruce M and Bruce A Stanton (2017). *Berne and levy physiology e-book*. Elsevier Health Sciences.

Korotkoff, N S (1905). "On methods of studying blood pressure". In: *Proceedings of the Russian Imperial Military Medical Academy* 11.1, p. 365.

Krogh, August (1912). "The Regulation of the Supply of Blood to the Right Heart". In: *Skandinavisches Archiv Physiologie* 27.2, pp. 227–248.

Lakhal, Karim, Stephan Ehrmann, and Thierry Boulain (2016). "Assessing the Effects of Passive Leg Raising: Fast, Not Furious". In: *Critical Care Medicine* 44.8.

Lakhal, Karim, Stephan Ehrmann, Isabelle Runge, Dalila Benzekri-Lefèvre, Annick Legras, Pierre François Dequin, Emmanuelle Mercier, Michel Wolff, Bernard Régnier, and Thierry Boulain (2010). "Central venous pressure measurements improve the accuracy of leg raising-induced change in pulse pressure to predict fluid responsiveness". In: *Intensive Care Medicine* 36.6, pp. 940–948.

Lakhal, Karim, Maëlle Martin, Sofian Faiz, Stephan Ehrmann, Yvonnick Blanloeil, Karim Asehnoune, Bertrand Rozec, and Thierry Boulain (2016). "The CNAP™ Finger Cuff for Noninvasive Beat-To-Beat Monitoring of Arterial Blood Pressure: An Evaluation in Intensive Care Unit Patients and a Comparison with 2 Intermittent Devices". In: *Anesthesia and Analgesia* 123.5.

Lee, Chen-Tse, Tzong-Shiun Lee, Ching-Tang Chiu, Hsiao-Chun Teng, Hsiao-Liang Cheng, and Chun-Yu Wu (2020). "Mini-fluid challenge test predicts stroke volume and arterial pressure fluid responsiveness during spine surgery in prone position: A STARD-compliant diagnostic accuracy study". In: *Medicine* 99.6, e19031.

Levy, M N (1979). "The cardiac and vascular factors that determine systemic blood flow." In: *Circulation Research* 44.6, pp. 739–747.

Lewis, Thomas (1930). "Remarks on early signs of cardiac failure of the congestive type". In: *British medical journal* 1.3618, p. 849.

Lin Wang, Yuh-Ying (2019). "Did you know developing quantitative pulse diagnosis with realistic haemodynamic theory can pave a way for future personalized health care." In: *Acta physiologica* 227.3, e13260–e13260.

Long, Elliot, Ed Oakley, Trevor Duke, and Franz E. Babl (2017). "Does Respiratory Variation in Inferior Vena Cava Diameter Predict Fluid Responsiveness: A Systematic Review and Meta-Analysis". In: *Shock* 47.5, pp. 550–559.

Maas, Jacinta J, Bart F Geerts, Paul C M van den Berg, Michael R Pinsky, and Jos R C Jansen (2009). "Assessment of venous return curve and mean systemic filling pressure in postoperative cardiac surgery patients*". In: *Critical Care Medicine* 37.3, pp. 912–918.

Maas, Jacinta J, Michael R Pinsky, Leon P Aarts, and Jos R Jansen (2012). "Bedside assessment of total systemic vascular compliance, stressed volume, and cardiac function curves in intensive care unit patients." eng. In: *Anesthesia and analgesia* 115.4, pp. 880–887.

Maas, Jacinta J, Michael R Pinsky, Bart F Geerts, Rob B de Wilde, and Jos R Jansen (2012). "Estimation of mean systemic filling pressure in postoperative cardiac surgery patients with three methods". In: *Intensive Care Medicine* 38.9, pp. 1452–1460.

Mackay, I F, P Van Loon, J T Campos, and N De Jesus (1967). "A technique for the indirect measurement of the velocity of induced venous pulsations." eng. In: *American heart journal* 73.1, pp. 17–23.

Magder, S (2006). "Point:Counterpoint: The classical Guyton view that mean systemic pressure, right atrial pressure, and venous resistance govern venous return is/is not correct". In: *Journal of Applied Physiology* 101.5, pp. 1523–1525.

Magder, S (2016). "Volume and its relationship to cardiac output and venous return". In: *Critical Care* 20.1, pp. 1–11.

Magder, Sheldon (2012). "Bench-to-bedside review: An approach to hemodynamic monitoring–Guyton at the bedside." eng. In: *Critical care* 16.5, p. 236.

Magder, Sheldon (2015). "Understanding central venous pressure: not a preload index?" In: *Current opinion in critical care* 21.5, pp. 369–375.

Magder, Sheldon (2017). "Right Atrial Pressure in the Critically Ill: How to Measure, What Is the Value, What Are the Limitations?" In: *Chest* 151.4, pp. 908–916.

Magnino, Corrado, Pierluigi Omedè, Eleonora Avenatti, Davide Presutti, Andrea Iannaccone, Michela Chiarlo, Claudio Moretti, Fiorenzo Gaita, Franco Veglio, and Alberto Milan (2017). "Inaccuracy of Right Atrial Pressure Estimates Through Inferior Vena Cava Indices." eng. In: *The American journal of cardiology* 120.9, pp. 1667–1673.

Mahjoub, Yazine, Jérémie Touzeau, Norair Airapetian, Emmanuel Lorne, Mustapha Hijazi, Elie Zogheib, François Tinturier, Michel Slama, and Hervé Dupont (2010). "The passive leg-raising maneuver cannot accurately predict fluid responsiveness in patients with intra-abdominal hypertension". In: *Critical Care Medicine* 38.9, pp. 1824–1829.

Malbrain, ML, PE Marik, IC Witters, AW Cordemans, DJ Kirkpatrick, N Roberts, and Van Regenmortel (2014). "Fluid overload, de-resuscitation, and outcomes in critically ill or injured patients: a systematic review with suggestions for clinical practice". In: *Anaesthesiology Intensive Therapy* 46.5.

Mancini, D M, L Bolinger, H Li, K Kendrick, B Chance, and J R Wilson (1994). "Validation of near-infrared spectroscopy in humans". In: *Journal of Applied Physiology* 77.6, pp. 2740–2747.

Marik, Paul E (2013). "Noninvasive Cardiac Output Monitors: A State-of the-Art Review". In: *Journal of Cardiothoracic and Vascular Anesthesia* 27.1, pp. 121–134.

Marik, Paul E, Michael Baram, and Bobbak Vahid (2008). "Does central venous pressure predict fluid responsiveness? A systematic review of the literature and the tale of seven mares." eng. In: *Chest* 134.1, pp. 172–178.

Marik, Paul E and Rodrigo Cavallazzi (2013). "Does the Central Venous Pressure Predict Fluid Responsiveness? An Updated Meta-Analysis and a Plea for Some Common Sense*". In: *Critical Care Medicine* 41.7.

Martin, J T (1995). "The Trendelenburg position: a review of current slants about head down tilt." In: *Journal of the American Association of Nurse Anesthetists* 63.1, pp. 29–36.

Mesin, Luca, Stefano Albani, and Gianfranco Sinagra (2019). "Non-invasive Estimation of Right Atrial Pressure Using Inferior Vena Cava Echography." eng. In: *Ultrasound in Medicine and Biology* 45.5, pp. 1331–1337.

Mesin, Luca, Tatiana Giovinazzo, Simone D'Alessandro, Silvestro Roatta, Alessandro Raviolo, Flavia Chiacchiarini, Massimo Porta, and Paolo Pasquero (2019). "Improved Repeatability of the Estimation of Pulsatility of Inferior Vena Cava". In: *Ultrasound in Medicine and Biology* 45.10, pp. 2830–2843.

Mesin, Luca, Paolo Pasquero, Stefano Albani, Massimo Porta, and Silvestro Roatta (2015). "Semi-automated Tracking and Continuous Monitoring of Inferior Vena Cava Diameter in Simulated and Experimental Ultrasound Imaging". In: *Ultrasound in Medicine and Biology* 41.3, pp. 845–857.

Mesin, Luca, Paolo Pasquero, and Silvestro Roatta (2019). "Tracking and Monitoring Pulsatility of a Portion of Inferior Vena Cava from Ultrasound Imaging in Long Axis". In: *Ultrasound in Medicine and Biology* 45.5, pp. 1338–1343.

Mesin, Luca, Paolo Pasquero, and Silvestro Roatta (2020). "Multi-directional Assessment of Respiratory and Cardiac Pulsatility of the Inferior Vena Cava From Ultrasound Imaging in Short Axis". In: *Ultrasound in Medicine and Biology* 46.12, pp. 3475–3482.

Mesin, Luca, Silvestro Roatta, Paolo Pasquero, and Massimo Porta (2020). "Automated volume status assessment using Inferior Vena Cava pulsatility". In: *Electronics* 9.10, p. 1671.

Mesquida, Jaume, Guillem Gruartmoner, and Ricard Ferrer (2017). "Passive leg raising for assessment of volume responsiveness: A review". In: *Current Opinion in Critical Care* 23.3, pp. 237–243.

Messere, Alessandro and Silvestro Roatta (2013). "Influence of cutaneous and muscular circulation on spatially resolved versus standard Beer-Lambert near-infrared spectroscopy." eng. In: *Physiological reports* 1.7, e00179.

Messina, Antonio, Antonio Dell'Anna, Marta Baggiani, Flavia Torrini, Gian Marco Maresca, Victoria Bennett, Laura Saderi, Giovanni Sotgiu, Massimo Antonelli, and Maurizio Cecconi (2019). "Functional hemodynamic tests: a systematic review and a metanalysis on the reliability of the end-expiratory occlusion test and of the mini-fluid challenge in predicting fluid responsiveness". In: *Critical Care* 23.1, p. 264.

Milan, Alberto, Gaia Zocaro, Dario Leone, Francesco Tosello, Irene Buraioli, Domenica Schiavone, and Franco Veglio (2019). "Current assessment of pulse wave velocity: Comprehensive review of validation studies". In: *Journal of Hypertension* 37.8, pp. 1547–1557.

Miller, Joseph, Chuan Xing Ho, Joy Tang, Richard Thompson, Jared Goldberg, Ahmed Amer, and Bashar Nahab (2016). "Assessing Fluid Responsiveness in Spontaneously Breathing Patients". In: *Academic Emergency Medicine* 23.2, pp. 186–190.

Miller, Wayne L (2016). "Fluid volume overload and congestion in heart failure". In: *Circulation: Heart Failure* 9.8, pp. 1–9.

Millington, Scott J (2019). "Ultrasound assessment of the inferior vena cava for fluid responsiveness: easy, fun, but unlikely to be helpful". eng. In: *Canadian journal of anaesthesia* 66.6, pp. 633–638.

Minten, Jaak, Frans Van De Werf, André Auber, Hugo Kasteloot, and Hilaire De Geest (1983). "Apparent pulse wave velocity in canine superior vena cava". In: *Cardiovascular Research* 17.10, pp. 627–632.

Monnet, Xavier, Paul Marik, and Jean-Louis Teboul (2016). "Passive leg raising for predicting fluid responsiveness: a systematic review and meta-analysis". In: *Intensive Care Medicine* 42.12, pp. 1935–1947.

Monnet, Xavier, Paul E Marik, and Jean Louis Teboul (2016). "Prediction of fluid responsiveness: an update". In: *Annals of Intensive Care* 6.1, pp. 1–11.

Monnet, Xavier and Michael R Pinsky (2015). "Predicting the determinants of volume responsiveness". eng. In: *Intensive care medicine* 41.2, pp. 354–356.

Monnet, Xavier and Jean Louis Teboul (2018). "Assessment of fluid responsiveness: Recent advances". In: *Current Opinion in Critical Care* 24.3, pp. 190–195.

Monnet, Xavier and Jean-Louis Teboul (2015). "Passive leg raising: five rules, not a drop of fluid!" In: *Critical Care* 19.1, p. 18.

Nakamura, Kensuke, Makoto Tomida, Takehiro Ando, Kon Sen, Ryota Inokuchi, Etsuko Kobayashi, Susumu Nakajima, Ichiro Sakuma, and Naoki Yahagi (2013). "Cardiac variation of inferior vena cava: new concept in the evaluation of intravascular blood volume". In: *Journal of Medical Ultrasonics* 40.3, pp. 205–209.

Nayak, Suraj K, Arindam Bit, Anilesh Dey, Biswajit Mohapatra, and Kunal Pal (2018). "A Review on the Nonlinear Dynamical System Analysis of Electrocardiogram Signal". In: *Journal of Healthcare Engineering* 2018. Ed. by Maria Lindén, p. 6920420.

Nieto, Orlando Ruben Pérez, Adrian Wong, Jorgelópez L. Fermín, Eder Iván Zamarrón López, José Antonio Meade Aguilar, Ernesto Deloya Tomas, Jorge Daniel Carrión Moya, Gabriela Castillo Gutiérrez, María Guadalupe Olvera Ramos, Xiomara García Montes, Manuel Alberto Guerrero Gutiérrez, Fernando George Aguilar, Jesús Salvador Sánchez Díaz, Raúl Soriano Orozco, Eduardo Ríos Argaiz, Thierry Hernandez-Gilsoul, Roberto Secchi Del Rio, Silvio Antonio Ñamendys-Silva, and Manu L.N.G. Malbrain (2021). "Aiming for zero fluid accumulation: First, do no harm". In: *Anaesthesiology Intensive Therapy* 53.2, pp. 162–178.

Nippa, Jurgen, Raymond Alexander, and Roland Folse (1971). "Pulse wave velocity in human veins". In: *Journal of Applied Physiology* 30.4, pp. 558–563.

Orso, Daniele, Irene Paoli, Tommaso Piani, Francesco L. Cilenti, Lorenzo Cristiani, and Nicola Guglielmo (2020). "Accuracy of Ultrasonographic Measurements of Inferior Vena Cava to Determine Fluid Responsiveness: A Systematic Review and Meta-Analysis". In: *Journal of Intensive Care Medicine* 35.4, pp. 354–363.

Pang, Catherine C.Y. (2001). "Autonomic control of the venous system in health and disease: effects of drugs". In: *Pharmacology and Therapeutics* 90.2-3, pp. 179–230.

Pasquero, Paolo, Stefano Albani, Elena Sitia, Anna Viola Taulaigo, Lorenzo Borio, Paola Berchialla, Franco Castagno, and Massimo Porta (2015). "Inferior vena cava diameters and collapsibility index reveal early volume depletion in a blood donor model". eng. In: *Critical ultrasound journal* 7.1, p. 17.

Pereira, Tânia, Carlos Correia, and João Cardoso (2015). "Novel methods for pulse wave velocity measurement". In: *Journal of Medical and Biological Engineering* 35.5, pp. 555–565.

Pickett, Joya D., Elizabeth Bridges, Patricia A. Kritek, and Jo Anne D. Whitney (2017). "Passive leg-raising and prediction of fluid responsiveness: Systematic review". In: *Critical Care Nurse* 37.2, pp. 32–48.

Pugsley, Jacob and Adam B Lerner (2010). "Cardiac Output Monitoring: Is There a Gold Standard and How Do the Newer Technologies Compare?" In: *Seminars in Cardiothoracic and Vascular Anesthesia* 14.4, pp. 274–282.

Quarteroni, Alfio, Alessandro Veneziani, and Christian Vergara (2016). "Geometric multiscale modeling of the cardiovascular system, between theory and practice". In: *Computer Methods in Applied Mechanics and Engineering* 302, pp. 193–252.

Repessé, Xavier, Cyril Charron, Julia Fink, Alain Beauchet, Florian Deleu, Michel Slama, Guillaume Belliard, and Antoine Vieillard-Baron (2015). "Value and determinants of the mean systemic filling pressure in critically ill patients". In: *American Journal of Physiology-Heart and Circulatory Physiology* 309.5, H1003–H1007.

Rhodes, Andrew et al. (2017). "Surviving Sepsis Campaign: International Guidelines for Management of Sepsis and Septic Shock: 2016". In: *Intensive Care Medicine* 43.3, pp. 304–377.

Ritchie, Hannah and Max Roser (2018). "Causes of Death". In: *Our World in Data*.

Rizkallah, Jacques, Megan Jack, Mahwash Saeed, Leigh Anne Shafer, Minh Vo, and James Tam (2014). "Non-invasive bedside assessment of central venous pressure: scanning into the future". In: *PloS one* 9.10, e109215.

Rothe, Carl (1983). "Reflex control of veins and vascular capacitance." eng. In: *Physiological reviews* 63.4, pp. 1281–1342.

Rothe, Carl (2006). "The classical Guyton view that mean systemic pressure, right atrial pressure, and venous resistance govern venous return is/is not correct". In: *Journal of Applied Physiology* 101.5, p. 1529.

Rothe, Carl (2011). *Venous System: Physiology of the Capacitance Vessels*. Major Reference Works, pp. 397–452.

Safar, Michel E (2018). "Arterial stiffness as a risk factor for clinical hypertension". In: *Nature Reviews Cardiology* 15.2, pp. 97–105.

Sakr, Yasser, Paolo Nahuel Rubatto Birri, Katarzyna Kotfis, Rahul Nanchal, Bhagyesh Shah, Stefan Kluge, Mary E. Schroeder, John C. Marshall, and Jean Louis Vincent (2017). "Higher Fluid Balance Increases the Risk of Death from Sepsis: Results from a Large International Audit". In: *Critical Care Medicine* 45.3, pp. 386–394.

Sangkum, Lisa, Geoffrey L Liu, Ling Yu, Hong Yan, Alan D Kaye, and Henry Liu (2016). "Minimally invasive or noninvasive cardiac output measurement: an update". In: *Journal of Anesthesia* 30.3, pp. 461–480.

Sathish, N., Naveen Singh, P. Nagaraja, B. Sarala, C. Prabhushankar, Manasa Dhananjaya, and N. Manjunatha (2016). "Comparison between noninvasive measurement of central venous pressure using near infrared spectroscopy with an invasive central venous pressure monitoring in cardiac surgical Intensive Care Unit". In: *Annals of Cardiac Anaesthesia* 19.3, pp. 405–409.

Saugel, Bernd, Phillip Hoppe, Julia Y Nicklas, Karim Kouz, Annmarie Körner, Julia C Hempel, Jaap J Vos, Gerhard Schön, and Thomas W L Scheeren (2020). "Continuous noninvasive pulse wave analysis using finger cuff technologies for arterial blood pressure and cardiac output monitoring in perioperative and intensive care medicine: a systematic review and meta-analysis". In: *British Journal of Anaesthesia* 125.1, pp. 25–37.

Saugel, Bernd, Jean-Louis Vincent, and Julia Y Wagner (2017). "Personalized hemodynamic management". In: *Current Opinion in Critical Care* 23.4.

Schulz, Luis, Guillaume Geri, Antoine Vieillard-Baron, Philippe Vignon, Geoffrey Parkin, and Anders Aneman (2021). "Volume status and volume responsiveness in postoperative cardiac surgical patients: An observational, multicentre cohort study". In: *Acta Anaesthesiologica Scandinavica* 65.3, pp. 320–328.

Scultetus, Anke H., J.Leonel Villavicencio, and Norman M. Rich (2001). "Facts and fiction surrounding the discovery of the venous valves". In: *Journal of Vascular Surgery* 33.2, pp. 435–441.

Sequí-Domínguez, Irene, Iván Cavero-Redondo, Celia Álvarez-Bueno, Diana P Pozuelo-Carrascosa, Sergio Nuñez de Arenas-Arroyo, and Vicente Martínez-Vizcaíno (2020). "Accuracy of Pulse Wave Velocity Predicting Cardiovascular and All-Cause Mortality. A Systematic Review and Meta-Analysis". In: *Journal of Clinical Medicine* 9.7, p. 2080.

Shah, Parth and Martine A Louis (2021). "Physiology, Central Venous Pressure." eng. In.

Shi, Rui, Xavier Monnet, and Jean Louis Teboul (2020). "Parameters of fluid responsiveness". In: *Current Opinion in Critical Care* 26.3, pp. 319–326.

Shirwany, Najeeb A and Ming-hui Zou (2010). "Arterial stiffness: a brief review". In: *Acta Pharmacologica Sinica* 31.10, pp. 1267–1276.

Shlyakhto, Eugene and Alexandra Conrady (2005). "Korotkoff sounds: what do we know about its discovery?" In: *Journal of Hypertension* 23.1, pp. 3–4.

Si, Xiang, Hailin Xu, Zimeng Liu, Jianfeng Wu, Daiyin Cao, Juan Chen, Minying Chen, Yongjun Liu, and Xiangdong Guan (2018). "Does Respiratory Variation in Inferior Vena Cava Diameter Predict Fluid Responsiveness in Mechanically Ventilated Patients? A Systematic Review and Meta-analysis". In: *Anesthesia and Analgesia* 127.5.

Silva, João M, Amanda Maria RibasRosa de Oliveira, Fernando Augusto Mendes Nogueira, Pedro Monferrari Monteiro Vianna, Marcos Cruz Pereira Filho, Leandro Ferreira Dias, Vivian Paz Leão Maia, Cesar de Souza Neucamp, Cristina Prata Amendola, Maria Jose Carvalho Carmona, and Luiz M Sá Malbouisson (2013). "The effect of excess fluid balance on the mortality rate of surgical patients: a multicenter prospective study". In: *Critical Care* 17.6, R288.

Skinner, James E, Ary L Goldberger, Gottfried Mayer-Kress, and Raymond E Ideker (1990). "Chaos in the Heart: Implications for Clinical Cardiology". In: *Nature Biotechnology* 8.11, pp. 1018–1024.

Sonoo, Tomohiro, Kensuke Nakamura, Takehiro Ando, Kon Sen, Akinori Maeda, Etsuko Kobayashi, Ichiro Sakuma, Kent Doi, Susumu Nakajima, and Naoki Yahagi (2015). "Prospective analysis of cardiac collapsibility of inferior vena cava using ultrasonography". In: *Journal of Critical Care* 30.5, pp. 945–948.

Stepanyan, Ivan V and Alexey A Mekler (2020). "Chaotic Algorithms of Analysis of Cardiovascular Systems and Artificial Intelligence BT - Advances in Artificial Systems for Medicine and Education III". In: ed. by Zhengbing Hu, Sergey Petoukhov, and Matthew He. Cham: Springer International Publishing, pp. 231–240.

Stiles, Thomas W, Alejandra E Morfin Rodriguez, Hanifa S Mohiuddin, Hyunjin Lee, Fazal A Dalal, Wesley W Fuertes, Thaddeus H Adams, Randolph H Stewart, and Christopher M Quick (2021). "Algebraic formulas characterizing an alternative to Guyton's graphical analysis relevant for heart failure". In: *American Journal of Physiology-Regulatory, Integrative and Comparative Physiology* 320.6, R851–R870.

Suehiro, Koichi (2020). "Update on the assessment of fluid responsiveness." eng. In: *Journal of anesthesia* 34.2, pp. 163–166.

Sunagawa, Kenji (2017). "Guyton's venous return curves should be taught at medical schools (complete English translation of Japanese version)". In: *The Journal of Physiological Sciences* 67.4, pp. 447–458.

Suzuki, Susumu, Sumio Takasaki, Takeo Ozaki, and Yukio Kobayashi (1999). "Tissue oxygenation monitor using NIR spatially resolved spectroscopy". In: *Optical tomography and spectroscopy of tissue III* 3597, pp. 582–592.

Tijsseling, A S and A Anderson (2012). "A. Isebree Moens and D.J. Korteweg: On the speed of propagation of waves in elastic tubes". In: *BHR Group - 11th International Conferences on Pressure Surges*, pp. 227–245.

Tobin, M. J., M. J. Mador, S. M. Guenther, R. F. Lodato, and M. A. Sackner (1988). "Variability of resting respiratory drive and timing in healthy subjects". In: *Journal of Applied Physiology* 65.1, pp. 309–317.

Toppen, William, Elizabeth Aquije Montoya, Stephanie Ong, Daniela Markovic, Yuhan Kao, Xueqing Xu, Alan Chiem, Maxime Cannesson, David Berlin, and Igor Barjaktarevic (2018). "Passive Leg Raise: Feasibility and Safety of the Maneuver in Patients With Undifferentiated Shock". In: *Journal of Intensive Care Medicine* 35.10, pp. 1123–1128.

Townsend, Raymond R, Ian B Wilkinson, Ernesto L Schiffrin, Alberto P Avolio, Julio A Chirinos, John R Cockcroft, Kevin S Heffernan, Edward G Lakatta, Carmel M McEniery, Gary F Mitchell, Samer S Najjar, Wilmer W Nichols, Elaine M Urbina, and Thomas Weber (2015). "Recommendations for Improving and Standardizing Vascular Research on Arterial Stiffness: A Scientific Statement From the American Heart Association." eng. In: *Hypertension* 66.3, pp. 698–722.

Truijen, Jasper, Morten Bundgaard-Nielsen, and Johannes J. Von Lieshout (2010). "A definition of normovolaemia and consequences for cardiovascular control during orthostatic and environmental stress". In: *European Journal of Applied Physiology* 109.2, pp. 141–157.

Tyberg, John V (2002). "How changes in venous capacitance modulate cardiac output." eng. In: *European journal of physiology* 445.1, pp. 10–17.

Unal Akoglu, Ebru and Haldun Akoglu (2021). "Does respiratory variation in inferior vena cava diameter predict fluid responsiveness in adult patients? A systematic review and meta-analysis of diagnostic accuracy studies". In: *Hong Kong Journal of Emergency Medicine*, p. 10249079211029781.

Uthoff, H, M Siegemund, M Aschwanden, L Hunziker, T Fabbro, U Baumann, K A Jaeger, S Imfeld, and D Staub (2012). "Prospective comparison of noninvasive, bedside ultrasound methods for assessing central venous pressure". In: *Ultraschall in der Medizin* 33.7, pp. 256–262.

Veneziani, Alessandro and Christian Vergara (2013). "Inverse problems in Cardiovascular Mathematics: toward patient-specific data assimilation and optimization". In: *International Journal for Numerical Methods in Biomedical Engineering* 29.7, pp. 723–725.

Via, Gabriele, Guido Tavazzi, and Susanna Price (2016). "Ten situations where inferior vena cava ultrasound may fail to accurately predict fluid responsiveness: a physiologically based point of view". In: *Intensive care medicine* 42.7, pp. 1164–1167.

Vistisen, Simon T and Peter Juhl-Olsen (2017). "Where are we heading with fluid responsiveness research?" In: *Current Opinion in Critical Care* 23.4, pp. 318–325.

Wagner, Julia Y, Annmarie Körner, Leonie Schulte-Uentrop, Mathias Kubik, Hermann Reichenspurner, Stefan Kluge, Daniel A Reuter, and Bernd Saugel (2018). "A comparison of volume clamp method-based continuous noninvasive cardiac output (CNCO) measurement versus intermittent pulmonary artery thermodilution in postoperative cardiothoracic surgery patients". In: *Journal of Clinical Monitoring and Computing* 32.2, pp. 235–244.

Wallace, David J, Michael Allison, and Michael B Stone (2010). "Inferior vena cava percentage collapse during respiration is affected by the sampling location: an ultrasound study in healthy volunteers". eng. In: *Academic Emergency Medicine* 17.1, pp. 96–99.

Wardhan, R and K Shelley (2009). "Peripheral venous pressure waveform". In: *Current Opinion in Anaesthesiology* 22.6, pp. 814–821.

Werner-Moller, Per, David Berger, and Jukka Takala (2020). "Letter to the Editor: Venous return and the physical connection between distribution of segmental pressures and volumes". In: *American Journal of Physiology-Heart and Circulatory Physiology* 318.1, H203–H204.

Wolf, Martin, Marco Ferrari, and Valentina Quaresima (2007). "Progress of near-infrared spectroscopy and topography for brain and muscle clinical applications." eng. In: *Journal of biomedical optics* 12.6, p. 62104.

Wong, D. H., K. K. Tremper, J. Zaccari, J. Hajduczek, H. N. Konchigeri, and S. M. Hufstedler (1988). "Acute cardiovascular response to passive leg raising". In: *Critical Care Medicine* 16.2, pp. 123–125.

Yu, Y, K Zhang, L Zhang, H Zong, L Meng, and R Han (2018). "Cerebral near-infrared spectroscopy (NIRS) for perioperative monitoring of brain oxygenation in children and adults". In: *Cochrane Database of Systematic Reviews* 2018.1.

Zhang, Zhongheng, Xiao Xu, Sheng Ye, and Lei Xu (2014). "Ultrasonographic measurement of the respiratory variation in the inferior vena cava diameter is predictive of fluid responsiveness in critically ill patients: systematic review and meta-analysis." eng. In: *Ultrasound in Medicine and Biology* 40.5, pp. 845–853.

Appendix

The original scientific papers, on which this PhD thesis is founded, are collected in this chapter. They are presented in the following order:

Paper I. **Ermini L**, Ferraresi C, De Benedictis C, Roatta S* *"Objective Assessment of Venous Pulse Wave Velocity in Healthy Humans"* Ultrasound in Medicine & Biology, 2020; 46(3):849-854.

Paper II. **Ermini L**, Chiarello NE, De Benedictis C, Ferraresi C, Roatta S* *"Venous Pulse Wave Velocity variation in response to a simulated fluid challenge in healthy subjects"* Biomedical Signal Processing and Control, 2021; 63(102177):1-7.

Paper III. Ferraresi C, Franco W, Maffiodo D, De Benedictis C*, Paterna M, Quiñones P D, **Ermini L**, Roatta S *"Applications of intermittent pneumatic compression for diagnostic and therapeutic purposes"* Proceedings of I4SDG Workshop 2021, Mechanisms and Machine Science, 2022; 108(1):209-218.

Paper IV. Barbagini A, **Ermini L***, Pertusio R, Roatta S *"A portable device for the measurement of venous Pulse Wave Velocity"* Applied Sciences, 2022; *under review.*

Paper V. **Ermini L***, Seddone S, Policastro P, Mesin L, Pasquero P, Roatta S *"The cardiac caval index. Improving non-invasive assessment of cardiac preload"* Journal of Ultrasound in Medicine, 2021; 9999:1-12, *Epub ahead of print.*

Paper VI. Seddone S, **Ermini L**, Policastro P, Mesin L, Roatta S* *"Evidence that large vessels do affect near infrared spectroscopy"* Scientific Reports, 2022; *in press.*

Paper VII. Mesin L*, Albani S, Pasquero P, Porta M, Policastro P, Leonardi G, Albera C, Scacciatella P, Melchiorri C, Pellicori P, Stolfo D, Fabris B, Grillo A, Bini R, Giannoni A, Pepe A, **Ermini L**, Seddone S, Sinagra G, Antonini-Canterin F, Roatta S *"Assessment of phasic changes of vascular size by automated edge tracking - State of the art and clinical perspectives"* Frontiers in Cardiovascular Medicine, 2022; 8(775635):1-9.

* Corresponding Author

In addition, it is also reported the Italian patent concerning the methodology to assess non-invasively venous Pulse Wave Velocity, developed at the beginning of my PhD project:

Patent. **Ermini L**, Franco W, Maffiodo D, De Benedictis C, Ferraresi C, Mesin L, Pasquero P, Porta M, Roatta S, Pertusio R *"Apparato per la misurazione della velocità di un'onda pressoria propagantesi nel distretto venoso di un individuo e procedimento corrispondente"* Italian Ministry of Economic Development, 2019; Application number 102019000007803, Classification A61B, Deposit number BIT22246.

Paper I

Ultrasound in Med. & Biol., Vol. 46, No. 3, pp. 849–854, 2020

0301-5629/$ - see front matter

https://doi.org/10.1016/j.ultrasmedbio.2019.11.003

● *Clinical Note*

OBJECTIVE ASSESSMENT OF VENOUS PULSE WAVE VELOCITY IN HEALTHY HUMANS

Leonardo Ermini,* Carlo Ferraresi,† Carlo De Benedictis,† and Silvestro Roatta*

* Laboratory of Integrative Physiology, Department of Neuroscience, University of Torino, Torino, Italy; and † Department of Mechanical and Aerospace Engineering, Politecnico of Torino, Torino, Italy

(*Received* 6 *August* 2019; *revised* 1 *October* 2019; *in final from* 6 *November* 2019)

Abstract—Central venous pressure and volume status are relevant parameters for characterization of a patient's hemodynamic condition; however, their invasive assessment is affected by various risks while non-invasive approaches provide limited and subjective indications. Here we explore the possibility of assessing venous pulse wave velocity (vPWV), a potential indicator of venous pressure changes. In eight healthy patients, pressure pulses were generated artificially in the leg veins by rapid compression of the foot, and their propagation was detected at the level of the superficial femoral vein with Doppler ultrasound. Changes in leg venous pressure were obtained by raising the trunk from the initial supine position by 30° and 60°. vPWV increased from 1.78 ± 0.06 m/s (supine) to 2.26 ± 0.19 m/s (60°) ($p < 0.01$) and exhibited an overall linear relationship with venous pressure. These results indicate that vPWV can be easily assessed, and is a non-invasive indicator of venous pressure changes. (E-mail: silvestro.roatta@unito.it)

Key Words: **Pulse wave velocity, Central venous pressure, Echo Doppler, Hemodynamics.**

INTRODUCTION

The central venous pressure and volemic status of the patient are relevant hemodynamic variables in understanding a patient's condition and the management of fluid therapies (Monnet and Teboul 2018). Given the risk associated with invasive measurements, there is a compelling need for reliable non-invasive assessment techniques. Different non-invasive approaches have been proposed, each suffering some limitation (Uthoff et al. 2012). Analysis of the pulsatility of the inferior vena cava is commonly adopted (Nagdev et al. 2010), although the caval index is affected by several confounding factors (Via et al. 2016). The traditional assessment of the point of collapse of the jugular vein (Rizkallah et al. 2014; Xing et al. 2015) cannot be used in supine patients or in the presence of surgical interventions or treatments in the neck area. Compression of superficial veins has recently been proposed for assessing peripheral venous pressure (Crimi et al. 2016), which, however, only approximates central venous pressure in certain patient conditions (Rizkallah et al. 2014; Via et al. 2016). On this basis, it is appropriate to consider alternative/additional methodologies such the assessment of pulse wave velocity (PWV) in the venous compartment. PWV has been largely investigated in arteries, and it is by now a well-established index of cardiovascular risk (Boutouyrie et al. 2009; Pereira et al. 2015) while investigations on venous PWV (vPWV) are scarce, possibly because of the lack of a regular natural pulsation in the venous flux and the small associated blood pressure changes. To our knowledge only two studies have investigated vPWV in human patients: one conducted on patients with "prominent superficial veins", the pressure pulse being generated by their digital compression/decompression (Mackay et al. 1967), and the other based on the small natural pulsation of the venous flux detected by echo-Doppler at the level of subclavian and femoral arteries (Nippa et al. 1971). Although these early investigations consistently indicated a linear dependence of vPWV on venous blood pressure (Mackay et al. 1967; Anliker et al. 1969; Nippa et al. 1971; Minten et al. 1983), this line of research was not followed up, possibly because of ineffective methodologies.

The aim of this study was to develop a non-invasive, objective method to measure vPWV as a preliminary step

Address correspondence to: Silvestro Roatta, c.so Raffaello 30, 10125, Torino, Italy. E-mail: silvestro.roatta@unito.it

before carrying out more thorough investigations on its reliability and sensitivity to hemodynamic challenges functional in possible future applications in the clinical setting. To work with clear-cut and repeatable pulse waves, we externally generated the waves by pneumatic compression of the foot and proximally detected the waves at the level of the femoral vein by Doppler ultrasound while leg venous pressure (LVP) was modulated by changing the reclination of the trunk.

METHODS

Patients

The experiment was conducted on eight healthy volunteers (aged 31 ± 9 y) with no exclusion criteria. The study was approved by the ethics committee of the University of Torino (March 23, 2015), and all participants gave their informed consent according to the principles of the Helsinki Declaration.

Measurement setup

Figure 1 is an overview of the experimental setup. A rapid compressive stimulus is delivered to the foot by rapid inflation (peak pressure: 200 mm Hg, duration: 1 s, inflation time: 400 ms) of a pneumatic cuff (49 × 15 cm, GIMA, Gessate, Italy). This is achieved with a custom PC-controlled system previously developed for the investigation of compression-induced rapid dilation in skeletal muscles (Messere et al. 2017b, 2018). Adapted, semi-rounded plastic foam paddings were applied under the sole and above the dorsum of the foot to achieve a quasi-cylindrical shape, adequate to be wrapped by the cuff. The trigger for the stimulus is provided by the participant by pressing a hand-held button. The foot compression generates a pressure pulse that propagates proximally along venous vessels and can be detected by Doppler ultrasound (MyLab 25 Gold, ESAOTE, Genova, Italy; equipped with linear probe LA523) at the level of the superficial femoral vein (SFV), distal to the inguinal ligament. Venous blood velocity is recorded by means of a linear probe, with the transverse approach and an incident angle of about 60° (Messere et al. 2017a). The cuff pressure was continuously monitored by a pressure sensor placed at the cuff outlet (pressure monitor BP-1, WPI, Sarasota, FL, USA), and the corresponding electrical signal was acquired by the acquisition system (Micro 1401 IImk, CED, Cambridge, UK, with Spike2 software), along with the Doppler signal and the signal from the button. The same digital board provided the trigger for cuff inflation by the pneumatic system.

Vessel size and peripheral venous pressure

The cross-sectional area of the SFV was calculated from a transverse echographic scan in B-mode, the linear probe oriented at 90° with respect to the vein axis. Leg venous pressure (in mm Hg) in the SFV was estimated as the hydrostatic load relative to the vertical distance (VD, in cm) between the venous point of collapse (*i.e.,* the point at which venous pressure approaches 0 mm Hg) and the leg (its mid-height), lying horizontally on the bed: LVP = 1.05 × 1.36 × VD. The venous point of collapse was echographically sought along the jugular vein (Rizkallah et al. 2014; Xing et al. 2015) when the trunk was reclined at 30° and 60° and along the basilic vein, when the participant was completely supine (trunk angle of 0°), the right arm being transiently and passively raised vertically for this purpose. The venous point of collapse was visualized with a

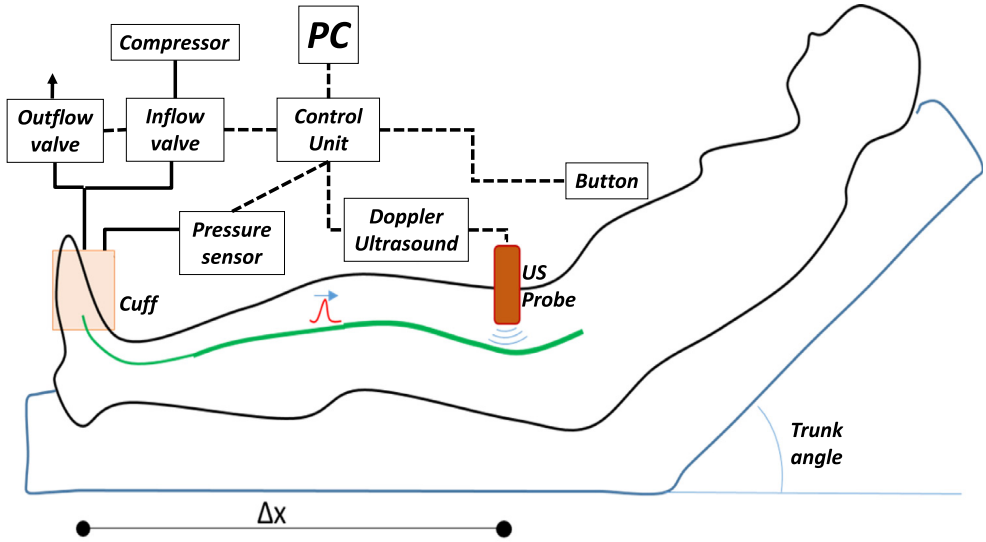

Fig. 1. Experimental setup. Electrical and pneumatic connections are indicated by *dashed and solid lines*, respectively.

second dedicated ultrasound machine (Mylab 25 XView, Esaote, with linear array LA 523).

Experimental protocol

The participant remained supine for at least 30 min (Hagan et al. 1978; Folino et al. 2017) before starting with the measurements; then the participant assumed three different positions. The legs were maintained horizontal while the trunk was reclined to 0°, 30° or 60°, in random order, thus affecting LVP through modification of the hydrostatic load (Uthoff et al. 2012; Xing et al. 2015). The participant, while breathing normally, was asked to periodically (approximately every 20−30 s) press the hand-held button at the end of the expiratory phase, thus triggering delivery of the pressure pulse. This allowed us to focus the measurement on the most reproducible respiratory condition (functional residual capacity) and exclude the potential interference of respiratory activity with vPWV, given its effects on venous blood pressure and flow (Folino et al. 2017). The control unit made sure that consecutive pulses were at least 20 s apart, ignoring the button signal otherwise. A series of 15 pulses were delivered in each position to assess vPWV 15 times consecutively. After a series was completed, the vessel cross-sectional area was measured and the LVP estimated (see above).

Data analysis

The Doppler signal was sampled at the rate of 10 kHz and was exported from Spike2 (Fig. 2a) to MATLAB for offline analysis: a custom-made algorithm was developed to extract the maximum velocity profile from the time−frequency representation of the signal and to identify the footprint of that profile (Boutouyrie et al. 2009). As a first step, the signal was cut into 1-s epochs, using the instant at which the control unit delivered the trigger for cuff inflation (t_0) as reference time, to isolate only those portions of the entire recording in which the passage of the PW definitely occurred. Then, the signal was digitally bandpass filtered with cutoff frequencies of 100 and 2000 Hz (approximately equivalent to 3−60 cm/s in terms of blood velocity). Afterward, the signal was transformed to be analyzed in the time−frequency plane by means of the wavelet synchrosqueezed transform. We chose this technique because, besides being a continuous wavelet transform (CWT) and therefore appropriate for dealing with signals whose frequency spectrum varies rapidly over time (Boashash 2015), it presents a reduced energy smearing with respect to classic CWTs and preserves the native resolution in the time domain (Thakur et al. 2013). The latter two properties were very useful in the present case because of the low intensity of the venous flow and the need to precisely

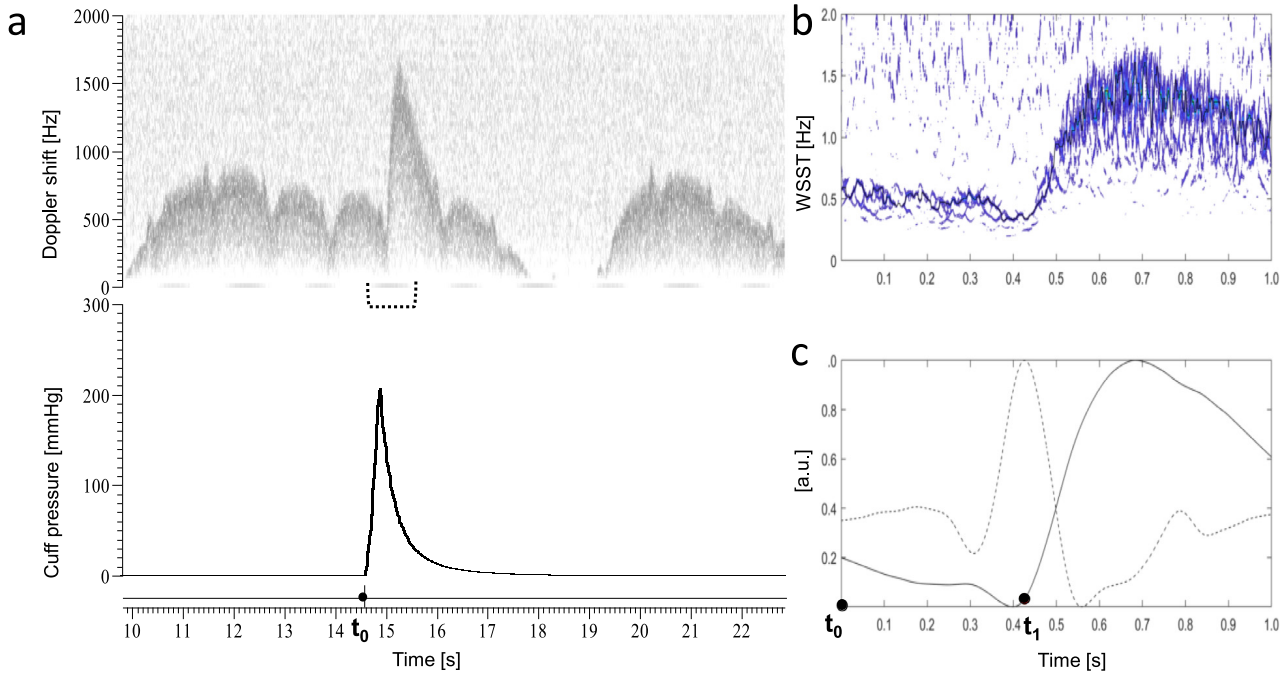

Fig. 2. Representative recording and processing. (a) Venous pulse wave as detected by Doppler ultrasound (upper trace), at the superficial femoral vein, after delivery of a compressive stimulus to the foot (lower trace) at time t_0. Post-processing of the 1-s epoch indicated by the *dashed line* is on the right: (b) Wavelet synchrosqueezed transform (WSST) of the Doppler signal. (c) Smoothed normalized maximum energy profile of WSST (*solid line*) and its normalized second derivative (*dashed line*), whose maximum identifies the footprint of the profile (t_1).

localize the reference point in time, respectively. Once the signal was transformed (Fig. 2b), the maximum velocity profile was extracted by linking all the maximum energy points along the time axis. The profile was subsequently smoothed by a local regression using the weighted linear least-squares method, and a first-degree polynomial model was applied by a sliding window of 200 ms. Finally, the footprint was identified as the instant t_1 at which the second derivative of the velocity profile reaches its maximum (Fig. 2c). The pulse wave (PW) transit time, from ankle to insonation site, was computed as $\Delta t = t_1 - t_0 -$ Lat, where t_0 is the time at which the control unit delivered the trigger for cuff inflation, and Lat is latency between t_0 and the time at which the PW can be detected along the great saphenous vein at the ankle level. This latency, which accounts for most of the mechanical delays in the pneumatic circuit, was set to 50 ms, based on measurements carried out in preliminary experiments. The vPWV was then calculated as the ratio of the traveled distance (Δx = ankle−probe distance) and the PW transit time: vPWV = $\Delta x/\Delta t$. Occasional odd vPWV values, attributed to failure of the algorithm because of low signal-to-noise ratio of the Doppler signal, were automatically identified as values beyond three times the mean absolute deviation and removed.

The intra-participant variability of the vPWV measurements was quantified by the coefficient of variation (CoV = standard deviation [SD]/mean × 100), and the average vPWV value was then computed for each condition. The effect of trunk position on vPWV was assessed by a paired one-way analysis of variance, followed by the Tukey−Kramer *post hoc* test. The same was done for LVP and vessel cross-sectional area. Finally, the correlation between LVP and vPWV was assessed with Pearson's coefficient.

All values reported in the Results section are expressed as the mean ± SD.

RESULTS

Body posture significantly affected blood pressure ($p < 0.01$) and volume ($p < 0.01$) of the leg venous compartment. The estimated LVP increased from 8 ± 3 to 26 ± 2 mm Hg, and the cross-sectional area of the superficial femoral vein, from 34 ± 22 to 67 ± 34 mm^2, when the trunk was reclined from 0° (supine position) to 60°. The change in posture also affected PW transit time (Δt) ($p < 0.01$), which decreased from 0.384 ± 0.038 s (supine) to 0.303 ± 0.021 s (60°); therefore, vPWV increased from 1.78 ± 0.06 m/s (supine) to 2.26 ± 0.19 m/s (60°). The variability in cuff−probe distance (Δx) was 0.68 ± 0.07 m. These results are graphically summarized in Figure 3. Notably, vPWV exhibits a linear dependence on venous pressure ($r = 0.82$). On the contrary, vessel size exhibits a curvilinear pattern, suggestive of increasing vessel stiffness with increasing pressure.

Single measurements of vPWV exhibited little intra-participant variability, as expressed by the CoV: 5.6 ± 2.5% when averaged across all patients and conditions. Individual values of vPWV were also quite similar in the supine condition (CoV = 3.1%) but did spread over a wider range at increased LVP (see error bars in Fig. 3a).

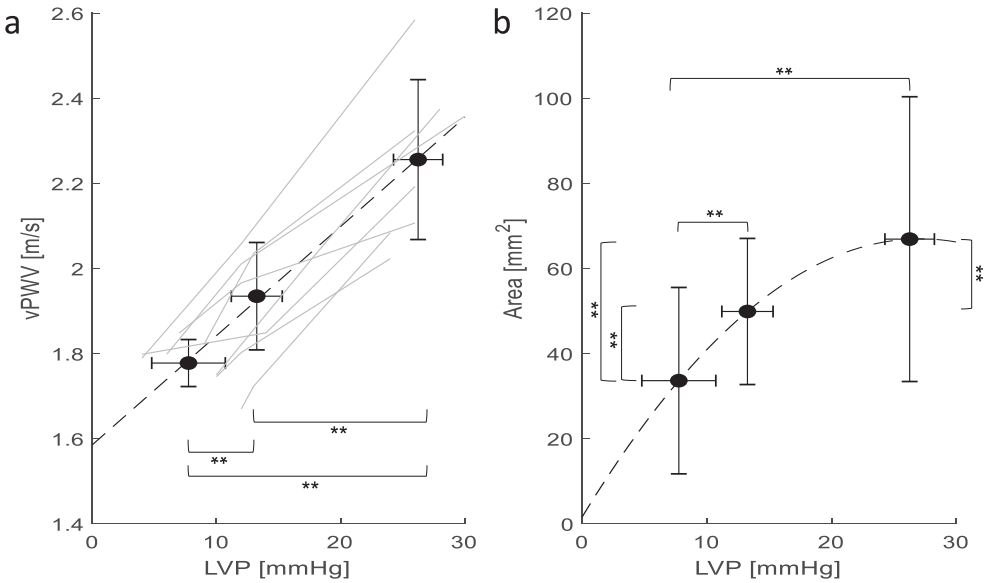

Fig. 3. Average effects of trunk position. The effects on venous pulse wave velocity (a) and vessel size (b) are displayed as a function of the effects on venous pressure in the leg (LVP). *Gray lines* (a) represent the individual responses. The *dashed lines* indicate the best linear (a) and quadratic (b) fitting. Error bars represent standard deviations. *$p < 0.05$. †$p < 0.01$.

DISCUSSION

The present study provides a proof of concept for a new methodology for the assessment of vPWV in humans. Although the reported vPWV values could be slightly overestimated, because we did not subtract the average blood velocity from the measurement, the results are compatible with those of other studies performed in different models and with different techniques, reporting values in the range 1−3 m/s in the supine position (Anliker et al. 1969; Nippa et al. 1971; Minten et al. 1983), while values of 4−15 m/s were reported at venous pressures of 20−80 mm Hg in the arm (Mackay et al. 1967). The linear dependence of vPWV on LVP (Fig. 3a) is also in line with the literature (Mackay et al. 1967; Anliker et al. 1969; Nippa et al. 1971; Minten et al. 1983) and reflects the increase in vessel stiffness at increasing transmural pressure, which is also indicated by the dependence of vessel size on LVP (Fig. 3b). With respect to previous studies, new and relevant achievements may be evidenced: (i) the automatic detection of the footprint of the Doppler signal associated with the pulse wave, thanks to the synchronization between pulse delivery and signal acquisition and to the implementation of specific signal processing algorithms; (ii) the high precision of the measurement (CoV ≈ 6%) compared with previous reports (CoV = 14%) (Nippa et al. 1971). Several reasons have contributed to the latter result: (i) the sharpness of the externally generated pulse wave compared with natural oscillations of venous flow and pressure; (ii) the long distance between delivery and detection of the pulse wave (>60 cm in the present case); and (iii) the synchronization of the measurement with respiratory activity, which cyclically modulates venous pressure (Nippa et al. 1971; Minten et al. 1983).

In the present implementation we included a single Doppler measurement, assuming delay in generation of the pressure pulse to be the same in all patients. Although a measurement based on two simultaneous Doppler readings, at the ankle and the thigh, would be more precise, the present approach has the advantage of requiring a simpler setup and measuring procedure. Future studies will help to shape the best trade-off or to design dedicated measuring devices.

Simultaneous measurement of vPWV and invasive CVP in patients with central venous access may be one way to investigate the direct relation between the two variables. On the other hand, vPWV may turn out to be particularly sensitive to detect changes in hemodynamic conditions, as observed by Felix et al. (1971) in dogs exposed to progressive blood losses. In addition, the possibility of using vPWV to implement automatic and long-term monitoring of the status of the venous compartment is particularly attractive. However, further technical improvements may have to be implemented, and additional studies will be necessary to assess the reliability and validity of this methodology before recommending its possible clinical application.

Acknowledgments—We thank Luca Pastore for his help in running the experiments, as part of his Master's thesis in Biomedical Engineering.

Conflict of interest disclosure—A patent application on the measurement of venous pulse wave velocity has been submitted.

REFERENCES

Anliker M, Wells MK, Ogden E. The transmission characteristics of large and small pressure waves in the abdominal vena cava. IEEE Trans Biomed Eng 1969;16:262–273.
Boashash B. Time−frequency signal analysis and processing: A comprehensive reference. London/San Diego: Academic Press; 2015.
Boutouyrie P, Briet M, Vermeersch S, Pannier B. Assessment of pulse wave velocity. Artery Res 2009;3:3–8.
Crimi A, Makhinya M, Baumann U, Thalhammer C, Szekely G, Goksel O. Automatic measurement of venous pressure using B-mode ultrasound. IEEE Trans Biomed Eng 2016;63:288–299.
Felix R, Sigel B, Amatneek K, Marshall C. Venous pulse propagation velcity in hemorrage. Arch Surg 1971;102:53–56.
Folino A, Benzo M, Pasquero P, Laguzzi A, Mesin L, Messere A, Porta M, Roatta S. Vena cava responsiveness to controlled isovolumetric respiratory efforts. J Ultrasound Med 2017;36:2113–2123.
Hagan RD, Diaz FJ, Horvath SM. Plasma volume changes with movement to supine and standing positions. J Appl Physiol 1978;45:414–417.
Mackay I, Van Loon P, Campos J, de Jesus N. A tecnique for the indirect measurement of the velocity of induced venous pulsation. Am Heart J 1967;73:17–23.
Messere A, Ceravolo G, Franco W, Maffiodo D, Ferraresi C, Roatta S. Increased tissue oxygenation explains the attenuation of hyperemia upon repetitive pneumatic compression of the lower leg. J Appl Physiol 2017a;123:1451–1460.
Messere A, Turturici M, Millo G, Roatta S. Repetitive muscle compression reduces vascular mechano-sensitivity and the hyperemic response to muscle contraction. J Physiol Pharmacol 2017b;68:427–437.
Messere A, Tschakovsky M, Seddone S, Lulli G, Franco W, Maffiodo D, Ferraresi C, Roatta S. Hyper-oxygenation attenuates the rapid vasodilatory response to muscle contraction and compression. Front Physiol 2018;9:1078.
Minten J, Van De Werf F, Auber A, Kasteloot H, De Geest H. Apparent pulse wave velocity in canine superior vena cava. Cardiovasc Res 1983;17:627–632.
Monnet X, Teboul JL. Assessment of fluid responsiveness: Recent advances. Curr Opin Crit Care 2018;24:190–195.
Nagdev AD, Merchant RC, Tirado-Gonzalez A, Sisson CA, Murphy MC. Emergency department bedside ultrasonographic measurement of the caval index for noninvasive determination of low central venous pressure. Ann Emerg Med 2010;55:290–295.
Nippa J, Alexander R, Folse R. Pulse wave velocity in human veins. J Appl Physiol 1971;30:558–563.
Pereira T, Correia C, Cardoso J. Novel methods for pulse wave velocity measurement. J Med Biol Eng 2015;35:555–565.
Rizkallah J, Jack M, Saeed M, Shafer LA, Vo M, Tam J. Non-invasive bedside assessment of central venous pressure: Scanning into the future. PLoS One 2014;9 e109215.
Thakur G, Brevdo E, Fučkar NS, Wu HT. The Synchrosqueezing algorithm for time-varying spectral analysis: Robustness properties and new paleoclimate applications. Signal Process 2013;93:1079–1094.
Uthoff H, Siegemund M, Aschwanden M, Hunziker L, Fabbro T, Baumann U, Jaeger KA, Imfeld S, Staub D. Prospective comparison of noninvasive, bedside ultrasound methods for assessing central venous pressure. Ultraschall Med 2012;33:256–262.

Via G, Tavazzi G, Price S. Ten situations where inferior vena cava ultrasound may fail to accurately predict fluid responsiveness: A physiologically based point of view. Intensive Care Med 2016;42: 1164–1167.

Xing CY, Liu YL, Zhao ML, Yang RJ, Duan YY, Zhang LH, De Sun X, Yuan LJ, Cao TS. New method for noninvasive quantification of central venous pressure by ultrasound. Circ Cardiovasc Imaging 2015;8 e003085.

Paper II

Biomedical Signal Processing and Control 63 (2021) 102177

Contents lists available at ScienceDirect

Biomedical Signal Processing and Control

journal homepage: www.elsevier.com/locate/bspc

Venous Pulse Wave Velocity variation in response to a simulated fluid challenge in healthy subjects

Leonardo Ermini [a], Nadia Elvira Chiarello [b], Carlo De Benedictis [b], Carlo Ferraresi [b], Silvestro Roatta [a,*]

[a] Laboratory of Integrative Physiology, Department of Neuroscience, University of Torino, c.so Raffaello 30, 10125, Torino, Italy
[b] Department of Mechanical and Aerospace Engineering, Politecnico of Torino, c.so Duca degli Abruzzi 24, 10129, Torino, Italy

ARTICLE INFO

Keywords:
Passive leg raising
Venous return
Vessel stiffness
Volume status

ABSTRACT

Purpose: The evaluation of a mini or simulated fluid challenge is still a complex and open issue in the clinical setting and it is of paramount significance for the fluid therapy optimization. We here investigated the capacity of a new hemodynamic parameter, the venous Pulse Wave Velocity (vPWV), to detect the effect of passive leg raising (PLR).

Materials and methods: In 15 healthy volunteers (7 M, 8 F, age 26 ± 3) venous pressure pulses were elicited by pneumatic compressions of the left hand and proximally detected by ultrasound for calculation of the vPWV. We also non-invasively measured the basilic vein (BV) cross-sectional perimeter, and peripheral venous pressure (PVP). The PLR manoeuvre was performed twice to evaluate reliability of the assessment.

Results: The PLR had an overall statistically significant effect on the entire set of variables (MANOVA, $p < 0.05$): vPWV increased from 2.11 ± 0.46 to 2.30 ± 0.47 m/s ($p = 0.01$; average increase: 10%). This effect was transient and dropped below 5% after about 3 min. A significant increase was also exhibited by BV size and PVP. In consecutive measurements vPWV showed little intra-subject variability (CoV = 8%) and good reliability (ICC = 0.87). Finally, the vPWV responses to the two PLRs exhibited good agreement (paired T-test: $p = 0.96$), and moderate reliability (ICC = 0.57).

Conclusion: These results demonstrated that vPWV can be non-invasively, objectively and reliably measured in healthy subjects and that it is adequate to detect small pressure/volume variations, as induced by PLR-from-supine. These characteristics make it suitable for clinical applications.

1. Introduction

In the last decade, the hemodynamics of the venous compartment has begun to receive more and more attention from the medical community, for its fundamental role in maintaining the cardiovascular equilibrium for correct tissue perfusion [1–3]. Since veins are compliant vessels and host 70% of the total blood volume, an albeit small modulation of such big capacity has the potential of redistributing significantly the blood volume among the body compartments, in particular from/to the splanchnic circulation [4]. This possibility has stimulated the interest of intensivists. Indeed, the patient haemodynamic status assessment for optimal fluid management is nowadays a critical and debated problem of paramount importance in intensive care units' everyday life [5,6] and becomes even more complicated when dealing with patients without catheterization. Despite some recent progress regarding the assessment of fluid responsiveness [7,8], an observational study [9] has shown that its clinical relevance is still underestimated and the commonly adopted procedures are often obsolete. For these reasons, during the last years, a lot of effort has been put in developing non-invasive methods, shifting the paradigm from static to dynamic measurements [8,10]. For instance, the hemodynamic transients associated with respiratory activity have been exploited to assess the respiratory variations in pulse pressure, stroke volume and inferior vena cava diameter. However, all these indicators suffer from specific limitations,

Abbreviations: ANOVA, analysis of variance; BSL, baseline; BV, basilic vein; CoV, coefficient of variation; ECG, electrocardiogram; HR, heart rate; ICC, intraclass correlation coefficient; MANOVA, multivariate analysis of variance; PLR, passive leg raising; PVP, peripheral venous pressure; PWV, pulse wave velocity; STD, standard deviation; vPWV, venous Pulse Wave Velocity.

* Corresponding author.
E-mail address: silvestro.roatta@unito.it (S. Roatta).

https://doi.org/10.1016/j.bspc.2020.102177
Received 9 April 2020; Received in revised form 28 July 2020; Accepted 22 August 2020

due to the inherent variability in the respiratory pattern and appeared to be poor predictors of fluid responsiveness in spontaneously breathing patients [10,11]. Compared to spontaneous breathing, passive leg raising (PLR) appears to produce a more reliable hemodynamic perturbation whose response is normally assessed by continuous cardiac output monitoring [12,13], which however is not commonly available [9]. Irrespectively of the adopted monitoring techniques, the emergent concept regarding fluid responsiveness is the willingness to abandon the dichotomous way of thinking (i.e., classifying patients as responders and non-responders) in favour of a continuous classification of the patient haemodynamic status [8,14], possibly integrating more than a single parameter. Based on the above considerations, there is a need for additional indicators of current volume status and of fluid responsiveness.

In line with the above considerations, we here explore a novel approach to the characterization of the venous compartment, potentially adequate to provide additional indications on the patient haemodynamic status [15,16], based on the assessment of a novel haemodynamic parameter: the venous Pulse Wave Velocity (vPWV). The PWV is generally measured in arteries as a widely adopted marker of cardiovascular health, being directly proportional to the vessel stiffness [17–19]. Such relation is potentially exploitable also in veins but with two important differences: 1) the lack of a natural pulsatility in venous blood pressure, which may require that artificial pulses are generated and 2) the low venous pressure, which can be easily disturbed by respiratory as well as cardiac activity. These limitations likely discouraged the investigation of vPWV although it was already shown to be linearly dependent on venous pressure [20–23] and sensitive to blood volume losses [24]. An experimental methodology was recently developed which addresses the above-mentioned limitations by artificially generating a venous pressure pulse at a limb extremity with a pneumatic cuff synchronized with the respiratory cycle, the generated pulse wave being then proximally detected by Doppler Ultrasound [25]. Promising results showed that large (8–26 mmHg) changes in leg venous pressure consistently produced proportional changes in leg vPWV (1.78–2.26 m/s). However, whether this assessment is sensitive enough to detect mild hemodynamic challenges has never been explored in humans.

Thus, this study aimed at assessing whether and to what extent the vPWV responds to a simulated fluid challenge, as provoked by the PLR manoeuvre.

Because of methodological constraints, the PLR had to be conducted from the supine position, thus producing an even smaller hemodynamic challenge than the PLR from the semi-recumbent position [26]. However, compared to our previous study, the stability of the measurement was further improved by synchronizing the measurement non only with the respiratory but also with the cardiac activity. To get an indication of the reliability of the vPWV response, the manoeuvre was repeated twice on each subject. The perimeter of the cross-sectional area of the insonated vein and the peripheral venous pressure were non-invasively assessed as individual quantitative indicators of the magnitude of the fluid challenge.

2. Materials and methods

2.1. Subjects

The experiment was conducted on 15 healthy volunteers (7 M, 8 F, age 26 ± 3) with no exclusion criteria. The study was approved by the ethics committee of the University of Torino (March 23, 2015) and all participants gave their informed consent according to the principles of the Helsinki Declaration.

2.2. Experimental set-up

As anticipated in the introduction, a system was devised for the measurement of vPWV along the arm, based on 1) generation of a pressure wave in venous blood by means of a rapid compression of the hand, 2) synchronous delivery of this compression with respiratory and cardiac activity, 3) proximal detection of the propagated pressure wave by Doppler ultrasound and calculation of the vPWV. Changes in vPWV will be sought during PLR, as compared to the supine position. An overview of the experimental set-up is given in Fig. 1. A pneumatic cuff (49 × 15 cm, GIMA, Gessate, Italy), wrapped around subject's hand, is employed to deliver rapid compressive stimuli to the hand (peak pressure: 400 mmHg, duration: ~1 s, inflation time: 400 ms). This is achieved by a custom PC-controlled system, previously developed for the investigation of the compression-induced rapid dilatation in skeletal muscles [27,28], composed by a compressed air supply (1 bar) and by two, digitally controlled, electro-pneumatic valves (VXE2330-02F-6D01, SMC, Tokyo, Japan), for inflation and deflation of the cuff. A hand sized hot water bag (filled with water at about 40 °C) was placed on the palm of the hand in order to 1) keep the hand warm and well perfused and 2) permit effective wrapping and compression by the cuff. The hand compression generates a pressure pulse that propagates proximally along venous vessels its passage being monitored by Doppler ultrasound (MyLab 25 Gold, ESAOTE, Genova, Italy) equipped with a linear probe (LA523, ESAOTE, Genova, Italy), at the level of the basilic vein (BV), distally to the armpit, with a transversal approach and an incident angle of about 60 deg [29].

Since venous blood flow and pressure may be affected by both respiratory and cardiac activity, the measurements were always performed 1) at the end of the expiratory phase, that is the most reproducible respiratory position (functional residual capacity) [30], and 2) at the same time position within the cardiac cycle: the one corresponding to the lowest blood velocity (which allowed better detection of the pulse wave).

To this aim, the subject was asked to signal the end of expiration by pressing a hand-held button. After the button was pressed, the occurrence of an R-wave was detected on the ECG (recorded by a Grass Physiodata Amplifier Model 15LT, Astro-Med Inc., West Warwick, USA), according to a threshold crossing criterion. The pneumatic compression was then started after adding a further adjustable delay of 0–800 ms from the R-wave detection. Such delay was individually set, after few preliminary trials, at the beginning of each experiment to locate the Doppler-detected pulse wave at the point where blood velocity in the BV exhibited the minimum value, within the cardiac cycle (Fig. 2). In fact, the superposition of the generated pulse wave with the spontaneous oscillations of cardiac origin of the venous blood flow could affect the correct detection of the pulse footprint. By adding this further delay to the detection time of the R-wave it was possible to locate the footprint in-between cardiac fluctuations, thus optimizing its detection.

Finally, the cuff pressure was continuously monitored (to locate, precisely in time, the beginning of the compressive stimulus) by a pressure sensor placed at the cuff outlet (Pressure monitor BP-1, WPI, Sarasota, FL, USA) and digitally recorded (Micro 1401 IImk, CED, Cambridge, UK, with Spike2 software), along with the Doppler audio signal, the ECG and the digital signal from the handheld start button, operated by the subject. The same digital board (Micro 1401 IImk) was also used to drive the two electro-pneumatic valves, which were responsible for the compressive stimuli delivery.

2.3. Vessel size and peripheral venous pressure

The cross-sectional perimeter of the BV was calculated from a transversal echographic scan in B-mode, the linear probe oriented at 90 deg with respect to the vein axis. The blood pressure in the BV (PVP, Peripheral Venous Pressure, in mmHg) was estimated as the hydrostatic load relative to the vertical distance (*vd*, in cm) between the venous point of collapse [31,32], i.e., the point in which venous pressure approaches 0 mmHg, and the mid-height of the chest along the anteroposterior direction: PVP = 1.05 * 1.36 * *vd*. The venous point of

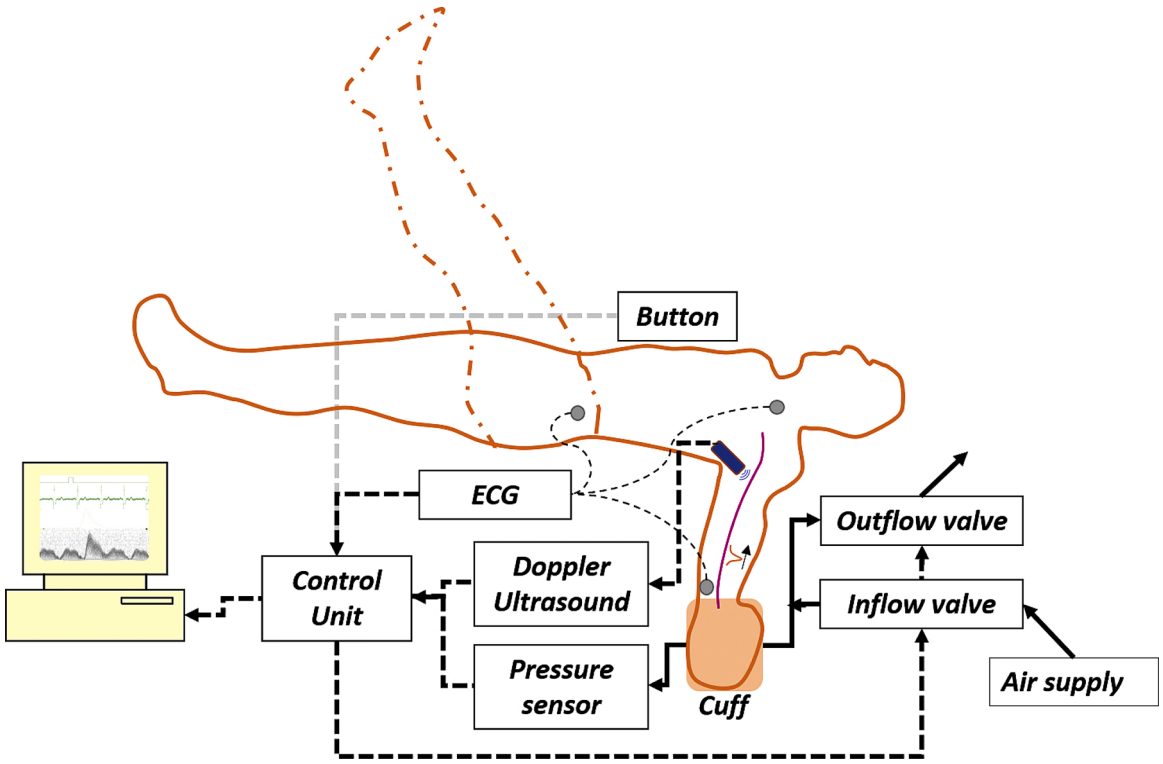

Fig. 1. Experimental set-up: electrical and pneumatic connections are indicated by dashed and solid lines, respectively.

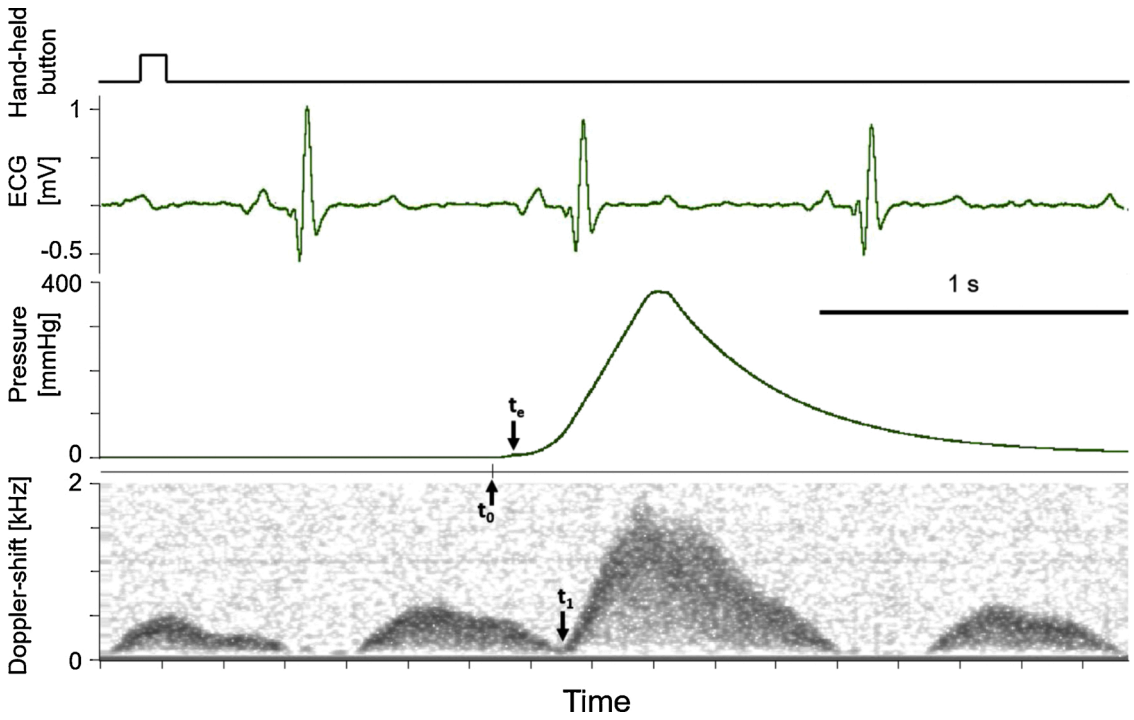

Fig. 2. Illustration of the synchronization process. From top to bottom: signal from the hand-held button, electrocardiogram, cuff pressure and Doppler shift from the ultrasound monitoring of blood velocity in basilica vein. The button is pressed by the subject at the end of expiration; the algorithm then detects the first R-wave on the ECG trace and after a pre-set delay, opens the inflation valve at t0, detects the beginning of cuff inflation at te, and of the passage of the pulse wave at t1.

collapse was echographically sought along the BV of the right arm, which was transiently and passively raised vertically to this purpose. The venous point of collapse was visualized with a second dedicated ultrasound machine (Mylab 25 XView, Esaote, Genova, Italy, with linear array LA 523).

2.4. Experimental protocol

The subject remained supine for at least 30 min [30,33] before starting the experimental protocol: two PLR manoeuvres were performed, PLR1 and PLR2, each lasting about 5 min and separated by

8-min rest in the supine position. The PLR was performed by an operator with the help of a pulley, raising and maintaining the extended legs at an angle of about 45 deg. A series of 8 pneumatic compressions were delivered to the hand during both PLRs (PLR1 and PLR2) and baselines i.e., the 5-min intervals preceding each PLR (BSL1 and BSL2), a vPWV measurement being performed for each pulse. In addition, measurements of BV diameter and peripheral venous pressure were also performed in all conditions.

2.5. Data analysis

The Doppler audio signal was sampled at a rate of 10 kHz and it was exported from Spike2 to Matlab for off-line analysis: a custom-made algorithm was developed to compute the time-domain envelope and to identify the footprint of that profile [17]. As first step, the relevant epochs of 1-s width, starting from the time (t_0) at which the control unit delivered the trigger for cuff inflation, were identified (Fig. 2). Then, the signal was digitally band-pass filtered between 100 and 2000 Hz (approximately equivalent to 3–60 cm/s in terms of blood velocity), after noticing, by visual inspection of the time-frequency representation of the recordings, that no relevant signal component exceeded that frequency band. Afterwards, the upper root-mean-square envelope of the signal was computed [34,35] and subsequently smoothed by a local regression using the weighted linear least squares method and a 1st-degree polynomial model applied by means of a sliding window of 200 ms. Then, the footprint of the velocimetric profile, containing the detected PW, was identified as the instant t_1 at which the envelope reaches 5% of its baseline-to-peak amplitude. Finally, the PW transit time, from wrist to insonation site, was computed as $\Delta t = t_1 - t_e$, where t_e is the instant at which the cuff pressure rose above 2 mmHg i.e., the instant at which the compression of the hand really begins and therefore it is also the instant at which the PW is generated (Fig. 2). The vPWV was then calculated as the ratio of the travelled distance (Δx = wrist-probe distance) and the PW transit time: vPWV = Δx / Δt. Occasional odd vPWV values, attributed to the failure of the algorithm due to low signal-to-noise ratio of the Doppler signal, were automatically identified as the values beyond three times the Mean Absolute Deviation and then removed.

The Heart Rate (HR) was computed, from the instantaneous heart rate derived from the ECG signal, as the average over a 20-s interval prior to each pressure pulse delivery in order to include several respiratory cycles, as HR is modulated by respiration. The vessel cross-sectional perimeter was measured both before (P_{start}) and after (P_{end}) the delivery of the series of 8 compressive stimuli, while the PVP was estimated only at the end of each series.

A preliminary assessment of the transient effect of PLR on vPWV was performed in order to define the time interval over which the response to the manoeuvre could be evaluated. All the vPWV measurements were expressed as percentage change relative to the respective baseline value (average of all values in BSL1 or BSL2) and aligned in time with respect to the moment of legs raising; then, the linear regression (robust least-squares fit, based on a bisquare weighting of the residuals, as provided by the Matlab function '*fit*') of the entire data set was used to model the trend and to select the time at which the PLR effect on vPWV fell below 5% (arbitrarily set upon visual inspection): only data points preceding that time were used to compute the average vPWV value during PLR and the others were excluded from the subsequent analysis. The same time interval was used to assess the effect on HR. This procedure for the definition of the time interval based on experimental data was adopted because the time course of the PLR induced effect on vPWV was not known *a priori*.

2.6. Statistics

As a first step, a multivariate analysis of variance (2-way repeated measurements MANOVA) was performed taking into account the absolute values of the entire set of variables, in order to evaluate the effect of the 2 within-subject factors i.e., the manoeuvre (BSL vs. PLR) and its repetition (1 vs. 2), and eventually assess their interaction. Prior check of multivariate normality assumption was performed by multiple univariate Shapiro-Wilk tests. Then, in order to evaluate the two above mentioned factors on vPWV alone (i.e., from a univariate point of view), a 2-way repeated measurements ANOVA was performed. Finally, since the experimental design didn't allow to apply post-hoc (no between-subject factors), multiple paired T-tests were performed in order to compare, separately, BSL1 vs. PLR1, BSL2 vs. PLR2, BSL1 vs. BSL2 and PLR1 vs. PLR2, for each variable.

Reliability of vPWV response to PLR was assessed comparing the two consecutive PLR-induced changes with respect to the averaged baseline value (i.e., ΔvPWV), specifically assessing the effect of the manoeuvre irrespective of the alterations in the baseline values, by means of paired T-test, Spearman correlation coefficient and single-measurement, absolute-agreement, 2-way mixed-effects model Intraclass Correlation Coefficient (ICC) [36]. Finally, the intra-subject variability of the vPWV measurements acquired during BSL1, was quantified by the coefficient of variation (CoV = STD / mean * 100), averaged across all subjects, while their level of reliability was assessed by the multiple-measurements, absolute-agreement, 2-way mixed-effects model ICC.

All the values reported in the results section are expressed in terms of MEAN ± STD and the level of significance, was set at 0.05 for each statistical test, unless otherwise reported.

3. Results

Single measurements of vPWV in resting conditions (BSL1) exhibited little intra-subject variability, as expressed by the CoV = 7.7 ± 2.9%, and a good level of reliability, as expressed by the ICC = 0.87 (95% confidence interval = 0.75–0.94).

In response to PLR vPWV transiently increased. The regression line fitted to the vPWV data, collected during PLR1 and normalized to baseline, exhibited a negative slope of 3.7%/min and crossed the +5% threshold at 179 s (~3 min), while during PLR2 the rate was 1.2%/min and the cross happened at 242 s (~4 min).

On a multivariate basis (i.e., considering all the physiological variables measured) the 2-way repeated measurements MANOVA showed that PLR had an overall statistically significant effect ($p = 0.02$) with no significant difference between PLR1 and PLR2 ($p = 0.13$). However, on a univariate basis (i.e., considering only the vPWV absolute values) the 2-ways repeated measurements ANOVA showed that vPWV was significantly affected by PLR ($p < 0.01$) and manoeuvre repetition ($p < 0.05$). The results of the T-tests are reported graphically in Fig. 3, by means of symbols.

During PLR1 (Fig. 3) vPWV increased from 2.11 ± 0.46 to 2.30 ± 0.47 m/s ($p = 0.01$), HR decreased slightly from 74 ± 7 to 70 ± 9 bpm ($p = 0.02$), P_{start} increased from 17.9 ± 2.8 to 19.0 ± 3.4 mm ($p = 0.04$) while P_{end} was practically unaffected ($p = 0.44$) and PVP increased slightly from 11.1 ± 1.9 to 11.6 ± 2.4 mmHg ($p = 0.05$). The response to PLR2 (Fig. 3) was similar, with vPWV increasing from 1.93 ± 0.40 to 2.12 ± 0.46 m/s ($p = 0.01$), while HR change was no longer significant ($p = 0.77$) and P_{end} remained significantly above the pre-PLR2 value ($p = 0.02$).

In terms of percentage change, vPWV exhibited a large increment compared to the other variables: vPWV showed a variation of 10 ± 14% and 10 ± 15%, HR of -3 ± 4% and 1 ± 11%, P_{start} of 6 ± 10% and 8 ± 8%, P_{end} of 2 ± 7% and 6 ± 9 and PVP of 4 ± 7% and 6 ± 9%, for PLR1 and PLR2 respectively.

A comparison of the vPWV response to PLR1 (X-axis) and PLR2 (Y-axis) for the different subjects is qualitatively shown in Fig. 4. It can be observed that most subjects responded similarly to the two manoeuvres (segments oriented at about 45 deg), while only few, having a small magnitude of response, exhibited markedly different patterns. On an individual basis, vPWV exhibited a mean increase of at least 5%, with

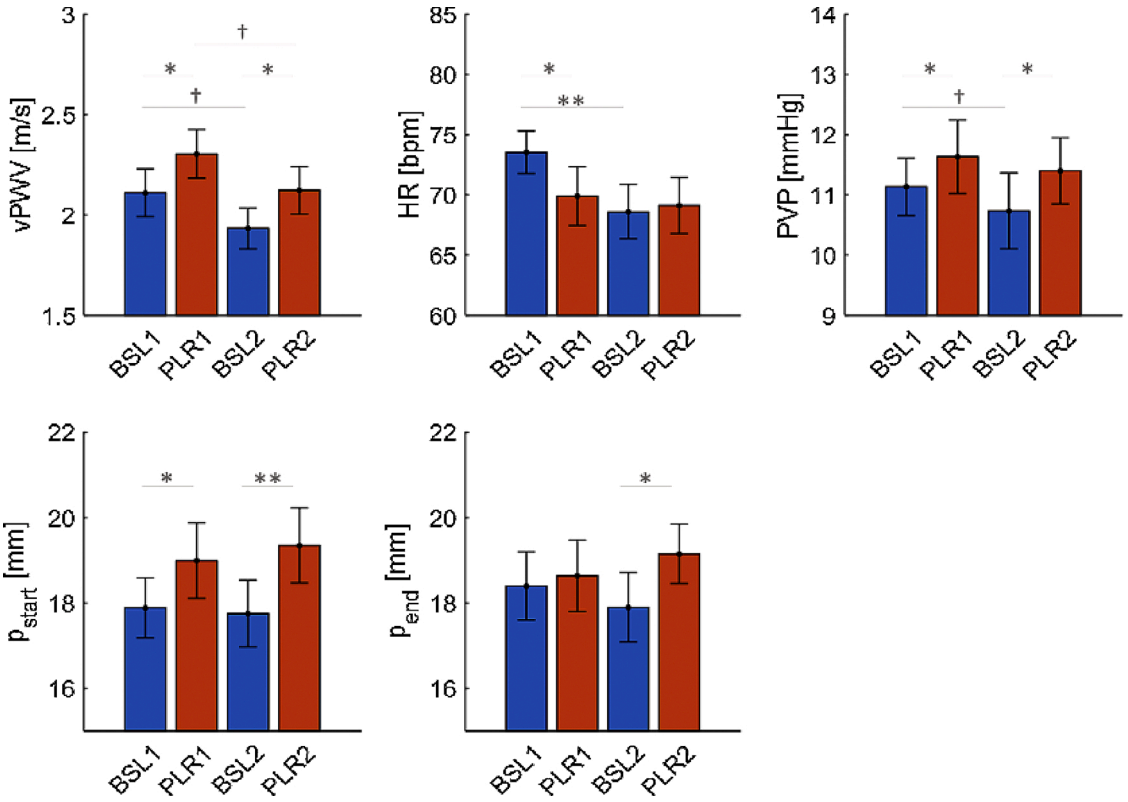

Fig. 3. Average effect of PLR on physiological parameters. The blue bars represent the baselines values and the red ones the values recorded during PLRs. Error bars represent standard errors. Statistical significance, as assessed by paired T-test, is also reported (†: $p < 0.10$; *: $p < 0.05$; **: $p < 0.01$).

respect to the mean baseline value, in 10/15 and 8/15 subjects (i.e., responders) in response to PLR1 and PLR2, respectively. It is worth to notice that the 8 responders to PLR2 were also responders to PLR1. Although the responses of vPWV (ΔvPWV) to PLR1 and PLR2 were moderately correlated (Spearman correlation coefficient: 0.56, $p < 0.05$) and their level of reliability was moderate (ICC = 0.57, 95% CI = -0.36–0.86), they showed good agreement when compared by paired T-test ($p = 0.96$).

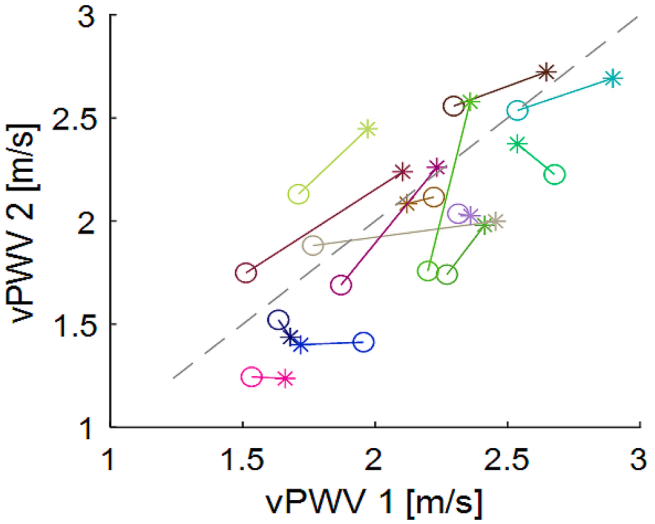

Fig. 4. Comparison of vPWV responses to PLR1 and PLR2. The X-axis and Y-axis report the vPWV values during BSL1 and BSL2 (circles) and PLR1 and PLR2 (stars), respectively, straight lines joining circle and star of individual subjects. The dashed grey line is a 45-degree reference line indicating the slope corresponding to ideal reproducibility.

4. Discussion

With the present study, we showed for the first time that by assessing vPWV it is possible to detect simulated changes in blood volume, as produced by PLR in healthy subjects. Although transient in nature (1–3 min) [5,26,37,38], the effect was quite consistently observed in 2 PLR manoeuvres performed in sequence.

In this respect, it is important to emphasize that the PLR from the supine position, as was performed in the present study, is a rather mild hemodynamic stimulus: indeed, in order to maximize the volume of blood that is displaced from the legs to the rest of the body, it is generally advisable to start the PLR from the semi-recumbent position, in which case the amount of displaced blood is estimated in the order of 300 mL [26,39]. Based on the observation that the cross-sectional area of the superficial femoral vein decreases by approximately 50% when moving from the semi-recumbent (60-deg inclination of the trunk) to the supine position [25] we can roughly estimate that the blood volume displaced by the PLR is also reduced by the same amount, if starting from the supine rather than the semi-recumbent position, i.e., resulting in about 150 mL. For this reason, PLR from supine may be little effective [26,40] and result as a poor predictor of fluid responsiveness [12,41]. In the present study, we could not start from the semi-recumbent position, due to the methodological constraints related to the vPWV measurement in upper limbs. In spite of the relative weakness of the PLR-from-supine manoeuvre confirmed by the small changes observed in PVP, HR, and basilic vein size, vPWV effectively detected the hemodynamic challenge, exhibiting an overall significant increase and moderate repeatability in the response to the two manoeuvres. Notably, a PLR-induced increase in vPWV larger than 5% was observed only in about 2/3 of the subjects, which can be ascribed to the weakness of the stimulus as well as to individual differences in basal volume status, in the compliance of central venous compartments and in autonomic reactivity. This result is in line with other studies which identified responders and non-responders to

simulated fluid challenges [37,42].

To our knowledge, the vPWV variation in response to a real or simulated fluid challenge has not been previously investigated in humans. The only similar study was performed in anaesthetized dogs during progressive haemorrhage [24]. Interestingly the authors already noticed better sensitivity of vPWV to blood loss, as compared to standard haemodynamic parameters such as arterial blood pressure, highlighting the potentiality of this parameter, that, it is worth remembering, takes into account not only the pressure alone but the working status of the vessels in terms of compliance, which is a more holistic approach. Unfortunately, after few investigations carried out in the seventies [20–24] the interest on vPWV decreased, possibly due to the lack of proper instrumentation and/or to the high variability in the measurement, e.g. CoV = 14% [23].

The low variability (CoV about 8%), good reliability (ICC = 0.87) and, consequently, the good sensitivity of vPWV to simulated changes in blood volume achieved in the present study likely depends on the methodological arrangements implemented in the measurement. In particular, the generation of the compressive stimuli was synchronized both with respiration and with the ECG, which allowed to deliver the pulse always in the same respiratory phase (end of expiration) and in the same phase of the cardiac cycle. In this way, we could get rid of two major disturbing factors given that venous blood flow and pressure are affected by large respiratory modulation [22,23,43], as well as by cardiac perturbations, backward propagating from the right heart and/or directly transmitted from pulsating neighbouring arteries [22,43,44]. In addition, the implementation of a dedicated algorithm to automatize the footprint detection and therefore the vPWV estimation, allowed us to obtain a totally operator-free and objective measurement.

The vPWV variation in response to PLR1 was not correlated with that of PVP. This is only apparently in contrast with previous observations reporting a dependence of vPWV on venous pressure [20–23,25]. In fact, in the present case, each point refers to a different subject and the changes in venous pressure are in the order of 1 mm Hg or less, i.e., a very low value and, as such, poorly measured by the non-invasive technique adopted. However, PLR also produced a significant increase in BV size, as indicated by P_{start} (+ 6%). It should also be observed that a larger figure would be exhibited by a vessel size expressed in terms of cross-sectional area (which reflects the changes in volume, the vessel length being constant). On this basis, it may be reasonably concluded that the simulated increase in blood volume by PLR affected mainly the "unstressed volume" of the upper body [3,4].

It is interesting to analyse the post-effects of PLR by comparing BSL2 vs. BSL1. While the BV size is unchanged, there is a tendency towards lower PVP ($p = 0.08$), and an almost significant decrease in vPWV ($p = 0.06$) (see Fig. 3): this is suggestive of a decreased sympathetically-mediated vascular tone of the venous compartment. The hypothesis of reduced sympathetic outflow is in line with the observed concomitant decrease in HR (Fig. 3) and find supports in the literature. In fact, it has been reported that central volume loading, as can be obtained for example by head-down tilt [45] or lower body positive pressure, produces sympathetic inhibition [46], with effects that may outlast the duration of the stimulus [47]. It is remarkable that, in spite of the post-effects of PLR1 and the ensuing differences between BSL1 and BSL2, the vPWV response to PLR2 was still quite well correlated to PLR1 (Fig. 4), achieving moderate reliability.

4.1. Potential for clinical applications

Besides a few potential drawbacks, namely the complexity of equipment and experimental set-up and the necessity to operate on a full limb, the proposed technique has several appealing characteristics for clinical applications. First of all, this measurement has a high sensitivity to mild hemodynamic challenges, whose demonstration is a major outcome of the present study. Secondly, the measurement is objective, the intervention of the operator being limited to positioning electrodes and probes and in selecting the delay for appropriate delivery of the pulse with respect to the R-wave of the ECG. Thirdly, the measurement is non-invasive and can be repeatedly performed. The maximum time resolution (related to the maximum frequency of the measurement) has not been specifically tested, as yet. A minimum time interval is required for the limb extremity to refill and this may depend on the actual circulatory conditions. A frequency of about 2–3/min as operated in the present study is rather high and adequate to describe fast hemodynamic transients, such as the response to PLR.

With these characteristics the technique is adequate for long term patient monitoring and, for example, it could be potentially useful to provide quantitative and objective monitoring of progressive vascular filling during fluid administration in depleted patients or for early detection of excessive fluid depletion in patients undergoing dialysis. As for the capacity of vPWV to predict fluid responsiveness, additional studies are necessary in which vPWV is compared to other parameters, like cardiac output or stroke volume, in response to simulated fluid challenges.

5. Limitations

The subjects had to actively signal the end-expiratory phase. In future studies, the automatic detection of the end-expiratory phase should be implemented in order to avoid any active involvement of the subject, which could possibly influence the autonomic balance and affect the measurement.

Due to the above limitation, the measurements were not perfectly timed with respect to the start of PLR, in addition, the different variables were measured at different times. This may have underestimated the maximum variations exhibited by the different variables. In fact, it is generally known that adaptation occurs in the system and that the hemodynamic effect of PLR tends to fade away within minutes. This phenomenon appears poorly described in the literature [37,48] but it deserves attention as it could reveal additional characteristics of the body response to fluid challenges. In this respect, vPWV could be one of the meaningful variables to consider.

Finally, the comparison between PLR1 and PLR2 cannot constitute a real repeatability study, since the two manoeuvres were separated by a short resting interval and the variables were not completely returned to control (pre-PLR1) levels.

6. Conclusions

The vPWV was shown to effectively detect a mild central volume loading, as obtained by the passive leg raising form the supine position, which produced only minor changes in peripheral venous pressure (<1 mmHg). This new hemodynamic index is objectively and non-invasively assessed, sensitive to mild hemodynamic challenges and characterized by low variability and good reliability of the measurement. For these reasons, it appears to have great potential for clinical applications.

CRediT authorship contribution statement

Leonardo Ermini: Conceptualization, Methodology, Software, Formal analysis, Data curation, Writing - original draft, Writing - review & editing, Visualization. **Nadia Elvira Chiarello:** Software, Validation, Formal analysis, Writing - original draft, Visualization. **Carlo De Benedictis:** Methodology, Writing - review & editing. **Carlo Ferraresi:** Methodology, Resources, Writing - review & editing, Supervision. **Silvestro Roatta:** Conceptualization, Methodology, Resources, Writing - review & editing, Supervision.

Acknowledgments

This activity was supported by local grants (ROAS_RILO_17_01,

University of Torino). No conflicts of interest, financial or otherwise, are declared by the authors.

Declaration of Competing Interest

The authors LE, CDB, CF, and SR have submitted a patent application concerning the assessment of venous pulse wave velocity.

References

[1] H.D. Aya, M. Cecconi, Can (and should) the venous tone be monitored at the bedside? Curr. Opin. Crit. Care 21 (2015) 240–244, https://doi.org/10.1097/MCC.0000000000000199.

[2] D.J. Funk, E. Jacobsohn, A. Kumar, The role of venous return in critical illness and shock-Part I: physiology, Crit. Care Med. 41 (2013) 255–262, https://doi.org/10.1097/CCM.0b013e3182772ab6.

[3] S. Gelman, Venous Function and Central Venous Pressure, Anesthesiology 108 (2008) 735–748, https://doi.org/10.1097/ALN.0b013e3181672607.

[4] C.C. Pang, Autonomic control of the venous system in health and disease: effects of drugs, Pharmacol. Ther. 90 (2001) 179–230.

[5] W.L. Miller, Fluid volume overload and congestion in heart failure, Circ. Hear. Fail. 9 (2016) 1–9, https://doi.org/10.1161/CIRCHEARTFAILURE.115.002922.

[6] A. Rhodes, L.E. Evans, W. Alhazzani, M.M. Levy, M. Antonelli, R. Ferrer, A. Kumar, J.E. Sevransky, C.L. Sprung, M.E. Nunnally, B. Rochwerg, G.D. Rubenfeld, D. C. Angus, D. Annane, R.J. Beale, G.J. Bellinghan, G.R. Bernard, J.-D. Chiche, C. Coopersmith, D.P. De Backer, C.J. French, S. Fujishima, H. Gerlach, J.L. Hidalgo, S.M. Hollenberg, A.E. Jones, D.R. Karnad, R.M. Kleinpell, Y. Koh, T.C. Lisboa, F. R. Machado, J.J. Marini, J.C. Marshall, J.E. Mazuski, L.A. McIntyre, A.S. McLean, S. Mehta, R.P. Moreno, J. Myburgh, P. Navalesi, O. Nishida, T.M. Osborn, A. Perner, C.M. Plunkett, M. Ranieri, C.A. Schorr, M.A. Seckel, C.W. Seymour, L. Shieh, K.A. Shukri, S.Q. Simpson, M. Singer, B.T. Thompson, S.R. Townsend, T. Van der Poll, J.-L. Vincent, W.J. Wiersinga, J.L. Zimmerman, R.P. Dellinger, Surviving sepsis campaign: international guidelines for management of sepsis and septic shock: 2016, Intensive Care Med. 43 (2017) 304–377, https://doi.org/10.1007/s00134-017-4683-6.

[7] P.E. Marik, J. Lemson, Fluid responsiveness: an evolution of our understanding, Br. J. Anaesth. 112 (2014) 617–620, https://doi.org/10.1093/bja/aet590.

[8] X. Monnet, J.L. Teboul, Assessment of fluid responsiveness: recent advances, Curr. Opin. Crit. Care 24 (2018) 190–195, https://doi.org/10.1097/MCC.0000000000000501.

[9] M. Cecconi, C. Hofer, J.-L. Teboul, V. Pettila, E. Wilkman, Z. Molnar, G. Della Rocca, C. Aldecoa, A. Artigas, S. Jog, M. Sander, C. Spies, J.-Y. Lefrant, D. De Backer, FENICE Investigators, ESICM Trial Group, Fluid challenges in intensive care: the FENICE study, Intensive Care Med. 41 (2015) 1529–1537, https://doi.org/10.1007/s00134-015-3850-x.

[10] X. Monnet, P.E. Marik, J.L. Teboul, Prediction of fluid responsiveness: an update, Ann. Intensive Care 6 (2016) 1–11, https://doi.org/10.1186/s13613-016-0216-7.

[11] G. Via, G. Tavazzi, S. Price, Ten situations where inferior vena cava ultrasound may fail to accurately predict fluid responsiveness: a physiologically based point of view, Intensive Care Med. 42 (2016) 1164–1167.

[12] X. Monnet, P. Marik, J.-L. Teboul, Passive leg raising for predicting fluid responsiveness: a systematic review and meta-analysis, Intensive Care Med. 42 (2016) 1935–1947, https://doi.org/10.1007/s00134-015-4134-1.

[13] S.T. Vistisen, P. Juhl-Olsen, Where are we heading with fluid responsiveness research? Curr. Opin. Crit. Care 23 (2017) 318–325, https://doi.org/10.1097/MCC.0000000000000421.

[14] K. Cooke, R. Sharvill, S. Sondergaard, A. Aneman, Volume responsiveness assessed by passive leg raising and a fluid challenge: a critical review focused on mean systemic filling pressure, Anaesthesia 73 (2018) 313–322, https://doi.org/10.1111/anae.14162.

[15] S. Gelman, L. Bigatello, The physiologic basis for goal-directed hemodynamic and fluid therapy: the pivotal role of the venous circulation, Can. J. Anesth. 65 (2018) 294–308, https://doi.org/10.1007/s12630-017-1045-3.

[16] S. Magder, Volume and its relationship to cardiac output and venous return, Crit. Care 20 (2016) 1–11, https://doi.org/10.1186/s13054-016-1438-7.

[17] P. Boutouyrie, M. Briet, S. Vermeersch, B. Pannier, Assessment of pulse wave velocity, Artery Res. 3 (2009) 3–8, https://doi.org/10.1016/j.artres.2008.11.002.

[18] M.E. Safar, Arterial stiffness as a risk factor for clinical hypertension, Nat. Rev. Cardiol. 15 (2018) 97–105, https://doi.org/10.1038/nrcardio.2017.155.

[19] Y.-Y. Lin Wang, Did you know developing quantitative pulse diagnosis with realistic haemodynamic theory can pave a way for future personalized health care, Acta Physiol. Oxf. (Oxf) 227 (2019) e13260, https://doi.org/10.1111/apha.13260.

[20] M. Anliker, M.K. Wells, E. Ogden, The transmission characteristics of large and small pressure waves in the abdominal vena cava, IEEE Trans. Biomed. Eng. BME-16 (1969) 262–273, https://doi.org/10.1109/TBME.1969.4502658.

[21] I. Mackay, P. Van Loon, J. Campos, N. de Jesus, A technique for the indirect measurement of the velocity of induced venous pulsation, Am. Heart J. 73 (1967) 17–23.

[22] J. Minten, F. Van De Werf, A. Auber, H. Kasteloot, H. De Geest, Apparent pulse wave velocity in canine superior vena cava, Cardiovasc. Res. 17 (1983) 627–632.

[23] J. Nippa, R. Alexander, R. Folse, Pulse wave velocity in human veins, J. Appl. Physiol. 30 (1971) 558–563.

[24] R. Felix, B. Sigel, K. Amatneek, C. Marshall, Venous pulse wave propagation velocity in hemorrhage, Arch Surg. 102 (1971) 53–56.

[25] L. Ermini, C. Ferraresi, C. De Benedictis, S. Roatta, Objective assessment of venous pulse wave velocity in healthy humans, Ultrasound Med. Biol. 46 (2019) 849–854, https://doi.org/10.1016/j.ultrasmedbio.2019.11.003.

[26] X. Monnet, J.-L. Teboul, Passive leg raising: five rules, not a drop of fluid!, Crit. Care 19 (2015) 18, https://doi.org/10.1186/s13054-014-0708-5.

[27] A. Messere, M. Turturici, G. Millo, S. Roatta, Repetitive muscle compression reduces vascular mechano-sensitivity and the hyperemic response to muscle contraction, J. Physiol. Pharmacol. 68 (2017) 427–437.

[28] A. Messere, M. Tschakovsky, S. Seddone, G. Lulli, W. Franco, D. Maffiodo, C. Ferraresi, S. Roatta, Hyper-oxygenation attenuates the rapid vasodilatory response to muscle contraction and compression, Front. Physiol. 9 (2018) 1078, https://doi.org/10.3389/fphys.2018.01078.

[29] A. Messere, G. Ceravolo, W. Franco, D. Maffiodo, C. Ferraresi, S. Roatta, Increased tissue oxygenation explains the attenuation of hyperemia upon repetitive pneumatic compression of the lower leg, J. Appl. Physiol. 123 (2017) 1451–1460, https://doi.org/10.1152/japplphysiol.00511.2017.

[30] A. Folino, M. Benzo, P. Pasquero, A. Laguzzi, L. Mesin, A. Messere, M. Porta, S. Roatta, Vena cava responsiveness to controlled isovolumetric respiratory efforts, J. Ultrasound Med. 36 (2017) 2113–2123, https://doi.org/10.1002/jum.14235.

[31] J. Rizkallah, M. Jack, M. Saeed, L.A. Shafer, M. Vo, J. Tam, Non-invasive bedside assessment of central venous pressure: scanning into the future, PLoS One 9 (2014), e109215.

[32] C.Y. Xing, Y.L. Liu, M.L. Zhao, R.J. Yang, Y.Y. Duan, L.H. Zhang, X. De Sun, L. J. Yuan, T.S. Cao, New method for noninvasive quantification of central venous pressure by ultrasound, Circ. Cardiovasc. Imaging 8 (2015), https://doi.org/10.1161/CIRCIMAGING.114.003085.

[33] R.D. Hagan, F.J. Diaz, S.M. Horvath, Plasma volume changes with movement to supine and standing positions, J. Appl. Physiol. 45 (1978) 414–417, https://doi.org/10.1152/jappl.1978.45.3.414.

[34] L. Marple, Computing the discrete-time analytic signal via FFT, IEEE Trans, Signal Process. 47 (1999) 2600–2603, https://doi.org/10.1109/78.782222.

[35] A.V. Oppenheim, R.W. Schafer, Discrete-time Signal Processing, Pearson, 2014.

[36] T.K. Koo, M.Y. Li, A guideline of selecting and reporting intraclass correlation coefficients for reliability research, J. Chiropr. Med. 15 (2016) 155–163, https://doi.org/10.1016/J.JCM.2016.02.012.

[37] M.H. Elwan, A. Roshdy, J.A. Reynolds, E.M. Elsharkawy, S.M. Eltahan, T.J. Coats, What is the normal haemodynamic response to passive leg raise? A study of healthy volunteers, Emerg. Med. J. 35 (2018) 544–549, https://doi.org/10.1136/emermed-2017-206836.

[38] X. Monnet, M. Rienzo, D. Osman, N. Anguel, C. Richard, M.R. Pinsky, J.-L. Teboul, Passive leg raising predicts fluid responsiveness in the critically ill*, Crit. Care Med. 34 (2006) 1402–1407, https://doi.org/10.1097/01.CCM.0000215453.11735.06.

[39] J. Jabot, J.L. Teboul, C. Richard, X. Monnet, Passive leg raising for predicting fluid responsiveness: importance of the postural change, Intensive Care Med. 35 (2009) 85–90, https://doi.org/10.1007/s00134-008-1293-3.

[40] G.E.P. Godfrey, S.W. Dubrey, J.M. Handy, A prospective observational study of stroke volume responsiveness to a passive leg raise manoeuvre in healthy non-starved volunteers as assessed by transthoracic echocardiography, Anaesthesia 69 (2014) 306–313, https://doi.org/10.1111/anae.12560.

[41] K. Lakhal, S. Ehrmann, I. Runge, D. Benzekri-Lefèvre, A. Legras, P.F. Dequin, E. Mercier, M. Wolff, B. Régnier, T. Boulain, Central venous pressure measurements improve the accuracy of leg raising-induced change in pulse pressure to predict fluid responsiveness, Intensive Care Med. 36 (2010) 940–948, https://doi.org/10.1007/s00134-010-1755-2.

[42] R.C. de F. Chaves, T.D. Corrêa, A.S. Neto, B. de A. Bravim, R.L. Cordioli, F. T. Moreira, K.T. Timenetsky, M.S.C. de Assunção, Assessment of fluid responsiveness in spontaneously breathing patients: a systematic review of literature, Ann. Intensive Care 8 (2018) 21, https://doi.org/10.1186/s13613-018-0365-y.

[43] K. Nakamura, M. Tomida, T. Ando, K. Sen, R. Inokuchi, E. Kobayashi, S. Nakajima, I. Sakuma, N. Yahagi, Cardiac variation of inferior vena cava: new concept in the evaluation of intravascular blood volume, J. Med. Ultrason. 40 (2013) 205–209, https://doi.org/10.1007/s10396-013-0435-6.

[44] A.A. Joseph, D. Voit, J. Frahm, Inferior vena cava revisited – real-time flow MRI of respiratory maneuvers, NMR Biomed. 33 (2020), https://doi.org/10.1002/nbm.4232.

[45] K. Nagaya, F. Wada, S. Nakamitsu, S. Sagawa, K. Shiraki, Responses of the circulatory system and muscle sympathetic nerve activity to head-down tilt in humans, Am. J. Physiol. 268 (1995) R1289–1294, https://doi.org/10.1152/ajpregu.1995.268.5.R1289.

[46] J. Cui, Z. Gao, C. Blaha, M.D. Herr, J. Mast, L.I. Sinoway, Distension of central great vein decreases sympathetic outflow in humans, Am. J. Physiol. - Hear. Circ. Physiol. 305 (2013) H378, https://doi.org/10.1152/ajpheart.00019.2013.

[47] D. Bosone, V. Ozturk, S. Roatta, A. Cavallini, P. Tosi, G. Micieli, Cerebral haemodynamic response to acute intracranial hypertension induced by head-down tilt, Funct. Neurol. 19 (2004) 31–35, http://www.ncbi.nlm.nih.gov/pubmed/15212114. (Accessed 14 March 14 2020).

[48] N. Duus, D.J. Shogilev, S. Skibsted, H.W. Zijlstra, E. Fish, A. Oren-Grinberg, Y. Lior, V. Novack, D. Talmor, H. Kirkegaard, N.I. Shapiro, The reliability and validity of passive leg raise and fluid bolus to assess fluid responsiveness in spontaneously breathing emergency department patients, J. Crit. Care 30 (2015) 217.e1–217.e5, https://doi.org/10.1016/j.jcrc.2014.07.031.

Paper III

Applications of Intermittent Pneumatic Compression for Diagnostic and Therapeutic Purposes

Carlo Ferraresi[1], Walter Franco[1], Daniela Maffiodo[1], Carlo De Benedictis[1(✉)], Maria Paterna[1], Daniel Pacheco Quiñones[1], Leonardo Ermini[2], and Silvestro Roatta[2]

[1] Department of Mechanical and Aerospace Engineering, Politecnico di Torino, Turin, Italy
carlo.debenedictis@polito.it

[2] Laboratory of Integrative Physiology, Department of Neuroscience, University of Torino, Turin, Italy

Abstract. Intermittent Pneumatic Compression (IPC) technique is prescribed for several treatments, as the management of venous leg ulcers or the prevention of deep vein thrombosis. Commercial devices do not enable the full customization of the compressive patterns due to design specifications and low dynamics. However, IPC can be implemented in a wide scenario of clinical protocols, and not only as a therapeutic tool. In this paper, the results of the research on IPC devices conducted at the Politecnico di Torino (Turin, Italy) are presented. In particular, applications regarding the treatment of the end-diastolic volume (EDV) reduction, the investigation of vascular phenomena as hyperemia, and the assessment of venous pulse wave velocity (vPWV) are discussed. The outcomes of the research demonstrate that IPC technology can lead to the creation of widely used diagnostic, therapeutic and rehabilitative devices.

Keywords: SDG3 · Therapeutic and rehabilitative devices · Intermittent pneumatic compression · Hemodynamics · Hyperemia · vPWV · Pneumotronics · Human-machine interaction

1 Introduction

In an extensive sense, Intermittent Pneumatic Compression (IPC) represents the application of mechanical pressure stimuli on a person's body, which can be either periodic or impulsive. An IPC device consists of one or more inflatable sleeves and an inflating system that allows a controlled and well-defined pressure trend to be applied to the lower or upper limbs of patients. In a first possible application, the applied compression may mimic the action of the muscle pump and promote venous return. For this reason, it can be used for the treatment of various pathologies, such as lymphedema, venous leg ulcers [3–5], prevention of deep vein thrombosis [6, 7], and for the treatment of subjects with limited mobility due to recent surgery or pathological condition.

IPC devices come with either single or multi-chamber sleeves [5]. The latter can provide sequential compression that can push the blood to the central part of the

G. Quaglia et al. (Eds.): I4SDG 2021, MMS 108, pp. 209–218, 2022.
https://doi.org/10.1007/978-3-030-87383-7_23

patient's body; the single-chamber devices, instead, produce controlled compression that is focused to a defined point of the body. The choice of one or the other type of device depends only on the specific application. In recent years, in order to improve the venous blood return and to prevent a reduction in left ventricle end-diastolic volume (EDV) in subjects with a walking disability, a multi-chamber IPC device has been developed at Politecnico di Torino [8–10].

In another application, Ferraresi et al. [11] describe a single chamber IPC device with high dynamic performance and capable to apply a customizable pressure pattern to the limbs of the subject. The device is therefore particularly suitable for research purposes oriented to better understand the mechanism behind the hyperemic response that develops in response to compression stimuli and its attenuation following consecutive compressions [12, 13]. The same device was also employed in a different application, oriented to the non-invasive assessment of a subject's volemic status [14, 15]. It is based on the generation and measurement of the propagation velocity of a pressure wave in the veins, namely the venous Pulse Wave Velocity (vPWV), which is related to vessel stiffness and therefore to vascular filling. The PWV has been used for years to monitor the stiffness of the arteries [16–18], but it is difficult to use it to monitor the venous compartment due to the lack of natural pulsations that therefore must be generated by the IPC device.

This work presents the outcomes of the research activity on IPC devices carried out by the group of functional biomechanics at the Department of Mechanical and Aerospace Engineering (DIMEAS) of Politecnico di Torino, Italy. The activity detailed in this work was carried out in collaboration with relevant research centers, in particular the Laboratory of Integrative Physiology of the University of Torino, Italy and the Laboratory of Sports Physiology of the University of Cagliari, Italy. The diversity of the applications shown in this paper and in the literature signals the relevancy of the research theme. In fact, the improvement of treatments for cardiovascular diseases and the definition of new methodologies for the investigation of hemodynamics are well in agreement with the rationale behind SDG3 promoted by the United Nations, which aims at ensuring healthy lives and well-being.

2 IPC Device for the Improvement of Venous Blood Return

Patients with a walking disability are subjected to a reduction in the EDV of the left ventricle, since the blood pressure gradient between the right atrium and the postcaval vein is normally supplied by effects related to locomotion, as the rhythmic contraction of the triceps surae which compresses the veins in the calf. For this reason, a device aiming to generate intermittent stimulation to the lower limbs can be effectively used to improve the cardiac functionality in those patients.

Ferraresi et al. [8], on the basis of a mathematical modeling, created a multi-bladder IPC device designed to favor the return of venous blood in people with motor deficit in the lower limbs. The mechatronic system was provided with six inflatable bladders integrated within two shells, each mounted on a separate segment (calf and foot, see Fig. 1). The bladders were designed to direct the pneumatic energy towards the limb without dispersion related to the deformation of the materials. Thanks to compliant and

air-tight material, as well as to proper shaping of each bladder, it was possible to achieve good performance of the IPC device.

The control system was based on a group of six 3-way electro-pneumatic valves, six pressure sensors and a programmable logic controller. The valves and pressure sensors were mounted on the calf shell, in order to improve the dynamic performance of the pneumatic system.

Subsequently, Manuello Bertetto et al. [9] applied this device in experimental trials, for objective evaluation of its effectiveness in the enhancement of venous blood return. To assess EDV non-invasively, an equipment able to measure the thoracic electrical bioimpedance was used.

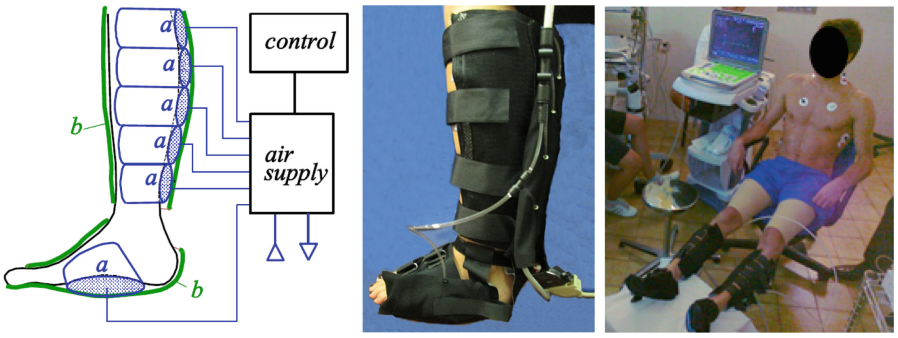

Fig. 1. Pneumotronic IPC device for the improvement of venous blood return; application in experimental trials for EDV assessment.

Compression-relaxation protocols were designed considering the alternating activation of two sleeves to simulate the muscle pattern during locomotion. The mechatronic device was tested on 19 healthy voluntary participants, which were initially monitored for 3 min to collect TEB baseline values. During the experimentation, which involved activation-deactivation sequences following a peristaltic compression (caudal-rostral trend), the EDV increased of about 10% with respect to preliminary observation done during initial monitoring of the subjects.

Although the study did not consider patients unable to walk or bed-ridden, it confirmed the relevance of the implementation of such IPC devices for the treatment of conditions related to reduction of venous blood return.

3 IPC Device for the Study of Vascular Phenomena

Besides therapeutic treatments, IPC devices can be effectively used to examine in-depth vascular phenomena as hyperemia. Ferraresi et al. [11] presented the design and modeling of an IPC device aimed at providing customizable pressure profiles to human limbs, whereas Messere et al. [12, 13] showed applications of such device on a set of healthy subjects, aimed at developing protocols for the study of the mechanisms behind hyperemia (i.e., the local increase of blood flow to tissues).

The device, shown in Fig. 2, was based on a pneumatic circuit used to inflate a blood pressure cuff wrapped around the limb to stimulate. In order to achieve appropriate responses, it was designed to control the pressure with a step reference of magnitude between 0 and 250 mmHg, with critical attention given to static and dynamic performance.

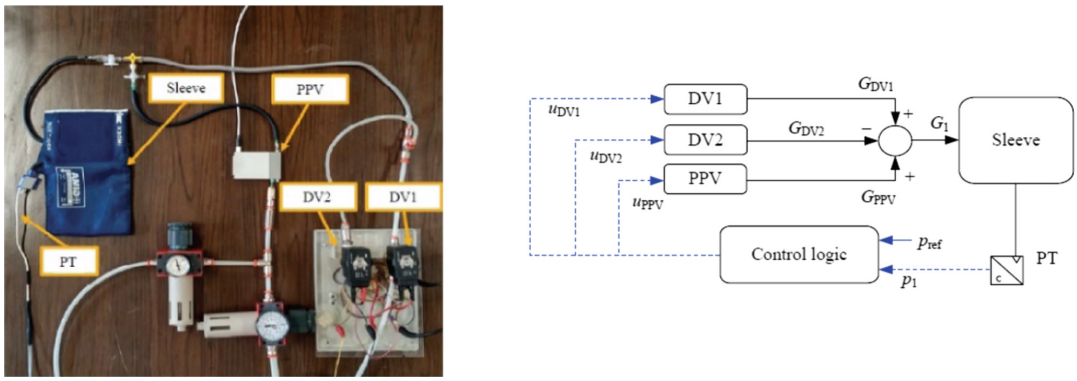

Fig. 2. Picture (left) and scheme (right) of the pneumotronic system [11]. DV1 and DV2 are the digital valves respectively used to charge and discharge the cuff, PPV is the pressure proportional valve, PT is the pressure transducer.

In order to fulfil the required specifications of accuracy and short time response, a pneumatic circuit based on the combination of 2/2 digital solenoid valves and a pressure proportional valve, shown in Fig. 2, was designed. The digital valves (DV1 and DV2) were used to quickly charge and discharge the cuff, while the compact pressure proportional valve (PPV) was used to accurately control the level of pressure inside the cuff. A control system, combined with a pressure transducer PT positioned inside the cuff, was used in the final architecture to drive the valves, depending on the operating conditions of the system.

In order to investigate the sensitivity of the device to the variation of some physical parameters, an analytical model was implemented. In particular, the interaction between the cuff and the biological tissues was studied to achieve an accurate matching between the model and experimental data.

The final design of the pneumotronic IPC device showed high dynamic performance and was able to provide sharp, customizable stimuli to the limb of a subject (see Fig. 3) in a wide range of pressure, necessary for the investigation of several vascular phenomena with different dynamics.

3.1 Investigation of Vascular Reactivity to Mechanical Stimuli

Resistance vessels in skeletal muscle exhibit a rapid dilatation in response to mechanical stimuli, such as short-lasting external compressions, whose underlying mechanisms are still unclear. Messere et al. [12] performed an analysis on 10 healthy volunteers with the IPC device described in the previous section. The subjects sat on a chair with a backrest, the leg fully extended with the cuff wrapped distally to the knee. The protocol started after 10 min of rest and provided customized pressure patterns. With respect

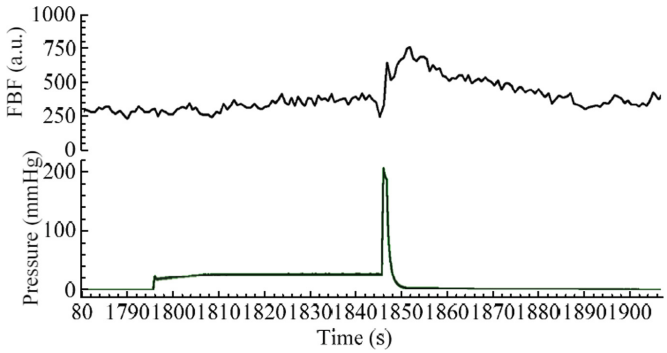

Fig. 3. Recordings of a post-compression hyperemia from a representative subject: femoral artery blood flow (FBF) and cuff pressure [11].

to traditional devices, that are often meant to apply fast and short-lasting stimuli, the custom-design IPC device was necessary to generate sequences of static pressure levels that can be considered to modulate vascular filling in venous compartments as well as pressure gradients across the wall of the vessels.

During the compressions, the blood flow of the femoral artery (FBF) was measured by Eco-Doppler sonography. The flow response highlighted a significant increase of FBF after the occurrence of the high-level compression. Preliminary investigations showed suitable performance of the device for the investigation of vascular phenomena behind the compression-induced rapid hyperemia that still do not have a univocal interpretation [19–24].

Another relevant issue recently investigated is the role of tissue oxygenation in shaping the magnitude of this mechanically-induced rapid hyperemia. Messere et al. [13] hypothesized that increased tissue oxygenation could explain the progressive attenuation of the hyperemia in response to repetitive stimulation. To measure local hemodynamic changes, a continuous wave near-infrared spectroscopy (NIRS) device was used, providing a tissue oxygenation index. The NIRS measurement was obtained for wrist extensor muscles and for the lateral head of the gastrocnemius muscle of the right leg, since two different stimulation points were considered (Fig. 4).

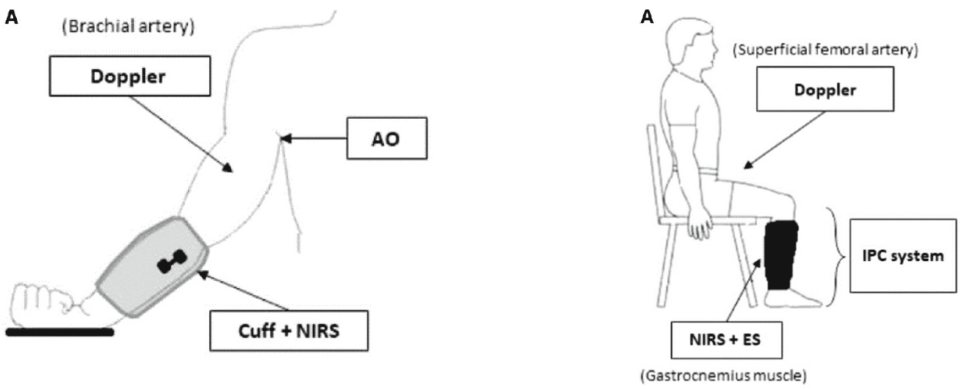

Fig. 4. Set-up of the 1st (left) and 2nd (right) protocol for the investigation of hyperemia [13].

In the first protocol, the IPC device was used to deliver two series of two compressive stimuli to the forearm with a time interval of 25 s between each compression, with peak

pressure 250 mmHg and duration 1 s (Fig. 4, left). In the first series, the hyperemia was not limited, whereas it was prevented after the first compression in the second series. It was observed that preventing the hyperemia and the ensuing increases in oxygenation also prevented the attenuation of the hyperemic response to a subsequent stimulus.

The second protocol was designed to understand if the tissue oxygenation produced by a compression or a muscle contraction (which similarly compresses intramuscular vessels) affects the hyperemia generated by a subsequent compression or contraction of the same muscle (Fig. 4, right). During this protocol, the lateral gastrocnemius of the right leg was stimulated by means of an electrical stimulator at 20 Hz frequency. Compression of the leg was obtained with an IPC system including four bladders, with peak pressure 150 mmHg and duration of about 2–3 s. Several combinations of muscle contraction and pneumatic compression were considered.

The results of the study demonstrated that the hemodynamic responses to muscle contraction and to limb compression are very similar, suggesting a common underlying mechanism related to mechanical deformation of blood vessels. Moreover, the results showed, for the first time in humans, that the tissue hyper-oxygenation has a significant role in limiting further responses in skeletal muscle.

4 IPC in the Study of Venous Compartment Hemodynamics

As discussed in Sect. 3, IPC technique can be employed to investigate vascular phenomena and not only as a therapeutic tool in patients with some deficits as EDV reduction (Sect. 2). Moreover, IPC devices can also be used to generate pressure pulses in veins to allow for the measurement of Pulse Wave Velocity (vPWV).

4.1 IPC as a Tool in a System for the Measurement of Venous PWV

Ermini et al. [14] carried out a study on 8 healthy volunteers with a revised version of the IPC device shown in Sect. 3. The experimental set-up is shown in Fig. 5. A compressive stimulus was delivered directly to the foot by inflating a pneumatic cuff. The peak pressure considered was equal to 200 mmHg, with a duration of 1 s and inflation time of 400 ms. The foot compression was used to create a pressure pulse that propagated along the veins until it was detected by a Doppler ultrasound system at superficial femoral vein (SFV) level. The venous blood velocity was recorded with a linear probe positioned on the leg, with an incident angle of about 60°.

A pressure transducer was positioned on the cuff outlet and used to monitor the pressure inside the inflating volume (Fig. 6a, bottom), whereas leg venous pressure (LVP) was estimated as the hydrostatic load relative to the vertical distance between the leg and the venous point of collapse, which was detected by a second dedicated ultrasound system. The Doppler signal was sampled at 10 kHz (Fig. 6a, top) and used to extract the maximum velocity profile (Fig. 6c). The footprint of the latter, detected by a custom-made algorithm, was used to calculate the transit time of the pulse wave. The vPWV was then calculated as the ratio between the traveled distance (measured between the ankle and the probe positions) and transit time.

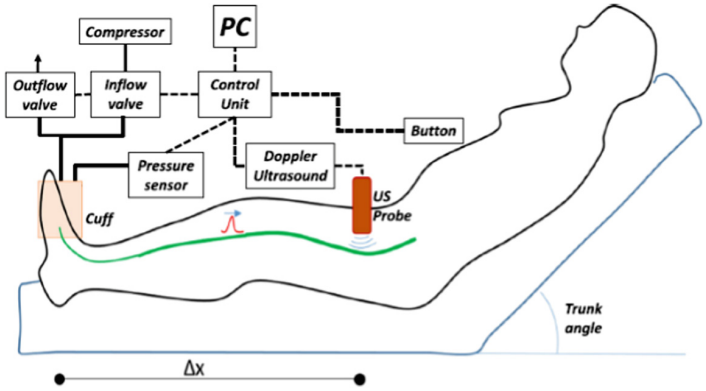

Fig. 5. Set-up for the measurement of vPWV in response of different trunk orientation [14].

The trigger of the stimulation was provided directly by the participant subject with a button, at the end of the expiratory phase in order to reduce the interference between the vPWV assessment and the respiratory activity and to improve the reproducibility of the measurements.

This study provided a significant proof of concept for a new methodology focused on the calculation of vPWV. Although PWV can be reliably assessed in arteries, where it is a well-established marker of cardiovascular risk, the measurement of vPWV has not been investigated with the same attention. In particular, the lack of relevant pulsation in the venous compartment, as well as the low blood pressure levels involved, represent significant limitations for a reliable measurement. For these reasons, the use of an IPC device can be really effective in generating the pressure pulse required for such measurement. The results of the study, in terms of vPWV values, were compatible with those obtained with different techniques (1–3 m/s for supine position, 4–15 m/s in the arm for venous pressures of 20–80 mmHg). Moreover, the linear relationship observed between vPWV and LVP was compatible with the literature [25–28] and confirmed that vPWV assessment could represent an indirect estimation of the venous pressure, which is directly connected to the volemic status of a patient.

4.2 Estimation of vPWV in Response to a Simulated Fluid Change

Ermini et al. [15] conducted an experiment on 15 healthy volunteers with a modified version of the IPC device shown in the previous section. In particular, the system was used to measure the vPWV along the arm, through a synchronous delivery of the compression (at the hand) with respiratory and cardiac cycles. The hemodynamic perturbation was realized by means of passive leg raising (PLR) maneuvers. An overview of the experimental set-up is given in Fig. 7. A fast compression (peak pressure: 400 mmHg, lasting about 1 s, inflation time: 400 ms) was delivered to the hand of each subject through the cuff.

A Doppler ultrasound system was used to detect the pressure pulse propagating proximally at the level of the basilic vein (BV). To further improve the quality of the measurements, the detection was synchronized with both respiratory and cardiac activities. In particular, the measurement was always performed at the end of the expiratory phase and at the same time instant within the cardiac cycle, corresponding to the lowest

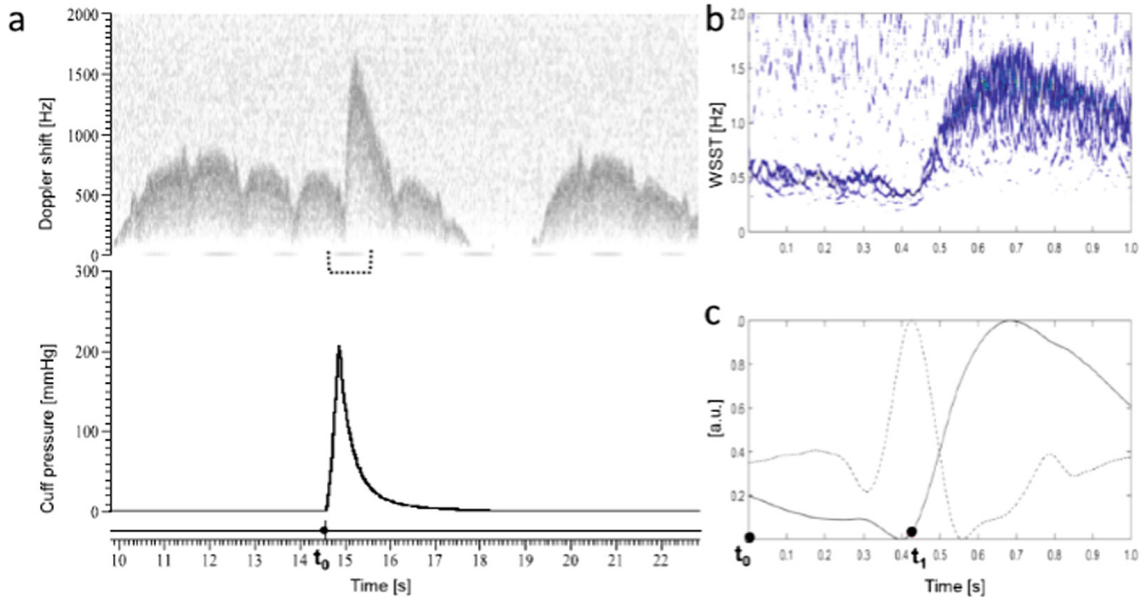

Fig. 6. Representative acquired and processed signals. (a) Venous pulse wave detected by Doppler ultrasound (top) and compressive stimulus profile (bottom). (b) Wavelet synchro-squeezed transform (WSST) of the Doppler signal. (c) Smoothed normalized maximum energy profile of WSST (solid line) and its normalized second derivative (dashed line), whose maximum identifies the footprint of the profile which was used to calculate the transit time of the pulse wave [14].

blood velocity. Cardiac synchronization was assessed by monitoring of the R-wave with a commercial ECG system.

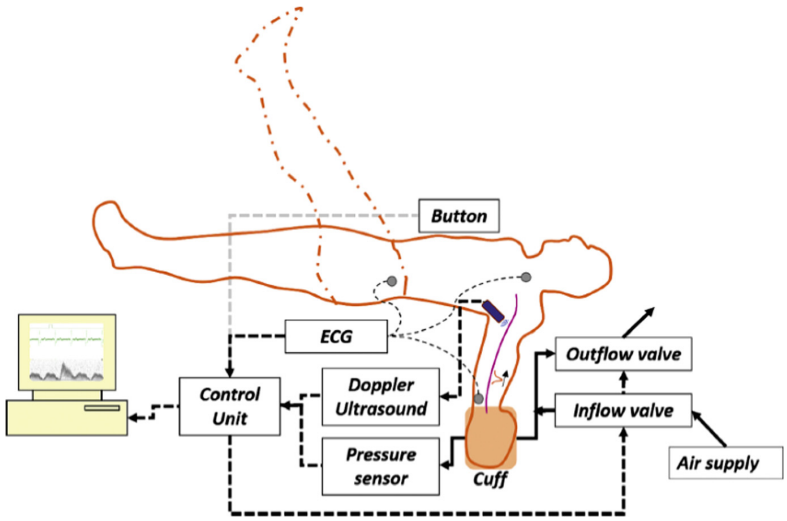

Fig. 7. Set-up to estimate vPWV in response of passive leg rising maneuvers [15].

This study showed for the first time that vPWV is sensitive to simulated changes in blood volume, as produced by PLR. With respect to traditional techniques, this methodology is objective. Furthermore, the measurement is sensitive even to limited hemodynamic challenges, and it is not invasive. Given the relationship between vPWV and the volemic status of a patient, this technique could be used for monitoring purposes

or to provide a quantitative assessment of vascular filling during fluid administration in patients.

5 Conclusions

The applications of IPC technique can be of a therapeutic and rehabilitative type, such as the improvement of the return of venous blood to the heart in people with disorders to the cardiovascular system, or of a diagnostic type, such as the measure of the propagation velocity of a pressure wave in the venous compartment, which allows an indirect evaluation of the volemic status of a subject. Further applications can deepen the study of still poorly defined phenomena in the cardiovascular system.

The variety of applications from the physiological point of view requires that the specific IPC device must be designed and manufactured with non-common techniques, to meet the required precision and dynamic performance.

The applications of IPC are completely non-invasive, and this constitutes a fundamental element for the realization of devices of limited cost, easy to use and therefore very widespread. They can therefore represent an important means of spreading well-being and good health widely, in the spirit of the SDG3 of the United Nations Development Program.

References

1. Johansson, K., Lie, E., Ekdahl, C., Lindfeldt, J.: A randomized study comparing manual lymph drainage with sequential pneumatic compression for treatment of postoperative arm lymphedema. Lymphology **31**, 56–64 (1998)
2. Zaleska, M., Olszewski, W.L., Durlik, M.: The effectiveness of intermittent pneumatic compression in long-term therapy of lymphedema of lower limbs. Lymphat Res. Biol. **12**(2), 103–109 (2014)
3. Comerota, A.J.: Intermittent pneumatic compression: physiologic and clinical basis to improve management of venous leg ulcers. J. Vasc. Surg. **53**, 1121–1129 (2011)
4. Nelson, E.A., Mani, R., Thomas, K., Vowden, K.: Intermittent pneumatic compression for treating venous leg ulcers. Cochrane Database Syst. Rev. **16**(2), CD001899 (2011)
5. Sparks-DeFriese, B.J.: Vascular Ulcers. In: Physical Rehabilitation, pp. 777–802, W.B. Saunders (2007)
6. Flam, E., Berry, S., Coyle, A., Dardik, H., Raab, L.: Blood-flow augmentation of intermittent pneumatic compression systems used for the prevention of deep vein thrombosis prior to surgery. Am. J. Surg. **171**, 312–315 (1996)
7. Zhang, D., Li, F., Li, X., Du, G.: Effect of Intermittent pneumatic compression on preventing deep vein thrombosis among stroke patients: a systematic review and meta-analysis. Worldviews Evid. Based Nurs. **15**(3), 189–196 (2018)
8. Ferraresi, C., Maffiodo, D., Hajimirzaalian, H.: A model-based method for the design of intermittent pneumatic compression systems acting on humans. Proc. Inst. Mech. Eng. PART H **228**(2), 118–126 (2014)
9. Manuello Bertetto, A., Meili, S., Ferraresi, C., Maffiodo, D., Crisafulli, A., Concu, A.: A mechatronic pneumatic device to improve diastolic function by intermittent action on lower Limbs. Int. J. Autom. Technol. **11**(3), 501–508 (2017)

10. Maffiodo, D., De Nisco, G., Gallo, D., Audenino, A., Morbiducci, U., Ferraresi, C.: A reduced-order model-based study on the effect of intermittent pneumatic compression of Limbs on the cardiovascular system. Proc. Inst. Mech. Eng. Part H **230**(4), 279–287 (2016)
11. Ferraresi, C., et al.: Design and simulation of a novel pneumotronic system aimed to the investigation of vascular phenomena induced by Limb compression. J. Bionic. Eng. **16**, 550–562 (2019)
12. Messere, A., et al.: Delivery of customizable compressive patterns to human limbs to investigate vascular reactivity. Biomed. Phys. Eng. Express **4**(6), 067003 (2018)
13. Messere, A., et al.: Hyper-oxygenation attenuates the rapid vasodilatory response to muscle contraction and compression. Front. Physiol. **9**, 1078 (2018)
14. Ermini, L., Ferraresi, C., De Benedictis, C., Roatta, S.: Objective assessment of venous pulse wave velocity in healthy humans. Ultrasound Med. Biol. **46**(3), 849–854 (2019)
15. Ermini, L., Chiarello, N., De Benedictis, C., Ferraresi, C., Roatta, S.: Venous Pulse Wave Velocity variation in response to a simulated fluid challenge in healthy subjects. Biomed. Signal Process. Control **63**, 102177 (2021). https://doi.org/10.1016/j.bspc.2020.102177
16. Boutouyrie, P., Briet, M., Vermeersch, S., Pannier, B.: Assessment of pulse wave velocity. Artery Res. **3**, 3–8 (2009)
17. Safar, M.E.: Arterial stiffness as a risk factor for clinical hypertension. Nat. Rev. Cardiol. **15**, 97–105 (2018)
18. Lin Wang, Y.Y.: Did you know developing quantitative pulse diagnosis with realistic haemodynamic theory can pave a way for future personalized health care. Acta Physiol. **227**(3), e13260 (2019). https://doi.org/10.1111/apha.13260
19. Mohrman, D.E., Sparks, H.V.: Myogenic hyperemia following brief tetanus of canine skeletal muscle. Am. J. Physiol. **227**, 531–535 (1974)
20. Tschakovsky, M.E., Sheriff, D.D.: Immediate exercise hyperemia: contributions of the muscle pump versus rapid vasodilation. J. Appl. Physiol. **97**, 739–747 (2004)
21. Clifford, P.S., Tschakovsky, M.E.: Rapid vascular responses to muscle contraction. Exerc. Sport Sci. Rev. **36**, 25–29 (2008)
22. Turturici, M., Mohammed, M., Roatta, S.: Evidence that the contraction-induced rapid hyperemia in rabbit masseter muscle is based on a mechanosensitive mechanism, not shared by cutaneous vascular beds. J. Appl. Physiol. **113**, 524–531 (2012)
23. Turturici, M., Roatta, S.: Inactivation of mechano-sensitive dilatation upon repetitive mechanical stimulation of the musculo-vascular network in the rabbit. J. Physiol. Pharmacol. **64**, 299–308 (2013)
24. Jasperse, J.L., Shoemaker, J.K., Gray, E.J., Clifford, P.S.: Positional differences in reactive hyperemia provide insight into initial phase of exercise hyperemia. J. Appl. Physiol. **1985**(119), 569–575 (2015)
25. Mackay, I., Van Loon, P., Campos, J., de Jesus, N.: A tecnique for the indirect measurement of the velocity of induced venous pulsation. Am. Heart J. **73**, 17–23 (1967)
26. Anliker, M., Wells, M.K., Ogden, E.: The transmission characteristics of large and small pressure waves in the abdominal vena cava. IEEE Trans. Biomed. Eng. **16**, 262–273 (1969)
27. Minten, J., Van De Werf, F., Auber, A., Kasteloot, H., De Geest, H.: Apparent pulse wave velocity in canine superior vena cava. Cardiovasc Res. **17**, 627–632 (1983)
28. Nippa, J., Alexander, R., Folse, R.: Pulse wave velocity in human veins. J. Appl. Physiol. **30**, 558–563 (1971)

Paper IV

MDPI

Article

A portable device for the measurement of venous Pulse Wave Velocity

Agata Barbagini [1], Leonardo Ermini [1], Raffaele Pertusio [1], Carlo Ferraresi [2], Silvestro Roatta [1]

[1] Laboratory of Integrative Physiology, Department of Neuroscience, University of Torino, c.so Raffaello 30, 10125, Torino, Italy
[2] Department of Mechanical and Aerospace Engineering, Politecnico of Torino, c.so Duca degli Abruzzi 24, 10129, Torino, Italy
* Correspondence: leonardo.ermini@unito.it

Abstract: Pulse wave velocity in veins (vPWV) has recently been reconsidered as a potential index of vascular filling. The measurement requires that an exogenous pressure pulse is generated in the venous blood stream, by an external pneumatic compression, and that the compression is delivered synchronously with both heart and respiratory activity. However, no device currently exists to serve this purpose. A portable prototype for the assessment of vPWV is here presented. It is based on the PC-board Raspberry PI, equipped with A/D board. It acquires the respiratory and ECG signal as well as the Doppler shift from the ultrasound monitoring of blood velocity from the relevant vein, drives the pneumatic cuff inflation and returns multiple measurements of vPWV. The device was tested in four healthy volunteers (2M, 2F, age 33 ± 13 yr.), subjected to the passive leg raising (PLR) manoeuvre, simulating a transient increase in blood volume. Measurement of vPWV in the basilic vein exhibited a low coefficient of variation ($3.6 \pm 1.1\%$), a significant increase during PLR in all subjects, consistent with previous findings. This compact device makes it possible to carry-out investigations in hospital wards on different patient populations, as necessary to assess the actual clinical potential of vPWV.

Keywords: Raspberry Pi; Pulse Wave Velocity; volume status; vascular stiffness; venous compliance; bioengineering;

Citation: Barbagini, A.; Ermini, L.; Pertusio, R.; Ferraresi, C.; Roatta, S. A portable device for the measurement of venous Pulse Wave Velocity. *Appl. Sci.* **2022**, *1*, 0. https://doi.org/

Received:
Accepted:
Published:

1. Introduction

Nowadays, the estimation of the volaemic status (or volaemia) of a patient through a non-invasive method is not trivial but, at the same time, its development could be of great utility, given that the interest in the patient volaemia spans across several different hospital departments [1]. An innovative method for assessing the volaemic status of patients has recently been proposed: the Pulse Wave Velocity in veins, termed venous Pulse Wave Velocity (vPWV) [2,3]. The relation between vPWV, venous pressure and changes in blood volume was first observed in the seventies [4,5], but the methodology was subsequently abandoned, possibly due to the difficulty of achieving reliable measurements. In fact, the pulse wave velocity is commonly measured in arteries, widely used as a marker of cardiovascular risk [6]. PWV measurement is considerably easier in arteries than veins, due to an higher blood pressure in arteries and the presence of a natural cardiac pulsatility, which is absent in veins. However, in recent studies, an improved methodology was devised in which a pneumatic compression applied to a limb extremity (e.g., the hand), generates the pressure pulse (i.e., the pulse wave) in the venous compartment, which propagates centrally and it is detected proximally (e.g., at the basilic vein) by Doppler ultrasound. Knowing the distance between the cuff and the ultrasound probe, it is possible to calculate the vPWV. In addition, to limit the confounding effect of respiratory and cardiac modulation of venous blood pressure, the compression is delivered synchronously with heart and respiratory activity. [2,3]. In this way it was possible to measure vPWV with reasonable reliability and to confirm a linear correlation among vPWV and venous pressure [2]. vPWV also exhibited good sensitivity to simulated changes in blood volume, associated

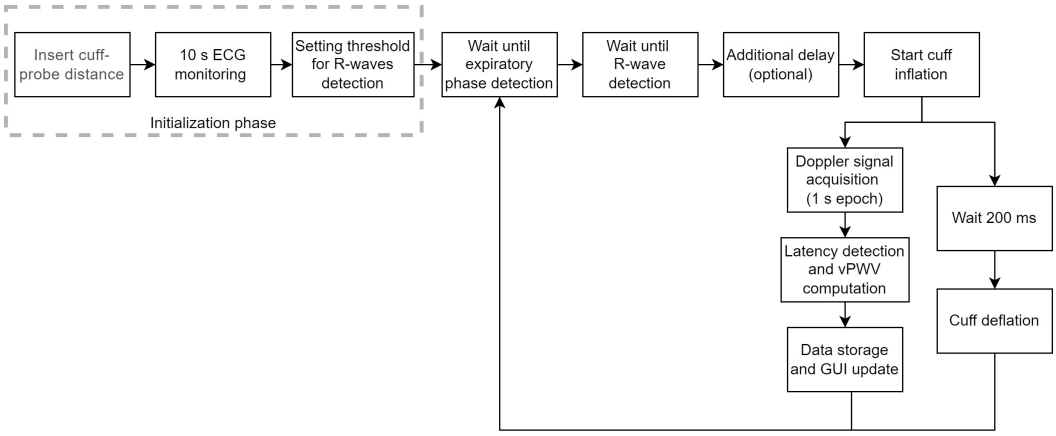

Figure 1. Flow-chart of the measurement. The compressive stimulus is synchronized with the respiratory and the cardiac cycle. The transition of the PW under the Doppler probe allows calculating the vPWV.

with minor changes in venous pressure as observed in healthy subjects in response to Passive Leg Raising (PLR) [3]. These results were achieved also thanks to the development of an automatic method for calculating vPWV by analysing the Doppler shift signal, as acquired by the echograph machine [2]. Thanks to this feature, the measurement can be carried out continuously, and it is thus adequate for long-term monitoring.

Following these promising results in healthy subjects, clinical trials need to be carried out in order to assess the usefulness of vPWV as diagnostic haemodynamic parameter. However, experimental series in hospital wards are not feasible with the cumbersome laboratory instrumentation, and no dedicated device is available on the market, as yet. Aim of the study is to present a proof-of-concept prototype of a user-friendly, portable and electrically isolated device for vPWV measurement. The entire hardware composing the device is embedded in a small, handy box, thanks to a single board computer, the Raspberry Pi, wirelessly connected to a PC, where a graphic interface allows to interact with the device. The performance of the RPi-based device is tested in 4 healthy subjects subjected to PLR and it is compared with the measurements performed by the original laboratory equipment (PC-based system).

2. Materials and Methods

The devised methodology for vPWV measurement requires the acquisition of several signals, including:

- ECG;
- Respiratory signal;
- Echo-Doppler ultrasound;

The flow chart of measurement process is reported in Figure 1, while a schematic representation of the device is shown in Figure 2. Examples of acquired signals are reported in Figure 3, showing typical timing of acquisition. In order to synchronize the delivery of the compressive stimulus both with respiratory and cardiac cycles, the system first identifies the expiratory phase in the respiratory signal and than the rising edge of the R-wave in the ECG signal. This latter event triggers the delivery of the compressive stimulus, after an optional delay defined by the user, and the acquisition of the haemodynamic response (i.e., the Doppler shift). This signal is then processed to identify the footprint that corresponds to the passage of the pulse wave under the probe. In this way the transit time of the pulse wave (i.e., the pulse transit time) can be estimated and its velocity calculated, based on the cuff-probe distance.

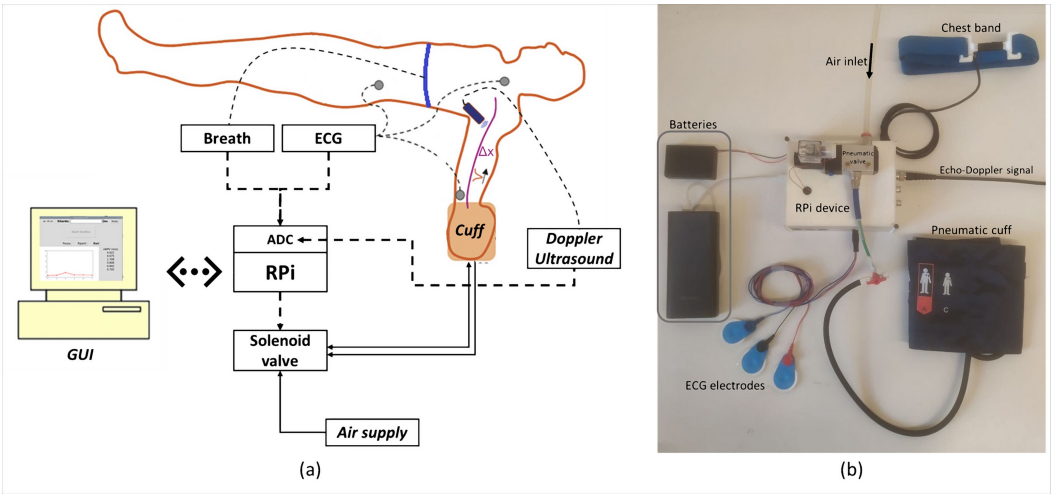

Figure 2. Device schematic and photographic representation. (**a**) Functional scheme. Electrical and pneumatic connections are indicated by dashed and solid lines, respectively. The Raspberry Pi (RPi) is the control unit, wirelessly connected to a graphical computer interface on a PC. (**b**) Picture of the prototype, enclosed in a 3D-printed box and connected to the external batteries, ECG electrodes, chest band and Doppler signal (ultrasound machine not shown)l. Note also the pneumatic valve, mounted on the top of the device, connected to the compressed air supply (not shown) and to the cuff.

2.1. Hardware

The PC board Raspberry Pi 4 B+ (Processor: Broadcom BCM2711 quad-core 64 bit ARM Cortex-A72, 1.5 GHz; RAM: 4 GB) has been chosen because of its small size, low-cost, and ability to be programmed using Python, which allows efficient signal processing. In addition, this solution offers easy design of graphical interface, the possibility of saving data, access to a large range of open source libraries and an easy connection to a remote PC. Alternative solutions based on microcontrollers would not provide all these possibilities. An analogue-to-digital converter (A/D converter) was used in combination with Raspberry Pi to acquire biological signals, exploiting the Serial Peripheral Interface (SPI) communication protocol: the Waveshare Raspberry Pi High-Precision AD/DA Expansion Board (Waveshare Electronics, Shenzhen, China) can be easily assembled on the top of Raspberry Pi. It embeds Texas Instrument's ADS1256 chip and provides eight channels for 24-bit single-ended acquisition of analogue signals, while maintaining free the RPi's forty General Purpose Input/Output (GPIO) pins. The hardware also includes printed circuits boards for conditioning respiratory signal as well as a relay and a pneumatic valve. The electrical power source is external consists of two batteries (5V, 3A) and, through DC/DC converter, it supplies:

- Raspberry Pi (5 V, 2 A)
- Pneumatic valve (12 V, 200 mA)
- Breathing signal conditioning circuit (12 V, 200 mA)

Other components requiring power supply, such as the relay and the ECG board, are connected to the Raspberry Pi's output pins, each of which can supply either 5 V or 3.3 V (max 16 mA). As such, the device has a floating ground and is electrically safe.

2.2. Respiratory signal

A custom-made chest band (3 cm wide) made of elastic material, and integrating a resistive sensor (strain gauge), is used to monitor respiratory movement. Before being digitally sampled (50 Hz), the respiratory signal is high-pass filtered (cut off frequency: 0.1 Hz) to remove slow trends in signal. It is offset to about 1.6 V by a summing circuit, to fit the input range of the acquisition board (0-5 V). RPi identifies the expiratory phase when the signal drops below the average value (about 1.6 V), as shown in Figure 3.

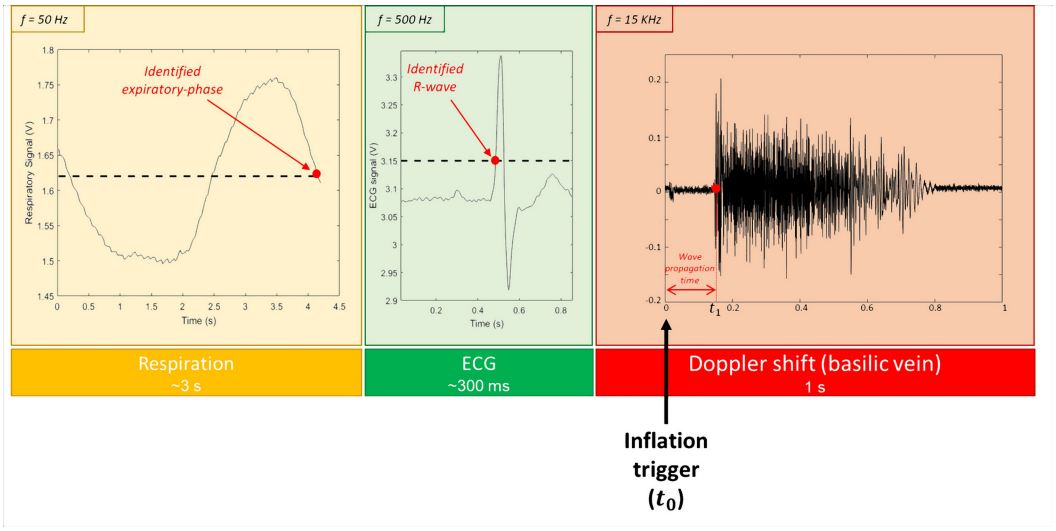

Figure 3. Signal acquisition timeline, typical timing and signal waveforms are shown. On the right, the haemodynamic response to the compressive stimulus is reported in the time domain. Note that the compressive stimulus is delivered at time 0 of Doppler acquisition, and that the pulse transit time t_1 can be easily estimated.

2.3. ECG

The ECG is provided by an integrated signal conditioning block: AD8232 SparkFun Single Lead Heart Rate Monitor (SparkFun, Niwot, Colorado). It presents a jack plug connection for three ECG electrodes (two measuring electrodes and one reference), and yields a fully positive, amplified and low-pass filtered analog output, which can be directly fed to the acquisition board and sampled at 500 Hz. ECG is monitored for 10 seconds at the beginning of the experimental session (initialization phase), in order to estimate an appropriate threshold for R-wave detection: the threshold is initially set at 15% of the baseline-to-peak amplitude. It is subsequently raised if an excessive number of peaks are crossed within the recorded 10 seconds. R-waves waves are then automatically detected by upward crossing of the threshold, as shown in Figure 3. AD8232 needs to be powered at 3.3 V, which is provided by one of RPi's output pins.

2.4. Compressive stimulus

Immediately after the detection of the R-wave, the Raspberry Pi triggers the compressive stimulus. The command is imparted through a digital output (3.3 V) which activates a relay (KY-019 5V Relais module) which, in turn, drives a solenoid valve (3V210-08 12VDC 3-Way, Heschen, Zhejiang, China), connecting a compressed air supply (2 bar), to the cuff (49×15cm, GIMA, Gessate, Italy) wrapped around the wrist. Inflation lasts for 200 ms. After that, RPi lowers the digital output, which releases the valve so the cuff passively deflates.

2.5. Ultrasound Doppler shift signal

The Doppler shift signal is generally provided by ultrasound machines as an audio signal output (e.g., from the headphones output). In the present study a MyLab25 Gold (ESAOTE, Genova, Italy) equipped with a linear probe (LA523, ESAOTE, Genova, Italy) was employed. The probe was located in the medial side of the arm, about 15 cm proximal to the elbow, with an angle of about 60 degrees to the basilic vein (BV). The Doppler shift is fed to the acquisition board (sampling frequency: 7.5 kHz). The acquisition of a 1-s lasting epoch is started immediately after the trigger of the compressive stimulus. After completing the acquisition, the Doppler shift is processed in the time domain as follows. The root mean square envelope of the signal is extracted. The latter is smoothed through a moving average filter (sliding square window of 100 ms). The footprint is then identified as the instant t_1 at which the envelope reaches 5% of its baseline-to-peak amplitude. The

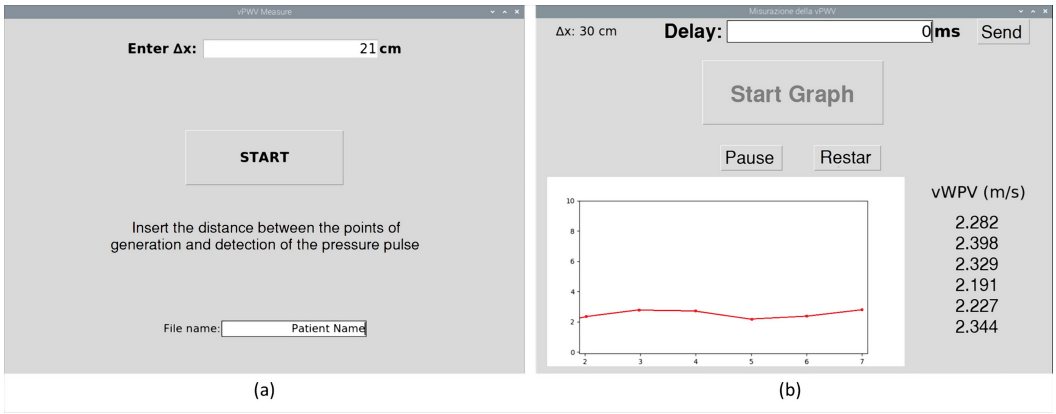

Figure 4. Graphical user interface. **(a)** GUI's firs page allows to enter the preliminary information, such as the distance between the cuff and the ultrasound probe (Δx), and the name for saving the data. **(b)** In working mode, the GUI displays numerical and graphical representation of measured vPWV values, and allows to adjust the additional delay for the delivery of the the compressive stimulus.

latency (i.e., the pulse transit time) is then estimated as $\Delta t = t_1 - t_0$ (where t_0 corresponds to the instant when the trigger is delivered, equal to zero in Figure 3) and, finally, the vPWV can be calculated as $\frac{\Delta x}{\Delta t}$.

2.6. Graphical interface

A graphical interface has been developed to interact with the device. Raspberry Pi is configured as an access point, so it offers a Wi-Fi network that allows a remote PC to connect and interact with the graphical interface, while avoiding any electrical connection to the PC. The GUI shows in graphical and numerical form the vPWV values, periodically updating the display at each new measurement. Moreover, it allows the measurement process to be paused and resumed at any time, after the initialisation phase. The user is asked to insert the Δx cuff-probe distance value at beginning of the process, necessary for vPWV computation. Also, the user has the possibility to adjust the delay of the compressive stimulus with respect to R-wave detection. This feature can be exploited to optimize the timing of the pressure pulse generation with respect to the spontaneous fluctuations of venous blood flow (of cardiac origin) which may disturb the detection of the pulse wave footprint in the Doppler shift. All acquired signals and vPWV values are locally stored and can be transferred to the PC at the end of the session, for further processing. An example of the GUI layout is shown in Figure 4.

3. Device validation

3.1. Procedure

In order to verify the performance of the device, vPWV measurements were carried out on four healthy subjects (two males and two females, age 33 ± 13 yr.), during resting condition in supine position and during a simulated increase in blood volume, in the trunk, as obtained by PLR. Each subject lied in supine position for at least 30 minutes before starting the measurement, in order to achieve a stable haemodynamic condition [7]. The cuff for the delivery of the pneumatic compressive stimuli was placed around the wrist and the Doppler ultrasound probe was placed over the BV about 15 cm proximally to the elbow. An electric compressor supplied the high pressure air. Respiratory movements and ECG were also collected and all transducers and devices were connected to the prototype as described above. In addition, all signals were also continuously sampled by an external acquisition board (Micro 1401 IImk, CED, Cambridge, UK, with Spike2 software) and off-line processed in Matlab®, according to the original methodology [3]. After the initialisation phase, 10 vPWV values were collected while the subject remained at rest in supine position

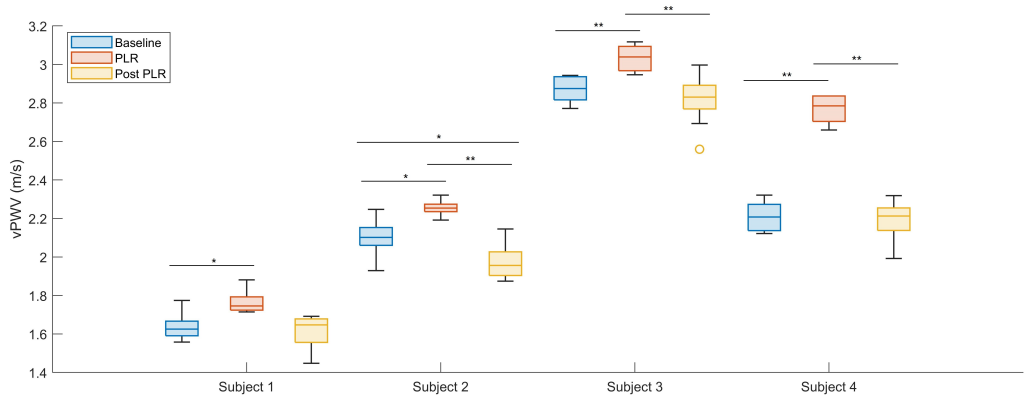

Figure 5. Distributions of vPWV values measured pre-, during and post-PLR, distinctly presented for the 4 subjects. Note the consistent increase of vPWV during PLR (*: $p < 0.05$; **: $p < 0.01$).

(baseline), then the PLR was performed by an operator, manually raising the subject's leg at about 45 degree. Other 5 to 7 vPWV readings were taken in this position, and other 5 to 10 readings after returning to supine position (post-PLR). A time interval of 15-30 s elapsed between subsequent measurements. The whole session lasted about 45 min.

3.2. Data analysis

After the acquisition with the RPi-based device, the data were cleaned, by removing values acquired during a movement of the ultrasound probe or a lack of contact with the arm. The reliability of the measurement was assessed by the coefficient of variation (CoV = STD / MEAN * 100), calculated over the 10 vPWV values collected during rest in the supine position. Afterwards, the impact of PLR on vPWV was investigated. The basal value was set as the average of the values relative to the supine position. vPWV collected during PLR were expressed as a percent changes with respect to the baseline. Moreover, the sensitivity of the measurement to simulated blood volume changes was assessed by individually comparing data collected during baseline, PLR and post-PLR, by student's T-test with Bonferroni correction for multiple comparisons. Finally, the accuracy of the measurement was assessed by comparing each individual vPWV value yielded by the prototype with the corresponding value measured by the original PC-based system. The difference among them was expressed in percentage terms with respect to the mean of the two values.

4. Results

In resting condition in the supine position, vPWV had an average value across all subjects of 2.2 ± 0.5 m/s, and the CoV of the measurement was 3.6 ± 1.1 %. The PLR maneuver consistently and significantly increased vPWV in all subjects as shown by the box plots of Figure 5. The percentage increases from baseline are reported in Table 1.

Table 1. Percentage increases in vPWV during PLR with respect to baseline, for each subject.

Subject	Percentage increase
1	$7.6 \pm 4.1\%$
2	$6.9 \pm 2.2\%$
3	$5.7 \pm 2.4\%$
4	$25.3 \pm 3.4\%$

Note also that vPWV tends to decrease after PLR (significantly in 3 out of 4 subjects). Figure 6 shows the time course of vPWV during the experimental session in one subject and compares the values obtained by the RPi-based prototype and by the original PC-based

system. The relative percentage difference distribution between the two was $-3.22 \pm 0.67\%$ (average of all collected values, from all subjects). The negative value indicates that RPi generally measures a lower velocity value than the PC-based system.

5. Discussion

For the first time, a prototype for the measurement of the pulse wave velocity in the venous compartment has been presented and validated. The device integrates all necessary electrical and pneumatic features, while remaining compact, battery powered, and with floating ground. This features make it electrically safe and suitable to be used on patients, in hospital wards. The validation test demonstrated that the quality of the measurement is comparable with previous reports based on a personal computer and laboratory instrumentation [2,3], achieving good reliability (CoV < 4%) and sensitivity. In fact, in all the 4 tested subjects, vPWV in the arm was significantly affected by a simulated fluid challenge: the PLR. This maneuver, performed from the supine position, is considered to displace from the legs to the upper body about 150 ml of blood, with an ensuing increase in peripheral venous pressure of less than 1 mmHg [3].

Over the last two decades, technological advancement and lower costs have led to the widespread use of single board computer platforms, such as Raspberry Pi or Jetson Nano, in a variety of fields. In particular, Raspberry Pi platform has been employed in several applications in the field of biological and physiological research [8], e.g., for impedance cardiography measurement [9] and for monitoring the anaesthetic status of a patient [10].Indeed, Raspberry Pi offers a wide range of board connectivity, custom plug-ins and interfaces that allow to develop low-cost solution. However, a limitation of the RPi is the lack of analogue to digital converters. In fact, all devices that integrate RPi with the purpose of signal acquisition, present necessary an A/D converter and some circuits for signal conditioning and amplification. The A/D converter can be either on a System on a Chip (SoC) [9], as in our case, or directly embedded in a microcontroller [10]. The add-on A/D board we adopted had problems in acquiring simultaneously from multiple channels and we observed the appearance of sampling noise at the highest sampling frequencies. We could, however, achieve satisfactory performance by sampling one analog channel at the time and by limiting the sampling rate to 7.5 kHz. Small delays related to the sequential handling of the different channels are probably responsible for the small difference observed in vPWV values estimated by RPi and the PC-based system.

Passing digital data from A/D converter device to RPi can take advantage of different communication protocols, most common are SPI and Inter Integrated Circuit (I^2C). Both are serial protocols, and they are based on a master-slave architecture. I^2C can handle more than one master at the same time and offers the advantage of easy addition of any new slaves [9,10]. SPI, on the other hand, presents a more restrictive architecture, but offers higher speed of communication [9]. In the same project both protocols can be used for different purposes. In this approach, it is possible to exploit the advantages of both and adapt to the communication protocol offered by the A/D converter that best suits the needs [9]. In our case, the A/D plug-in board was equipped with an SPI bus.

In addition, RPi provides convenient features concerning the possibility of autonomous data processing as well as wireless communication with a remote PC for input of working settings and data display and storage. In our case, this functionality was used to manage the measurement process via GUI from a wirelessly connected computer. But, this relevant feature offers much wider possibilities. In fact, many examples of RPi-based Internet of Things (IoT) systems can be found in the literature [11,12]. RPi can be programmed to send data to a remote web database via WiFi or ethernet, adding the MAC address of the board to an IoT website. Some of this works combined the single board computer with sensors to collect some simple monitoring signals (temperature, respiratory signal, ECG, humidity...) and embedded in an IoT system for implementing a home care monitoring strategy.

As for the pneumatic circuit, it is meant to transmit a sharp compressive stimulus in order for the generated pressure wave to be clearly identifiable. Expensive professional

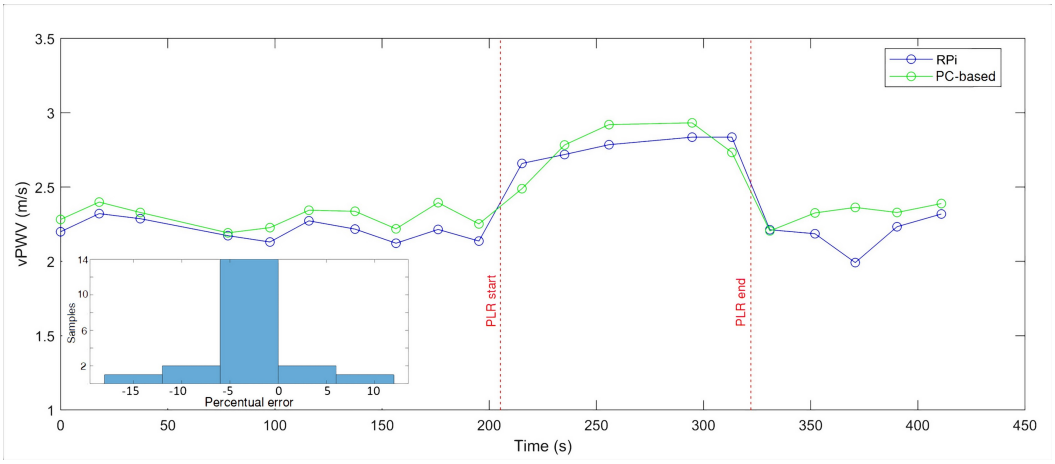

Figure 6. Time course of vPWV during the experimental session in one subject. Values yielded by the RPi-based prototype (blue) are compared with those returned by the original PC-based system (green).

machines are generally adopted to the purpose of eliciting rapid tissue compressions [13]. We faced this need when investigating the muscular and skin reactivity to compressive stimuli [14,15] and have developed a custom system based on PC driven valves for controlled rapid inflation and deflation of the cuff [14,16], as recently reviewed [17]. For the present application, a single 3-ways valve is adopted for both inflation and deflation. The valve is directly mounted on the top of the device a can be conveniently connected to the compressed air line, available in most hospitals.

Different approaches have been proposed for non-invasively assessing venous pressure or the volume status, which are mostly based on echographic monitoring of size and pulsatility of large and central veins like the inferior vena cava [1] and the jugular vein [18]. However, they all suffer of important limitations. Locating the point of collapse of the jugular vein is complicated by the pulsatile nature of jugular venous pressure and the necessity to estimate the hydrostatic gradient between this point and the right atrium. A rough indication about volaemic status of the patient may also be obtained by the assessment of respiro-phasic changes in size of the inferior vena cava [1]. This assessment has however been criticized in the literature [19] for the low specificity [20] due to the many confounding factors, among which the irregularity of spontaneous respiration [7,21] and the respiration-related displacements of the vena cava, affecting the echographic measurements [22,23], even though methodological improvements have been proposed [24–26]. A non invasive assessment of peripheral venous pressure has also been proposed, based on detecting the point of collapse of superficial veins in limbs when compressed by an externally applied pressure [27], which however is limited to superficial visible veins. The present methodology overcomes most of the disadvantages of the mentioned techniques. It concerns the peripheral venous compartment (limbs) but may focus on the blood stream of large veins, which are likely to play a more relevant role in the systemic haemodynamics than the small superficial ones. Moreover, thanks to the implemented synchronism with respiratory and cardiac activity, the vPWV measurement is virtually unaffected by their intrinsic variability in amplitude and frequency.

The lack of a dedicated device has likely hindered the research in this field for many years: to our knowledge, no studies on vPWV have been published in the last 40 years, in spite of the early promising results [4,5]. The prototype here presented will hopefully pave the way to the clinical studies that are necessary to verify the usefulness of vPWV, as a possible index of peripheral vascular filling or of venosclerosis.

5.1. Limitations

The current implementation of the device requires the use of a Doppler ultrasound for the proximal detection of the pulse wave, which has the disadvantage of been expensive and of requiring some experience for positioning and holding the probe in place. Moreover, the transit time of the pulse wave is measured starting from the time of triggering the cuff inflation, and thus erroneously includes the electro-pneumatic delay that precedes the actual generation of the intravascular pulse wave. This could slightly affect the accuracy of the measurement, in terms of a slight underestimation of the vPWV value. Future implementations may address these limitations. In particular, other methodologies may possibly be adopted for the pulse wave detection (e.g. tonometry [6,28,29]), which may provide a cheaper and simpler solution then Doppler ultrasound. Such an approach would also allow for a two-point detection of the pulse wave, thus eliminating the problem of the electro-pneumatic delay. Alternatively, acquisition and reference to the rise of air pressure in the cuff (rather than to the electrical command to the valve) could as well contribute to increase the accuracy of the measurement.

6. Conclusions

A first compact and battery powered device for the measurement of vPWV has been presented and validated, demonstrating good reliability and good sensitivity to simulated fluid challenges. The device will make it possible to extend the investigation of vPWV from healthy subjects in a laboratory to patients in hospital wards. This is necessary to initiate clinical studies oriented to understand the potential of this new parameter in characterizing the haemodynamic condition of the patient and in supporting the management of fluid therapies.

7. Patents

An Italian patent concerning the present methodology for vPWV measurement was deposited by University of Torino and Politecnico of Torino (BIT22246-AF/PS).

Author Contributions: conceptualization, L.E., C.F. and S.R.; methodology, A.B., L.E., R.P. and S.R.; software, A.B., L.E.; validation, A.B., L.E. and R.P.; formal analysis, A.B.; investigation, A.B.; resources, S.R.; data curation, A.B.; writing—original draft preparation, A.B.; writing—review and editing, A.B., L.E., C.F. and S.R.; supervision, L.E. and S.R.; funding acquisition, S.R. All authors have read and agreed to the published version of the manuscript.

Funding: A fellowship (A.B.) was covered by a donation from Prof. Magda Passatore.

Institutional Review Board Statement: The study was conducted according to the guidelines of the Declaration of Helsinki, and approved by the Institutional Review Board (or Ethics Committee) of the University of Torino (March 23 2015).

Informed Consent Statement: Informed consent was obtained from all subjects involved in the study.

Data Availability Statement: The python code used to control the device is available at the following link https://github.com/leonardoermini/vPWV_on_RPi.git, while the experimental data presented in this study are available as supplementary material.

Acknowledgments: The authors thank Daiana Billia for her help in developing the first version of the code used to control A/D board, as part of her Master's thesis in Biomedical Engineering.

Conflicts of Interest: A patent concerning the assessment of venous pulse wave velocity was deposited by University of Torino and Politecnico of Torino. The funders had no role in the design of the study; in the collection, analyses, or interpretation of data; in the writing of the manuscript, or in the decision to publish the results.

Abbreviations

The following abbreviations are used in this manuscript:

A/D	Analog to Digital
ADC	Analog to Digital Converter
CoV	Coefficient of Variation
ECG	Electrocardiogram
GUI	Graphical User Interface
I^2C	Inter Integrated Circuit
IoT	Internet of Things
MAC	Media Access Control
PC	Personal Computer
PLR	Passive Leg Raising
RPi	Raspberry Pi
SoC	System on a Chip
SPI	Serial Peripheral Interface
STD	Standard Deviation
vPWV	venous Pulse Wave Velocity

References

1. Meisn, L.; Albani, S.; Pasquero, P.; Porta, M.; Policastro, P.; Leonardi, G.; Albera, C.; Scacciatella, P.; Melchiorri, C.; Pellicori, P.; et al. Assessment of phasic changes of vascular size by automated edge tracking -State of the art and clinical perspectives. *Frontiers in Cardiovascular Medicine* **2021**.
2. Ermini, L.; Ferraresi, C.; De Benedictis, C.; Roatta, S. Objective assessment of venous pulse wave velocity in healthy humans. *Ultrasound in medicine & biology* **2020**, *46*, 849–854.
3. Ermini, L.; Chiarello, N.E.; De Benedictis, C.; Ferraresi, C.; Roatta, S. Venous Pulse Wave Velocity variation in response to a simulated fluid challenge in healthy subjects. *Biomedical Signal Processing and Control* **2021**, *63*, 102177.
4. Felix, W.R.; Sigel, B.; Amatneek, K.V.; Chrablow, M.H. Venous pulse wave propagation velocity in hemorrhage. *Archives of Surgery* **1971**, *102*, 53–56.
5. Nippa, J.H.; Alexander, R.H.; Folse, R. Pulse wave velocity in human veins. *Journal of applied physiology* **1971**, *30*, 558–563.
6. Tomiyama, H.; Yamashina, A. Ankle-Brachial Pressure Index and Pulse Wave Velocity in Cardiovascular Risk Assessment. In *Encyclopedia of Cardiovascular Research and Medicine*; Vasan, R.S.; Sawyer, D.B., Eds.; Elsevier: Oxford, 2018; pp. 111–122. doi:https://doi.org/10.1016/B978-0-12-809657-4.99592-9.
7. Folino, A.; Benzo, M.; Pasquero, P.; Laguzzi, A.; Mesin, L.; Messere, A.; Porta, M.; Roatta, S. Vena cava responsiveness to controlled isovolumetric respiratory efforts. *Journal of Ultrasound in Medicine* **2017**, *36*, 2113–2123.
8. Jolles, J.W. Broad-scale applications of the Raspberry Pi: A review and guide for biologists. *Methods in Ecology and Evolution* **2021**, *12*, 1562–1579.
9. Hafid, A.; Benouar, S.; Kedir-Talha, M.; Abtahi, F.; Attari, M.; Seoane, F. Full impedance cardiography measurement device using raspberry PI3 and system-on-chip biomedical instrumentation solutions. *IEEE journal of biomedical and health informatics* **2017**, *22*, 1883–1894.
10. Stradolini, F.; Tuoheti, A.; Ros, P.M.; Demarchi, D.; Carrara, S. Raspberry pi based system for portable and simultaneous monitoring of anesthetics and therapeutic compounds. 2017 New Generation of CAS (NGCAS). IEEE, 2017, pp. 101–104.
11. Kumar, R.; Rajasekaran, M.P. An IoT based patient monitoring system using raspberry Pi. 2016 International Conference on Computing Technologies and Intelligent Data Engineering (ICCTIDE'16). IEEE, 2016, pp. 1–4.
12. Rakesh, P.; Prakash, I.M. Raspberry Pi based E–Health System over Internet of Things. IOP Conference Series: Materials Science and Engineering. IOP Publishing, 2020, Vol. 981, p. 042008.
13. Sheldon, R.D.; Roseguini, B.T.; Thyfault, J.P.; Crist, B.D.; Laughlin, M.H.; Newcomer, S.C. Acute impact of intermittent pneumatic leg compression frequency on limb hemodynamics, vascular function, and skeletal muscle gene expression in humans. *Journal of Applied Physiology* **2012**, *112*, 2099–2109.
14. Messere, A.; Pertusio, R.; Macrì, C.; Maffiodo, D.; Franco, W.; De Benedictis, C.; Ferraresi, C.; Roatta, S. Delivery of customizable compressive patterns to human limbs to investigate vascular reactivity. *Biomedical Physics & Engineering Express* **2018**, *4*, 067003.
15. Stefano, S.; Alessandro, M.; Silvestro, R. Vascular reactivity of cutaneous circulation to brief compressive stimuli, in the human forearm. *European journal of applied physiology* **2020**, *120*, 1041–1050.
16. Ferraresi, C.; De Benedictis, C.; Maffiodo, D.; Franco, W.; Messere, A.; Pertusio, R.; Roatta, S. Design and simulation of a novel pneumotronic system aimed to the investigation of vascular phenomena induced by limb compression. *Journal of Bionic Engineering* **2019**, *16*, 550–562.
17. Ferraresi, C.; Franco, W.; Maffiodo, D.; De Benedictis, C.; Paterna, M.; Pacheco Quiñones, D.; Ermini, L.; Roatta, S. Applications of Intermittent Pneumatic Compression for Diagnostic and Therapeutic Purposes. International Workshop IFToMM for Sustainable Development Goals. Springer, 2021, pp. 209–218.
18. Xing, C.Y.; Liu, Y.L.; Zhao, M.L.; Yang, R.J.; Duan, Y.Y.; Zhang, L.H.; Sun, X.D.; Yuan, L.J.; Cao, T.S. New method for noninvasive quantification of central venous pressure by ultrasound. *Circulation: Cardiovascular Imaging* **2015**, *8*, e003085.

19. Millington, S.J. Ultrasound assessment of the inferior vena cava for fluid responsiveness: easy, fun, but unlikely to be helpful. *Canadian Journal of Anesthesia/Journal canadien d'anesthésie* **2019**, *66*, 633–638.
20. Das, S.K.; Choupoo, N.S.; Pradhan, D.; Saikia, P.; Monnet, X. Diagnostic accuracy of inferior vena caval respiratory variation in detecting fluid unresponsiveness: a systematic review and meta-analysis. *European Journal of Anaesthesiology| EJA* **2018**, *35*, 831–839.
21. Tobin, M.J.; Mador, M.J.; Guenther, S.M.; Lodato, R.F.; Sackner, M.A. Variability of resting respiratory drive and timing in healthy subjects. *Journal of Applied Physiology* **1988**, *65*, 309–317.
22. Mesin, L.; Pasquero, P.; Albani, S.; Porta, M.; Roatta, S. Semi-automated tracking and continuous monitoring of inferior vena cava diameter in simulated and experimental ultrasound imaging. *Ultrasound in medicine & biology* **2015**, *41*, 845–857.
23. Blehar, D.J.; Resop, D.; Chin, B.; Dayno, M.; Gaspari, R. Inferior vena cava displacement during respirophasic ultrasound imaging. *Critical Ultrasound Journal* **2012**, *4*, 1–5.
24. Mesin, L.; Roatta, S.; Pasquero, P.; Porta, M. Automated volume status assessment using Inferior Vena Cava pulsatility. *Electronics* **2020**, *9*, 1671.
25. Ermini, L.; Seddone, S.; Policastro, P.; Mesin, L.; Pasquero, P.; Roatta, S. The Cardiac Caval Index: Improving Noninvasive Assessment of Cardiac Preload. *Journal of Ultrasound in Medicine* **2021**.
26. Mesin, L.; Giovinazzo, T.; D'Alessandro, S.; Roatta, S.; Raviolo, A.; Chiacchiarini, F.; Porta, M.; Pasquero, P. Improved repeatability of the estimation of pulsatility of inferior vena cava. *Ultrasound in medicine & biology* **2019**, *45*, 2830–2843.
27. Crimi, A.; Makhinya, M.; Baumann, U.; Thalhammer, C.; Szekely, G.; Goksel, O. Automatic measurement of venous pressure using B-mode ultrasound. *IEEE Transactions on Biomedical Engineering* **2015**, *63*, 288–299.
28. Baulmann, J.; Schillings, U.; Rickert, S.; Uen, S.; Düsing, R.; Illyes, M.; Cziraki, A.; Nickenig, G.; Mengden, T. A new oscillometric method for assessment of arterial stiffness: comparison with tonometric and piezo-electronic methods. *Journal of hypertension* **2008**, *26*, 523–528.
29. Miyata, M. Noninvasive assessment of arterial stiffness using oscillometric methods: baPWV, CAVI, API, and AVI. *Journal of atherosclerosis and thrombosis* **2018**, *25*, 790–791.
30. Minten, J.; Van de Werf, F.; Aubert, A.E.; Kesteloot, H.; Geest, H.D. Apparent pulse wave velocity in the canine superior vena cava. *Cardiovascular research* **1983**, *17*, 627–632.
31. Nagdev, A.D.; Merchant, R.C.; Tirado-Gonzalez, A.; Sisson, C.A.; Murphy, M.C. Emergency department bedside ultrasonographic measurement of the caval index for noninvasive determination of low central venous pressure. *Annals of emergency medicine* **2010**, *55*, 290–295.

Paper V

The Cardiac Caval Index

Improving Noninvasive Assessment of Cardiac Preload

Leonardo Ermini, MS, Stefano Seddone, MS, Piero Policastro, MS, Luca Mesin, MS, PhD, Paolo Pasquero, MD, Silvestro Roatta, MS, PhD

Objectives—Inferior vena cava (IVC) pulsatility quantified by the Caval Index (CI) is characterized by poor reliability, also due to the irregular magnitude of spontaneous respiratory activity generating the major pulsatile component. The aim of this study was to test whether the IVC cardiac oscillatory component could provide a more stable index (Cardiac CI-CCI) compared to CI or respiratory CI (RCI).

Methods—Nine healthy volunteers underwent long-term monitoring in supine position of IVC, followed by 3 minutes passive leg raising (PLR). CI, RCI, and CCI were extracted from video recordings by automated edge-tracking and CCI was averaged over each respiratory cycle (aCCI). Cardiac output (CO), mean arterial pressure (MAP) and heart rate (HR) were also recorded during baseline (1 minutes prior to PLR) and PLR (first minute).

Results—In response to PLR, all IVC indices decreased ($P < .01$), CO increased by 4 ± 4% ($P = .055$) while HR and MAP did not vary. The Coefficient of Variation (CoV) of aCCI (13 ± 5%) was lower than that of CI (17 ± 5%, $P < .01$), RCI (26 ± 7%, $P < .001$) and CCI (25 ± 7%, $P < .001$). The mutual correlations in time of the indices were 0.81 (CI-RCI), 0.49 (CI-aCCI) and 0.2 (RCI-aCCI).

Conclusions—Long-term IVC monitoring by automated edge-tracking allowed us to evidence that 1) respiratory and averaged cardiac pulsatility components are uncorrelated and thus carry different information and 2) the new index aCCI, exhibiting the lowest CoV while maintaining good sensitivity to blood volume changes, may overcome the poor reliability of CI and RCI.

Key Words—automatic edge-tracking; fluid responsiveness; inferior vena cava; passive leg raising; volume status

In the clinical setting, deciding whether and what amount of fluid to administer intravenously to a patient, that is, the prediction of fluid responsiveness, is a long-standing open issue, whose relevance is paramount. Indeed, it has been shown that only half of the hemodynamic unstable patients exhibits a positive outcome after a fluid challenge,[1] while the remaining ones are exposed to the risk of fluid overload.[2–4] Since no satisfactory solution to this problem has been found yet, improvements in the existing techniques as well as new methodological approaches are constantly investigated.[5–9]

Due to its fast and noninvasive approach, the echographic assessment of the inferior vena cava (IVC) pulsatility (often also termed "collapsibility") is a widely adopted monitoring technique.[7] From the analysis of pulsatility, it is possible to infer about the mechanical characteristics of blood vessels, such as stiffness

Received September 11, 2021, from the Laboratory of Integrative Physiology, Department of Neuroscience, Università di Torino, Torino, Italy (L.E., S.S., S.R.); Mathematical Biology and Physiology, Department of Electronics and Telecommunications, Politecnico di Torino, Torino, Italy (P.P., L.M.); and Department of Medical Sciences, Università di Torino, Torino, Italy (P.P.). Manuscript accepted for publication November 19, 2021.

This activity was supported by local grants (ROAS_RILO_17_01), University of Torino, and by Proof of Concept "Vein Image Processing for Edge Rendering—VIPER," supported by the Italian Ministry of Economic Development, CUP C16I20000080006.

An instrument implementing the algorithm used in this report to automatically track IVC edges and to extract the mean IVC diameter was patented by Politecnico di Torino and Università di Torino (WO 2018/134726).

Address correspondence to Leonardo Ermini, MS, c.so Raffaello 30, 10125 Torino, Italy.

E-mail: leonardo.ermini@unito.it

Abbreviations

aCCI, averaged Cardiac Caval Index; CCI, Cardiac Caval Index; CI, Caval Index; CO, Cardiac Output; CoV, Coefficient of Variation; CVP, Central Venous Pressure; HR, Heart Rate; IVC, Inferior Vena Cava; MAP, Mean Arterial Pressure; PLR, Passive Leg Raising; RCI, Respiratory Caval Index; ROC, Receiver Operating Characteristic; US, Ultrasound

doi:10.1002/jum.15909

and compliance, and about their determinants, such as blood pressure, blood volume, vessel tone, etc.[10] IVC pulsatility is often quantified by means of the Caval Index (CI), which conveniently normalizes the respirophasic diameter variation (d_{max}–d_{min}) to d_{max}, thus accounting for individual differences in IVC size (d_{max} and d_{min} being the maximum and minimum diameters, as measured at the end of the expiratory and inspiratory phases, respectively). However, this index suffers of a large variability and, consequently, of poor reliability.[11–13] Based on the development of new image processing algorithms, several sources of variability were recently investigated and compensated for, for example, by tracking the displacement of the vessel with respect to the ultrasound (US) probe[14,15] and by averaging the measurements over several IVC diameters in either short[16] or long-axis,[15,17] which contributed to improve the repeatability of the measurements.[16,17] However, a major source of variability in the respirophasic oscillation of IVC size is the intrinsic variability of spontaneous respiratory activity, in terms of magnitude, frequency and relative extent of thoracic/diaphragmatic respiration,[18,19] all these aspects providing consistent effects on IVC pulsatility.[19–22] A possible solution to this problem was originally suggested by Nakamura[23] who proposed to consider the cardiac component of IVC pulsatility rather than the respiratory. The issue was followed-up in few subsequent studies.[16,17,20,24] In these studies, the automated analysis of US video clips yielded the continuous description of IVC size changes with high time resolution (equal to the frame rate of the US video recording), so that the cardiac and respiratory components of IVC pulsatility could be easily separated, based on their different frequency contents, and independently analyzed.[16,17,24] On this basis, the Respiratory Caval Index (RCI) and the Cardiac Caval Index (CCI), specifically quantifying the respiratory and cardiac component of IVC pulsatility, were introduced and compared. The results showed that also the CCI could be used as an index of vascular filling[23,24] and that it was characterized by a lower variability (as quantified by the coefficient of variation, CoV) than the RCI, although, contrary to the expectation, not lower than the variability of the CI.[17] Two reasons may possibly explain this observation: 1) the above-mentioned results refer to index variability over different subjects and measurement sessions, while the actual CCI variability over time has never been assessed; 2) the cardiac pulsatility may still be affected by a respiratory modulation, as apparent from published recordings[17,25] and confirmed in preliminary observations. However, to our knowledge, all studies generally considered only short time intervals lasting 10 to 15 seconds, and the time correlation between pulsatile components has never been investigated.

We hypothesized that 1) by further improving the signal processing we could effectively reduce the respiratory modulation of CCI and obtain a more stable hemodynamic index of vascular filling; 2) due to its different nature, the CCI could differ from RCI and CI in terms of time course and responsiveness to fluid challenges.

To this purpose, continuous and long-duration recordings of B-mode IVC imaging were performed with the help of a dedicated probe holder, in resting conditions and during a simulated fluid challenge, as produced by a passive leg raising (PLR).

Materials and Methods

Subjects

Nine healthy volunteers (7 M, 2 F, age 34 ± 9) were included in the study, with the only exclusion criteria being a poor quality of the echographic imaging. The study was approved by the Ethics Committee of the University of Torino (March 23, 2015) and all participants gave their informed consent according to the principles of the Helsinki Declaration.

Experimental Setup and Protocol

Participants remained supine on a clinical bed for at least 30 minutes before starting the experiment, in order to stabilize the equilibrium between fluid compartments.[20,26] A two-dimensional B-mode longitudinal view of the IVC was recorded by means of a MyLab 25 Gold system (ESAOTE, Genova, Italy) equipped with a convex 2 to 5 MHz US probe, according to a *sub-xyphoid* transabdominal long-axis approach (2–3 cm caudal to the right atrial junction).[27] To achieve long-lasting US monitoring, we made use of a probe holder, as successfully implemented in previous studies for stable echo-Doppler monitoring of arteries and veins of upper and lower limbs.[9,28–31] In the

present case, the probe holder was stemming from one side of the bed and its 40-cm long horizontal arm was allowed to freely rotate about a joint at one of its ends. The US probe, located at the other end, due to its own weight, could then exert a light pressure on the abdomen and maintain adequate acoustic contact, accommodating with virtually vertical displacements the small abdominal movements during respiration. This arrangement allowed us to continuously monitor the IVC for the whole duration of the protocol (4 minutes).

The experimental protocol consisted of 1 minutes of rest in supine position (baseline), followed by 3 minutes during which the legs were passively raised and maintained at about 45° (PLR) and 1 minutes of rest, again in supine position. During the entire protocol, the US video of the IVC longitudinal section (in the sagittal plane) was recorded for the subsequent processing and analysis. In addition, heart rate (HR), mean arterial pressure (MAP) and cardiac output (CO) were non-invasively monitored by photoplethysmography (CNAP®, CNSystems Medizintechnik, Graz, Austria) while breathing was monitored by means of a custom-made strain gauge band placed around the chest (the recorded signal is referred to as Breath in the following). All these signals were digitally and synchronously recorded by a general-purpose acquisition board (Micro 1401 IImk, CED, Cambridge, UK, with Spike2 software): IVC videos were acquired at about 30 fps while HR, MAP, CO, and breathing were sampled at 10 Hz.

IVC Segmentation

US videos were processed by a custom-made software (implemented in MATLAB 2020a, The MathWorks, Natick, MA) for IVC edge-tracking. The routines were based on a previously developed algorithm.[15] The tracking algorithm was improved to attenuate the effect of small drifts, which would produce detrimental effects with videos of long duration considered here (manuscript in preparation). The edges of the IVC were estimated as previously described,[15] by sampling along 21 directions crossing the blood vessel, considering a portion selected by an operator (PPo), who was blinded to the results. Along each direction, the software estimated the US pixel intensity by interpolation. Then, abrupt variations of this estimated US intensity were identified as the locations of the two IVC edges along the considered direction (see Mesin et al[15] for additional details). The length of the segment between each couple of points placed on the upper and lower vein edges was the IVC diameter along that direction.

The median axis of the vein was estimated (as the mean of the two sampled edges), interpolated by a second-order polynomial and used to rotate the 21 diameters mentioned above to be orthogonal to it. By considering all frames of the US video, each diameter was a time series. High-frequency contributions in these time series of diameters (mostly related to superimposed noise) were removed. For the identification of the cut-off frequency, the power spectrum density (PSD) of the diameters was first computed (Burg method, with order 40[32]), from which the highest frequency of our interest was identified as follows. First, we have searched for a peak in the PSD between 40 and 120 bpm, which reflected the cardiac component. Then, the median (across diameters) of peak frequencies (mf) was computed (this parameter was used later to define the cut-off frequency of the filter). Then, a portion of 15 mm around the position of the diameter showing the highest peak of the cardiac component was selected (assuming that such a diameter provided reliable information on the cardiac contribution and that it was less affected by noise than the other diameters). Upper and lower border points of this portion of the vein were then interpolated with two straight lines. Finally, the *mean IVC diameter*, for each frame, was calculated as the area of the IVC section considered above, divided by its length (ie, 15 mm).

Such a mean diameter was low-pass filtered, with cut-off frequency equal to $mf + 0.5$ Hz (Chebyshev of type I, stop band starting at $mf + 1.5$ Hz, minimum attenuation of 30 dB, passband from 0 to $mf + 0.5$ Hz with ripple of 0.5 dB), and indicated with *dIVC*.

The respiratory and cardiac components of IVC pulsatility were estimated from the mean diameter just obtained. The respiratory diameter, indicated as *R-dIVC*, was estimated by the first step of the Empirical Mode Decomposition applied to the mean diameter. Specifically, two curves were first obtained by interpolating the local maxima and the local minima of *dIVC*. The curve *R-IVC* was defined as the mean of these two curves. Notice that this technique allows to

estimate each respiration cycle. On the other hand, a filter with fixed passband was used in previous works[17]: such a filter had lower performances than the one used here, especially with our long recordings, in which respiration cycles could have very different durations (thus, being attenuated differently by a fixed filter). The cardiac diameter, called C-dIVC, was computed as $C\text{-}dIVC = dIVC\text{-}R\text{-}dIVC + s\text{-}dIVC$ and is equivalent to the mean diameter deprived of the respiratory oscillations. The term *s-dIVC* indicates the low-pass filtered mean diameter with cut-off 0.05 Hz (Chebyshev filter of type I, stop band starting at 0.5 Hz, minimum attenuation of 30 dB, passband ripple of 0.5 dB), where only the *slow* subrespiratory frequencies are left. This low-pass filter was chosen in order to remove any oscillation and keep only the low-frequency trend reflecting slow IVC size variations induced by the PLR.

At this point of the analysis, the three diameters, *dIVC*, *R-dIVC*, and *C-dIVC* were available as time series (see Figure 1) and were used to estimate the pulsatility indicators CI, RCI and Cardiac Caval Index (CCI) respectively, according to the usual formula: $(d_{\max} - d_{\min})/d_{\max}$ (Figure 1, bottom). Note that, while for CI and RCI one estimate per respiratory cycle is obtained, the CCI yields one estimate per cardiac cycle.

In addition, an *averaged* version of the CCI, aCCI, was computed by averaging the CCI over distinct respiratory cycles. The aCCI estimates could then be considered synchronous with CI and RCI (one estimate per respiratory cycle).

Figure 1. Tracings from a representative subject, in resting condition. The time course of each one of the following variables is shown: heart rate (HR), mean arterial pressure (MAP), respiration (Breath), inferior vena cava (IVC) respiratory (R-dIVC) and cardiac (C-dIVC) components of the native diameter trace (dIVC) and their respective indexes, namely, Caval Index (CI), Respiratory Caval Index (RCI) and averaged Cardiac Caval Index (aCCI). In the latter graph, the markers indicate the exact sample of each IVC pulsatility indexes, as described in the legend, while the continuous gray lines are the respective cubic interpolation that were superimposed for a better visualization.

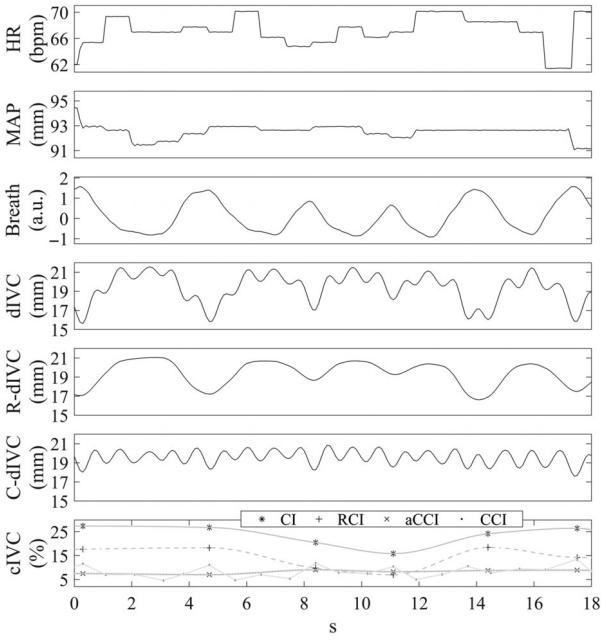

Data Analysis

HR, MAP and CO were exported from Spike2 software to MATLAB® (version 2020b) for off-line analysis. As a first step, they were aligned in time with the time-series of the IVC pulsatility indexes, computed separately as explained above, that presented a non-uniform sampling rate due to their nature. Indeed, CI, RCI, and aCCI had one sample per respiratory cycle while CCI one per heartbeat: The sample location in time, within the respiratory cycle, was arbitrary and we chose to be at the minimum of the IVC diameter component for all the three indexes.

The intrasubject variability in time of each IVC pulsatility index was quantified during baseline by the coefficient of variation $(\text{CoV} = (\text{std/mean}) \times 100)$ and averaged across all subjects. The correlation of time course in baseline was tested among CI, RCI, and aCCI, for each subject, using the Pearson correlation coefficient (ρ); then, the mean ρ across subjects was computed by averaging the individual ρ values after a Fisher Z-transformation and subsequently applying an inverse transformation to the result.

In order to perform the correlation of IVC indices with other signals, they were resampled at 10 Hz, after a shape-preserving piecewise cubic interpolation. This was necessary to test the correlation of CCI and aCCI with the respiratory pattern. However, since the delay between the respiratory effort and the resulting changes in size of the IVC cannot be assumed constant neither across subject nor over time, the normalized cross-correlation function on the appropriately standardized signals, instead of Pearson

correlation coefficient, was employed and its maximum value, irrespective of the delay, was chosen as the correlation coefficient (ρ). Then, the ρ values obtained were averaged across subjects using the Fisher transformation as explained above.

The response to the PLR is known to take place within the first minute after raising the legs[33] and, for each of the variables, it was assessed as the difference between the mean value calculated during the first minute of PLR and during the whole baseline (1 minutes), as DELTA = PLR-baseline, and considered in both absolute and relative (percentage) terms. For both basal and DELTA values, mutual correlations among CI, RCI, and aCCI were quantified by the Pearson correlation coefficient, presented along with the 95% confidence interval in between brackets. The effect of PLR on each variable was assessed considering the distribution of DELTA values and testing if the mean differed from zero with a level of significance set at 0.05, by means of the Wilcoxon signed rank test. The same test was used to compare the variability in time (as expressed by the CoV) of aCCI with CI and RCI. The IVC indices accuracy in predicting the subject response to the simulated fluid challenge, as induced by PLR, was analyzed by means of ROC curves built using a 10% increase in CO as marker of fluid responsiveness.[6,34]

Finally, it is worth to mention that, given the nonuniform sampling rate for the IVC pulsatility indexes, their average time course, across subjects, was obtained by averaging the interpolated curves.

Results

Basal Conditions

An example of the original tracings from a representative subject is shown in Figure 1 which includes the continuous recordings of some systemic variables like HR, MAP, and respiratory activity as well as variables extracted from the US monitoring of the IVC, that is, the IVC diameter (average diameter of the considered IVC segment), the respiratory diameter (high-frequency components are filtered out) and the cardiac diameter (the respiratory component is filtered out). At the bottom of the figure are the different indices, automatically calculated. Two aspects need to be observed.

1. A strong correspondence exists between the magnitude of respiratory acts and the respiratory changes in IVC diameter. Accordingly, CI and RCI (bottom) are also modulated by the depth of respiration, in particular, it is worth to notice how CI and RCI drop (the variation is in the order of 10%) around the fourth second of the recording, concomitantly with a reduced inspiratory depth, as revealed by the Breath signal.
2. Even the cardiac pulsatility is modulated by the respiratory activity. Accordingly, such modulation is preserved in CCI and affects its variability in time.

We first tested whether the averaging over single respiratory cycles, as implemented for the calculation of aCCI, was effective in reducing the respiratory modulation affecting CCI: The averaged maxima of cross-correlation with respiration dropped from 0.4 (CCI) to 0.02 (aCCI). Then, we tested whether this new feature was effective in reducing the overall variability in time, as assessed by the CoV. In Figure 2, it is possible to observe the distribution of the individual CoVs, depicted by means of box and whiskers plots, for each IVC pulsatility index, including the original CCI. The mean $\pm$ STD CoV values of CI, RCI, CCI and aCCI are, respectively, $17 \pm 5\%$, $26 \pm 7\%$, $25 \pm 7\%$, $13 \pm 5\%$. As expected, aCCI exhibited a lower variability than CCI. The improved stability over time can also be observed by comparing the corresponding tracings in Figure 1. Moreover, aCCI also achieved a lower CoV than CI ($P < .01$).

Response to PLR

On a different timescale, the full representation of the response to PLR of a representative subject is shown in Figure 3. It can be observed that during PLR, starting at time 0 seconds, both cardiac and respiratory pulsatile components are reduced, and that the IVC diameter is increased. This results in a reduction of all indices during PLR, as displayed at the bottom.

In Figure 4, the averaged (across subjects) time course of HR, MAP, and CO are presented in terms of percentage changes with respect to the mean baseline value (ie, DELTA in percentage terms). It can be observed that at the beginning of PLR (time 0 seconds), HR and MAP exhibit only small fluctuations while CO immediately begins to rise reaching a

Figure 2. Coefficient of variation (CoV) of pulsatility indexes of the inferior vena cava. The CoV distributions across subjects computed during baseline are shown for Caval Index (CI), Respiratory Caval Index (RCI), Cardiac Caval Index (CCI) and averaged Cardiac Caval Index (aCCI). The red dots indicate the individual data.

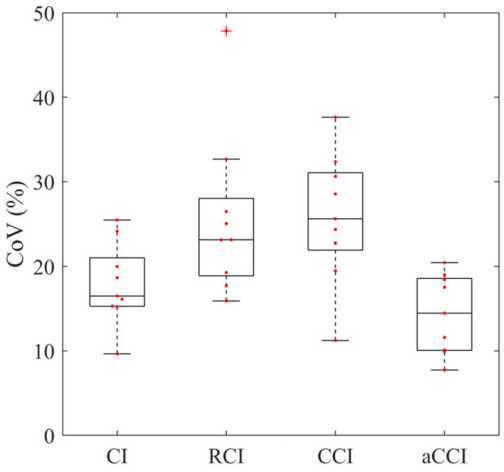

peak at around 30 seconds and returning to the basal value at around 60 seconds, before the end of PLR (180 seconds).

Figure 5 shows, on the same timescale, the averaged (across subjects) time course of IVC pulsatility indexes, namely CI, RCI, and aCCI (with CCI superimposed as dashed line). Here the variations with respect to the mean baseline values are not translated in percentage terms, since the indexes are already expressed as percentages, so that absolute variations (of a percentage) are considered (ie, DELTA in absolute terms). It can be observed that all indices exhibit a consistent decrease, which is maintained throughout PLR, and that aCCI exhibited a sharper decrease at the beginning of PLR, compared to CI and RCI.

In Table 1, the values averaged across subjects for baseline, PLR, and DELTA (in percentage terms) for all the physiological variables of interest are listed, as well as the statistical significance against the null hypothesis of no effects induced by PLR. As it can be noticed, HR and MAP did not change following PLR while CO and all the IVC pulsatility indexes did.

Finally, regarding the prediction of fluid responsiveness, both CI and aCCI performed as perfect classifiers (ie, AUCROC 1) with threshold of 21 and 9%,

Figure 3. Example of a complete individual recording. The time course of each one of the following variables is shown: heart rate (HR), mean arterial pressure (MAP), respiration (Breath), inferior vena cava (IVC) respiratory (R-dIVC) and cardiac (C-dIVC) components of the native diameter trace (dIVC) and their respective indexes, namely Caval Index (CI), Respiratory Caval Index (RCI) and averaged Cardiac Caval Index (aCCI). In the latter graph, the markers indicate the exact sample of each IVC pulsatility indexes, as described in the legend, while the continuous gray lines are the respective cubic interpolation that were superimposed for a better visualization.

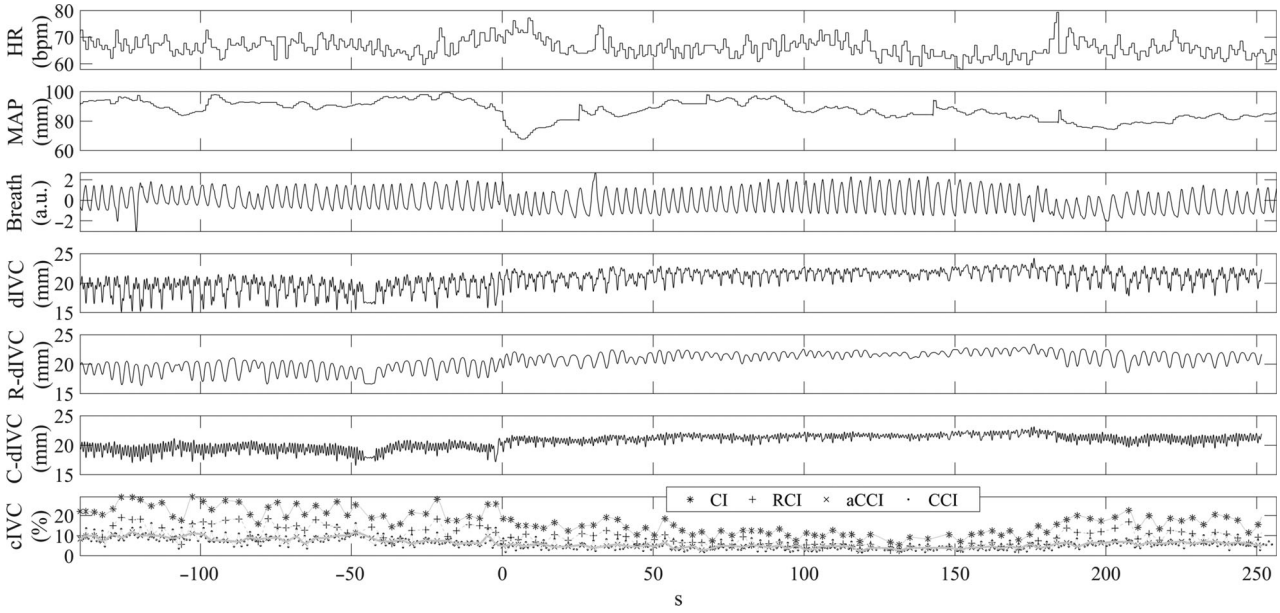

Figure 4. Hemodynamic variables averaged (across subjects) time course. Percentage changes with respect to the mean baseline value of heart rate (ΔHR), mean arterial pressure (ΔMAP), and cardiac output (ΔCO): The black solid line represents the mean while the shaded gray error bar represent mean ± std. The vertical dashed lines mark the beginning (left one) and the end (right one) of the PLR.

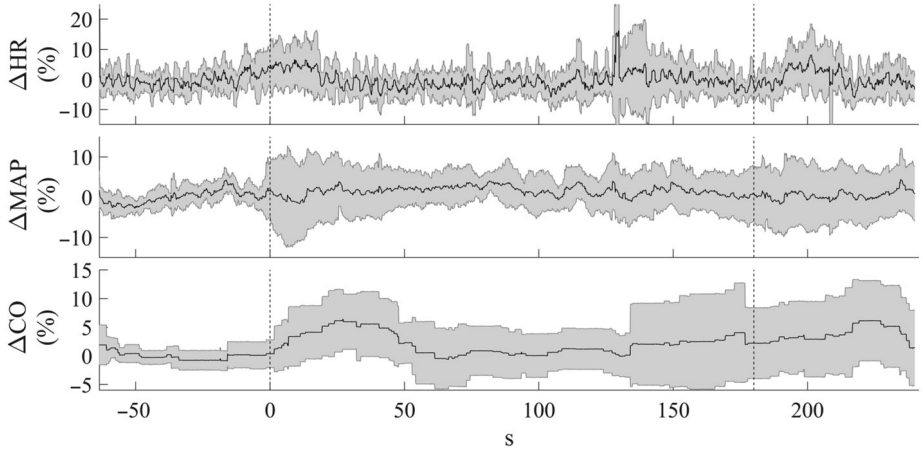

Figure 5. Inferior Vena Cava pulsatility indexes averaged (across subjects) time course. Absolute changes with respect to the mean baseline value of Caval Index (ΔCI), Respiratory Caval Index (ΔRCI) and averaged Cardiac Caval Index (ΔaCCI): The black solid line represents the mean while the shaded gray error bar represents mean ± std. The latter graph presents also a superimposed dashed line trace that is the native Cardiac Caval Index: Note the oscillations due to the respiratory modulation of the cardiac induced pulsatility which are removed in the aCCI trace (black solid line). The vertical dashed lines mark the beginning (left one) and the end (right one) of the PLR.

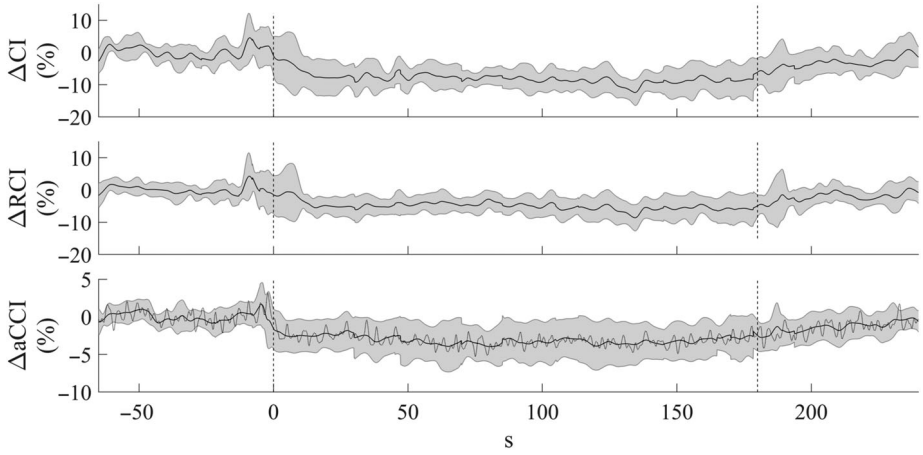

respectively, while RCI reached a poorer performance (AUCROC 0.78).

Correlations Among Indices

The individual mutual correlations in time among the IVC pulsatility indexes are reported below (the original CCI is no longer considered): The biggest correlation is between CI and RCI (mean value 0.81), while the smallest one is between RCI and aCCI (mean value 0.2) and the intermediate one is between CI and aCCI (mean value 0.49). It is worth to mention that the CI-RCI distribution presents a narrower interquartile range compared to the CI-aCCI distribution, highlighting the robustness of the link between the former two indexes. Finally, the Pearson correlation coefficient among the averaged baseline values of CI-RCI, CI-aCCI, and RCI-aCCI was 0.92 (0.66, 0.98), 0.76 (0.19, 0.95), and 0.50 (−0.25, 0.87),

Table 1. Averaged Values of Heart Rate, Mean Arterial Pressure, Cardiac Output, Caval Index (CI), Respiratory Caval Index, and averaged Cardiac Caval Index (aCCI) in absolute values, during baseline and PLR, and in terms of percentage variation during PLR w.r.t. the mean baseline value (DELTA)

Variable	Baseline	PLR	DELTA %	*P*-Value
Heart rate (bpm)	59 ± 9	59 ± 10	0 ± 3	.82
Mean arterial pressure (mmHg)	89 ± 11	90 ± 9	1 ± 6	.43
Cardiac output (L/min)	5.0 ± 0.8	5.1 ± 0.7	4 ± 4	.03
Caval Index (%)	27 ± 6	19 ± 7	−31 ± 17	.004
Respiratory Caval Index (%)	14 ± 4	9 ± 4	−35 ± 17	.004
averaged Cardiac Caval Index (%)	13 ± 4	9 ± 4	−28 ± 21	.008

Values are expressed as mean ± std. Last column reports the *P*-value of the paired statistical comparison, by means of a paired Wilcoxon signed rank test, among the two distributions of PLR and baseline individually averaged values.

respectively. The same coefficients for the DELTA values, following the same order, were 0.74 (0.16, 0.94), 0.73 (0.13, 0.94), and 0.2 (−0.53, 0.76).

Discussion

The present study allowed to confirm preliminary observations and to achieve new relevant results, which can be synthetized as follows:

1. Although the CI is generally considered as an index of the respiratory-induced pulsatility of the IVC, it is heavily affected (or disturbed) by a pulsatility of cardiac nature.
2. The magnitude of the cardiac pulsatility of IVC is still modulated by the respiratory activity, which negatively impacts on the reliability of the CCI.
3. Averaging the CCI over single respiratory cycles effectively eliminates the respiratory modulation and improves its stability in time.
4. The aCCI responsiveness to PLR is uncorrelated to that of RCI, suggesting that the two indices may carry different information.

To our knowledge, this is the first study reporting a long-term monitoring and analysis of IVC pulsatility, which was achieved thanks to a newly devised experimental setup and consolidated image processing algorithms.[14,15,17,25,35] With this approach, a continuous time series of the average IVC diameter, with high time resolution, could be analyzed along with other physiological variables: Such an analysis included the identification of the oscillatory components of the IVC diameter of respiratory and cardiac origin and the automated calculation of the corresponding pulsatility indices RCI and CCI (Figure 1).[17]

The Pivotal Role of Heart in Inferior Vena Cava Respirophasic Oscillations

The aforementioned framework gave us the possibility to carefully observe the interplay between respiration and heartbeat in generating the IVC pulsatility. Indeed, although IVC pulsatility has been already the object of hundreds of studies[12,13] and its use in the clinical settings, as predictor of fluid responsiveness[6,7] or as surrogate measure of central venous pressure,[35] has been extensively investigated, only recently the cardiac component of the IVC pulsatility has been described.[23] This component was probably too weak or too fast to be detected and disentangled from the slower respiratory component by means of just the visual assessment and the standard tools available on US machines. On the one hand, these limitations delayed the recognition and the investigation of the characteristics and meaning of the cardiac component, on the other hand, the unrecognized cardiac oscillation, merging with the primary respiratory oscillation, decreased the "signal-to-noise ratio" and increased the variability of the oscillatory pattern. We speculate that this overlooked "disturbance" on the assessment of IVC diameter may at least partly explain the poor reliability and clinical applicability of the CI.[12,13] Notably, in the present study, removal of the cardiac pulsatility reduced the IVC pulsatility index by about 50% (ie, RCI is about 50% of CI) and, accordingly, the aCCI approximately accounts for the other 50% (see Table 1, baseline). These results challenge the concept that the classical IVC CI quantifies the "respirophasic" changes in IVC diameter.

As shown in the representative recordings of Figure 1, as well as in other figures previously published,[16,17] the cardiac pulsatility is modulated by respiration: the magnitude of the oscillation increases at low IVC diameter, which occurs approximately at the end of the inspiratory phase (maximum lung volume). This modulatory pattern fits with the idea that the pulse pressure, mainly provided by the atrial contraction, results in a lower volume increase (reflected by a lower IVC diameter increase) when the IVC compliance is lower, which occurs at larger IVC size.[10] Surprisingly an opposite pattern is shown in Figure 4 of the study from Sonoo et al,[24] that is, wider cardiac pulsatility during expiration compared to inspiration. However, their average findings (collected from 142 patients enrolled in an emergency department) confirm a higher CCI during inspiration (13.8%) compared to expiration (11.0%). This modulatory action is responsible for the high CoV of the CCI in time, similar to the CoV of CI (Figure 2)[17] and negatively impacts on its potential clinical usefulness. By simply averaging over single respiratory cycles (aCCI), this problem was effectively addressed and the CoV in time considerably reduced.

As discussed above, cardiac pulsatility is larger when the vessel size is smaller and vessel compliance is larger. As such, aCCI candidates as a possible indicator of IVC compliance and of poor vascular filling. In this respect, it is interesting to observe that it was shown to correlate to CI, both in time (intrasubject) and across different subjects (in basal conditions). Moreover, it was significantly affected by PLR (-28%, $P < .01$).

On the other hand, while a similar performance was reported by RCI (good correlation with CI and significant decrease during PLR), aCCI and RCI were very poorly correlated: their spontaneous oscillations in resting conditions are uncorrelated, their absolute values assessed in resting conditions are uncorrelated, their responses to a (simulated) fluid challenge are uncorrelated. These results strongly suggest that RCI and CCI are carrier of different information (although both sensitive to fluid challenges). Their different time course in the response to PLR (Figure 5, aCCI exhibiting a faster and sharper response than RCI) further supports this proposition.

Clinical Implications

While further studies are necessary to understand the distinct physio-pathological meaning of the two indices and their possible integration for clinical purposes, the possibility to get increased and more reliable information from the same fast and noninvasive US examination is intriguing. To date, only few studies have included a cardiac IVC pulsatility index in their outcomes. In particular, the presence of CCI enhanced the capacity to predict the volume status[25] and right atrial pressure in patients.[35] However, no one has yet investigated the potential of CCI in predicting a fluid challenge. For this reason, although we were curious to perform such an investigation, we are aware that, given our small dataset ($N = 9$) and the limitations of the photoplethysmographic fingercuff pulse contour analysis techniques in reliably monitoring CO,[36] the extrapolated ROC analysis presented in this work are not relevant for a valid fluid responsiveness study. Beyond that, we believe that the present findings, although obtained on healthy volunteers, can add new useful information to the widespread use of the IVC pulsatility indexes in predicting the fluid responsiveness in patients.

Physiologic Response to Passive Leg Raising

A final comment concerns the general response to PLR in this group of healthy subjects, which provides a nice description of the physiological adaptation of the body to the new situation (Figures 4 and 5): no apparent effect on MAP, only a minor (pre-) activation of HR, probably an increase in alertness due to the passive leg movement, along with a small but visible transient increase in CO.[33] In comparison, all the IVC indices detect a net variation during PLR. Interestingly the exhibited changes are not transient, but last throughout the 3-minutes duration of the test, which likely indicates that this time is too short for adjustments in blood volume. Moreover, they show that the duration of the transients is shorter at the onset (<15 seconds) than at the termination of PLR (about 1 minutes).

Limitations

One limitation of the study is related to the way IVC videos were acquired, that is, with the probe held in place by a probe holder rather than by the hand of the echographer. While this was a necessary implementation to achieve stable recordings lasting several minutes, it is not without drawbacks, as involuntary spontaneous movements of the subject as well as

movements resulting from the PLR maneuver could occasionally interrupt the correct IVC tracking. However, thanks to the prompt intervention of the operators, the proper probe orientation was generally restored within seconds with no impact on the subsequent analysis. Prospectively, with the increasing adoption of 4D US machines, the edge-tracking will be likely extended to 3D images, which will minimize misalignment problems related to latero-lateral displacement of IVC: At present, a potential confounding factor in long-axis imaging of IVC, irrespective of whether the US probe is held by hand or fixed supports.

Secondly, the experiment was performed only on healthy volunteers posing some limitations to the extrapolation of the results to the clinical setting. Moreover, we had to exclude subjects that could not present good quality imaging of the IVC, as required by the image processing routines. This criterion slightly biased the recruited sample toward a prevalence of males, possibly due to their lower thickness of abdominal adipose tissue layer. However, we are not aware of sex-related differences in IVC indices that could have affected the general validity of the present results. Unfortunately, this is a known limitation of US studies that require high-quality imaging.

Finally, the possibility exists that CCI could be influenced by additional factors related to pathological alterations of cardiac function (concerning rhythm, contractility, stiffness, and valvular efficiency), of other variables such as pulmonary arterial pressure and intra-abdominal pressure, as well as of hemodynamic phenomena at the confluence of superior and inferior vena cava. These pathological states may alter the magnitude and the morphology of the cardiac component of CVP pulsatility irrespective or in addition to the mean CVP value. For instance, in atrial fibrillation the absence of the atrial systole and the irregularity of the ventricular rhythm would profoundly alter the pulsatile pattern of right atrial pressure. This is likely to introduce a pathology-dependent variability in the absolute value of CCI, although relative changes in CCI should still effectively detect or monitor acute changes in CVP and volume status. The influence of pathological conditions on the CCI remains to be explored through further studies on specific patient populations.

Conclusions

With this methodological study on healthy subjects, we evidenced that through echographic long-term monitoring of the IVC longitudinal section, in association with an automated edge-tracking software, it is possible to record the IVC diameter and distinct respiratory and cardiac pulsatility indexes as continuous time-series. A newly defined aCCI exhibited 1) the lowest variability in time, 2) good sensitivity to simulated blood volume changes, as induced by PLR and 3) poor correlation with the RCI in time, among subjects, and in their response to PLR, supporting the hypothesis that they carry different information. Therefore, we believe that aCCI has the potential to overcome the poor reliability of the classical CI in the fluid responsiveness prediction. Further studies in patients are needed to understand its specificity and explore its applicability in the clinical practice.

References

1. Bentzer P, Griesdale DE, Boyd J, MacLean K, Sirounis D, Ayas NT. Will this hemodynamically unstable patient respond to a bolus of intravenous fluids? *JAMA* 2016; 316:1298–1309. https://doi.org/10.1001/JAMA.2016.12310.
2. Sakr Y, Rubatto Birri PN, Kotfis K, et al. Higher fluid balance increases the risk of death from sepsis: results from a large international audit. *Crit Care Med* 2017; 45:386–394. https://doi.org/10.1097/CCM.0000000000002189.
3. Malbrain MLNG, Van Regenmortel N, Saugel B, et al. Principles of fluid management and stewardship in septic shock: it is time to consider the four D's and the four phases of fluid therapy. *Ann Intensive Care* 2018; 8:66. https://doi.org/10.1186/s13613-018-0402-x.
4. Silva JM, de Oliveira AMR, Nogueira FAM, et al. The effect of excess fluid balance on the mortality rate of surgical patients: a multicenter prospective study. *Crit Care* 2013; 17:R288. https://doi.org/10.1186/cc13151.
5. Monnet X, Marik PE, Teboul J-L. Prediction of fluid responsiveness: an update. *Ann Intensive Care* 2016; 6:1–11. https://doi.org/10.1186/S13613-016-0216-7.
6. Monnet X, Teboul JL. Assessment of fluid responsiveness: recent advances. *Curr Opin Crit Care* 2018; 24:190–195. https://doi.org/10.1097/MCC.0000000000000501.

7. Shi R, Monnet X, Teboul JL. Parameters of fluid responsiveness. *Curr Opin Crit Care* 2020; 26:319–326. https://doi.org/10.1097/MCC.0000000000000723.
8. Bednarczyk JM, Fridfinnson JA, Kumar A, et al. Incorporating dynamic assessment of fluid responsiveness into goal-directed therapy: a systematic review and meta-analysis. *Crit Care Med* 2017; 45: 1538–1545. https://doi.org/10.1097/CCM.0000000000002554.
9. Ermini L, Chiarello NE, De Benedictis C, Ferraresi C, Roatta S. Venous pulse wave velocity variation in response to a simulated fluid challenge in healthy subjects. *Biomed Signal Process Control* 2021; 63:102177. https://doi.org/10.1016/j.bspc.2020.102177.
10. Mesin L, Albani S, Policastro P, et al. Assessment of phasic changes of vascular size by automated edge tracking—state of the art and clinical perspectives. *Ultrasound Med Biol,* Submitted for publication.
11. Long E, Oakley E, Duke T, Babl FE. Does respiratory variation in inferior vena cava diameter predict fluid responsiveness: a systematic review and meta-analysis. *Shock* 2017; 47:550–559. https://doi.org/10.1097/SHK.0000000000000801.
12. Das SK, Choupoo NS, Pradhan D, Saikia P, Monnet X. Diagnostic accuracy of inferior vena caval respiratory variation in detecting fluid unresponsiveness: a systematic review and meta-analysis. *Eur J Anaesthesiol* 2018; 35:831–839. https://doi.org/10.1097/EJA.0000000000000841.
13. Orso D, Paoli I, Piani T, Cilenti FL, Cristiani L, Guglielmo N. Accuracy of ultrasonographic measurements of inferior vena cava to determine fluid responsiveness: a systematic review and meta-analysis. *J Intensive Care Med* 2020; 35:354–363. https://doi.org/10.1177/0885066617752308.
14. Mesin L, Pasquero P, Albani S, Porta M, Roatta S. Semi-automated tracking and continuous monitoring of inferior vena cava diameter in simulated and experimental ultrasound imaging. *Ultrasound Med Biol* 2015; 41:845–857. https://doi.org/10.1016/J.ULTRASMEDBIO.2014.09.031.
15. Mesin L, Pasquero P, Roatta S. Tracking and monitoring pulsatility of a portion of inferior vena cava from ultrasound imaging in long axis. *Ultrasound Med Biol* 2019; 45:1338–1343. https://doi.org/10.1016/J.ULTRASMEDBIO.2018.10.024.
16. Mesin L, Pasquero P, Roatta S. Multi-directional assessment of respiratory and cardiac pulsatility of the inferior vena cava from ultrasound imaging in short axis. *Ultrasound Med Biol* 2020; 46:3475–3482. https://doi.org/10.1016/J.ULTRASMEDBIO.2020.08.027.
17. Mesin L, Giovinazzo T, D'Alessandro S, et al. Improved repeatability of the estimation of pulsatility of inferior vena cava. *Ultrasound Med Biol* 2019; 45:2830–2843. https://doi.org/10.1016/J.ULTRASMEDBIO.2019.06.002.
18. Tobin MJ, Mador MJ, Guenther SM, Lodato RF, Sackner MA. Variability of resting respiratory drive and timing in healthy subjects. *J Appl Physiol* 1988; 65:309–317. https://doi.org/10.1152/JAPPL.1988.65.1.309.
19. Gignon L, Roger C, Bastide S, et al. Influence of diaphragmatic motion on inferior vena cava diameter respiratory variations in healthy volunteers. *Anesthesiology* 2016; 124:1338–1346. https://doi.org/10.1097/ALN.0000000000001096.
20. Folino A, Benzo M, Pasquero P, et al. Vena cava responsiveness to controlled isovolumetric respiratory efforts. *J Ultrasound Med* 2017; 36:2113–2123. https://doi.org/10.1002/JUM.14235.
21. Kimura BJ, Dalugdugan R, Gilcrease GW III, Phan JN, Showalter BK, Wolfson T. The effect of breathing manner on inferior vena caval diameter. *Eur J Echocardiogr* 2011; 12:120–123. https://doi.org/10.1093/ejechocard/jeq157.
22. Bortolotti P, Colling D, Colas V, et al. Respiratory changes of the inferior vena cava diameter predict fluid responsiveness in spontaneously breathing patients with cardiac arrhythmias. *Ann Intensive Care* 2018; 8:79. https://doi.org/10.1186/s13613-018-0427-1.
23. Nakamura K, Tomida M, Ando T, et al. Cardiac variation of inferior vena cava: new concept in the evaluation of intravascular blood volume. *J Med Ultrason* 2013; 40:205–209. https://doi.org/10.1007/S10396-013-0435-6.
24. Sonoo T, Nakamura K, Ando T, et al. Prospective analysis of cardiac collapsibility of inferior vena cava using ultrasonography. *J Crit Care* 2015; 30:945–948. https://doi.org/10.1016/J.JCRC.2015.04.124.
25. Mesin L, Roatta S, Pasquero P, Porta M. Automated volume status assessment using inferior vena cava pulsatility. *Electronics* 2020; 9: 1671. https://doi.org/10.3390/electronics9101671.
26. Hagan RD, Diaz FJ, Horvath SM. Plasma volume changes with movement to supine and standing positions. *J Appl Physiol* 1978; 45:414–418. https://doi.org/10.1152/JAPPL.1978.45.3.414.
27. Finnerty NM, Panchal AR, Boulger C, et al. Inferior vena cava measurement with ultrasound: what is the best view and best mode? *West J Emerg Med* 2017; 18:496. https://doi.org/10.5811/WESTJEM.2016.12.32489.
28. Messere A, Ceravolo G, Franco W, Maffiodo D, Ferraresi C, Roatta S. Increased tissue oxygenation explains the attenuation of hyperemia upon repetitive pneumatic compression of the lower leg. *J Appl Physiol* 2017; 123:1451–1460. https://doi.org/10.1152/japplphysiol.00511.2017.
29. Messere A, Turturici M, Millo G, Roatta S. Repetitive muscle compression reduces vascular mechano-sensitivity and the hyperemic response to muscle contraction. *J Physiol Pharmacol* 2017; 68: 427–437.
30. Messere A, Tschakovsky M, Seddone S, et al. Hyper-oxygenation attenuates the rapid vasodilatory response to muscle contraction and compression. *Front Physiol* 2018; 9:1078. https://doi.org/10.3389/fphys.2018.01078.
31. Ermini L, Ferraresi C, De Benedictis C, Roatta S. Objective assessment of venous pulse wave velocity in healthy humans. *Ultrasound Med Biol* 2020; 46:849–854. https://doi.org/10.1016/j.ultrasmedbio.2019.11.003.

32. Kay SM. *Modern Spectral Estimation: Theory and Application*. London, England: Pearson Education; 1988.
33. Monnet X, Teboul J-L. Passive leg raising: five rules, not a drop of fluid! *Crit Care* 2015; 19:18. https://doi.org/10.1186/s13054-014-0708-5.
34. Mesquida J, Gruartmoner G, Ferrer R. Passive leg raising for assessment of volume responsiveness: a review. *Curr Opin Crit Care* 2017; 23:237–243. https://doi.org/10.1097/MCC.0000000000000404.
35. Albani S, Pinamonti B, Giovinazzo T, et al. Accuracy of right atrial pressure estimation using a multi-parameter approach derived from inferior vena cava semi-automated edge-tracking echocardiography: a pilot study in patients with cardiovascular disorders. *Int J Cardiovasc Imaging* 2020; 36:1213–1225. https://doi.org/10.1007/s10554-020-01814-8.
36. Saugel B, Hoppe P, Nicklas JY, et al. Continuous noninvasive pulse wave analysis using finger cuff technologies for arterial blood pressure and cardiac output monitoring in perioperative and intensive care medicine: a systematic review and meta-analysis. *Br J Anaesth* 2020; 125:25–37. https://doi.org/10.1016/j.bja.2020.03.013.

Paper VI

scientific reports

Check for updates

OPEN

Evidence that large vessels do affect near infrared spectroscopy

Stefano Seddone[1], Leonardo Ermini[1], Piero Policastro[2], Luca Mesin[2] & Silvestro Roatta[1]✉

The influence of large vessels on near infrared spectroscopy (NIRS) measurement is generally considered negligible. Aim of this study is to test the hypothesis that changes in the vessel size, by varying the amount of absorbed NIR light, could profoundly affect NIRS blood volume indexes. Changes in haemoglobin concentration (tHb) and in tissue haemoglobin index (THI) were monitored over the basilic vein (BV) and over the biceps muscle belly, in 11 subjects (7 M – 4 F; age 31 ± 8 year) with simultaneous ultrasound monitoring of BV size. The arm was subjected to venous occlusion, according to two pressure profiles: slow (from 0 to 60 mmHg in 135 s) and rapid (0 to 40 mmHg maintained for 30 s). Both tHb and THI detected a larger blood volume increase (1.7 to 4 fold; $p < 0.01$) and exhibited a faster increase and a greater convexity on the BV than on the muscle. In addition, NIRS signals from BV exhibited higher correlation with changes in BV size than from muscle ($r = 0.91$ vs 0.55, $p < 0.001$ for THI). A collection of individual relevant recordings is also included. These results challenge the long-standing belief that the NIRS measurement is unaffected by large vessels and support the concept that large veins may be a major determinant of blood volume changes in multiple experimental conditions.

Abbreviations

BL	Beer–Lambert
BV	Basilic vein
HHb	Deoxy-haemoglobin
nAUC	Normalized area under the curve
NIR	Near-infrared light
NIRS	Near-infrared light spectroscopy
O_2Hb	Oxy-haemoglobin
SRS	Spatially-resolved spectroscopy
tHb	Total haemoglobin
THI	Total haemoglobin index
US	Ultrasound

Near-Infrared Spectroscopy (NIRS) has been extensively applied for the assessment of changes in tissue oxygenation and blood volume in skeletal muscles due to its non-invasiveness, its ability to operate in real-time and for being little affected by movement artefacts[1–3]. Briefly, the functioning of NIRS depends on the emission of a NIR light radiation from the emitting optode which travels through the underlying tissues and gets either absorbed or scattered, the backscattered fraction being collected by the receiving optode. Depending on the amount of returning light at different wavelengths, NIRS devices can assess changes in the concentration of Oxy-(Haemoglobin + Myoglobin) and Deoxy-(Haemoglobin + Myoglobin) (O_2Hb/HHb) thus providing indications on tissue oxygenation and blood volume.

The interpretation of NIRS signals is complicated by several limitations of the methodology, among which the inability to discriminate between haemoglobin and myoglobin, the difficulty to discriminate between superficial and deep tissues, the need to estimate or assess the actual optical pathlength of NIRS light, and the uncertainty about the actual vessels contributing to the measurement, with regard to type (arterial/capillary/venous) and size[4]. As for vessel size, it is generally assumed that only vessels smaller than 1-mm diameter contribute to the NIRS signal[4–6]. This assumption appears to stem from a consideration originally expressed by Mancini et al.[7] that the large vessels would completely absorb the incident light and preclude backscattering, due to the high heme

[1]Department of Neuroscience, Università degli Studi di Torino, Turin, Italy. [2]Department of Electronics and Telecommunications, Politecnico di Torino, Turin, Italy. ✉email: silvestro.roatta@unito.it

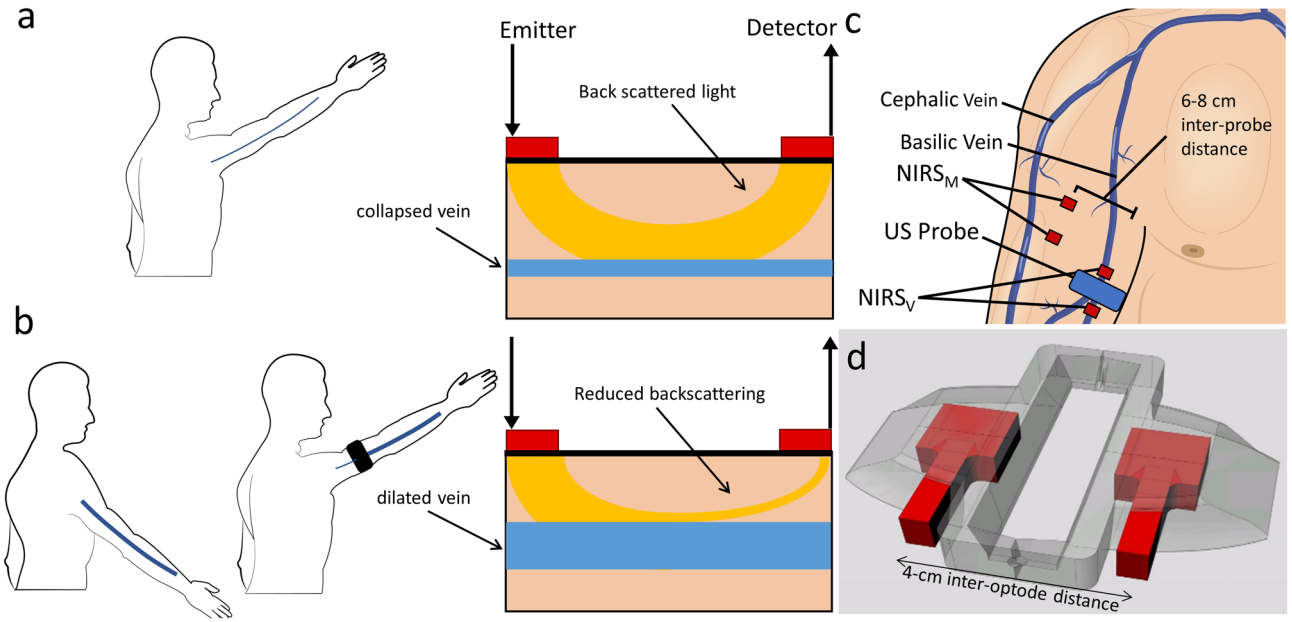

Figure 1. (**a**) Vein collapse during arm elevation results in little absorption of NIR light by the vein and consequently in high intensity of the light backscattered to the detector. (**b**) Vein dilation, during, e.g., arm lowering or venous occlusion, increases the absorption and reduces the amount of backscattered light, which produces an increase of NIRS blood volume indexes; (**c**) location of NIRS probes: one NIRS probe was positioned over the biceps muscle belly ($NIRS_M$) and one over the basilic vein ($NIRS_V$); an ultrasound probe was coupled with $NIRS_V$ to monitor size changes in the cross-sectional area of the basilic vein; (**d**) custom 3D-printed probe holder, designed to embed the linear US-probe (not drawn) in-between NIRS optodes (in red). The figure was created with Adobe Illustrator 2020, v. 24.1.1, www.adobe.com (**a,c**), MS PowerPoint 2019, v. 2111, www.microsoft.com (**b**), and Rhino 7 v.7.13, www.rhino3d.com (**d**).

concentration. Therefore, the collected light would arise mostly from small vessels, such as capillaries[6], arterioles, and venules[8,9]. However, we believe that this reasoning is correct only as long as the size of the large vessels does not change. In fact, an increase in vessel size would increase the amount of absorbed light and decrease the fraction of backscattered light, as described in Fig. 1a,b. The possibility that large vessels may change their size is particularly relevant for the highly compliant veins, which frequently exhibits large size changes in response to changes in intravascular and extravascular pressure, e.g., the vein size in a limb increases when the limb is moved from an independent (Fig. 1a) to a dependent position (Fig. 1b), due to increased hydrostatic blood pressure or may decrease due to the external compressions produced by muscle contractions. However, due to the consideration anticipated above, the possibility that large vessels may actually affect NIRS measurements in skeletal muscles is generally neglected, despite the issue has never been specifically addressed or experimentally verified. On the contrary, contamination of NIRS signals by superficial visible veins has been occasionally evidenced[10,11].

Aim of the present study was to test the hypothesis that large vessels may significantly affect NIRS signals. To this aim, NIRS monitoring was conducted in the biceps muscle, one probe being located over a vessel-free area and the other one over the basilic vein (BV). In order to allow for continuous monitoring of the BV cross-section by ultrasound imaging, that could be problematic during postural changes or exercise, repeatable changes in BV size were obtained in static conditions by controlled venous occlusion, proximally delivered. Evidences in support of the hypothesis were collected both from average responses to venous occlusions as well as from relevant observations derived from individual recordings.

Methods

Eleven healthy subjects were recruited in this study (31 ± 8 year—7 M 4F). The study was approved by the Bioethics Committee of the University of Torino, no diagnosed diseases were reported by any of the participants. All the experiments were performed in accordance with Declaration of Helsinki, each subject signed the informed consent form.

Subject setting. The subjects were seated on a comfortable and adjustable chair with the back supported, in a quiet room at a constant temperature of ~ 21–22° C. The left arm was elevated until reaching ~ 135° of shoulder flexion and passively maintained supine over a padded rigid support. A gentle bandage at the wrist served to secure and stabilize the arm position. This arrangement produced a collapse of the basilic vein in most subjects, due to the decrease in venous blood pressure according to hydrostatic gradients.

Venous occlusion. Controlled pneumatic compressions were elicited by the inflation of a pneumatic paediatric cuff (Gima, Gessate, Italy; width 5 cm), close to the armpit. The cuff inflation was operated by two sole-

noid valves (VXE2330-02F-6D01, SMC, Tokyo, Japan), granting rapid in-flow and out-flow, and a proportional valve (ITV0010, SMC, Tokyo, Japan), granting precise pressure maintenance at the desired level. Compressed air (1 bar) was provided by an air compressor, and the Spike2 software (version 9, Cambridge Electronic Design, Cambridge, UK) coupled with an I/O board (CED Micro 1041, Cambridge Electronic Design, Cambridge, UK) was used to drive the above-mentioned valves to implement both rapid and slow inflation/deflation patterns[12–14].

NIRS measurements. NIRS measurements were performed using a continuous wave spectrometer (NIRO200NX, Hamamatsu Photonics, Hamamatsu City, Japan), implementing the modified Beer–Lambert (BL) and spatially resolved spectroscopy (SRS) methods[15]. The former allows to detect changes in oxygenated (O_2Hb) and deoxygenated haemoglobin concentrations (HHb) expressed in µmol/L, assuming a *differential path-length factor* of 3.6[16]. The sum of these two components, tHb = O_2Hb + HHb, indicate changes in total blood volumes, with respect to a basal reference level, set to 0. The SRS technique provides an additional blood volume indicator, the tissue haemoglobin index (THI), which yields the relative change in haemoglobin concentration (dimensionless) with respect to the beginning of the recording, arbitrarily set to 1. Notably, NIRS spectrometers are unable to discriminate between haemoglobin and cytoplasmic myoglobin, therefore all measurements are actually referred to the sum of the two components (haemoglobin + myoglobin) in the sample volume.

Two NIRS measurements were simultaneously performed. One probe was positioned at the distal third of the arm, on the medial side, just over the BV and more laterally on the biceps brachii muscle, over an area virtually free of large vessels (Fig. 1c). Echographic guidance allowed for precise identification of the BV, whose orientation was marked with a marker on the overlying skin. A custom 3D-printed holder was designed to accommodate both the NIRS optodes (inter-optode distance of 4 cm; Fig. 1d), and a linear US probe (see below) in between and transversally to the NIRS probe, so that the NIRS probe could be oriented parallel to the BV while the US probe could be used to display and record its cross-sectional area. The NIRS optodes position over the biceps muscle belly were housed in their native probe holder (same inter-optode distance of 4 cm). The NIRS probes were sufficiently separated from each other (6–8 cm) to avoid interference and were stuck to the skin by double-sided medical adhesive tape and further secured by additional overlying tape. The 4-cm rather than the 3-cm inter-optode distance was chosen because it grants a better rejection of the interference from the cutaneous circulation (for the SRS parameter, THI) and increases the depth of the sample volume, considered to be about half of the inter-optode distance.

Ultrasound imaging. The cross-section of the BV was continuously monitored by B-mode US imaging (MyLab 15, Esaote S.p.A., Genoa, Italy) using a linear array (LA 523, Esaote, Genoa, Italy) oriented transversally to the vessel lumen at an insonation angle of ~ 90° (US frequency of 12 MHz). The US probe was maintained firmly in place by a mechanical arm, anchored to the same support holding the subject's arm[12]. From the B-mode scan, the thickness of cutaneous and subcutaneous tissue layer could be measured in all subjects.

Experimental protocol. After stabilization of hemodynamic signals, a randomized sequence of venous occlusions was performed according to the following pressure profiles: (i) a slow inflation from 0 to 60 mmHg in 135 s followed by a plateau, 60 mmHg for 30 s, followed by slow deflation 60–0 mmHg in 135 s; (ii) rapid inflation to 40 mmHg, achieved in 2 s, maintained for 30 s and passively deflated in about 2 s. The different occlusions were separated by at least 30 s. Other occlusion patterns or pressure levels were occasionally tested but were not systematically analysed. Venous occlusion led to a gradual rise of blood pressure in distal veins and the ensuing increase in BV size could be recorded by US imaging.

Data acquisition and processing. The NIRS signals were digitally acquired at 50 Hz along with the cuff pneumatic pressure (CED Micro 1041, Cambridge Electronic Design, Cambridge, United Kingdom) and stored for later analysis on the computer using Spike2 software (version 9.04b, Cambridge Electronic Design, Cambridge, United Kingdom). The analysis was limited to the blood volume indicators tHb and THI, collected from the probe positioned over the basilic vein (tHb_V and THI_V) and over the biceps muscle belly (tHb_M and THI_M). Responses to venous occlusion were characterized in terms of (1) maximum change in blood volume, as expressed by the peak value of the recordings (considering that basal, i.e., pre-occlusion levels for tHb and THI are 0 and 1, respectively); (2) convexity of the rising volume curve, quantified as the area comprised between the normalized curve and the virtual linear trend, divided by the duration of the rising phase (nAUC) so that nAUC is dimensionless and equals 0.5 for maximum convexity, 0 for a rising linear trend and − 0.5 for maximum concavity. The area is calculated over the whole rising phase, defined as the time interval between the moment at which the pressure exceeded 10 mmHg and the moment at which the blood volume reaches its maximum value (i.e. at the end of the plateau), while the normalization of the curve was achieved by subtracting the minimum to the original curve and subsequently dividing the resulting curve by its current maximum value. In this way the normalized rising volume curve had its minimum value at 0 and its maximum value at 1.

Volume-pressure curves were constructed by quadratic fitting of the average tHb and THI response to slow cuff deflation (from 60 to 0 mmHg in 135 s, described above). Compliance curves were then obtained as first analytical derivatives of the volume-pressure curves[17].

Video clips of US imaging of the BV, lasting for the whole duration of the venous occlusions, were recorded and later analysed by a custom image processing software, originally developed for the inferior vena cava[18,19], capable of tracking the vein borders, and reporting the time course of the vessel cross-sectional area during cuff inflation. Proper detection of vein borders was validated by visual inspection of the video clips with superimposed vessel reconstruction. Automatic vessel detection could fail due to poor quality of the US imaging or due to the collapse of the vein. In these cases, data were either discarded or integrated with manual measurements.

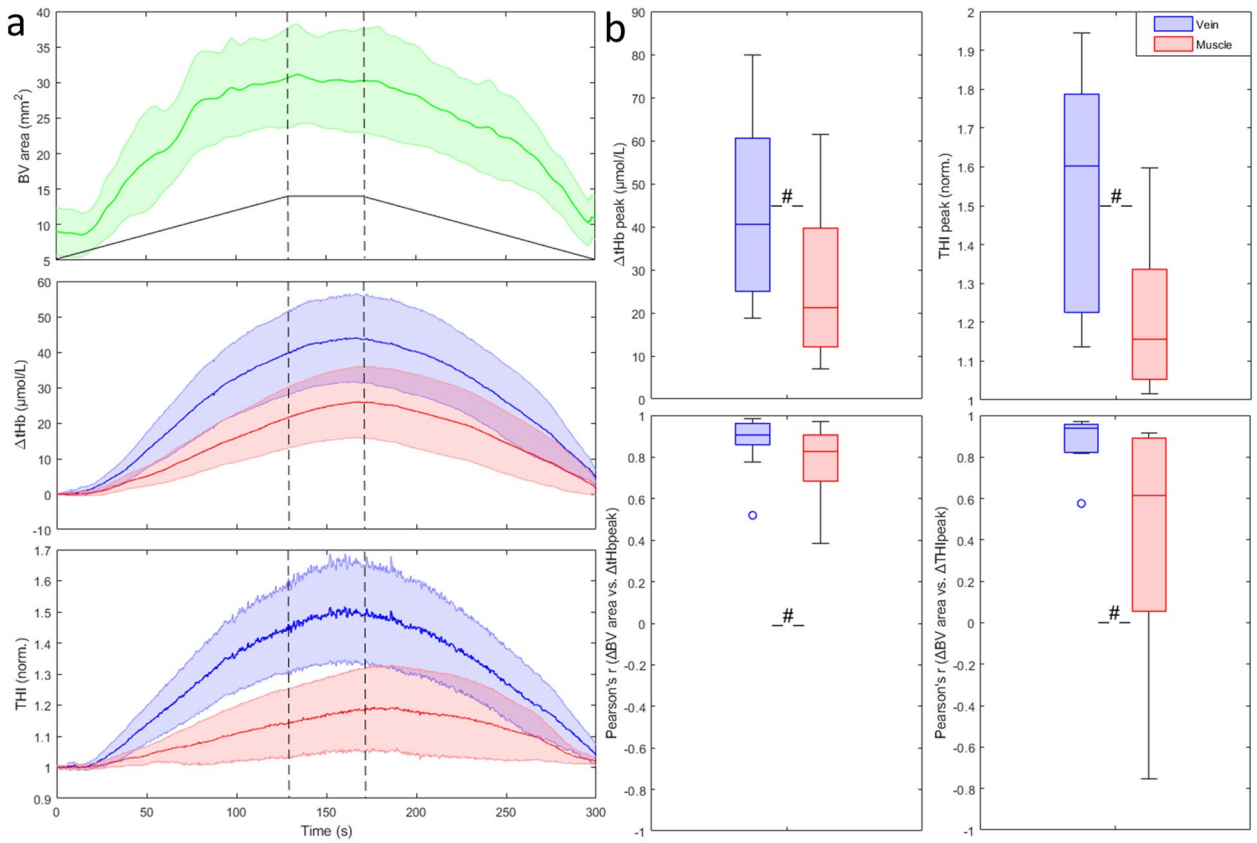

Figure 2. (**a**) Average response to slow venous occlusion of the cross-sectional area of the basilic vein (green) and of tHb and THI as detected on the muscle (red) and on the vein (blue). Shaded areas represent the 95% confidence interval of the mean. The black trapezoid depicted in the top graph qualitatively reproduces the cuff pressure during inflation to 60 mmHg, plateau and subsequent deflation to 0 mmHg, while the vertical dashed lines indicate end of inflation (first one) and beginning of deflation (second one). (**b**) Peak response of blood volume indexes, collected from vein and muscle probes (top), Pearson's coefficient of the correlation between changes in BV cross-sectional area and in blood volume indices (bottom). $^{*}p<0.05$; $^{\#}p<0.01$.

Statistical analysis. Comparisons between responses of NIRS signals from the two probes (vein vs. muscle), in terms of magnitude, latency and convexity were done using a non-parametric paired Wilcoxon T test. Similarity of the response of NIRS variables with changes in BV size, for each subject, was quantified by the Pearson's correlation coefficient, then Fisher transformation was applied to those ρ values, and finally each distribution was tested using a non-parametric Wilcoxon T test. The procedure was performed for both tHb and THI and for both slow and rapid venous occlusion profiles.

Results

In two subjects, THI_V saturated during venous occlusion. The measurements were then discarded and repeated after slightly displacing the NIRS probe by few millimetres. This problem was not encountered in signals collected from the muscle belly.

In the resting condition, the BV collapsed in most subjects. Average BV depth (centre of the vessel) was 10.2 ± 4.2 mm, extending from 7.4 ± 4.2 to 13.1 ± 4.2 mm at its maximum dilatation at the plateau of slow ramp occlusions. The thickness of cutaneous and subcutaneous tissue layers was assessed from the ultrasound scans and found to be 2.1 ± 0.3 mm.

Slow vein occlusions. The slow venous occlusion effectively increased the BV cross-sectional area from 8.9 ± 5.7 to 32.7 ± 12.1 mm^2 and produced a slow increase, followed by a slow decrease in blood volume indexes as shown in Fig. 2a. Notably, the indexes exhibited systematically larger changes over the BV than over the muscle belly, on average: $\Delta tHb_V = 44.8 \pm 21.3$ μmol/L vs. $\Delta tHb_M = 27.1 \pm 17.6$ μmol/L ($p<0.01$) and $THI_V = 54 \pm 31\%$ vs. $THI_M = 22 \pm 21\%$ ($p<0.002$) (Fig. 2b).

The time course of the responses was also slightly different between the two measurement areas: indeed, tHb_V exhibited a more rapid increase as compared to tHb_M as shown by the higher curvature nAUC (0.052 ± 0.076 vs. − 0.005 ± 0.045, $p=0.03$). For THI the differences did not reach statistical significance. However, it is worth to report that in 3 subjects THI_M did not increase or slightly decreased.

Both tHb_V and THI_V values were better correlated to BV size than the corresponding muscle indexes ($p<0.001$): tHb_V $\rho=0.92$, THI_V $\rho=0.91$, tHb_M $\rho=0.83$, THI_M $\rho=0.55$ (Fig. 2b).

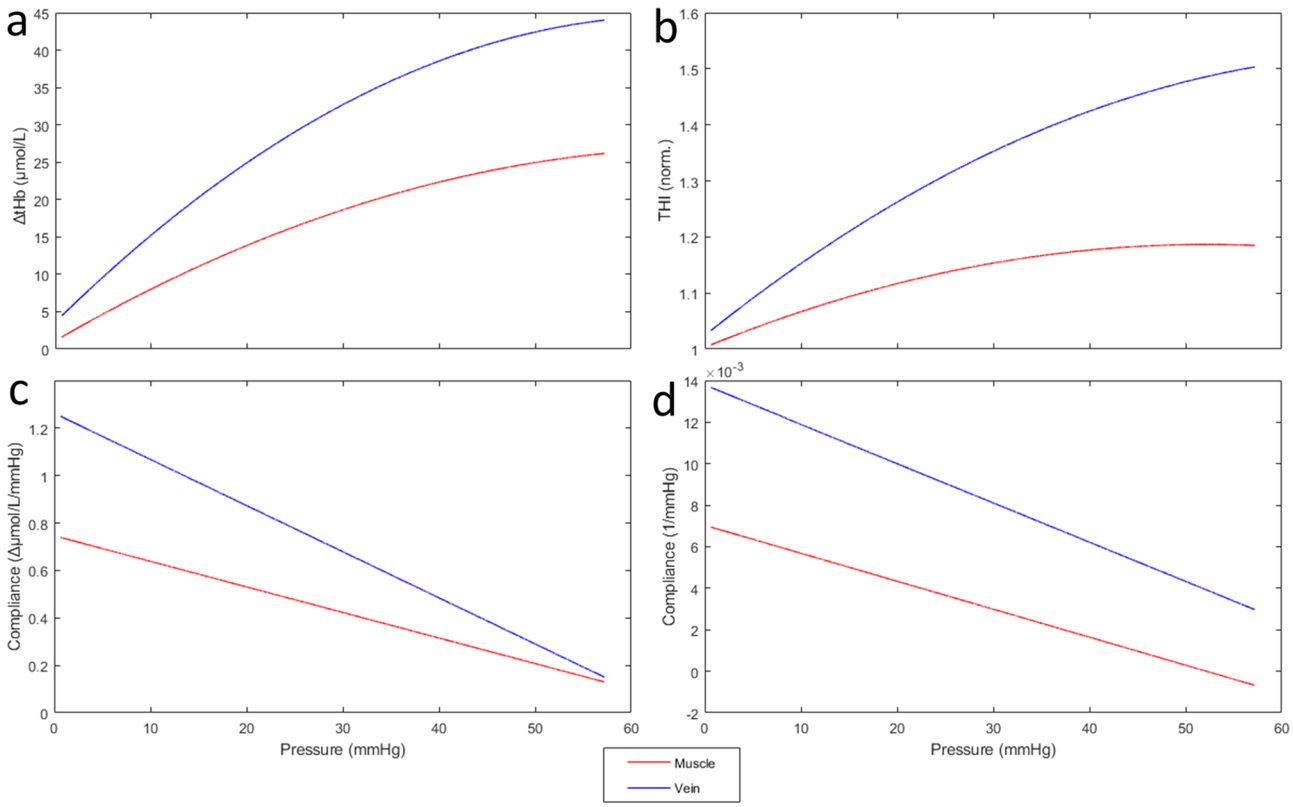

Figure 3. Volume-pressure curves, obtained by 2° order polynomial fitting of average responses to slow cuff-deflation of Fig. 2a (top), and compliance curves, obtained as the slopes of the corresponding volume-pressure curves (bottom), for tHb (left) and THI (right) collected from vein (blue) and muscle (red). Note the large difference in the compliance estimated from vein and muscle.

Volume-pressure and vascular compliance curves were constructed from the average tHb and THI curves of Fig. 2, collected from vein and muscle during cuff deflation (Fig. 3). Note that the compliance estimated from the probe on the vein is considerably higher than from the muscle.

Rapid vein occlusions. As described for slow-ramp occlusions, rapid occlusions also produced an increase in BV cross-sectional area from 8.8 ± 6.5 to 25.5 ± 13.4 mm^2, and relevant increase in blood volume indexes (Fig. 4a) with significantly larger changes in the vein than in the muscle: $\Delta tHb_V = 27.3 \pm 12.6$ μmol/L vs. $\Delta tHb_M = 11 \pm 7.1$ μmol/L ($p < 0.002$) and $THI_V = 32 \pm 21\%$ vs. $THI_M = 8 \pm 9\%$ ($p < 0.001$) (Fig. 4b). A clear-cut difference in time course between vein and muscle is here significantly achieved for tHb and THI, both exhibiting a higher convexity during the rising phase of blood volume (tHb: 0.18 ± 0.08 vs. 0.07 ± 0.10, $p < 0.05$; for THI: 0.16 ± 0.07 vs. 0.06 ± 0.12, $p < 0.05$), on the vein as compared to the muscle. Also in this case 4/11 subjects exhibited no change or slight decrease in THI_M.

As shown in Fig. 4b, vein indexes were generally better correlated to BV cross-sectional area than muscle indexes: average Pearson's ρ was 0.92 vs. 0.78 for tHb ($p < 0.01$) and 0.89 vs. 0.56 for THI ($p < 0.05$) in vein vs. muscle.

Single relevant cases. In addition to the afore-described differences in the NIRS signals averaged over all subjects, few relevant examples of individual recordings are presented below, further evidencing peculiar aspects of the influence that large vessels exert on NIRS signals.

(1) In Fig. 5 the execution of two occlusive stimuli in sequence produced markedly different responses in the tHb_V signal: while on the first occlusion (left) tHb_V reveals a normal progressive increase in blood volume, on the second occlusion the increase surprisingly takes place in two steps. Analysis of the US recording clarifies the phenomenon, showing that beside the basilic vein, one brachial vein also appears into the sample volume of the probe as exhibited in Supplementary Video S1 (https://doi.org/10.6084/m9.figshare.14694270). These veins are located at 2.4 and 5.1 mm of depth and, thus, within the sampling depth of the NIRS (about 2 cm, given the inter-optode distance of 4 cm). They have been separately tracked and the time course of their change in size is also reported; it can be observed that they simultaneously dilate in response to the first but not to the second venous occlusion. The delayed dilation of the basilic vein (green

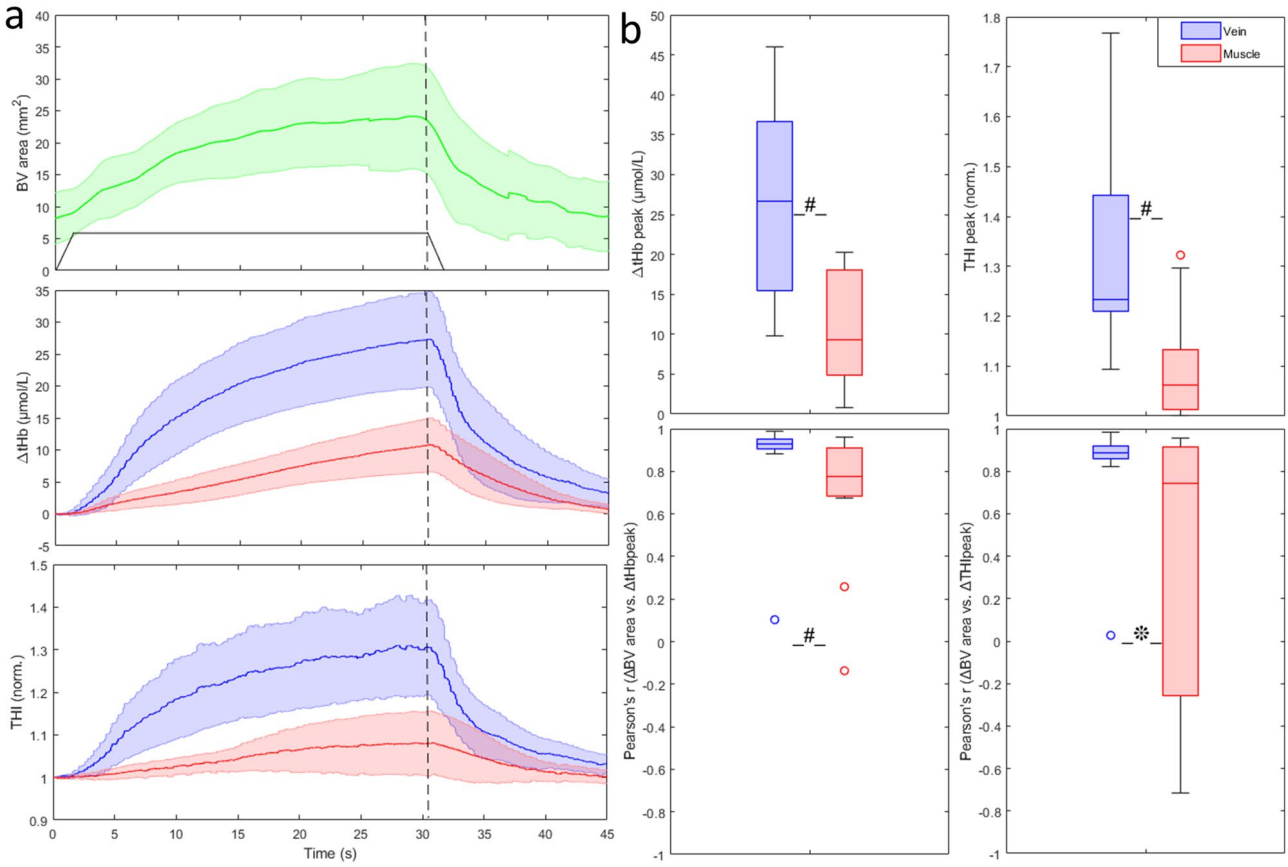

Figure 4. Average response to rapid venous occlusion of the cross-sectional area of the basilic vein (green) and of tHb and THI as detected on the muscle (red) and on the vein (blue). Shaded areas represent the 95% confidence interval of the mean. The black trapezoid depicted in the top graph qualitatively reproduces the cuff pressure during inflation to 40 mmHg, plateau and subsequent deflation to 0 mmHg, while the vertical dashed line indicates the beginning of deflation. (**b**) Peak response of blood volume indexes, collected from vein and muscle probes (top), Pearson's coefficient of the correlation between changes in BV cross-sectional area and in blood volume indices (bottom). $^{*}p < 0.05$; $^{\#}p < 0.01$.

trace) explain the discontinuous increase of tHb_V. Also note the relatively small increase exhibited by tHb_M compared to tHb_V.

(2) In Fig. 6, the response to two subsequent rapid occlusions is shown, in a different subject. It can be observed that (1) both tHb_V and THI_V, but not tHb_M and THI_M exhibit a regular oscillatory pattern (of respiratory origin) before and after the occlusion, the same oscillation being clearly visible on the BV cross-sectional area and (2) upon release of the first occlusion (but not the second) tHb_V and THI_V, but not tHb_M and THI_M, remain elevated with respect to the pre-occlusion levels, which again mirrors the pattern exhibited by the BV cross-sectional area. Notably, a respiratory pattern was never observed on NIRS signals collected from muscle.

(3) We mentioned above that, surprisingly, in 4 subjects no THI increase was observed in the muscle, during the rapid venous occlusion. Aiming to discern whether the effect was related to individual characteristics or to the specific position of the probe on the muscle belly, we have reinvestigated the issue. We observed that small displacements (in the order of 1 cm) of the NIRS probe could revert the THI_M response into a prominent increase (Fig. 7). In one case this was attributed to the presence of a small vein at a depth of 23 mm, hardly detectable by B-mode US imaging but visible through Color-Doppler imaging at the time of cuff deflation.

(4) Although it is well known that large changes in venous size may take place during postural changes, a representative recording is here reported to show that similar effects are produced by venous occlusion and displacement from an independent to a dependent position (Fig. 8a). A single NIRS probe is here located over the BV. It can be observed that, both tHb and THI reveal a blood volume fall when the arm is raised up and an equivalent increase when it is returned to the dependent position. Venous occlusion performed in the independent position produces comparable effects, while a smaller response is observed in the dependent position.

(5) In order to show that the influence on NIRS blood volume indexes by large veins also concerns muscle contractions, a specific experimental set-up was designed. Given that it is difficult to identify large veins in the biceps muscle, this recording was performed in calf muscles, during a light isometric plantar flexion of

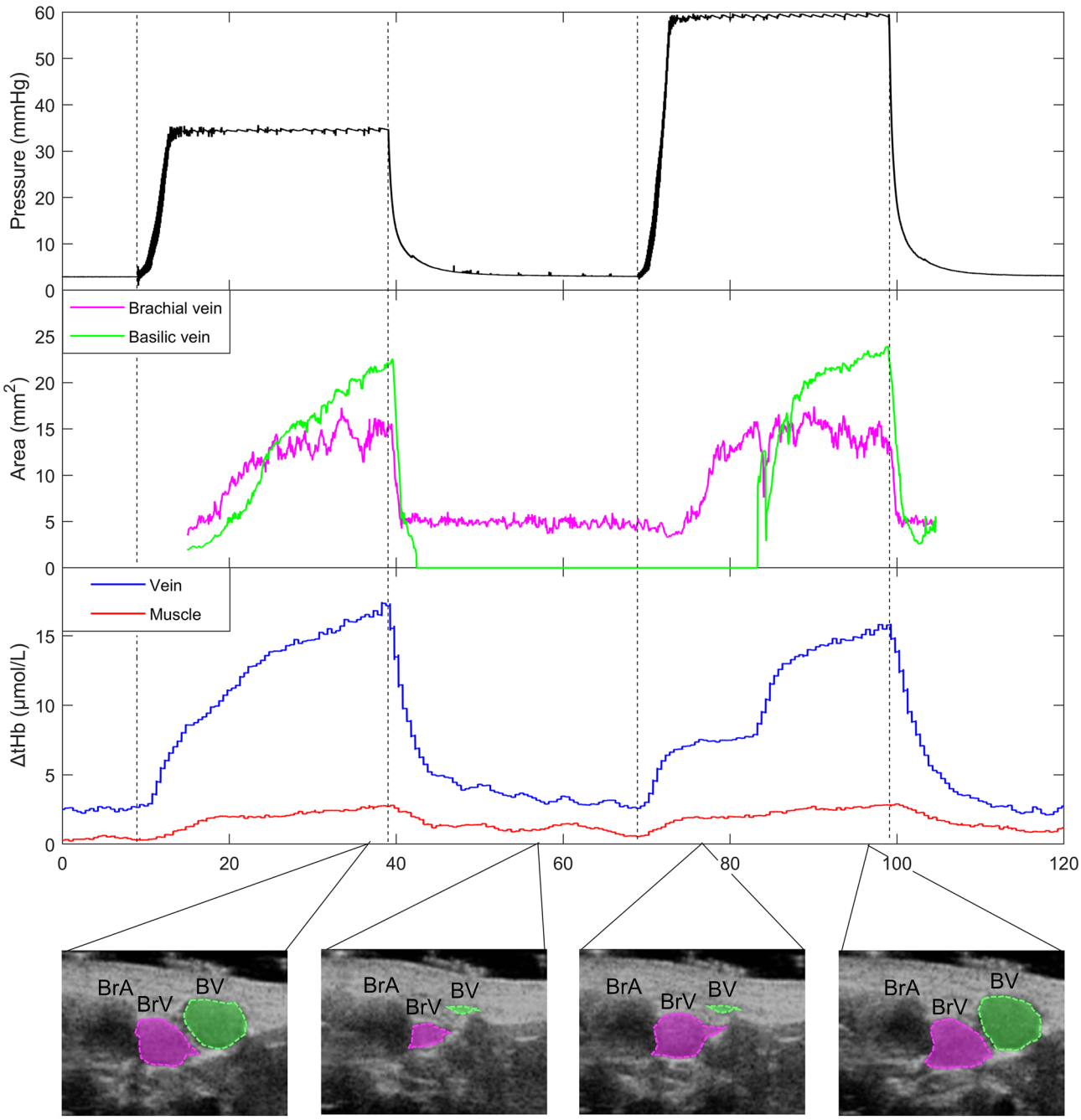

Figure 5. Original traces from a single subject showing the responses to two subsequent short lasting venous occlusions (30 and 60 mmHg, respectively). From top to bottom: cuff pressure; Cross-sectional area of brachial vein and basilic vein; tHb signals from the vein (blue) and muscle (red) probes. At the bottom, single frames of US imaging of blood vessels underneath the $NIRS_V$ probe (as indicated in Fig. 1b) are displayed, with superimposed coloured shadings indicating the extent of collapse/dilatation of the brachial (BrV) and basilic (BV) veins. The brachial artery (BrA) is also indicated. Note the unusual 2-steps increase in tHb_V in response to the second occlusion, which is explained by the delayed dilatation of the basilic vein. The fact that the increase in venous size is delayed, compared to tHb_V is due to the NIRS sample volume extending proximally to the US insonation site (during venous occlusion, venous pressure increases earlier at proximal than at distal sites, in the raised arm). Vertical dashed lines indicate start of cuff inflation and deflation.

the ankle. One NIRS probe was located over a large vein detected by US in the soleus muscle, while the other probe was located in an adjacent area of the same muscle, free of visible veins. The results are presented in Fig. 8b, whereby EMG and Force tracings document the duration and extent of the contraction. Note that the probe located over the vein detected a large decrease in blood volume during the contraction, compared

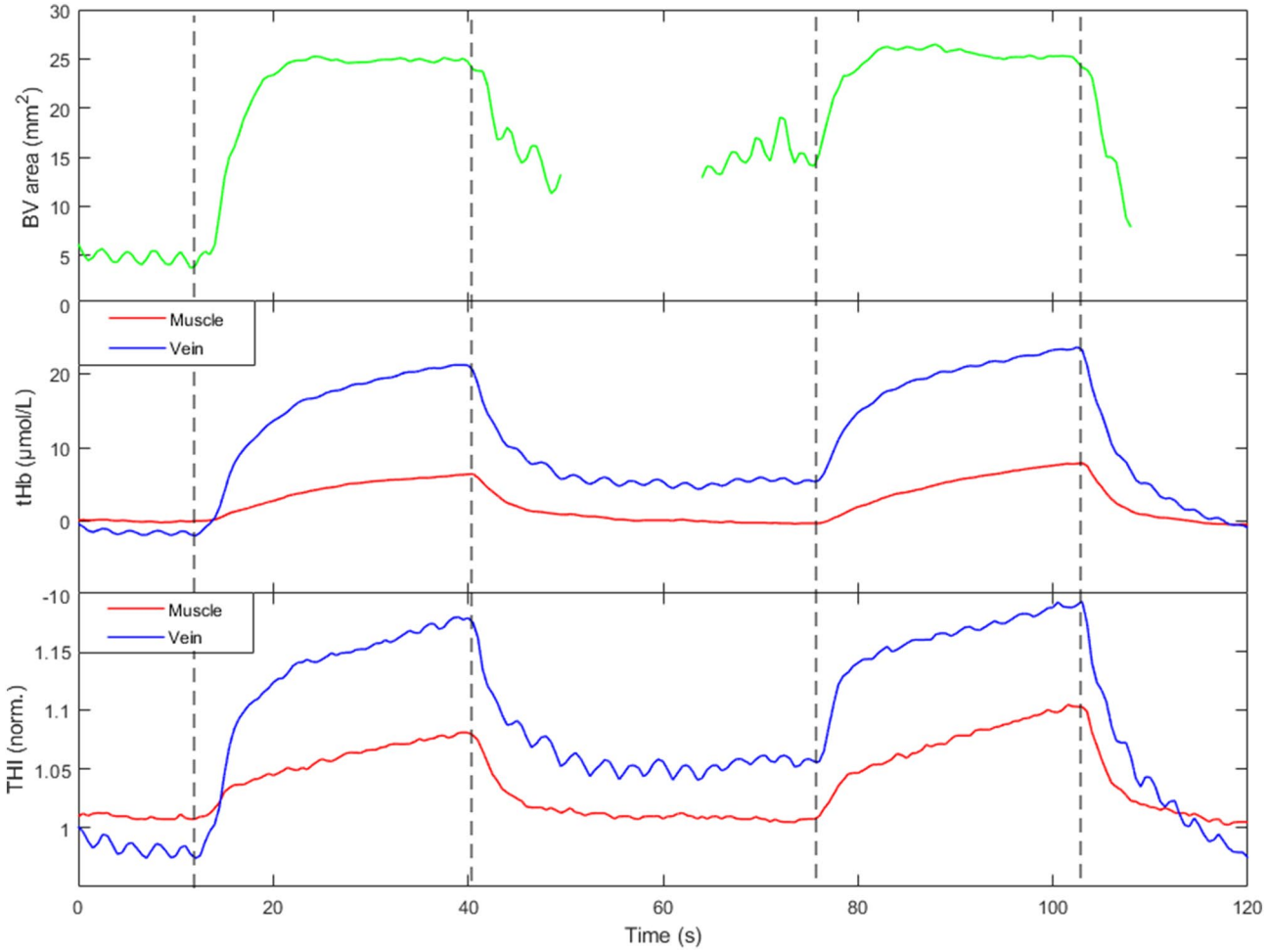

Figure 6. Original traces from a single subject showing the responses to two subsequent short lasting occluding stimuli (both at 40 mmHg). From top to bottom: cross-sectional area of the basilic vein (green), THI, and tHb signals collected from the vein (blue) and from the muscle (red). Note the presence of an oscillatory component of respiratory origin, synchronously appearing on the vessel cross-sectional area and on the venous NIRS signals only. Vertical dashed lines indicate start of cuff inflation and deflation.

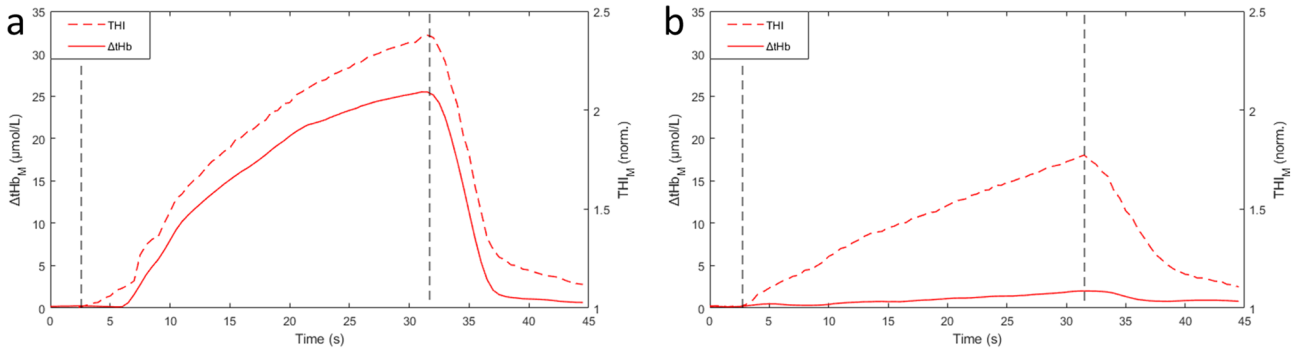

Figure 7. Original traces from the same subject showing tHb and THI responses to 40-mmHg venous occlusions subsequently recorded on the biceps brachii muscle belly at the original site (**a**) and after lateral displacement of 1 cm (**b**). Note the different response of THI, attributed to a small vein in the sample volume in (**b**). Vertical dashed lines indicate start of cuff inflation and deflation.

to the other probe. Simultaneous US monitoring of the vein confirmed the complete vein collapse during the contraction.

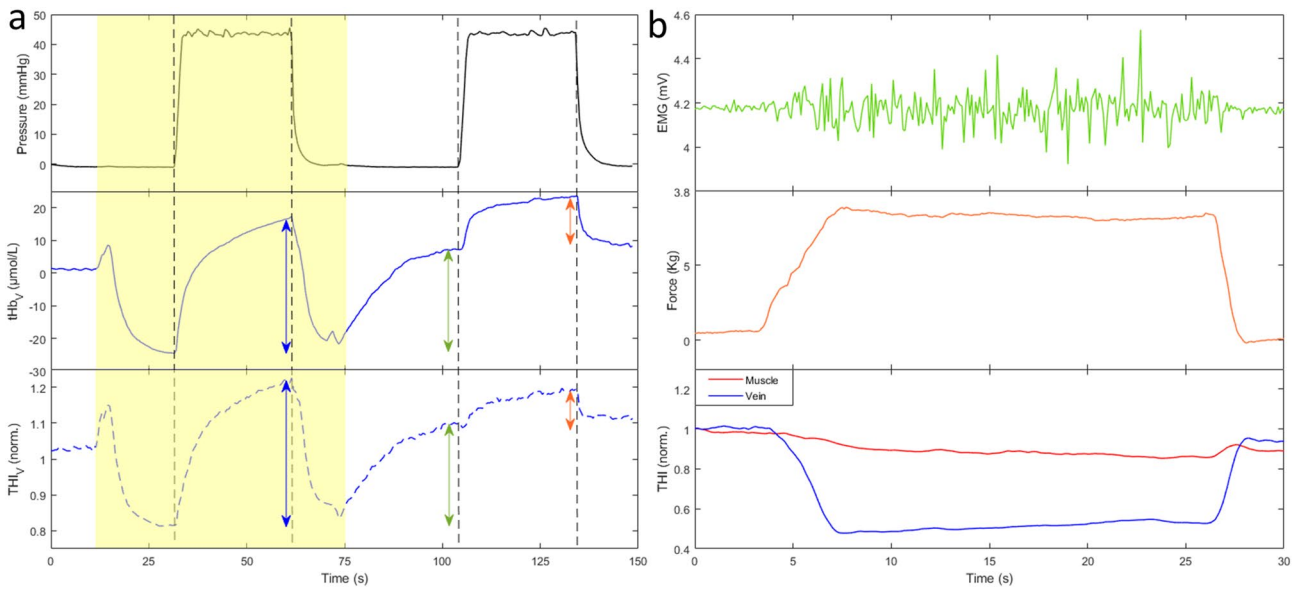

Figure 8. (**a**) Effect of postural changes on blood volume indices in a representative recording. From top to bottom, cuff pressure, tHb_V and THI_V collected from a single NIRS probe placed over the basilic vein (same set-up of Fig. 1b). The arm was moved from below to above (yellow-shaded area) and again returned to below heart level. Proximal venous occlusion (40 mmHg) was also performed for comparison, as indicated by the cuff pressure signal. Note that similar increases in blood volume are produced by venous occlusion (blue double-arrows) and arm lowering (green double-arrows). Much smaller effects are produced by venous occlusion when performed in the dependent arm (orange double-arrows). Vertical dashed lines indicate the beginning of cuff inflation and deflation. (**b**) Effect of muscle contraction on blood volume indices in a representative recording. Recordings are collected from the calf muscles during isometric plantar flexion of the ankle, the subject laying prone. From top to bottom, the electromyographic signal (EMG, measured over the distal portion of the soleus muscle), the force (measured at the forefoot) and THI signals form two probes, one located over an intramuscular soleus vein (blue) and one over a more distal portion of the same muscle (red). Note the different magnitude of contraction-related changes of THI at the two sites.

Discussion

In the present study, several points of evidence were gathered against the commonly held concept that large blood vessels do not affect the NIRS measurement. By comparing the blood volume measurements collected from the biceps muscle belly and from over the large basilic vein during venous occlusion, we showed that the increase in NIRS signal in the latter case (1) is 1.7 to 4 times larger, (2) exhibits a larger convexity and (3) is better correlated with the increase in size of the basilic vein. In addition, a number of representative recordings was shown to further describe the clear dependence of the NIRS variables from the underlying large vein(s).

In 1994, Mancini et al.[7] stated in the Introduction of their pioneering study that, due to the high Hb concentration in the blood, emitted NIR photons were unlikely to emerge from arteries and veins larger than 1 mm in diameter, and thus NIR light absorption changes would primarily depend on smaller vessels. Although this issue was not specifically investigated in the study, this paper is highly cited to support the assumption that the presence of large vessels in the NIRS sample volume can be *tout-court* neglected. However, based on the reasoning presented in Fig. 1a and the present experimental data, this assumption appears to be incorrect in all conditions in which the size of these large vessels changes. While in arteries relevant size changes are not common, in veins they are very frequent and may easily occur due to alteration of the intravascular as well as of the extravascular pressure. However, since these factors affect large as well as small veins, the contribution of large veins is difficult to discriminate and, to our knowledge, has not been previously investigated, although some hints can be found in the literature.

Several studies pointed out that the NIRS measurement yields different results depending on probe location. For example, the impact of probe location was specifically addressed in healthy subjects by comparing the changes in tissue oxygenation in thenar and forearm muscles in response to a vascular occlusion test[20]. A significantly faster O_2 desaturation in thenar than in forearm muscles was attributed to different anatomical structures (muscle and subdermal tissues) at the two sites. Among these, the large veins in the forearm could have played a role, considering that during arterial occlusion redistribution of the blood from arteries to veins takes place. In fact, it was also reported that the forearm exhibits a larger volume decrease than the thenar in response to lower-body negative pressure[21]. While a different sensitivity of the two regions to hypovolemic stress is possible, the higher blood volume decrease in the forearm could also be explained by a higher density of large veins undergoing emptying in the forearm than in thenar.

Interestingly, in two studies a NIRS probe was intentionally placed over visible (superficial) veins, for comparing the signals with a probe located on a virtually vein-free area[11,15]. In the first study, aimed to infer venous saturation from respiratory oscillations in venous blood volume, the authors noticed that blood volume signals

collected from the vastus medialis over a visible vein had larger respiratory oscillations and provided more reliable estimation of venous oxygen saturation than signals from a vein free area of the vastus lateralis muscle[11]. This suggests that the veins may have exerted a direct influence on NIRS measurements. This interpretation is supported by the present data: respiratory oscillations were only observed on signals collected from the vein and were mirrored by respiratory changes in BV cross-sectional area (Fig. 6). The influence of superficial veins on NIRS blood volume indicators was also recently pointed out with a different approach: it was observed that the peripheral (remote) cutaneous hyperaemia, obtained by selective hand warming, produced a significant tHb increase at the forearm, with a tendency to larger effects if the probe was placed over a superficial visible vein than over a vein-free area[15]. Since no heat-induced hyperaemia was observed at the forearm, those results indicated that increased venous outflow from the hand could be detected by NIRS at the forearm.

Subjects exhibiting a different pattern of response. In a relevant fraction of subjects (4 out of 11) the expected blood volume increase in response to venous occlusion was regularly recorded at the site over the basilic vein (tHb_V and THI_V), and in the superficial (cutaneous) layers over the muscle belly (tHb_M increased) but not in the deeper muscle tissue (THI_M exhibited a negligible increase or even a decrease during cuff inflation). However, by reinvestigating the relevant subjects we showed that a prominent THI_M increase could be detected after slight displacement of the probe over the muscle belly (Fig. 7).

This means that the possible lack of response of THI_M to venous occlusion does not necessarily reflect a characteristic of that subject or of that muscle but may simply depend of the specific probe position with respect to deep veins.

Along the same line, NIRS signals may exhibit different patterns of response to muscle contraction, i.e., marked reduction if a large vein is included in the sample volume or negligible changes otherwise as shown in the example recordings of Fig. 8b.

Whether the likelihood of including a large vein in the sample volume depends on muscle mass, training, sex or other factors remains to be investigated.

Beer–Lambert vs. spatially-resolved spectroscopy. Spatially resolved spectroscopy is known to focus the measurement in depth, thereby being less affected than the standard Beer–Lambert spectroscopy by hemodynamic changes taking place in superficial tissue layers, as has been reported for both the cerebral and muscle investigations by our and other groups[10,15,22–24]. We here observed remarkably similar responses of tHb (BL) and THI (SRS) blood volume indicators from the probe placed on the BV, in all subjects, and from the muscle probe from most subjects, which is only apparently in contrast with our previous study on the forearm, in which only tHb and not THI was affected by increased venous return from the hand[15]. In fact, in that case only the superficial venous circulation was affected, while in the present case the BV was located at a depth of about 1 cm, i.e., in a range relevant to both BL and SRS methodologies. Along the same line, the saturation of THI_V, initially observed in two subjects and later prevented by slight probe displacement, is reasonably attributable to excessive light absorption by the vein during venous occlusion.

Implications. NIR spectroscopy is employed to investigate several issues of physiological and clinical interest[4,25–27]. We here consider two applications that are concerned by the present results.

Assessment of *vascular compliance* by NIRS is a possible alternative to the classical strain-gauge plethysmography. Initially proposed by Binzoni et al.[28], this measurement is based on relating the increase in blood volume (ΔtHb) to the increase in venous pressure as may be obtained by performing a Head-Up Tilt Test[28,29], or by proximal venous occlusions[30,31]. With the present study we show that the presence of a large vein in the NIRS sample volume may magnify the blood volume change by a factor of 1.7 to 4 times (Figs. 2, 4) and alter the estimated compliance by a similar amount (Fig. 3). Although the present study was not designed to assess vascular compliance, qualitative volume-pressure and compliance curves could be obtained from the signals recorded during slow cuff deflation, highlighting the different responses at the two measuring sites (Fig. 3). The present findings are in agreement with the concept that small intramuscular vessels may have a limited dilatory capacity as compared to large extra muscular vessels. By monitoring the size of deep vessels by magnetic resonance imaging during venous occlusion, it was observed that dilatation of deep veins accounted for most of the limb volume increase, particularly at low pressures (up to 40 mmHg)[32,33]. Similar observations were reported by de Groot 2005[34]: the authors observed that, during venous occlusion, deep veins exhibited early dilatation and could reach a plateau in just 30 s, while standard plethysmography could require up to 2–3 min. These data fit with the present observation of larger and earlier changes and larger convexity of the NIRS tracings collected on the vein as compared to the muscle.

NIRS has also been used to provide indirect measurement of *muscle blood flow*. The procedure consists of assessing the blood volume increase (e.g., by means of tHb) in response to a rapid venous occlusion at subdiastolic pressure (60–80 mmHg)[3,35,36]. Blood flow is then estimated as the initial slope of the volume curve, e.g., considered in the first 1–4 cardiac cycles[37,38]. Although in some study a good reliability of blood flow measurement has been reported[3], other studies evidenced some variability, possibly dependent on the location of the NIRS probes[38]. By examining the initial slope of the volume responses to the rapid 40-mmHg venous occlusion of Fig. 4a, it is clear that the presence of a large vein in the sampling volume may lead to a dramatic overestimation of muscle blood flow. Conversely, low vascular compliance of muscles deprived of large veins may lead to its underestimation.

Limitations. Our NIRS device did not account for possible changes in the differential path-length factor. In addition, even the slow venous occlusion protocol might have been too short lasting to ensure matching

between venous and cuff pressures from the very beginning of cuff deflation, as required to correctly estimate volume-pressure curves (Fig. 3). However, these approximations are unlikely to explain the consistent differences between BV and muscle NIRS monitoring observed in the different conditions. The presence of subcutaneous tissue layer is also considered to affect the tissue measurement[3], however, given small and similar thickness of cutaneous and subcutaneous tissue layers at the two measurement sites they are unlikely responsible for the observed results.

Conclusions

For the first time NIRS blood volume indexes were collected over a large deep vein while simultaneously monitoring its size and were compared to indexes collected from the muscle belly. The results contradict the dogma that the NIRS measurement is unaffected by large vessels and confirm the hypothesis that the increase in size of large vessels determines considerable increases in NIRS blood volume indexes. Unlike superficial veins, size changes in deep veins affect Beer-Lambert as well as spatially resolved indexes. These results bear implication in all conditions affecting the vein transmural pressure, including exercise and postural changes, as well as the response to manoeuvres such as external compressions and venous occlusion.

Data availability

The datasets generated during and/or analysed during the current study are available from the corresponding author on reasonable request.

Received: 17 September 2021; Accepted: 12 January 2022
Published online: 09 February 2022

References

1. Ferrari, M., Mottola, L. & Quaresima, V. Principles, techniques, and limitations of near infrared spectroscopy. *Can. J. Appl. Physiol.* **29**, 463–487 (2004).
2. Ferrari, M., Muthalib, M. & Quaresima, V. The use of near-infrared spectroscopy in understanding skeletal muscle physiology: Recent developments. *Philos. Trans. R. Soc. A* **369**, 4577–4590 (2011).
3. Barstow, T. J. Understanding near infrared spectroscopy and its application to skeletal muscle research. *J. Appl. Physiol.* **126**, 1360–1376 (2019).
4. Grassi, B. & Quaresima, V. Near-infrared spectroscopy and skeletal muscle oxidative function in vivo in health and disease: A review from an exercise physiology perspective. *J. Biomed. Opt.* **21**, 091313 (2016).
5. Davis, M. L. & Barstow, T. Estimated contribution of hemoglobin and myoglobin to near infrared spectroscopy. *Respir. Physiol. Neurobiol.* **186**, 180–187 (2013).
6. McCully, K. K. & Hamaoka, T. Near-infrared spectroscopy: What can it tell us about oxygen saturation in skeletal muscle? *Exerc. Sport Sci. Rev.* **28**, 123–127 (2000).
7. Mancini, D. M. *et al.* Validation of near-infrared spectroscopy in humans. *J. Appl. Physiol.* **77**, 2740–2747 (1994).
8. Van Beekvelt, M. C., Colier, W. N., Wevers, R. A. & Van Engelen, B. G. Performance of near-infrared spectroscopy in measuring local O2 consumption and blood flow in skeletal muscle. *J. Appl. Physiol.* **90**, 511–519 (2001).
9. Hamaoka, T., McCully, K. K., Quaresima, V., Yamamoto, K. & Chance, B. Near-infrared spectroscopy/imaging for monitoring muscle oxygenation and oxidative metabolism in healthy and diseased humans. *J. Biomed. Opt.* **12**, 062105 (2007).
10. Messere, A. & Roatta, S. Influence of cutaneous and muscular circulation on spatially resolved versus standard Beer-Lambert near-infrared spectroscopy. *Physiol. Rep.* **1**, e00179 (2013).
11. Franceschini, M. A. *et al.* Near-infrared spiroximetry: Noninvasive measurements of venous saturation in piglets and human subjects. *J. Appl. Physiol.* **92**, 372–384 (2002).
12. Seddone, S., Messere, A. & Roatta, S. Vascular reactivity of cutaneous circulation to brief compressive stimuli, in the human forearm. *Eur. J. Appl. Physiol.* **120**, 1–10 (2020).
13. Messere, A. *et al.* Hyper-oxygenation attenuates the rapid vasodilatory response to muscle contraction and compression. *Front. Physiol.* **9**, 1078 (2018).
14. Ferraresi, C. *et al.* Design and simulation of a novel pneumotronic system aimed to the investigation of vascular phenomena induced by limb compression. *J. Bionic Eng.* **16**, 550–562 (2019).
15. Messere, A. & Roatta, S. Local and remote thermoregulatory changes affect NIRS measurement in forearm muscles. *Eur. J. Appl. Physiol.* **115**, 2281–2291 (2015).
16. Pirovano, I. *et al.* Effect of adipose tissue thickness and tissue optical properties on the differential pathlength factor estimation for NIRS studies on human skeletal muscle. *Biomed. Opt. Express.* **12**, 571–587 (2021).
17. Halliwill, J. R., Minson, C. T. & Joyner, M. J. Measurement of limb venous compliance in humans: Technical considerations and physiological findings. *J. Appl. Physiol.* **87**, 1555–1563 (1999).
18. Mesin, L., Pasquero, P. & Roatta, S. Multi-directional assessment of respiratory and cardiac pulsatility of the inferior vena cava from ultrasound imaging in short axis. *Ultrasound Med. Biol.* **46**, 3475–3482 (2020).
19. Folino, A. *et al.* Vena cava responsiveness to controlled isovolumetric respiratory efforts. *J. Ultrasound Med.* **36**, 2113–2123 (2017).
20. Bezemer, R. *et al.* Simultaneous multi-depth assessment of tissue oxygen saturation in thenar and forearm using near-infrared spectroscopy during a simple cardiovascular challenge. *Crit. Care* **13**, 1–5 (2009).
21. Bartels, S. A. *et al.* Multi-site and multi-depth near-infrared spectroscopy in a model of simulated (central) hypovolemia: Lower body negative pressure. *Intens. Care Med.* **37**, 671–677 (2011).
22. Canova, D., Roatta, S., Bosone, D. & Micieli, G. Inconsistent detection of changes in cerebral blood volume by near infrared spectroscopy in standard clinical tests. *J. Appl. Physiol.* **110**, 1646–1655 (2011).
23. Al-Rawi, P. G., Smielewski, P. & Kirkpatrick, P. J. Evaluation of a near-infrared spectrometer (NIRO 300) for the detection of intracranial oxygenation changes in the adult head. *Stroke* **32**, 2492–2500 (2001).
24. Tew, G. A., Ruddock, A. D. & Saxton, J. M. Skin blood flow differentially affects near-infrared spectroscopy-derived measures of muscle oxygen saturation and blood volume at rest and during dynamic leg exercise. *Eur. J. Appl. Physiol.* **110**, 1083–1089 (2010).
25. Boushel, R. *et al.* Monitoring tissue oxygen availability with near infrared spectroscopy (NIRS) in health and disease. *Scand. J. Med. Sci. Sports* **11**, 213–222 (2001).
26. Boushel, R. & Piantadosi, C. Near-infrared spectroscopy for monitoring muscle oxygenation. *Acta Physiol. Scand.* **168**, 615–622 (2000).
27. Boezeman, R. P., Moll, F. L., Ünlü, Ç. & de Vries, J. P. P. Systematic review of clinical applications of monitoring muscle tissue oxygenation with near-infrared spectroscopy in vascular disease. *Microvasc. Res.* **104**, 11–22 (2016).

28. Binzoni, T., Quaresima, V., Ferrari, M., Hiltbrand, E. & Cerretelli, P. Human calf microvascular compliance measured by near-infrared spectroscopy. *J. Appl. Physiol.* **88**, 369–372 (2000).
29. Truijen, J. *et al.* Orthostatic leg blood volume changes assessed by near-infrared spectroscopy. *Exp. Physiol.* **97**, 353–361 (2012).
30. De Blasi, R. A. *et al.* Microcirculatory changes and skeletal muscle oxygenation measured at rest by non-infrared spectroscopy in patients with and without diabetes undergoing haemodialysis. *Crit. Care* **13**, 1–10 (2009).
31. De Blasi, R. A. & Arcioni, R. Assessing skeletal muscle variations in microvascular pressure and unstressed blood volume at the bedside. *Microcirculation* **21**, 606–614 (2014).
32. Buckey, J. C., Peshock, R. M. & Blomqvist, C. G. Deep venous contribution to hydrostatic blood volume change in the human leg. *Am. J. Cardiol.* **62**, 449–453 (1988).
33. Neglen, P. & Raju, S. S. The pressure/volume relationship of the calf: A measurement of vein compliance? *J. Cardiovasc Surg.* **36**, 219–224 (1995).
34. de Groot, P. C., Bleeker, M. W. & Hopman, M. T. Ultrasound: A reproducible method to measure conduit vein compliance. *J. Appl. Physiol.* **98**, 1878–1883 (2005).
35. De Blasi, R. A. *et al.* Noninvasive measurement of forearm blood flow and oxygen consumption by near-infrared spectroscopy. *J. Appl. Physiol.* **76**, 1388–1393 (1994).
36. Southern, W. M., Ryan, T. E., Reynolds, M. A. & McCully, K. Reproducibility of near-infrared spectroscopy measurements of oxidative function and postexercise recovery kinetics in the medial gastrocnemius muscle. *Appl. Physiol. Nutr. Metab.* **39**, 521–529 (2014).
37. Cross, T. J. & Sabapathy, S. The impact of venous occlusion per se on forearm muscle blood flow: Implications for the near-infrared spectroscopy venous occlusion technique. *Clin. Physiol. Funct. Imaging* **37**, 293–298 (2017).
38. Lucero, A. A. *et al.* Reliability of muscle blood flow and oxygen consumption response from exercise using near-infrared spectroscopy. *Exp. Physiol.* **103**, 90–100 (2018).

Acknowledgements
The authors are grateful to Dr. Raffaele Pertusio for designing and developing the ultrasound probe holder.

Author contributions
Conception of the work: S.R., S.S., and L.E. Acquisition, analysis or interpretation of data for the work: S.R., S.S., L.E., and P.P. Drafting the work or revising it critically for important intellectual content: S.S., L.E., P.P., L.M., and S.R. All authors approved the final version of the manuscript, agree to be accountable for all aspects of the work in ensuring that questions related to the accuracy or integrity of any part of the work are appropriately investigated and resolved and confirm that all persons designated as authors qualify for authorship, and all those who qualify for authorship are listed.

Funding
This research was supported by local grants from the University of Torino (ROAS_RILO_17_01) and Supported by the Italian Ministry of Economic Development through the Proof of Concept (PoC-Off) project "Vein Image Processing for Edge Rendering—VIPER" (CUP C16I20000080006).

Competing interests
The authors declare no competing interests.

Additional information
Supplementary Information The online version contains supplementary material available at https://doi.org/10.1038/s41598-022-05863-y.

Correspondence and requests for materials should be addressed to S.R.

Reprints and permissions information is available at www.nature.com/reprints.

Publisher's note Springer Nature remains neutral with regard to jurisdictional claims in published maps and institutional affiliations.

Paper VII

frontiers in Cardiovascular Medicine

REVIEW
published: 21 January 2022
doi: 10.3389/fcvm.2021.775635

Assessment of Phasic Changes of Vascular Size by Automated Edge Tracking-State of the Art and Clinical Perspectives

Luca Mesin[1], Stefano Albani[2,3], Piero Policastro[1], Paolo Pasquero[4], Massimo Porta[4], Chiara Melchiorri[4], Gianluca Leonardi[4], Carlo Albera[4], Paolo Scacciatella[2], Pierpaolo Pellicori[5], Davide Stolfo[3], Andrea Grillo[3], Bruno Fabris[3], Roberto Bini[6], Alberto Giannoni[7,8], Antonio Pepe[9,10], Leonardo Ermini[11], Stefano Seddone[11], Gianfranco Sinagra[5], Francesco Antonini-Canterin[9] and Silvestro Roatta[11]*

[1] Mathematical Biology and Physiology, Department of Electronics and Telecommunications, Politecnico di Torino, Turin, Italy, [2] SC Cardiologia Ospedale Regionale U. Parini, Aosta, Italy, [3] Department of Medical, Surgical and Health Sciences, Universitá di Trieste, Trieste, Italy, [4] Department of Medical Sciences, Universitá di Torino, Turin, Italy, [5] Robertson Centre for Biostatistics, Research Institute of Health and Wellbeing, University of Glasgow, Glasgow, United Kingdom, [6] Chirurgia Generale e Trauma Team GOM Niguarda, Milan, Italy, [7] Scuola Superiore Sant'Anna, Pisa, Italy, [8] Fondazione Toscana G. Monasterio, Pisa, Italy, [9] Highly Specialized in Rehabilitation Hospital-ORAS S.p.A., Motta di Livenza, Italy, [10] Ospedale Unico di Santorso, AULSS7 Pedemontana, Italy, [11] Integrative Physiology Lab, Department of Neuroscience, Universitá di Torino, Turin, Italy

OPEN ACCESS

Edited by:
Stefania Paolillo,
University of Naples Federico II, Italy

Reviewed by:
Arturo Cesaro,
University of Campania Luigi Vanvitelli, Italy
Elisabetta Salvioni,
Monzino Cardiology Center, Scientific Institute for Research, Hospitalization and Healthcare (IRCCS), Italy

***Correspondence:**
Luca Mesin
luca.mesin@polito.it

Specialty section:
This article was submitted to Heart Failure and Transplantation, a section of the journal Frontiers in Cardiovascular Medicine

Received: *14 September 2021*
Accepted: *14 December 2021*
Published: *21 January 2022*

Citation:
Mesin L, Albani S, Policastro P, Pasquero P, Porta M, Melchiorri C, Leonardi G, Albera C, Scacciatella P, Pellicori P, Stolfo D, Grillo A, Fabris B, Bini R, Giannoni A, Pepe A, Ermini L, Seddone S, Sinagra G, Antonini-Canterin F and Roatta S (2022) Assessment of Phasic Changes of Vascular Size by Automated Edge Tracking-State of the Art and Clinical Perspectives. Front. Cardiovasc. Med. 8:775635. doi: 10.3389/fcvm.2021.775635

Assessment of vascular size and of its phasic changes by ultrasound is important for the management of many clinical conditions. For example, a dilated and stiff inferior vena cava reflects increased intravascular volume and identifies patients with heart failure at greater risk of an early death. However, lack of standardization and sub-optimal intra- and inter- operator reproducibility limit the use of these techniques. To overcome these limitations, we developed two image-processing algorithms that quantify phasic vascular deformation by tracking wall movements, either in long or in short axis. Prospective studies will verify the clinical applicability and utility of these methods in different settings, vessels and medical conditions.

Keywords: inferior vena cava, arterial stiffness, ultrasound imaging, pulsatility, fluid volume assessment, right atrial pressure

1. INTRODUCTION

Currently, the invasive measurement of central venous pressure (CVP) to estimate right atrial pressure (RAP) is routinely used only in critically ill patients to assess cardiac hemodynamics and volume status. Medical devices that provide this information non-invasively are under development, but not routinely used yet in clinical practice (1). A widely adopted non-invasive approach to estimate RAP is based on ultrasound (US) imaging of the inferior vena cava (IVC) diameter and of its respiratory changes (2, 3). These changes can be expressed in terms of the caval index (CI), defined as the variation of the vessel diameter during a respiration cycle, relative to the maximum diameter (4). This approach is not standardized (5) [for instance, it is performed in either long (6) or short axis (7) views], is operator-dependent (8) [with an important effect of experience (9)] and prone to measurement errors (10) [e.g., due to movements (8, 11) or to irregular shape of the IVC (12)]. Therefore, a single measurement might only provide limited—and misleading—information. The following sources of variability of the standard

US approach have been investigated (8): different respiration cycles (coefficient of variation, CoV=15%), specific longitudinal section (CoV=40%), inter- and intra-operator variability (CoV 35 and 28%, respectively). Furthermore, recent studies indicated that IVC collapsibility assessed with current methods is not a reliable predictor of fluid responsiveness (13) and its correlation with RAP is only modest (14, 15).

Alternative approaches to assess, non-invasively, the CVP or volemic status have been proposed. For instance, there is a good correlation between CVP with pressure measured in superficial veins at the forearm with an US probe equipped with a pressure transducer (16). Moreover, measuring with US the ratio of the internal jugular vein during a Valsalva maneuver to that at rest identifies patients with heart failure with more severe intravascular congestion at greater risk of poorer outcomes (17, 18). However these techniques are not routinely used in clinical practice, as they require a more robust validation.

The assessment of arterial wall properties is also useful to characterize the health of the cardiovascular system and can improve prediction of cardiovascular events beyond conventional risk factors (19). Measurement of aortic pulse wave velocity (PWV) is considered the current gold standard to assess arterial stiffness. It has acceptable degree of accuracy and reliability (10) and has demonstrated to predict cardiovascular events for patients with different cardiovascular risk factors or diseases (20), but requires a specialized equipment (arterial tonometry, piezoelectric sensors, photoplethysmography) and additional time and resources. Moreover, current assessment of PWV may exclude the proximal segment of the aorta and might not identify pathological segments along the arterial tree, the deformation of which could, potentially, be assessed by US if a reliable method existed (21, 22).

Recently, we have started to address some of the above mentioned issues and developed two semi-automated methods to delineate and track displacements of the IVC borders in long (4, 8, 23, 24) or short axis views (12). Our approaches could reduce the inter/intra-operator variability (8), assist in the interpretation of findings clinicians or sonographers with limited training and experience (25), and perhaps facilitate the diffusion of point-of-care US to guide clinical decisions. Our preliminary results suggest that the integration of indexes extracted by both algorithms could provide a more reliable estimation of the volemic status than using the standard IVC assessment (26) and call for extensions of research to larger databases and other vessels, like the arteries, the evaluation of which might improve cardiovascular risk stratification (27).

In this manuscript, we discuss these methods along with some possible future applications.

2. PHYSIOLOGICAL BASIS OF VESSEL PULSATILITY

Rapid changes in vascular size (irrespective of whether we deal with arteries or veins) are primarily produced by changes in transmural pressure P_{tm}, defined as $P_{tm} = P_{in} - P_{out}$, where P_{in} is the blood pressure inside and P_{out} the pressure outside the vessel wall (28, 29). The relation between vascular size and P_{tm} is generally represented by a volume-pressure (or capacitance) curve as qualitatively shown in **Figure 1**, whereby the vascular size, expressed in terms of vessel volume V, is shown to increase with increasing transmural pressure. This sketchy representation can be assumed to be a hypothetical experimental characterization of the vessel of interest. Ranges of volume and pressure are not indicated, as they vary widely along the cardiovascular system (30). Specifically, arteries are more rigid and exposed to larger pressure variations than veins. Pressure variations in the arteries are mainly determined by the pulsatile nature of the cardiac pump and they are also affected by peripheral resistances; whilst P_{tm} changes in the veins are largely influenced by a variation of the external pressure. However, this scheme is only a simplistic representation, as intrinsic vessel characteristics, circulating blood volume, medications and many other additional factors might influence intravascular pressure (31); moreover, the volume-pressure curve of a certain vessel or vascular district can be modulated by spontaneous or drug-mediated variations in vascular tone.

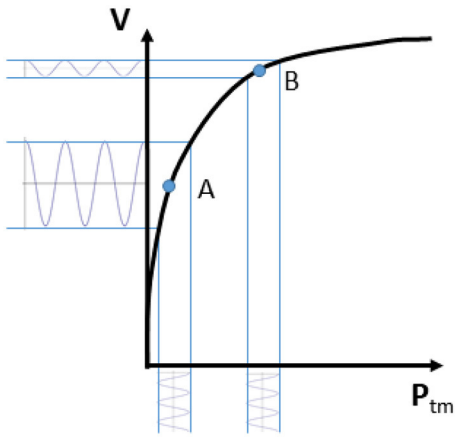

FIGURE 1 | Volume-pressure curve of a venous blood vessel relating the vessel size (volume V) to the transmural pressure (P_{tm}). Note that an oscillatory perturbation in blood pressure results in large volume changes if P_{tm} is low (A; high vessel compliance) and low pulsatility if P_{tm} is high (B; low vessel compliance).

Coming back to the simplified representation shown in **Figure 1**, it can however be observed that the curve has a tendency to flatten at high P_{tm}. This indicates a decreasing vessel compliance, defined as

$$C = \frac{\Delta V}{\Delta P_{tm}} \quad (1)$$

and representing the slope of the volume-pressure curve. A given perturbation of P_{tm}, such as a blood pressure change of cardiac or respiratory origin, would result in a corresponding vessel volume change, according to vessel compliance. As shown in **Figure 1**, the same change in P_{tm} will produce different changes in vessel size, depending on the resting (average) value of P_{tm} and V: if average P_{tm} is low (for instance, in the case of IVC, when

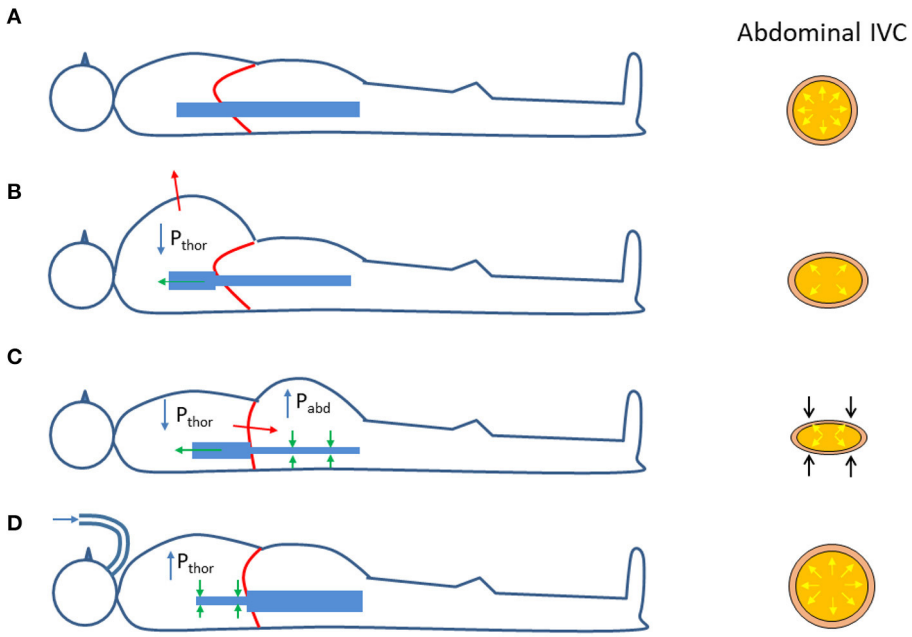

FIGURE 2 | Effects of respiration on the size of the abdominal inferior vena cava (IVC); see explanation in the text. P_{thor} = Intrathoracic pressure; P_{abd} = abdominal pressure. **(A)** Functional residual capacity (end expiration). **(B)** Thoracic inspiration. **(C)** Abdominal (diaphragmatic) inspiration. **(D)** Positive pressure ventilation (inspiration).

CVP or blood volume are normal) size changes will be large, while at a higher P_{tm} value the vessel size will be larger and its phasic changes (that we might call "pulsatility", for simplicity) will be smaller (for instance, when CVP is high or if there is hypervolemia).

The same considerations might apply, in theory, to the entire vascular system. Notably, P_{tm} is not just dependent on the inner blood pressure, but also on the outside pressure. The effect of changes in the outside pressure are particularly relevant in veins, given their low blood pressure.

It is worth to reconsider the changes in transmural pressure that take place in the (abdominal) IVC during respiration. As compared to the reference end-expiratory condition (**Figure 2A**), in which the IVC exhibits its maximum size, during a thoracic inspiration the IVC undergoes a slight reduction in size, due to the decrease in intrathoracic pressure which drains blood from the IVC, thus lowering blood pressure and its P_{tm} (**Figure 2B**). In addition, during inspiration, the diaphragm descends and abdominal pressure increases, with a further decrease in P_{tm} and IVC size (**Figure 2C**). The different implications of the respiratory pattern on IVC size have been evidenced experimentally during both spontaneous respiration (32) and in controlled isovolumetric respiratory efforts (33). Opposite effects, i.e., increased IVC size during inspiration, are observed during positive pressure ventilation, whereby the increase in intrathoracic pressure hinders venous return, thus increasing abdominal venous blood pressure and IVC size (**Figure 2D**).

Finally, the analysis of phasic changes of the vascular size should take in consideration an additional confounding factor: the extravascular compliance. Since blood vessels are embedded within other organs and tissues, their possibility to expand upon variations in blood pressure depends on the capacity of the extravascular tissues to accommodate such changes. In other words, when measuring vessel volume changes in response to given variations in blood pressure, we are actually assessing the total compliance (C_{tot}), which accounts for the vascular (C_v) and extravascular (C_{ev}) compliances according to the formula

$$C_{tot} = \frac{1}{\frac{1}{C_v} + \frac{1}{C_{ev}}} \tag{2}$$

C_{tot} resulting smaller than C_v.

In summary, 1) the vessel size depends on $P_{tm} = P_{in} - P_{out}$, according to a non-linear volume-pressure curve; 2) the vessel compliance ($C = \Delta V/\Delta P_{tm}$) generally decreases at increasing P_{tm}; 3) vessel phasic changes depend on vascular compliance; 4) low extravascular compliance may lead to underestimate actual vessel compliance.

3. ECHOGRAPHY PROCESSING

Vessels such as the IVC might have a complex geometry. In particular, as shown in **Figure 3**, the section of the IVC is not constant along the longitudinal axis and its cross-section is far from being like a perfect circle, with large variations across subjects and clinical conditions. Moreover, IVC is a very compliant vessel whose movements are also affected by surrounding structures to which it can be anchored. Therefore, measuring its size on a single plane might be largely inaccurate (as shown in **Figure 4**).

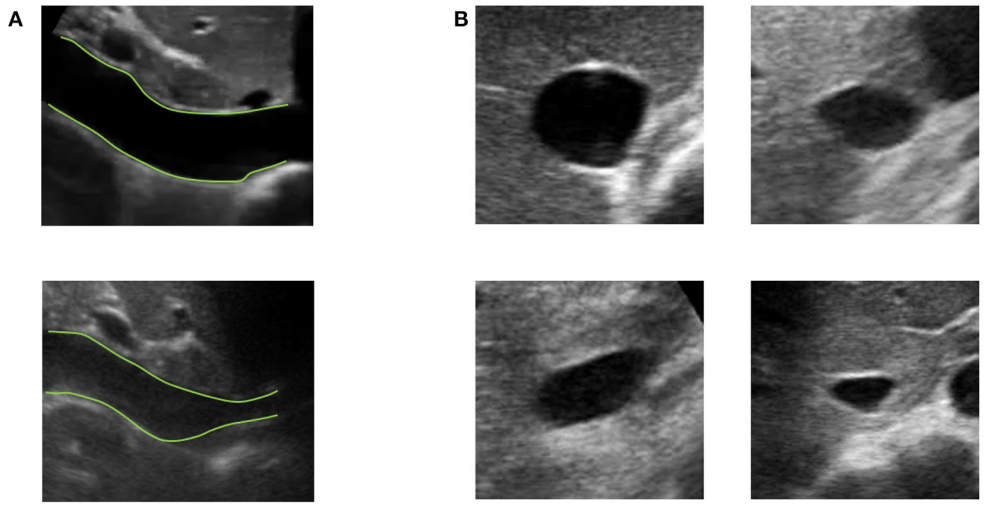

FIGURE 3 | Examples of long and short axis sections of inferior vena cava (IVC) from different subjects. **(A)** IVC in long axis: one IVC has a stable diameter whereas the other shows great variations along the longitudinal axis. **(B)** Different shapes of IVC cross-sections.

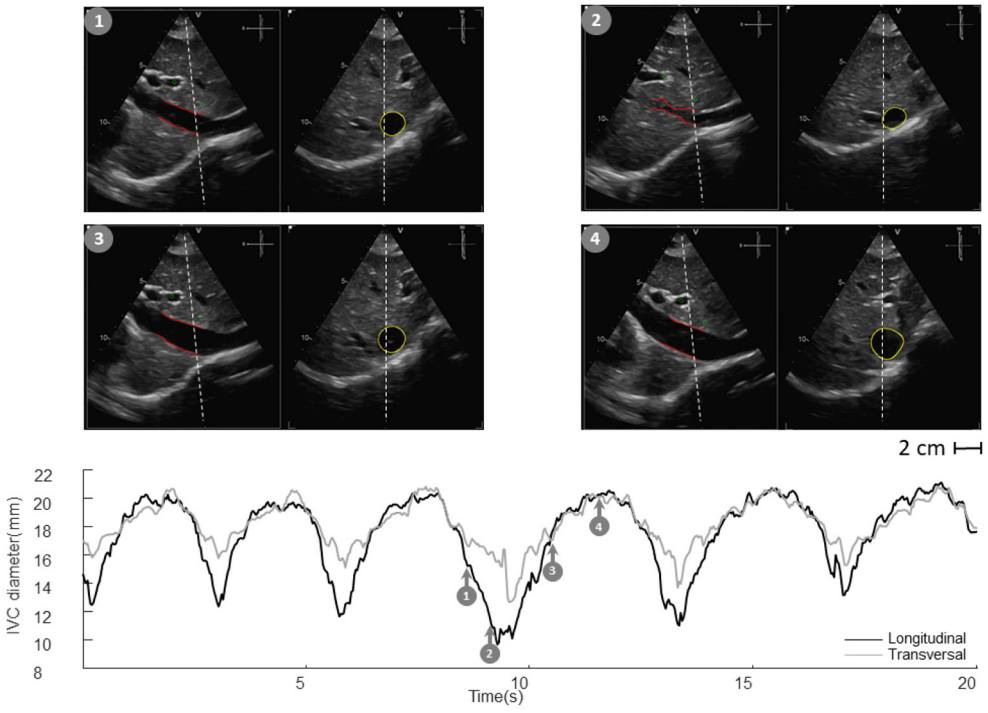

FIGURE 4 | Inferior vena cava (IVC) echography in x-plane. Both long and short axis views are available in synchronous scans. The sections can be displaced with respect to the center of the vessel. Moreover, they could be not orthogonal to the IVC axis. The estimation of the diameter in a single section can be largely affected.

US scans of IVC in B-mode provide limited information on its phasic changes, which occur in a three dimensional space. With our two algorithms we can estimate the IVC edges either in long or short axis views (12, 23).

In long axis, IVC movements are estimated by tracking two reference points selected by the user. Then, the edges are estimated in an entire longitudinal portion of the vessel. The diameters of different sections are then computed in directions orthogonal to the midline of the IVC, thus compensating for possible translations and rotations in the visualized plane (23).

In the case of the short axis view, the contour of the cross-section of the IVC is estimated, finding the edges along different directions starting from its center, identified in the previous frame as the centroid of the vessel border (12).

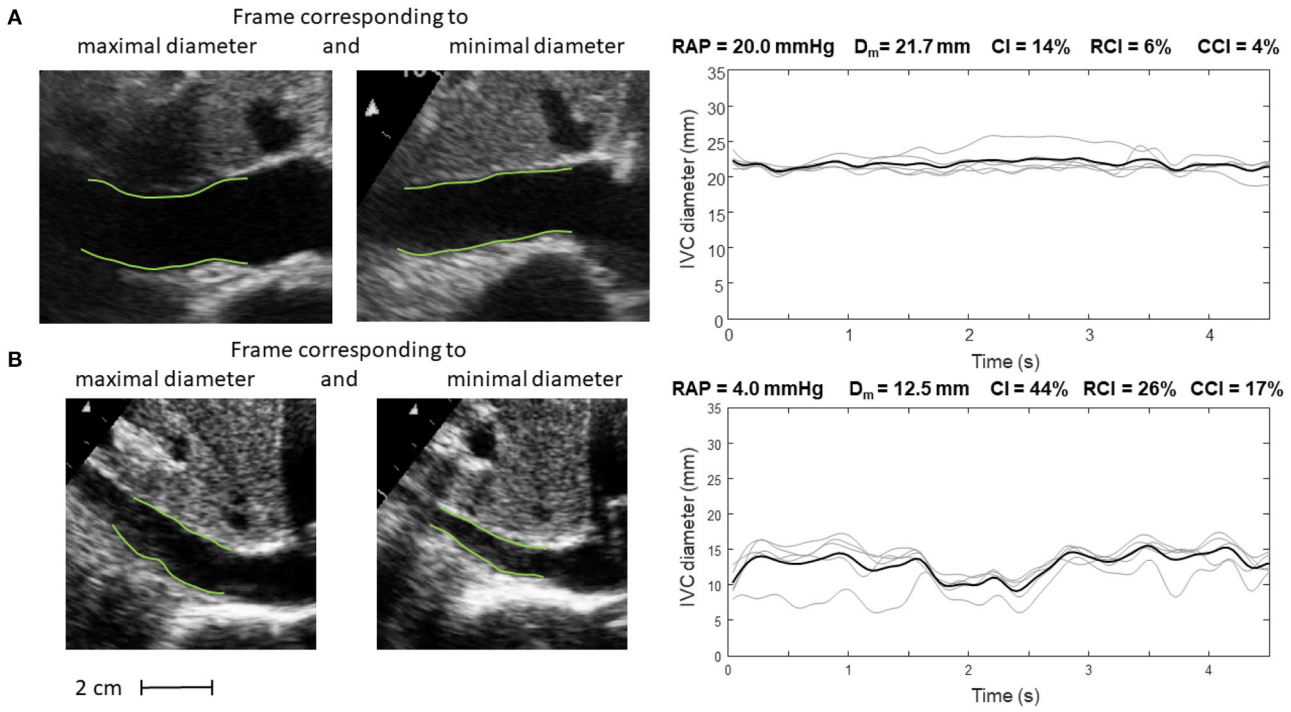

FIGURE 5 | Inferior vena cava (IVC) dynamics in patients with different right atrial pressure (RAP, measured invasively). **(A)** Patient with high RAP. **(B)** Patient with low RAP. Abbreviations used: average diameter D_m, caval index *CI*, respiratory caval index *RCI*, cardiac caval index *CCI*.

As the edges of the IVC are estimated in each frame of the US video, a temporal series is acquired, from which different measures of IVC size can be obtained (e.g., different diameters, their average, or the cross-sectional area). In particular, two main contributions are clearly visible in IVC dynamics described by those time series: a slow oscillation of IVC size induced by respiration (due to variations of intrathoracic and abdominal pressure) and another at higher frequency induced by the heartbeats (reflecting retrograde flow induced by right atrial contraction). These two components can be measured separately (respiratory caval index, RCI, and cardiac caval index, CCI) and potentially provide complementary information (4, 8, 12, 23, 24, 26, 34).

Alternative methods to assess phasic changes of vascular size have also been applied or developed by other colleagues (35–37). Specifically, a method widely used in echocardiography is based on tracking the speckle noise (38), i.e., a random mixture of interference patterns and US reflections characterizing each region of the tissue (like as a fingerprint) that is relatively stable on consecutive frames, allowing the region to be traced from one frame to the next. Speckle tracking has been applied to study the IVC deformation in long axis view (36) or to assess aortic or carotid stiffness (39, 40). Different processing techniques have also been used to segment blood vessels: for example, Otsu's thresholding (41) was combined with active contour on multiple short axis views to estimate the carotid in 3D (42); a semi-automated modified watershed method was applied to estimate the cross-section of IVC (43); snake and template matching (the latter approach, similar to speckle tracking) were tested for IVC edge detection in short axis (44); a novel energy functional for polar active contour was applied to the segmentation of IVC in short axis (45). More recently, deep learning approaches have been applied on the segmentation of IVC in short axis, obtaining moderately good performances in predicting fluid responsiveness (46). Edge-tracking methodology might exhibit a good compromise between computational cost and accuracy (12). We are currently working on the real time implementation and rendering over the US scan of the estimated vascular edges: this can provide the operators with visual feedback and guidance to obtain and acquire good quality images; moreover, the simultaneous measurement of quantitative indexes (e.g., mean diameter and pulsatility indexes) might be a valuable add-on for research and routine clinical practice.

4. CURRENT AND FUTURE APPLICATIONS

Our methods have been applied in two pilot studies, to estimate the RAP (24, 34) and volume status (26). Representative examples are shown in **Figures 5**, **6**.

Specifically, **Figure 5** shows frames corresponding to maximal and minimal IVC size for two patients, with invasively measured high (A) and low (B) RAP, respectively. The average size of IVC is larger in the patient with higher RAP (20 mmHg) and the IVC phasic changes are greater for the patient with lower RAP (4 mmHg): in the latter case, small variations of transmural pressure induce large changes of size in the vessel.

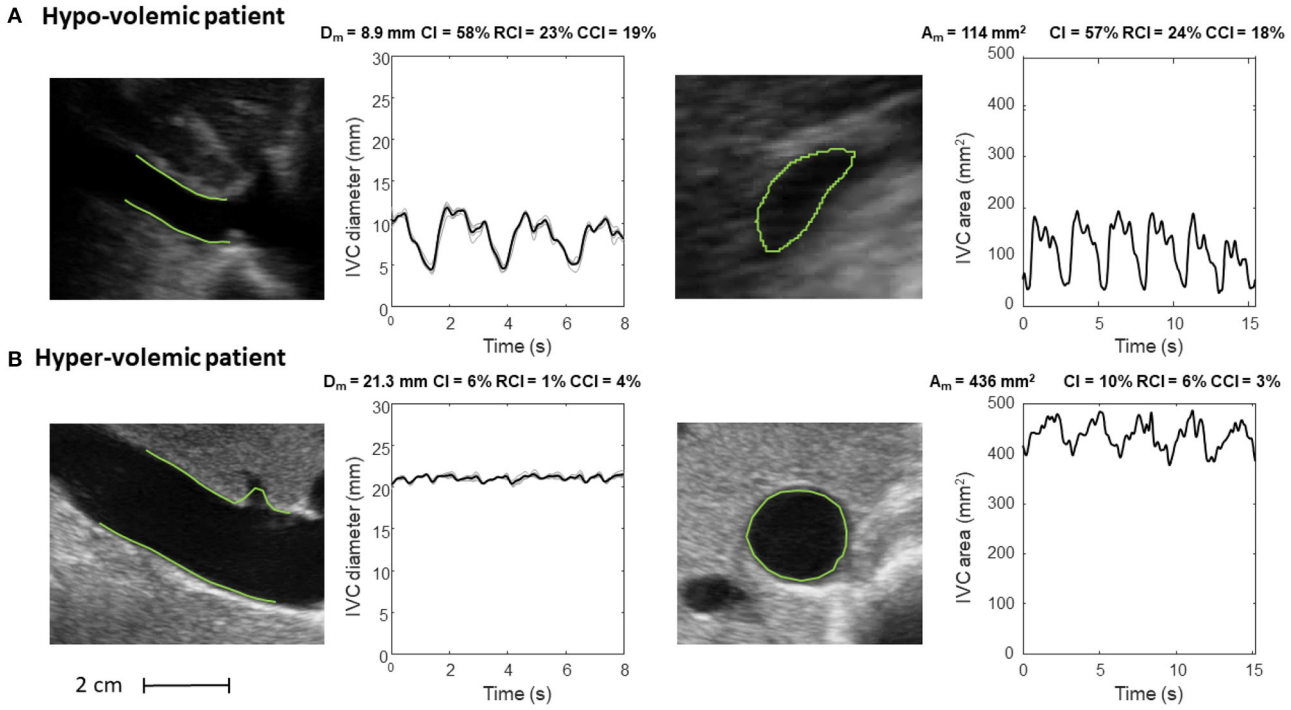

FIGURE 6 | Inferior vena cava (IVC) dynamics in patients with different volume status. **(A)** Hypo-volemic patient. **(B)** Hyper-volemic patient. Abbreviations used: average diameter D_m, average cross-sectional area A_m, caval index *CI*, respiratory caval index *RCI*, cardiac caval index *CCI*.

TABLE 1 | Current evaluation and potential clinical relevance of image-processing algorithms applied to vascular ultrasound.

Current evaluation	Potential clinical relevance
Tracking of IVC movements and phasic deformation, longitudinally or cross-sectionally	Assessment of volemic status Estimation of right atrial pressure Assessment of venous compliance and fluid redistribution
Tracking of peripheral veins deformation	Monitoring responses during renal dialysis, to diuretics or a fluid challenge
Tracking of arterial phasic deformation, longitudinally or cross-sectionally	Evaluation of arterial stiffness Assessment of cardiovascular health

Figure 6 shows the long and short axis of the IVC in a hypo- (**Figure 6A**) and hyper- (**Figure 6B**) volemic patient, respectively. Compared to patients with hypervolemia, in those with hypovolemia the IVC size is smaller and the pulsatility is larger; moreover, the IVC in the cross-section view has a flattened shape, whereas it is mostly circular in conditions of fluid overload.

In addition, the features offered by the automated algorithms (i.e., size and indexes of pulsatility of the blood vessel of interest) open the way to new applications. We here briefly overview those that are of particular interest to the authors, i.e., specific studies or applications that have recently been attempted and are close to completion or that belong to the author's different working fields in basic and clinical sciences and that will be addressed in the near future. These existing and potential application of the methodology are presented in **Table 1**, but many other applications may possibly be envisaged.

Edge tracking algorithms can be applied to peripheral veins to investigate, by ultrasound, the mechanical response to changes in transmural pressure, e.g., by venous occlusion, for the assessment of venous compliance (47, 48) and characterize the filling condition and the expanding capacity of the peripheral reservoir, a major pathway for venous return. Assessment of venous compliance could also be used to validate another recently proposed index of peripheral vascular filling, the venous pulse wave velocity (49, 50). Combining these methods with the IVC assessment might increase the understanding of the underlying mechanisms of fluid distribution and displacements across different body regions and compartments in various clinical contexts (28, 29).

In this respect, an interesting model of acute fluid redistribution is offered by the MuVIT technique (51), a procedure used to transiently lower aortic blood flow and pressure during thoracic or abdominal vascular interventions (e.g., stent graft placements) consisting in transiently increasing alveolar pressure up to about 30 mmHg. This maneuver provokes a substantial blood volume displacement from the pulmonary and arterial compartments to the systemic venous compartment resulting in a transient venous congestion. The possibility of simultaneous tracking size changes of abdominal and peripheral

veins may help to characterize the dynamic behavior of the full venous compartment.

Fluid overload, or congestion, is a key clinical feature in acute heart failure, but its management with diuretic is still very subjective (52). Controversial results have been documented in the literature about the potential utility of IVC diameter and distensibility to monitor the response to diuretics in patients with acute heart failure (53, 54). Quantifying with precision phasic IVC changes might potentially detect even small variations in intravascular fluids and possibly guide clinicians for a more objective use of diuretic therapy.

Similar considerations apply to renal failure patients undergoing dialysis, whereby automated continuous and unsupervised IVC monitoring may help to tailor the dialytic process according to the current volume status of the patient.

The possibility to detect a cardiac pulsatility of IVC in addition to the major oscillatory component of respiratory origin is still largely unexplored and many questions have to be addressed. May the cardiac pulsatility provide a more reliable index of IVC collapsibility than the classical caval index? Is cardiac pulsatility carrying additional or different information than respiratory phasic variations? Long term monitoring and correlation analysis of these oscillatory components as well as extending the investigation to specific patient groups is necessary to address these questions.

Finally, a relevant application concerns the assessment of arterial stiffness. Aortic stiffness is associated with incident cardiovascular events. In clinical practice, aortic stiffness is usually investigated indirectly in terms of the PWV. However, the PWV is usually measured from the carotid-femoral artery PWV, a global index, which does not reflect local stiffness variations. In theory, aortic stiffness could be estimated directly, by measuring with US the aorta pulsatility under a known pressure variation (systo-diastolic) (55), in different aortic segments (56). Whether segmental aortic stiffness measured by US might discriminate different patients' conditions and risk, it is worth exploring.

5. CONCLUSIONS

Rapid advances in US image processing have made now possible to obtain more objective information on the size of arteries and veins, but also to quantify their phasic changes with more precision, which can transform management of several conditions and potentially improve outcomes.

6. PATENTS

An instrument implementing the algorithms for IVC delineation used in this paper was patented by Politecnico di Torino and Universitá di Torino (WO 2018/134726).

AUTHOR CONTRIBUTIONS

LM, SA, and SR: methodology and writing–original draft preparation. LM and PPo: software. SA, SR, PPa, MP, and LE: data preparation. LM, SR, and PPo: visualization. MP, GS, PPe, FA-C, and SR: supervision. All authors conceptualization, writing–review, editing, read, and agreed to the published version of the manuscript.

FUNDING

Supported by the Italian Ministry of Economic Development through the Proof of Concept (PoC-Off) project Vein Image Processing for Edge Rendering–VIPER (CUP C16I20000080006).

REFERENCES

1. Pellicori P, Clark AL, Kallvikbacka-Bennett A, Zhang J, Urbinati A, Monzo L, et al. Non-invasive measurement of right atrial pressure by near-infrared spectroscopy: preliminary experience. A report from the SICA-HF study. *Eur J Heart Fail*. (2017) 19:883–92. doi: 10.1002/ejhf.825
2. Lang RM, Badano LP, Mor-Avi V, Afilalo J, Armstrong A, Ernande L, et al. Recommendations for cardiac chamber quantification by echocardiography in adults: an update from the American Society of Echocardiography and the European Association of Cardiovascular Imaging. *J Am Soc Echocardiogr*. (2015) 28:1–39.e14. doi: 10.1016/j.echo.2014.10.003
3. Ponikowski P, Voors AA, Anker SD, Bueno H, Cleland JG, Coats AJ, et al. 2016 ESC Guidelines for the diagnosis treatment of acute chronic heart failure: The Task Force for the diagnosis treatment of acute chronic heart failure of the European Society of Cardiology (ESC). Developed with the special contribution of the Heart Failure Association (HFA) of the ESC. *Eur J Heart* Fail. (2016). 18:891–975. doi: 10.1002/ejhf.592
4. Mesin L, Pasquero P, Albani S, Porta M, Roatta S. Semi-automated tracking and continuous monitoring of inferior vena cava diameter in simulated and experimental ultrasound imaging. *Ultrasound Med Biol*. (2015) 41:845–57. doi: 10.1016/j.ultrasmedbio.2014.09.031
5. Wallace DJ, Allison M, Stone MB. Inferior vena cava percentage collapse during respiration is affected by the sampling location: an ultrasound study in healthy volunteers. *Acad Emerg Med*. (2010) 17:96–9. doi: 10.1111/j.1553-2712.2009.00627.x
6. Barbier C, Loubieres Y, Schmit C, Hayon J, Ricome JL, Jardin F, et al. Respiratory changes in inferior vena cava diameter are helpful in predicting fluid responsiveness in ventilated septic patients. *Intensive Care Med*. (2004) 30:1740–6. doi: 10.1007/s00134-004-2259-8
7. Blehar DJ, Dickman E, Gaspari R. Identification of congestive heart failure via respiratory variation of inferior vena cava diameter. *Am J Emerg Med*. (2009) 27:71–5. doi: 10.1016/j.ajem.2008.01.002
8. Mesin L, Giovinazzo T, D'Alessandro S, Roatta S, Raviolo A, Chiacchiarini F, et al. Improved repeatability of the estimation of pulsatility of inferior vena cava. *Ultrasound Med Biol*. (2019) 45:2830–43. doi: 10.1016/j.ultrasmedbio.2019.06.002
9. Corl KA, Azab N, Nayeemuddin M, Schick A, Lopardo T, Zeba F, et al. Performance of a 25% inferior vena cava collapsibility in detecting fluid responsiveness when assessed by novice versus expert physician sonologists. *J Intensive Care Med*. (2020) 35:1520–8. doi: 10.1177/0885066619881123
10. Townsend RR, Wilkinson IB, Schiffrin EL, Avolio AP, Chirinos JA, Cockcroft JR, et al. Recommendations for improving and standardizing vascular research on arterial stiffness: a scientific statement from the American Heart Association. *Hypertension*. (2015) 66:698–722. doi: 10.1161/HYP.0000000000000033
11. Blehar D, Resop D, Chin B, Dayno M, Gaspari R. Inferior vena cava displacement during respirophasic ultrasound imaging. *Crit Ultrasound J*. (2012) 4:1–5. doi: 10.1186/2036-7902-4-18
12. Mesin L, Pasquero P, Roatta S. Multi-directional assessment of respiratory and cardiac pulsatility of the inferior vena cava from ultrasound

imaging in short axis. *Ultrasound Med Biol*. (2020) 46:3475–82. doi: 10.1016/j.ultrasmedbio.2020.08.027
13. Orso D, Paoli I, Piani T, Cilenti FL, Cristiani L, Guglielmo N. Accuracy of ultrasonographic measurements of inferior vena cava to determine fluid responsiveness: a systematic review and meta-analysis. *J Intensive Care Med*. (2020) 35:354–63. doi: 10.1177/0885066617752308
14. Bouzat P, Walther G, Rupp T, Levy P. Inferior vena cava diameter may be misleading in detecting central venous pressure elevation induced by acute pulmonary hypertension. *Am J Respir Crit Care Med*. (2014) 190:233–5. doi: 10.1164/rccm.201403-0488LE
15. Magnino C, Omedé P, Avenatti E, Presutti D, Iannaccone A, Chiarlo M, et al. Inaccuracy of right atrial pressure estimates through inferior vena cava indices. *Am J Cardiol*. (2017) 120:1667–73. doi: 10.1016/j.amjcard.2017.07.069
16. Thalhammer C, Aschwanden M, Odermatt A, Baumann UA, Imfeld S, Bilecen D, et al. Noninvasive central venous pressure measurement by controlled compression sonography at the forearm. *J Am Coll Cardiol*. (2007) 50:1584–9. doi: 10.1016/j.jacc.2007.07.022
17. Pellicori P, Kallvikbacka-Bennett A, Dierckx R, Zhang J, Putzu P, Cuthbert J, et al. Prognostic significance of ultrasound-assessed jugular vein distensibility in heart failure. *Heart*. (2015) 101:1149–58. doi: 10.1136/heartjnl-2015-307558
18. Pellicori P, Kallvikbacka-Bennett A, Zhang J, Khaleva O, Warden J, Clark AL, et al. Revisiting a classical clinical sign: jugular venous ultrasound. *Int J Cardiol*. (2014) 170:364–70. doi: 10.1016/j.ijcard.2013.11.015
19. Laurent S, Cockcroft J, Van Bortel L, Boutouyrie P, Giannattasio C, Hayoz D, et al. Expert consensus document on arterial stiffness: methodological issues and clinical applications. *Eur Heart J*. (2006) 27:2588–605. doi: 10.1093/eurheartj/ehl254
20. Ben-Shlomo Y, Spears M, Boustred C, May M, Anderson SG, Benjamin EJ, et al. Aortic pulse wave velocity improves cardiovascular event prediction: an individual participant meta-analysis of prospective observational data from 17,635 subjects. *J Ame Coll Cardiol*. (2014) 63:636–46. doi: 10.1016/j.jacc.2013.09.063
21. Salvi P, Scalise F, Rovina M, Moretti F, Salvi L, Grillo A, et al. Noninvasive estimation of aortic stiffness through different approaches: comparison with intra-aortic recordings. *Hypertension*. (2019) 74:117–29. doi: 10.1161/HYPERTENSIONAHA.119.12853
22. Hickson SS, Butlin M, Graves M, Taviani V, Avolio AP, McEniery CM, et al. The relationship of age with regional aortic stiffness and diameter. *JACC Cardiovasc Imaging*. (2010) 3:1247–55. doi: 10.1016/j.jcmg.2010.09.016
23. Mesin L, Pasquero P, Roatta S. Tracking and monitoring pulsatility of a portion of inferior vena cava from ultrasound imaging in long axis. *Ultrasound Med Biol*. (2019) 45:1338–43. doi: 10.1016/j.ultrasmedbio.2018.10.024
24. Albani S, Pinamonti B, Giovinazzo T, de Scordilli M, Fabris E, Stolfo D, et al. Accuracy of right atrial pressure estimation using a multi-parameter approach derived from inferior vena cava semi-automated edge-tracking echocardiography: a pilot study in patients with cardiovascular disorders. *Int J Cardiovasc Imaging*. (2020) 36:1213–25. doi: 10.1007/s10554-020-01814-8
25. Monti J. Revolution or evolution? A proposal for the integration of point-of-care ultrasound into physician assistant clinical practice. *J Physician Assist Educ*. (2017) 28:127–32. doi: 10.1097/JPA.0000000000000101
26. Mesin L, Pasquero P, Roatta S, Porta M. Automated volume status assessment using inferior vena cava pulsatility. *Electronics*. (2020) 9:1671. doi: 10.3390/electronics9101671
27. Laurent S, Boutouyrie P, Asmar R, Gautier I, Laloux B, Guize L, et al. Aortic stiffness is an independent predictor of all-cause and cardiovascular mortality in hypertensive patients. *Hypertension*. (2001) 37:1236–41. doi: 10.1161/01.HYP.37.5.1236
28. Brengelmann GL. Venous return and the physical connection between distribution of segmental pressures and volumes. *Am J Physiol Heart Circ Physiol*. (2019) 317:H939–53. doi: 10.1152/ajpheart.00381.2019
29. Gelman S. Venous function and central venous pressure: a physiologic story. *Anesthesiology*. (2008) 108:735–48. doi: 10.1097/ALN.0b013e3181672607
30. Guala A, Camporeale C, Ridolfi L, Mesin L. Non-invasive aortic systolic pressure and pulse wave velocity estimation in a primary care setting: an in silico study. *Med Eng Phys*. (2017) 42:91–98. doi: 10.1016/j.medengphy.2017.02.007
31. Van Bortel LM, Kool MJ, Boudier HA, Struijker Boudier HA. Effects of antihypertensive agents on local arterial distensibility and compliance. *Hypertension*. (1995) 26:531–4. doi: 10.1161/01.HYP.26.3.531
32. Kimura B, Dalugdugan R, Gilcrease G, Phan J, Showalter B, Wolfson T. The effect of breathing manner on inferior vena caval diameter. *Eur J Echocardiogr*. (2011) 12:120–3. doi: 10.1093/ejechocard/jeq157
33. Folino A, Benzo M, Pasquero P, Laguzzi A, Mesin A L Messere, Porta M, et al. Vena cava responsiveness to controlled isovolumetric respiratory efforts. *J Ultrasound Med*. (2017) 36:2113–23. doi: 10.1002/jum.14235
34. Mesin L, Albani S, Sinagra G. Non-invasive estimation of right atrial pressure using the pulsatility of inferior vena cava. *Ultrasound Med Biol*. (2019) 45:1331–7. doi: 10.1016/j.ultrasmedbio.2018.12.013
35. Nakamura K, Qian K, Ando T, Inokuchi R, Doi K, Kobayashi E, et al. Cardiac variation of internal jugular vein for the evaluation of hemodynamics. *Ultrasound Med Biol*. (2016) 42:1764–70. doi: 10.1016/j.ultrasmedbio.2016.03.003
36. Sonoo T, Nakamura K, Ando T, Sen K, Maeda A, Kobayashi E, et al. Prospective analysis of cardiac collapsibility of inferior vena cava using ultrasonography. *J Crit Care*. (2015) 30:945–8. doi: 10.1016/j.jcrc.2015.04.124
37. Tokunaga K, Nakamura K, Inokuchi R, Hayase N, Terada R, Tomioka Y, et al. Cardiac variation of internal jugular vein as a marker of volume change in hemorrhagic shock. *Shock*. (2020) 54:717–22. doi: 10.1097/SHK.0000000000001548
38. Oleynikov VE, Galimskaya VA, Kupriyanova SN, Burko NV. Use of the speckle tracking method for determining global parameters of heart contractility in healthy individuals. *MethodsX*. (2018) 5:125–35. doi: 10.1016/j.mex.2018.01.011
39. Bieseviciene M, Vaskelyte JJ, Mizariene V, Karaliute R, Lesauskaite V, Verseckaite R. Two-dimensional speckle-tracking echocardiography for evaluation of dilative ascending aorta biomechanics. *BMC Cardiovasc Disord*. (2017) 17:27. doi: 10.1186/s12872-016-0434-9
40. Yang EY, Dokainish H, Virani SS, Misra A, Pritchett AM, Lakkis N, et al. Segmental analysis of carotid arterial strain using speckle-tracking. *J Am Soc Echocardiogr*. (2011) 24:1276–1284. doi: 10.1016/j.echo.2011.08.002
41. Otsu N. A threshold selection method from gray-level histograms. *IEEE Trans Syst Man Cybern*. (1979) 9:62–6. doi: 10.1109/TSMC.1979.4310076
42. de Ruijter J, van Sambeek M, van de Vosse F, Lopata R. Automated 3D geometry segmentation of the healthy and diseased carotid artery in free-hand, probe tracked ultrasound images. *Med Phys*. (2020) 47:1034–47. doi: 10.1002/mp.13960
43. Bellows S, Smith J, Mcguire P, Smith A. Validation of a computerized technique for automatically tracking and measuring the inferior vena cava in ultrasound imagery. *Stud Health Technol Inform*. (2014) 207:183–92. doi: 10.3233/978-1-61499-474-9-183
44. Nakamura K, Tomida M, Ando T, Sen K, Inokuchi R, Kobayashi E, et al. Cardiac variation of inferior vena cava: new concept in the evaluation of intravascular blood volume. *J Med Ultrason*. (2013) 40:205–9. doi: 10.1007/s10396-013-0435-6
45. Karami E, M S Shehata MS, Smith A. Estimation and tracking of AP-diameter of the inferior vena cava in ultrasound images using a novel active circle algorithm. *Comput Biol Med*. (2018) 98:16–25. doi: 10.1016/j.compbiomed.2018.05.001
46. Blaivas M, Blaivas L, Philips G, Merchant R, Levy M, Abbasi A, et al. Development of a deep learning network to classify inferior vena cava collapse to predict fluid responsiveness. *J Ultrasound Med*. (2021) 40:1495–504. doi: 10.1002/jum.15527
47. de Groot PC, Bleeker MW, Hopman MT. Ultrasound: a reproducible method to measure conduit vein compliance. *J Appl Physiol*. (2005) 98:1878–83. doi: 10.1152/japplphysiol.01166.2004
48. Leinan IM, Aamot IL, Stoylen A, Karlsen T, Wisloff U. Upper arm venous compliance and fitness in stable coronary artery disease patients and healthy controls. *Clin Physiol Funct Imaging*. (2017) 37:498–506. doi: 10.1111/cpf.12324
49. Ermini L, Chiarello NE, De Benedictis C, Ferraresi C, Roatta S. Venous pulse wave velocity variation in response to a simulated fluid challenge in healthy subjects. *Biomed Signal Proc Control*. (2021) 63:102177. doi: 10.1016/j.bspc.2020.102177

50. Ermini L, Ferraresi C, De Benedictis C, Roatta S. Objective assessment of venous pulse wave velocity in healthy humans. *Ultrasound Med Biol*. (2020) 46:849–54. doi: 10.1016/j.ultrasmedbio.2019.11.003
51. Tsilimparis N, Abicht JM, Stana J, Konstantinou N, Rantner B, Banafsche R, et al. The munich valsalva implantation technique (MuVIT) for cardiac output reduction during TEVAR: vena cava occlusion with the valsalva maneuver. *J Endovasc Ther*. (2021) 28:7–13. doi: 10.1177/15266028209 61376
52. Pellicori P, Cleland JG, Zhang J, Kallvikbacka-Bennett A, Urbinati A, Shah P, et al. Cardiac dysfunction, congestion and loop diuretics: their relationship to prognosis in heart failure. *Cardiovasc Drugs Ther*. (2016) 30:599–609. doi: 10.1007/s10557-016-6697-7
53. Miller WL, Lobo R, Grill DE, Mullan BP. Diuresis-related weight loss reflects interstitial compartment decongestion with minimal impact on intravascular volume expansion or outcomes in post-acute heart failure: metrics of decongestion and volume status. *J Card Fail*. (2021) 27:445–52. doi: 10.1016/j.cardfail.2020.12.006
54. Pellicori P, Shah P, Cuthbert J, Urbinati A, Zhang J, Kallvikbacka-Bennett A, et al. Prevalence, pattern and clinical relevance of ultrasound indices of congestion in outpatients with heart failure. *Eur J Heart Fail*. (2019) 21:904–16. doi: 10.1002/ejhf.1383
55. Kuo MM, Barodka V, Abraham TP, Steppan J, Shoukas AA, Butlin M, et al. Measuring ascending aortic stiffness in vivo in mice using ultrasound. *J Vis Exp*. (2014) 94:52200. doi: 10.3791/52200
56. Antonini-Canterin F, Pepe A, Strazzanti M, Rivaben D, Nicolosi E, Pagliani L, et al. P1830 Single-beat aortic arch pulse wave velocity by dual-gate simultaneous Doppler technique: a novel method for arterial stiffness evaluation. *Eur Heart J Cardiovasc Imaging*. (2020) 21:jez319.1173. doi: 10.1093/ehjci/jez319.1173

Conflict of Interest: RB was employed by company Chirurgia Generale e Trauma Team GOM Niguarda.

The remaining authors declare that the research was conducted in the absence of any commercial or financial relationships that could be construed as a potential conflict of interest.

Publisher's Note: All claims expressed in this article are solely those of the authors and do not necessarily represent those of their affiliated organizations, or those of the publisher, the editors and the reviewers. Any product that may be evaluated in this article, or claim that may be made by its manufacturer, is not guaranteed or endorsed by the publisher.

Patent

ATTESTATO DI BREVETTO PER INVENZIONE INDUSTRIALE

Il presente brevetto viene concesso per l'invenzione oggetto della domanda:

N. 102019000007803

TITOLARE/I:	• POLITECNICO DI TORINO 38.0% • UNIVERSITA' DEGLI STUDI DI TORINO 62.0%
DOMICILIO:	Meindl Tassilo Bertram Buzzi, Notaro & Antonielli d'Oulx S.r.l. Corso Vittorio Emanuele II, 6 10123 Torino
INVENTORE/I:	• ERMINI LEONARDO • FRANCO WALTER • MAFFIODO DANIELA • DE BENEDICTIS CARLO • FERRARESI CARLO • MESIN LUCA • PASQUERO PAOLO • PORTA MASSIMO • ROATTA SILVESTRO • PERTUSIO RAFFAELE
TITOLO:	APPARATO PER LA MISURAZIONE DELLA VELOCITA' DI UN'ONDA PRESSORIA PROPAGANTESI NEL DISTRETTO VENOSO DI UN INDIVIDUO E PROCEDIMENTO CORRISPONDENTE
CLASSIFICA:	A61B
DATA DEPOSITO:	31/05/2019

Roma, 26/10/2021

Il Dirigente della Divisione VII
Loredana Guglielmetti

DESCRIZIONE dell'invenzione industriale dal titolo:
"Apparato per la misurazione della velocità di un'onda pressoria propagantesi nel distretto venoso di un individuo e procedimento corrispondente"
di: Università degli Studi di Torino, nazionalità italiana, via Verdi 8 – 10124 Torino; Politecnico di Torino, nazionalità italiana, Corso Duca degli Abruzzi 24 – 10129 Torino
Inventori designati: Leonardo ERMINI, Raffaele PERTUSIO, Walter FRANCO, Daniela MAFFIODO, Carlo DE BENEDICTIS, Carlo FERRARESI, Luca MESIN, Paolo PASQUERO, Massimo PORTA, Silvestro ROATTA
Depositata il: 31 maggio 2019

****

TESTO DELLA DESCRIZIONE

Campo tecnico

La descrizione si riferisce a tecniche per misurare la velocità di un'onda di pressione che si propaga nel distretto venoso di un individuo.

Sfondo tecnologico

Un'onda di pressione in un liquido, all'interno di un tubo elastico, si propaga con una velocità che è funzione delle caratteristiche geometriche e meccaniche del tubo elastico (quale può essere un vaso sanguigno) e delle proprietà meccaniche e/o fluidodinamiche del liquido (ad esempio, il sangue).

Tale fenomeno è stato ampiamente studiato in relazione all'analisi della propagazione di onde di pressione nel distretto arterioso, in quanto la velocità di propagazione dell'onda pulsatoria ("pulse wave velocity", PWV) risulta

essere un buon indicatore della rigidità dei vasi (in particolare, delle arterie) e, indirettamente, della pressione arteriosa (che influenza la rigidità vascolare). I valori di questi parametri sono importanti indici di rischio cardiovascolare per l'individuo.

Nel distretto arterioso, questo tipo di misurazione è facilitato dalla naturale presenza di onde di pressione prodotte dall'attività cardiaca (propriamente indicate come onde "pulsatorie") ed è tipicamente basata sulla misura del ritardo con cui tali onde pulsatorie raggiungono le arterie del polso o della caviglia rispetto alla carotide comune, in prossimità dell'arco aortico, dove hanno origine. In tale contesto, i seguenti documenti sono indicativi della tecnica nota:

- "Brachial-Ankle Pulse Wave Velocity: Background, Method, and Clinical Evidence", Munakata et al., Pulse, Vol. 3, No. 3-4, pp. 195-204, 2016, doi: 10.1159/000443740,

- "Assessment of pulse wave velocity", Boutouyrie et al., Artery Research, Vol. 3, No. 1, pp. 3-8, 2009, doi: 10.1016/j.artres.2008.11.002,

- "Aortic Pulse Wave Velocity Improves Cardiovascular Event Prediction", Ben-Shlomo et al., Journal of the American College of Cardiology, Vol. 63, No. 7, pp. 636-646, 2014, doi: 10.1016/j.jacc.2013.09.063,

- US 2 658 505 A, e

- US 6 331 162 B1.

Inoltre, sono noti vari sistemi e prodotti commerciali per la misurazione della PWV arteriosa, quali ad esempio i dispositivi disponibili al pubblico con le denominazioni commerciali VICORDER® di SMT Medical, VasoScreen® di medis, e Complior® di ALAM MEDICAL.

Tali sistemi sfruttano la pulsatilità cardiaca

intrinsecamente presente nelle arterie e risultano quindi essere costruttivamente piuttosto semplici.

Poiché la PWV arteriosa è un indicatore sia della rigidità delle pareti delle arterie, sia della pressione arteriosa, sono stati definiti diversi indici di interesse clinico (carotid-femoral PWV, femoral-ankle PWV, brachial-ankle PWV, ecc.) quali indicatori di rischio cardiovascolare di interesse in varie situazioni patologiche, quali ad esempio: ipertensione, diabete, sindrome metabolica, insufficienza renale cronica, arteriosclerosi, e altre.

Contrariamente alla PWV arteriosa, la velocità di propagazione di un'onda pressoria nel distretto venoso (venous PWV, vPWV) è un parametro poco indagato, oggetto di un numero estremamente limitato di studi scientifici.

In particolare, due documenti in letteratura indagano la vPWV di deboli onde pressorie, generate dall'attività contrattile dell'atrio destro, dal quale si propagano in senso retrogrado nelle grandi vene.

Il primo di tali documenti, "Apparent Pulse Wave Velocity in the Canine Superior Vena Cava", Minten et al., Cardiovascular Research 17:627-632, 1983, descrive uno studio dell'andamento della pulsatilità retrograda dell'atrio destro nella vena cava e nella giugulare, caratterizzandolo tramite diversi parametri, tra cui anche la vPWV. Tale studio è effettuato tramite tecniche dirette e quindi particolarmente invasive.

Il secondo di tali documenti, "Pulse Wave Velocity in Human Veins", Nippa et al., J. of App. Physio., Vol. 30, No. 4, 1971, descrive un metodo di stima del tempo di propagazione di un'onda pressoria nelle vene – anche in questo caso generata in senso retrogrado dalla contrazione

dell'atrio destro - tramite il posizionamento di due sonde eco-Doppler a una distanza nota tra loro.

Gli approcci descritti in Minten et al. e Nippa et al. presentano la difficoltà di riconoscere la debole pulsatilità cardiaca nel distretto venoso rispetto a fattori di disturbo, quali:

- fenomeni di riflessione delle onde pressorie nell'albero vascolare venoso,

- disturbi pressori derivanti dalla pulsatilità cardiaca delle arterie, che sonno anatomicamente localizzate in stretta vicinanza con le vene e ne possono pertanto influenzare la pressione, e

- la profonda modulazione che l'attività respiratoria opera sui volumi e sulle pressioni del comparto venoso.

In un solo studio, condotto su cani anestetizzati, è descritta la generazione artificiale di un'onda pressoria nel distretto venoso operando una compressione rapida di una zona distale di un arto. In tale studio, descritto nel documento "Venous Pulse Wave Propagation Velocity in Hemorrhage", Felix et al., Arch. Surg. Vol. 102, 1971, gli autori hanno stimato la vPWV nei cani anestetizzati per utilizzarla come indicatore di emorragie interne. La tecnica utilizzata consiste nell'applicare una compressione all'arto canino e utilizzare due sonde eco-Doppler per stimare due tempi di passaggio dell'onda pressoria generata da tale compressione. Essendo nota la distanza fra le due sonde eco-Doppler (pari ad alcuni centimetri), è possibile risalire alla vPWV. Tutti i passaggi per effettuare la misura sono stati compiuti manualmente dagli autori dello studio.

Nel campo della stima della vPWV, non sono rilevati documenti brevettuali di rilievo. Gli Inventori hanno

individuato due documenti genericamente pertinenti al campo della stima della pressione venosa centrale, senza però alcun riferimento alla stima della vPWV.

Ad esempio, il documento US 6 432 061 B1 descrive un sistema comprendente un manicotto la cui pressione di gonfiaggio viene fatta aumentare lentamente, e un sensore che misura la pulsatilità cardiaca in un'arteria distale rispetto al manicotto. Quando la pulsatilità misurata cambia in un modo significativo, la pressione di gonfiaggio del manicotto in quel preciso istante rispecchia la pressione venosa locale.

Il documento US 7 118 534 B2 descrive un sistema che utilizza un manicotto in maniera analoga al documento US 6 432 061 B1 precedentemente citato, ovvero per occludere il circolo venoso di un arto. In questo secondo documento, il sensore posizionato distalmente sull'arto è uno *strain gauge* (cioè, un sensore di deformazione) configurato per monitorare l'area della sezione dell'arto nel punto in questione. La misura di pressione venosa centrale viene ricavata al momento dello sgonfiaggio del manicotto, quando la curva di pressione del manicotto raggiunge la massima ripidezza.

Scopo e sintesi

Nonostante l'attività nel campo, sono desiderabili soluzioni migliorate.

Ad esempio, sono desiderabili soluzioni che possono facilitare la misurazione della velocità di propagazione di un'onda pressoria nel distretto venoso (vPWV) di un individuo, in quanto la vPWV può essere un importante indice dello stato emodinamico di un individuo (ad esempio, volemia e pressione venosa), al pari della PWV.

Uno scopo di una o più forme di attuazione è contribuire a fornire tali soluzioni migliorate.

Secondo una o più forme di attuazione, un tale scopo si può conseguire per mezzo di un apparato avente le caratteristiche esposte nelle rivendicazioni che seguono.

Una o più forme di attuazione possono essere relative a un corrispondente procedimento.

Le rivendicazioni sono una parte integrante dell'insegnamento tecnico qui fornito per quanto riguarda le forme di realizzazione.

In varie forme di attuazione, un apparato per la misurazione della velocità di un'onda pressoria propagantesi nel distretto venoso di un individuo comprende:

- un manicotto pneumatico configurato per essere calzato intorno a una estremità di un arto di detto individuo,

- un dispositivo pneumatico configurato per gonfiare detto manicotto pneumatico in modo impulsivo, e

- una unità elettronica di controllo accoppiata a detto dispositivo pneumatico e accoppiabile a un dispositivo di rilevazione, detto dispositivo di rilevazione comprendendo una sonda configurata per rilevare un segnale indicativo di una pressione in una vena prossimale dell'individuo.

In varie forme di attuazione, detta unità elettronica di controllo è configurata per:

- generare un segnale di attivazione di detto dispositivo pneumatico per comandare il gonfiaggio impulsivo di detto manicotto pneumatico a partire da un certo primo istante temporale, e

- rilevare tramite detta sonda detto segnale

indicativo di una pressione in una vena prossimale dell'individuo.

In varie forme di attuazione, detto dispositivo di rilevazione comprende un ecografo Doppler e detta sonda comprende una sonda eco-Doppler, e detto segnale indicativo di una pressione in una vena prossimale dell'individuo è un segnale velocimetrico indicativo della velocità del sangue in detta vena prossimale dell'individuo.

In varie forme di attuazione, detto dispositivo di rilevazione comprende un tonometro, e detto segnale indicativo di una pressione in una vena prossimale dell'individuo è un segnale di pressione rilevato sulla superficie cutanea in corrispondenza di detta vena prossimale dell'individuo.

In varie forme di attuazione, detto dispositivo di rilevazione comprende un accelerometro, e detto segnale indicativo di una pressione in una vena prossimale dell'individuo è un segnale di accelerazione rilevato sulla superficie cutanea in corrispondenza di detta vena prossimale dell'individuo.

In varie forme di attuazione, detto dispositivo di rilevazione comprende uno schermo di visualizzazione ed è configurato per visualizzare detto segnale di attivazione di detto dispositivo pneumatico e detto segnale indicativo di una pressione in una vena prossimale dell'individuo su detto schermo di visualizzazione.

In varie forme di attuazione, detto manicotto pneumatico comprende un sensore di pressione configurato per rilevare un segnale indicativo di una pressione di gonfiaggio di detto manicotto pneumatico.

In varie forme di attuazione, detto dispositivo di rilevazione comprende uno schermo di visualizzazione ed è

configurato per visualizzare detto segnale indicativo di una pressione di gonfiaggio di detto manicotto pneumatico e detto segnale indicativo di una pressione in una vena prossimale dell'individuo su detto schermo di visualizzazione.

In varie forme di attuazione, detto dispositivo di rilevazione è integrato in detta unità elettronica di controllo, e detta unità elettronica di controllo è configurata per:

- determinare un certo secondo istante temporale in cui detto segnale indicativo di una pressione in una vena prossimale dell'individuo comprende un fronte di salita indicativo di un'onda pressoria rilevata, e

- stimare un valore della velocità di detta onda pressoria rilevata in funzione di un intervallo temporale trascorso tra detto primo istante temporale e detto secondo istante temporale, e di una distanza tra detto manicotto pneumatico e detta sonda.

In varie forme di attuazione, detto primo istante temporale corrisponde ad un fronte di salita di detto segnale di attivazione di detto dispositivo pneumatico.

In varie forme di attuazione, detto primo istante temporale corrisponde a un istante in cui detto segnale indicativo di una pressione di gonfiaggio di detto manicotto pneumatico supera una certa soglia.

In varie forme di attuazione, detto dispositivo pneumatico e/o detta unità elettronica di controllo sono configurati per:

- gonfiare detto manicotto pneumatico con una velocità di gonfiaggio compresa tra 300 mmHg/s e 700 mmHg/s, preferibilmente tra 400 mmHg/s e 600 mmHg/s, ancora più preferibilmente tra 450 mmHg/s e 550 mmHg/s;

- completare il gonfiaggio di detto manicotto pneumatico in un tempo massimo compreso tra 100 ms e 300 ms, preferibilmente tra 150 ms e 250 ms, e

- mantenere gonfiato detto manicotto pneumatico per un intervallo temporale compreso tra 0.5 s e 1.5 s, preferibilmente tra 0.8 s e 1.2 s.

In varie forme di attuazione, detto manicotto pneumatico comprende dei mezzi riscaldanti atti a riscaldare detto manicotto pneumatico, preferibilmente a una temperatura compresa tra 37°C e 42°C.

In varie forme di attuazione, l'apparato comprende uno o più sensori configurati per rilevare un segnale indicativo dell'attività respiratoria dell'individuo, e detta unità elettronica di controllo è configurata per:

- rilevare, nel segnale indicativo dell'attività respiratoria dell'individuo, un istante temporale corrispondente alla fine di un atto di espirazione dell'individuo, e

- comandare il gonfiaggio impulsivo di detto manicotto pneumatico a partire da detto istante temporale corrispondente alla fine di un atto di espirazione dell'individuo.

In varie forme di attuazione, detto uno o più sensori configurati per rilevare un segnale indicativo dell'attività respiratoria dell'individuo comprende una fascia estensimetrica configurata per essere posizionata intorno al torace dell'individuo, e detto apparato comprende inoltre un insieme di elettrodi configurati per rilevare un segnale elettrocardiografico dell'individuo.

In varie forme di attuazione, detta unità elettronica di controllo è configurata per:

- rilevare, nel segnale elettrocardiografico

dell'individuo, una prima onda R successiva a detto istante temporale corrispondente alla fine di un atto di espirazione dell'individuo, e

- comandare il gonfiaggio impulsivo di detto manicotto pneumatico come risultato della rilevazione di detta prima onda R.

In varie forme di attuazione, un procedimento per la misurazione della velocità di un'onda pressoria propagantesi nel distretto venoso di un individuo tramite un apparato secondo una forma di attuazione comprende:

- calzare un manicotto pneumatico di detto apparato intorno a una estremità di un arto di detto individuo,

- generare un segnale di attivazione di un dispositivo pneumatico di detto apparato per comandare il gonfiaggio impulsivo del manicotto pneumatico a partire da un certo primo istante temporale, e

- rilevare un segnale indicativo di una pressione in una vena prossimale dell'individuo tramite una sonda di detto apparato.

In varie forme di attuazione, il procedimento comprende configurare una unità elettronica di controllo di detto apparato per:

- determinare un certo secondo istante temporale in cui detto segnale indicativo di una pressione in una vena prossimale dell'individuo comprende un fronte di salita indicativo di un'onda pressoria rilevata, e

- stimare un valore della velocità di detta onda pressoria rilevata in funzione di un intervallo temporale trascorso tra detto primo istante temporale e detto secondo istante temporale, e di una distanza tra detto manicotto pneumatico e detta sonda.

Breve descrizione delle figure

Una o più forme di realizzazione verranno ora descritte, solo a titolo di esempio, facendo riferimento alle figure annesse, in cui:

- la figura 1 è uno schema esemplificativo di un apparato per la misurazione della velocità di propagazione di un'onda pressoria nel distretto venoso (vPWV) secondo una o più forme di realizzazione,

- le figure 2 e 3 sono esemplificative del possibile andamento temporale di segnali in una o più forme di realizzazione, e

- la figura 4 è un grafico esemplificativo di una possibile relazione tra vPWV misurata e pressione venosa.

Descrizione dettagliata

Nella seguente descrizione sono illustrati uno o più dettagli specifici, mirati a fornire una comprensione approfondita di esempi di forme di realizzazione di questa descrizione. Le forme di realizzazione si possono ottenere senza uno o più dei dettagli specifici, o con altri procedimenti, componenti, materiali, ecc. In altri casi, strutture, materiali, o operazioni note non sono illustrate o descritte nel dettaglio in modo che certi aspetti delle forme di realizzazione non saranno resi poco chiari.

Il riferimento a "una forma di realizzazione" nel quadro della presente descrizione è destinato ad indicare che una particolare configurazione, struttura o caratteristica descritta in relazione alla forma di realizzazione è compresa in almeno una forma di realizzazione. Pertanto, una frase quale "in una forma di realizzazione" che può essere presente in uno o più punti della presente descrizione non si riferisce necessariamente

ad un’unica e alla stessa forma di realizzazione.

Inoltre, conformazioni, strutture o caratteristiche particolari possono essere combinate in un modo adatto qualsiasi, in una o più forme di realizzazione.

In tutte le figure qui annesse, parti o elementi simili sono indicati con riferimenti/numeri simili e una descrizione corrispondente non sarà ripetuta per brevità.

I riferimenti qui utilizzati sono forniti meramente per comodità e pertanto non definiscono la portata di protezione o l’ambito delle forme di realizzazione.

La figura 1 è esemplificativa di un apparato 10 per la misurazione della velocità di un’onda pressoria che si propaga nel distretto venoso (vPWV) di un individuo 1 secondo una o più forme di attuazione.

In particolare, l’apparato 10 comprende un sistema pneumatico configurato per generare un’onda di pressione nel distretto venoso dell’individuo 1 (di cui è schematicamente raffigurata una vena 12 nella figura 1, ad esempio, una vena femorale).

Un’onda di pressione può essere generata nel distretto venoso mediante una compressione rapida (impulsiva) dell’estremità di un arto dell’individuo, ad esempio un piede (come esemplificato nella figura 1) o una mano. Nell’apparato 10, tale compressione rapida dell’arto è generata da un manicotto pneumatico 100. Il manicotto pneumatico 100 può comprendere una sacca gonfiabile di forma tubolare da calzare intorno all’estremità dell’arto, collegata a un dispositivo pneumatico 102 controllato da una unità di controllo 104. In particolare, l’unità di controllo 104 è configurata per generare un segnale (impulsivo) di attivazione del dispositivo pneumatico 102 che comanda il gonfiaggio impulsivo del manicotto

pneumatico 100 a partire da un certo istante temporale.

L'unità di controllo 104 è accoppiata a un dispositivo di rilevazione 106 comprendente una sonda 108, ed è configurata per rilevare tramite la sonda 108 un segnale pressorio in corrispondenza di una vena prossimale dell'individuo 1 (ad esempio una vena femorale, come esemplificato nella figura 1, o una vena brachiale).

In una forma di attuazione preferita, il dispositivo di rilevazione 106 e la sonda 108 possono rilevare un segnale pressorio in corrispondenza della vena 12. Ad esempio, il dispositivo di rilevazione 106 può comprendere un tonometro arterioso e/o un accelerometro, o altri dispositivi atti a rilevare la pressione interna di un vaso sanguigno.

In una forma di attuazione alternativa, il dispositivo di rilevazione 106 comprende un ecografo Doppler a ultrasuoni e la sonda 108 comprende una sonda eco-Doppler. L'ecografo Doppler è configurato per rilevare un segnale velocimetrico (cioè, un segnale indicativo della velocità del sangue nella vena in prossimità della sonda 108, ad esempio espressa in cm/s). Le variazioni di tale segnale velocimetrico rilevato (ad esempio, un aumento di velocità) risultano sostanzialmente sincrone con le variazioni di pressione all'interno della vena 12 (ad esempio, un corrispondente aumento di pressione), e quindi possono essere utilizzate per rilevare il passaggio di un'onda pressoria.

In una forma di attuazione preferita, l'ecografo Doppler 106 comprende una macchina eco-Doppler convenzionale, come quelle comunemente disponibili nei reparti ospedalieri, che non presenta alcuna modifica di tipo hardware e/o software. In tale forma di attuazione,

l’unità di controllo 104 può essere collegata alla macchina eco-Doppler convenzionale 106 (ad esempio, tramite una porta di ingresso per segnale elettrocardiografico, normalmente presente nelle macchine eco-Doppler) permettendo di visualizzare, su uno schermo di visualizzazione della macchina eco-Doppler, il segnale *A* (impulsivo) di attivazione del dispositivo pneumatico 102 generato dall’unità di controllo 104 e il segnale velocimetrico *P* (indicativo di un’onda di pressione) rilevato dalla sonda 108 in corrispondenza di una vena prossimale dell’individuo 1, anche unitamente (si veda, ad esempio, la figura 2).

In una forma di attuazione alternativa, l’unità di controllo 104 può essere collegata a una macchina eco-Doppler 106 tramite una porta seriale presente sulla macchina eco-Doppler 106. In tale configurazione, il software (firmware) della macchina eco-Doppler 106 può essere opportunamente modificato per permettere di visualizzare, su uno schermo di visualizzazione della macchina eco-Doppler, il segnale *A* (e il segnale velocimetrico *P*, anche unitamente).

Negli esempi di forme di attuazione sopra descritti, è compito dell’ecografista individuare nel segnale velocimetrico *P* visualizzato a video un eventuale fronte di salita, indicativo di un’onda pressoria rilevata, e misurarne manualmente la latenza (cioè, il ritardo temporale) rispetto al fronte di salita del segnale di attivazione *A* del dispositivo pneumatico 102, anch’esso visualizzato a video, per calcolare la vPWV.

Come esemplificato nelle figure 1 e 2, la vPWV può essere calcolata come rapporto $\Delta x/\Delta t$, dove Δx è la distanza tra la sonda 108 (ad es., una sonda eco-Doppler) e

l’estremità dell’arto che ha subito la compressione impulsiva (cioè, l’arto su cui è calzato il manicotto pneumatico 100), e Δt è l’intervallo di tempo misurato tra il fronte di salita del segnale di attivazione *A* (istante t_1) e il fronte di salita della corrispondente onda pressoria rilevata nel segnale *P* (istante t_2), sia questo un segnale pressorio (quale quello misurato tramite un tonometro) o velocimetrico (quale quello misurato tramite un dispositivo eco-Doppler).

Varie forme di attuazione possono tenere in considerazione il fatto che può verificarsi un leggero ritardo tra il fronte di salita del segnale di attivazione *A* del dispositivo pneumatico 102 e l’effettivo aumento di pressione nel manicotto 100 con conseguente generazione dell’onda pressoria nella vena 12, ad esempio a causa di una fase di transitorio iniziale. Per risolvere tale inconveniente e fornire una maggiore precisione nella misura della vPWV, varie forme di attuazione possono comprendere un sensore di pressione 101 associato al manicotto pneumatico 100. Tale sensore di pressione 101 può fornire all’unità di controllo 104 un segnale *S* indicativo dell’effettiva pressione di gonfiaggio del manicotto 100 (si veda, ad esempio, la figura 3).

In una forma di attuazione, il segnale di pressione *S* rilevato dal sensore 101 viene visualizzato sullo schermo della macchina eco-Doppler (in sostituzione o in aggiunta alla visualizzazione del segnale di attivazione *A*), permettendo all’ecografista di valutare l’intervallo di tempo Δt rispetto all’effettivo istante t_3 di gonfiaggio del manicotto 100 (cioè, $\Delta t = t_2 - t_3$).

In alternativa o in aggiunta, il segnale di pressione *S* rilevato dal sensore 101 può essere elaborato dall’unità

di controllo 104 al fine di generare un ulteriore segnale di sincronismo *T* utile alla valutazione dell'intervallo di tempo Δt. Per esempio, l'unità di controllo 104 può essere configurata per rilevare un aumento di pressione nel segnale *S* superiore a una certa soglia (ad es., 5 mmHg), e generare tale segnale di sincronismo *T* avente un fronte di salita in corrispondenza di tale superamento della soglia (istante t_4 in figura 3), tale per cui è possibile misurare $\Delta t = t_2 - t_4$.

Una ulteriore forma di realizzazione può risolvere l'inconveniente del ritardo tra il fronte di salita del segnale di attivazione *A* e l'effettiva generazione dell'onda pressoria nella vena 12 prevedendo l'utilizzo di una sonda aggiuntiva rispetto alla sonda 108, anch'essa connessa al dispositivo di rilevazione 106. La sonda aggiuntiva può essere localizzata in corrispondenza della vena 12 in prossimità del manicotto pneumatico 100, e l'ecografista può determinare l'intervallo di tempo Δt assumendo come istante iniziale t_1 un istante corrispondente a un fronte di salita visualizzato nel segnale pressorio rilevato dalla sonda aggiuntiva (e adottando, come misura della lunghezza Δx, la distanza tra le due sonde).

Il fatto che il sistema secondo la presente invenzione possa essere implementato su macchine eco-Doppler convenzionali disponibili sul mercato lo rende particolarmente vantaggioso in ambiente ospedaliero, non solo per l'abbondanza di ecografi Doppler tipicamente già presenti nei reparti ospedalieri (dove pertanto può rappresentare una soluzione di basso costo), ma anche per la complessità minima dell'operazione richiesta all'operatore (cioè, l'ecografista) per effettuare la

misura. Ne deriva pertanto anche il vantaggio di ridurre le possibili fonti di errore rispetto alle metodologie note.

In un'altra forma di attuazione preferita, l'ecografo Doppler 106 può comprendere una macchina eco-Doppler ad-hoc o può costituire, insieme all'unità di controllo 104, un unico dispositivo hardware (ad esempio, l'ecografo Doppler 106 può essere integrato nell'unità di controllo 104).

In tale forma di attuazione preferita, l'unità di controllo 104 può svolgere anche funzioni di elaborazione del segnale *P* (pressorio o velocimetrico) rilevato dalla sonda 108. In particolare, l'unità di controllo (e di elaborazione) 104 può essere configurata per:

- rilevare all'interno del segnale (velocimetrico) *P*, tramite un certo algoritmo, un eventuale fronte di salita e determinare un certo istante temporale t_2 in cui tale fronte di salita ha luogo, e

- stimare un valore della vPWV in funzione dell'intervallo temporale Δt trascorso tra l'istante temporale t_1 (o t_4) in cui viene gonfiato impulsivamente il manicotto pneumatico 100 e l'istante temporale t_2, e della distanza Δx tra il manicotto pneumatico 100 e la sonda Doppler 108.

In tale forma di attuazione, pertanto, l'apparato di misurazione 10 può determinare una stima della vPWV richiedendo all'operatore solamente la misurazione della distanza Δx tra il manicotto pneumatico 100 e la sonda 108, da fornire come dato di input all'unità di controllo 104, risultando vantaggiosamente in una più rapida effettuazione della misura e in un margine d'errore ancora più ridotto.

In particolare, un algoritmo suscettibile di rilevare un fronte di salita nel segnale (velocimetrico) *P* può comprendere individuare il massimo della derivata seconda

del segnale *P*. In alternativa, è possibile utilizzare il metodo delle due linee tangenti descritto nel documento Boutouyrie et al., citato precedentemente. Ancora in alternativa, è possibile impostare un valore di soglia del segnale *P* (in valore assoluto, o in percentuale sul picco massimo rispetto alla *baseline* di riferimento), il cui superamento è fatto coincidere con l'istante t_2.

Nel contesto della presente descrizione, un gonfiaggio "impulsivo" del manicotto pneumatico 100 deve essere inteso come un gonfiaggio sufficientemente rapido da provocare la generazione di un'onda di pressione nel distretto venoso dell'arto cui viene applicato lo stimolo compressivo.

Preferibilmente, la velocità di incremento della pressione nel manicotto 100 è pari o superiore a 500 mmHg/s. Preferibilmente, la pressione massima raggiunta dal manicotto pneumatico 100 è pari a circa 100 mmHg (ottenibile preferibilmente in un tempo di gonfiaggio di circa 200 ms). Tale pressione massima può essere mantenuta per un periodo di circa 1 secondo.

In varie forme di attuazione, il manicotto pneumatico 100 può vantaggiosamente comprendere dei mezzi riscaldanti (ad esempio, delle resistenze alimentate elettricamente) per riscaldare il manicotto stesso, preferibilmente a una temperatura compresa fra 37°C e 42°C. In tale modo, il manicotto può produrre un riscaldamento dei tessuti dell'arto su cui è calzato, al fine di migliorarne la perfusione sanguigna e quindi il volume di sangue spostato dalla compressione applicata, risultando così in un segnale *P* più facilmente rilevabile dalla sonda 108.

In varie forme di attuazione, l'unità di controllo 104 può inoltre essere configurata per sincronizzare lo stimolo di compressione dell'estremità dell'arto (cioè, il segnale

di attivazione *A*) e la misura della vPWV con l'attività respiratoria e/o il battito cardiaco dell'individuo. Tale sincronizzazione può facilitare l'ottenimento di una maggiore ripetibilità e una maggiore sensibilità della misurazione della vPWV, in quanto l'attività respiratoria e il battito cardiaco possono modulare il flusso venoso e quindi inserire un fattore di variabilità nella misura se non opportunamente considerati.

Ad esempio, in una forma di attuazione preferita l'apparato 10 comprende uno o più sensori atti a rilevare l'attività respiratoria dell'individuo 1. Una fascia estensimetrica 110 può essere posizionata intorno al torace dell'individuo 1 per monitorarne l'attività respiratoria tramite analisi di un corrispondente segnale rilevato *B*. In tale caso, l'unità di controllo 104 è configurata per rilevare un istante temporale t_e corrispondente alla fine di un atto di espirazione dell'individuo 1, e innescare la compressione del manicotto 100 (cioè, innescare il segnale di attivazione *A*) in corrispondenza di tale istante temporale t_e.

In aggiunta o in alternativa, varie forme di attuazione preferite possono permettere di sincronizzare lo stimolo di compressione dell'estremità dell'arto con l'attività cardiaca dell'individuo 1. Ad esempio, un insieme di elettrodi 112 (ad esempio, 3 elettrodi) possono essere utilizzati per la rilevazione dell'attività elettrocardiaca (segnale *ECG*) dell'individuo 1 (si veda ancora la figura 3). In tale caso, l'unità di controllo 104 è configurata per rilevare, nel segnale elettrocardiografico *ECG* fornito dagli elettrodi 112, una prima onda R successiva all'istante temporale t_e, e innescare la compressione del manicotto 100 (cioè,

innescare il segnale di attivazione *A*) come risultato della rilevazione di tale prima onda R.

In varie forme di attuazione, l'istante temporale t_e di fine espirazione può essere identificato a 1.2 s da un picco inspiratorio rilevato, che corrisponde al massimo del segnale *B* fornito dalla fascia estensimetrica 110 (istante t_p in figura 3: t_e-t_p = 1.2 s).

In varie forme di attuazione, l'onda R può essere riconosciuta nel segnale *ECG* in corrispondenza del superamento di una soglia adattiva, ad esempio, tale soglia corrispondendo al 70% del picco R (massimo del segnale ECG) rilevato nei 2 secondi precedenti.

Risultati preliminari raccolti con una versione prototipale di un apparato secondo la presente invenzione indicano che la vPWV è influenzata da variazioni di pressione e volume ematico nel comparto venoso. Ad esempio, in dieci soggetti sani, in cui la pressione venosa negli arti inferiori è stata modulata attraverso alterazioni posturali del tronco, gli Inventori hanno osservato che la misura di vPWV è caratterizzata da una buona ripetibilità e da una relazione lineare con la pressione venosa (stimata sulla base dei gradienti idrostatici alterati dalla postura) in un'ampia gamma di valori, confermando le indicazioni raccolte dai primi studi sulla vPWV.

Ad esempio, la figura 4 è un grafico esemplificativo di una possibile relazione tra vPWV misurata (asse delle ordinate, m/s) e pressione venosa (asse delle ascisse, mmHg).

Parametri clinici come lo stato volemico e la pressione venosa centrale, di cui la vPWV può essere indicativa, sono estremamente utili per l'inquadramento clinico del paziente e per il monitoraggio delle terapie di

idratazione in diversi ambiti della medicina: dal pronto soccorso, alla medicina interna, alla dialisi, all'anestesia e rianimazione. In tutti questi contesti, sono particolarmente apprezzate le valutazioni non invasive, visti i rischi e le complicazioni associate all'inserimento di cateteri venosi centrali.

In particolare, la valutazione dello stato volemico con metodiche non invasive rappresenta un elemento cruciale nella definizione delle condizioni cliniche in circa il 50% dei pazienti ricoverati nei dipartimenti di medicina interna. Questa valutazione può risultare particolarmente difficoltosa nei pazienti complessi, con pluri-patologie o fragili, per la presenza di fattori interferenti con la pressione venosa o con il riempimento venoso. In questi casi la misurazione della vPWV consentirebbe di superare i limiti di altre metodiche non invasive quali la misurazione delle variazioni della vena cava inferiore, che risente della coesistenza di patologie respiratorie croniche (bronco pneumopatia cronica ostruttiva, interstiziopatie, fibrosi polmonare) oppure patologie addominali (cirrosi epatica scompensata, patologie acute e croniche intestinali).

La misurazione della vPWV mediante un apparato secondo la presente invenzione (con un approccio periferico/distale) migliora anche l'accessibilità, oltre a minimizzare la necessità di collaborazione richiesta al paziente. Tali caratteristiche risultano di interesse in molte condizioni quali il trauma, l'allettamento acuto o cronico, la scarsa collaborazione dovuta a vasculopatia cerebrale e/o demenza, eccetera.

Varie forme di attuazione possono trovare applicazione nell'ambito della ricerca pre-clinica e clinica che possa

identificare le caratteristiche della vPWV in relazione a parametri di interesse quali la rigidità vascolare, la pressione venosa, lo stato volemico.

Varie forme di attuazione possono fornire uno strumento per un'indicazione oggettiva, non invasiva e di rapida rilevazione dello stato di salute del distretto venoso e un'indicazione sullo stato volemico del paziente. Ad esempio, semplicità e rapidità di utilizzo permettono di impiegare una o più forme di attuazione per misurare e monitorare anche le variazioni dello stato volemico in corso di trattamento di espansione o riduzione della volemia, ad esempio per valutare l'adeguatezza e l'efficacia terapeutica.

In aggiunta, una o più forme di attuazione possono facilitare lo studio dello stato volemico in presenza di patologie respiratore cardiologiche e/o addominali, acute e/o croniche, che interferiscono con il ritorno venoso stesso. Si tratta di patologie frequenti nella popolazione, specie in quella anziana che viene osservata durante un ricovero ospedaliero, ed in particolare:

- patologie respiratorie croniche (BPCO) associate a insufficienza respiratoria, ipertensione polmonare, trombo embolia polmonare;

- patologie cardiovascolari e ischemiche con insufficienza cardiaca, pericardite costrittiva, tamponamento cardiaco; valvulopatie mitraliche e aortiche;

- cirrosi epatica in fase di scompenso ascitico, malattia ischemica intestinale, malattia sub occlusiva.

In questi casi, la possibilità di discriminare e di fornire una stima oggettiva della rigidità vascolare venosa tramite misurazione della vPWV può essere utile per una diagnosi più accurata e per una adeguata gestione del

trattamento.

Senza pregiudizio per i principi sottostanti, i dettagli e le forme di realizzazione possono variare anche notevolmente, rispetto a quanto descritto a titolo esclusivamente esemplificativo, senza discostarsi dall'ambito di protezione.

L'ambito di protezione è definito dalle rivendicazioni allegate.

RIVENDICAZIONI

1. Apparato (10) per la misurazione della velocità di un'onda pressoria propagantesi nel distretto venoso di un individuo (1), comprendente:

- un manicotto pneumatico (100) configurato per essere calzato intorno a una estremità di un arto di detto individuo (1),

- un dispositivo pneumatico (102) configurato per gonfiare detto manicotto pneumatico (100) in modo impulsivo, e

- una unità elettronica di controllo (104) accoppiata a detto dispositivo pneumatico (102) e accoppiabile a un dispositivo di rilevazione (106), detto dispositivo di rilevazione (106) comprendendo una sonda (108) configurata per rilevare un segnale (*P*) indicativo di una pressione in una vena prossimale (12) dell'individuo (1), detta unità elettronica di controllo (104) essendo configurata per:

  - generare un segnale di attivazione (*A*) di detto dispositivo pneumatico (102) per comandare il gonfiaggio impulsivo di detto manicotto pneumatico (100) a partire da un certo primo istante temporale (t_1, t_3, t_4), e

  - rilevare tramite detta sonda (108) detto segnale (*P*) indicativo di una pressione in una vena prossimale (12) dell'individuo (1).

2. Apparato (10) secondo la rivendicazione 1, in cui:

- detto dispositivo di rilevazione (106) comprende un ecografo Doppler e detta sonda (108) comprende una sonda eco-Doppler, e detto segnale (*P*) indicativo di una pressione in una vena prossimale (12) dell'individuo (1) è

un segnale velocimetrico indicativo della velocità del sangue in detta vena prossimale (12) dell'individuo (1); oppure

- detto dispositivo di rilevazione (106) comprende un tonometro, e detto segnale (*P*) indicativo di una pressione in una vena prossimale (12) dell'individuo (1) è un segnale di pressione rilevato sulla superficie cutanea in corrispondenza di detta vena prossimale (12) dell'individuo (1); oppure

- detto dispositivo di rilevazione (106) comprende un accelerometro, e detto segnale (*P*) indicativo di una pressione in una vena prossimale (12) dell'individuo (1) è un segnale di accelerazione rilevato sulla superficie cutanea in corrispondenza di detta vena prossimale (12) dell'individuo (1).

3. Apparato (10) secondo la rivendicazione 1 o la rivendicazione 2, in cui detto dispositivo di rilevazione (106) comprende uno schermo di visualizzazione ed è configurato per visualizzare detto segnale di attivazione (*A*) di detto dispositivo pneumatico (102) e detto segnale (*P*) indicativo di una pressione in una vena prossimale (12) dell'individuo (1) su detto schermo di visualizzazione.

4. Apparato (10) secondo una qualsiasi delle rivendicazioni precedenti, in cui detto manicotto pneumatico (100) comprende un sensore di pressione (101) configurato per rilevare un segnale indicativo di una pressione di gonfiaggio (*S*) di detto manicotto pneumatico (100).

5. Apparato (10) secondo la rivendicazione 4, in cui

detto dispositivo di rilevazione (106) comprende uno schermo di visualizzazione ed è configurato per visualizzare detto segnale indicativo di una pressione di gonfiaggio (*S*) di detto manicotto pneumatico (100) e detto segnale (*P*) indicativo di una pressione in una vena prossimale (12) dell'individuo (1) su detto schermo di visualizzazione.

6. Apparato (10) secondo una qualsiasi delle rivendicazioni precedenti, in cui detto dispositivo di rilevazione (106) è integrato in detta unità elettronica di controllo (104), e detta unità elettronica di controllo (104) è configurata per:

- determinare un certo secondo istante temporale (t_2) in cui detto segnale (*P*) indicativo di una pressione in una vena prossimale (12) dell'individuo (1) comprende un fronte di salita indicativo di un'onda pressoria rilevata, e
- stimare un valore della velocità di detta onda pressoria rilevata in funzione di un intervallo temporale (Δt) trascorso tra detto primo istante temporale (t_1, t_4) e detto secondo istante temporale (t_2), e di una distanza (Δx) tra detto manicotto pneumatico (100) e detta sonda (108).

7. Apparato (10) secondo la rivendicazione 6, in cui detto primo istante temporale corrisponde ad un fronte di salita (t_1) di detto segnale di attivazione (*A*) di detto dispositivo pneumatico (102).

8. Apparato (10) secondo la rivendicazione 4 e la rivendicazione 6, in cui detto primo istante temporale corrisponde a un istante (t_4) in cui detto segnale

indicativo di una pressione di gonfiaggio (*S*) di detto manicotto pneumatico (100) supera una certa soglia.

9. Apparato (10) secondo una qualsiasi delle rivendicazioni precedenti, in cui detto dispositivo pneumatico (102) e/o detta unità elettronica di controllo (104) sono configurati per:

- gonfiare detto manicotto pneumatico (100) con una velocità di gonfiaggio compresa tra 300 mmHg/s e 700 mmHg/s, preferibilmente tra 400 mmHg/s e 600 mmHg/s, ancora più preferibilmente tra 450 mmHg/s e 550 mmHg/s;
- completare il gonfiaggio di detto manicotto pneumatico (100) in un tempo massimo compreso tra 100 ms e 300 ms, preferibilmente tra 150 ms e 250 ms; e
- mantenere gonfiato detto manicotto pneumatico (100) per un intervallo temporale compreso tra 0.5 s e 1.5 s, preferibilmente tra 0.8 s e 1.2 s.

10. Apparato (10) secondo una qualsiasi delle rivendicazioni precedenti, in cui detto manicotto pneumatico (100) comprende dei mezzi riscaldanti atti a riscaldare detto manicotto pneumatico (100), preferibilmente a una temperatura compresa tra 37°C e 42°C.

11. Apparato (10) secondo una qualsiasi delle rivendicazioni precedenti, comprendente almeno un sensore (110) configurato per rilevare un segnale (*B*) indicativo dell'attività respiratoria dell'individuo (1), in cui detta unità elettronica di controllo (104) è configurata per:

- rilevare, nel segnale (*B*) indicativo dell'attività respiratoria dell'individuo (1), un istante temporale (t_e) corrispondente alla fine di un atto di espirazione

dell'individuo (1), e

- comandare il gonfiaggio impulsivo di detto manicotto pneumatico (100) a partire da detto istante temporale (t_e) corrispondente alla fine di un atto di espirazione dell'individuo (1).

12. Apparato (10) secondo la rivendicazione 11, in cui detto almeno un sensore (110) configurato per rilevare un segnale (*B*) indicativo dell'attività respiratoria dell'individuo (1) comprende una fascia estensimetrica (110) configurata per essere posizionata intorno al torace dell'individuo (1), detto apparato comprendendo inoltre un insieme di elettrodi (112) configurati per rilevare un segnale elettrocardiografico (*ECG*) dell'individuo (1),

in cui detta unità elettronica di controllo (104) è configurata per:

- rilevare, nel segnale elettrocardiografico (*ECG*) dell'individuo (1), una prima onda R successiva a detto istante temporale (t_e) corrispondente alla fine di un atto di espirazione dell'individuo (1), e

- comandare il gonfiaggio impulsivo di detto manicotto pneumatico (100) come risultato della rilevazione di detta prima onda R.

13. Procedimento per la misurazione della velocità di un'onda pressoria propagantesi nel distretto venoso di un individuo (1) tramite un apparato (10) secondo una qualsiasi delle rivendicazioni 1 a 12, in cui detto procedimento comprende:

- calzare detto manicotto pneumatico (100) di detto apparato (10) intorno a una estremità di un arto di detto individuo (1),

- generare un segnale di attivazione (*A*) di detto dispositivo pneumatico (102) di detto apparato (10) per comandare il gonfiaggio impulsivo del manicotto pneumatico (100) a partire da un certo primo istante temporale (t_1, t_3, t_4), e

- rilevare un segnale (*P*) indicativo di una pressione in una vena prossimale (12) dell'individuo (1) tramite detta sonda (108) di detto apparato (10).

14. Procedimento secondo la rivendicazione 13, comprendente configurare detta unità elettronica di controllo (104) di detto apparato (10) per:

- determinare un certo secondo istante temporale (t_2) in cui detto segnale (*P*) indicativo di una pressione in una vena prossimale (12) dell'individuo (1) comprende un fronte di salita indicativo di un'onda pressoria rilevata, e

- stimare un valore della velocità di detta onda pressoria rilevata in funzione di un intervallo temporale (Δt) trascorso tra detto primo istante temporale (t_1, t_4) e detto secondo istante temporale (t_2), e di una distanza (Δx) tra detto manicotto pneumatico (100) e detta sonda (108).

RIASSUNTO

E’ descritto un apparato (10) per la misurazione della velocità di un’onda pressoria che si propaga nel distretto venoso di un individuo (1). L’apparato comprende:

- un manicotto pneumatico (100) configurato per essere calzato intorno a una estremità di un arto di detto individuo (1),

- un dispositivo pneumatico (102) configurato per gonfiare detto manicotto pneumatico (100) in modo impulsivo, e

- una unità elettronica di controllo (104) accoppiata a detto dispositivo pneumatico (102) e accoppiabile a un dispositivo di rilevazione (106), detto dispositivo di rilevazione (106) comprendendo una sonda (108) configurata per rilevare un segnale indicativo di una pressione in una vena prossimale (12) dell’individuo (1).

L’unità elettronica di controllo (104) è configurata per:

- generare un segnale di attivazione di detto dispositivo pneumatico (102) per comandare il gonfiaggio impulsivo di detto manicotto pneumatico (100) a partire da un certo primo istante temporale, e

- rilevare tramite detta sonda (108) detto segnale indicativo di una pressione in una vena prossimale (12) dell’individuo (1).

(Figura 1)

FIG. 1

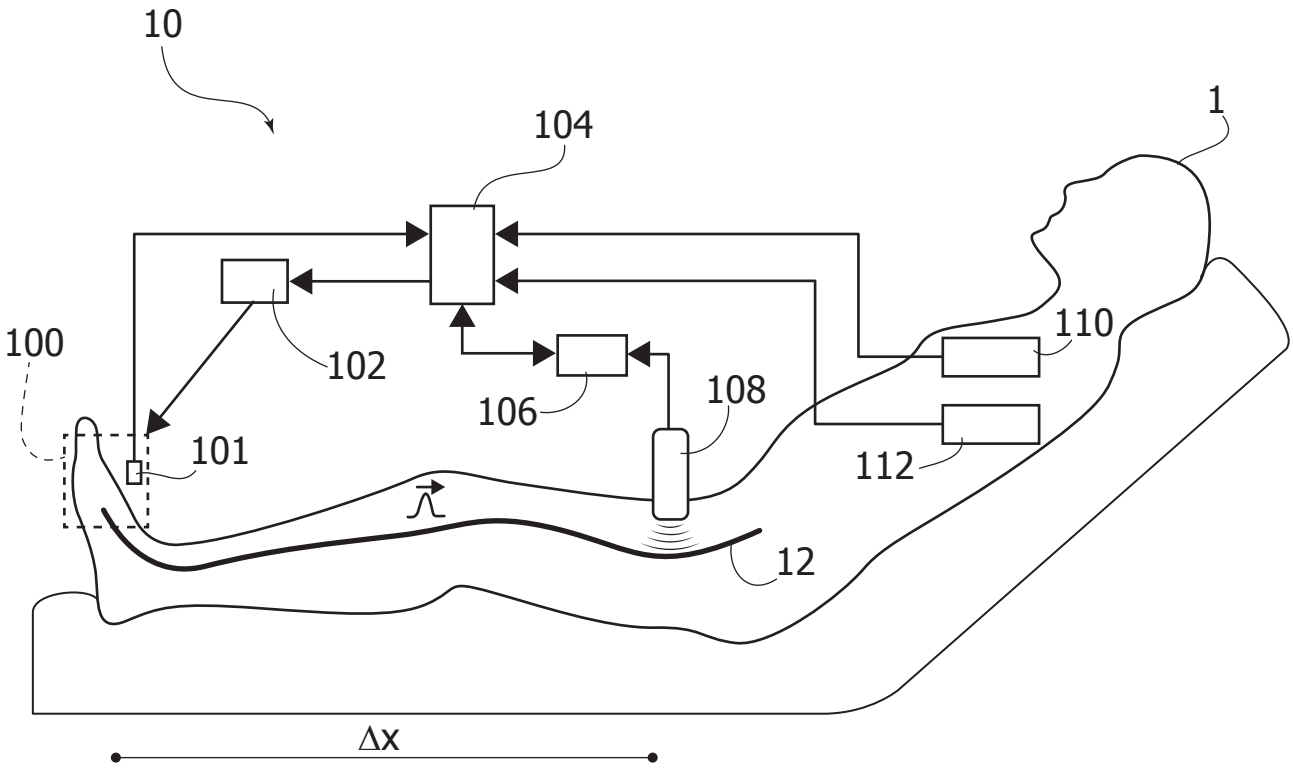

FIG. 2

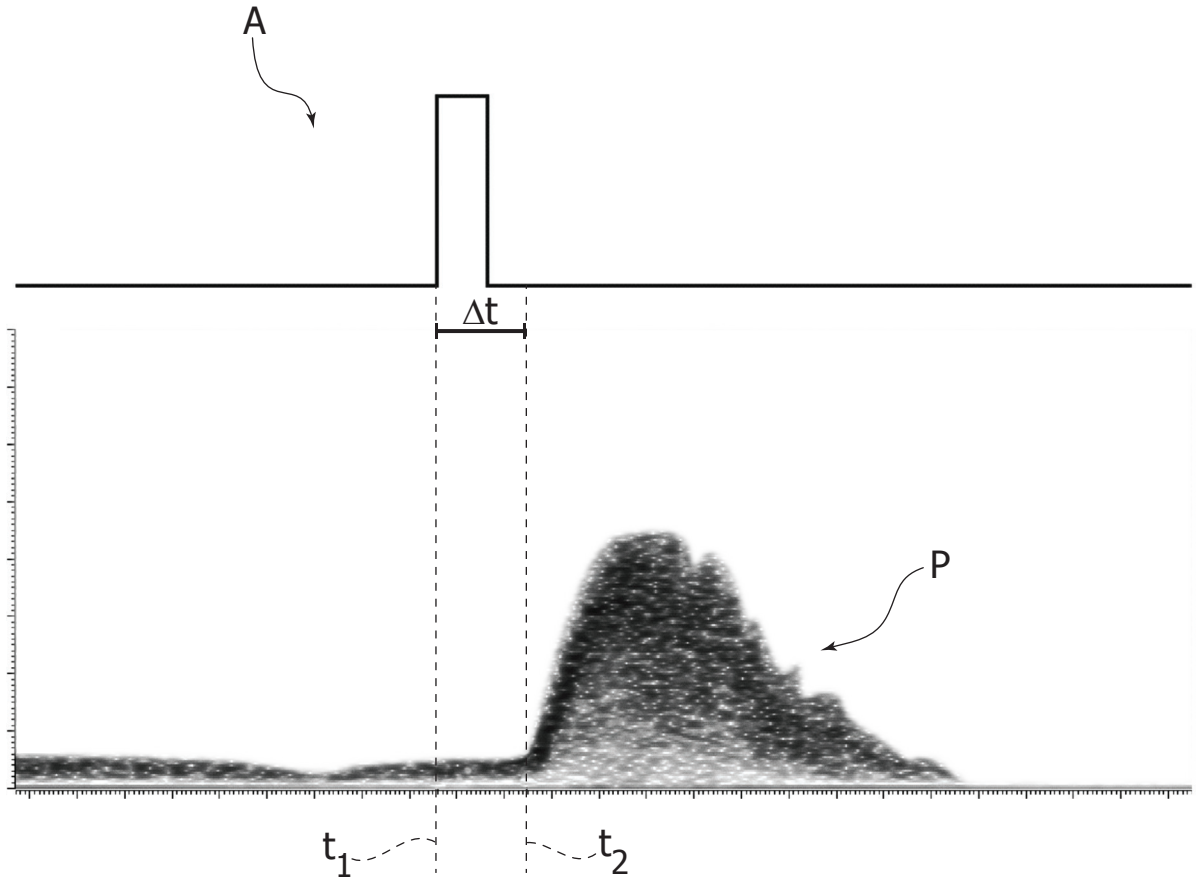

FIG. 3

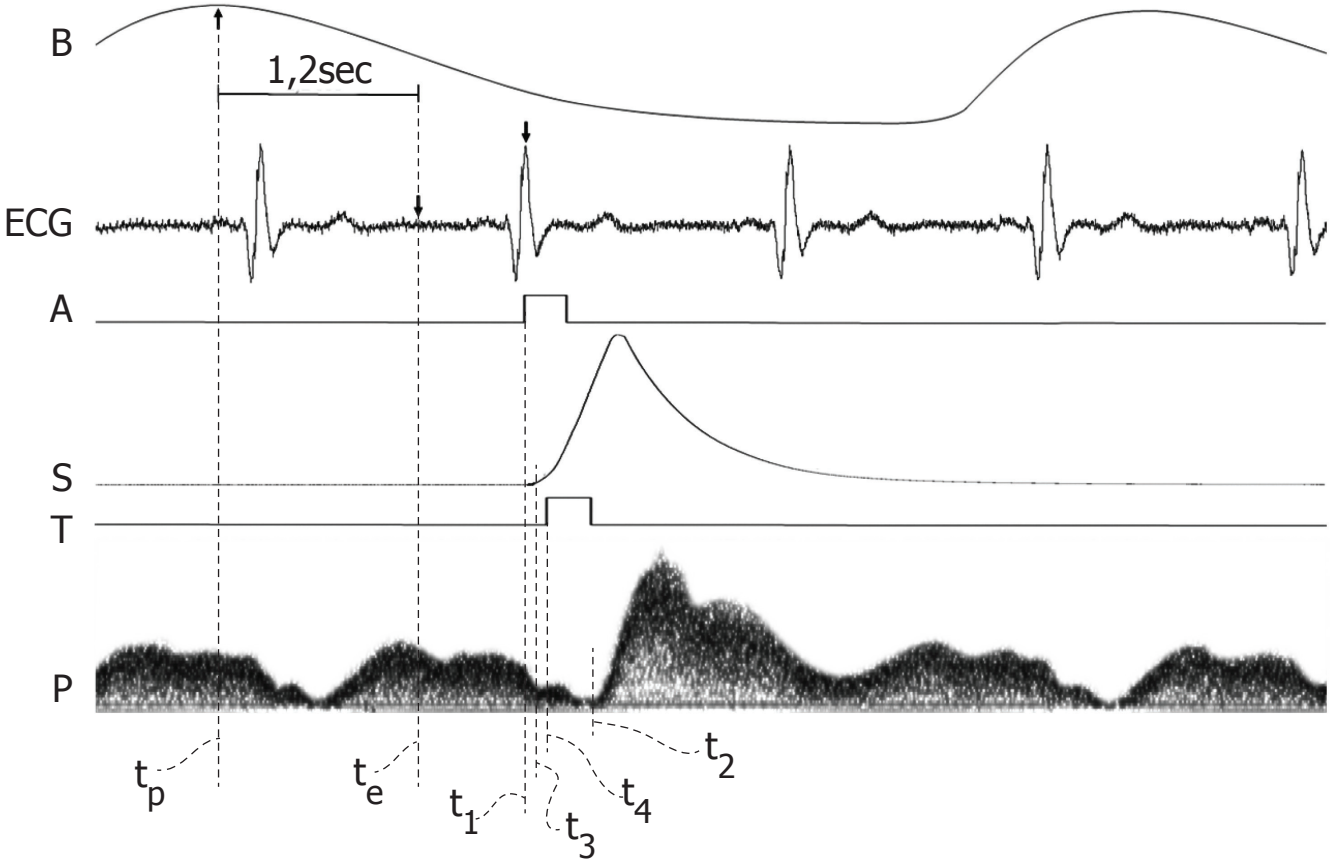
B
1,2sec
ECG
A
S
T
P
t_p
t_e
t_1
t_3
t_4
t_2

FIG. 4

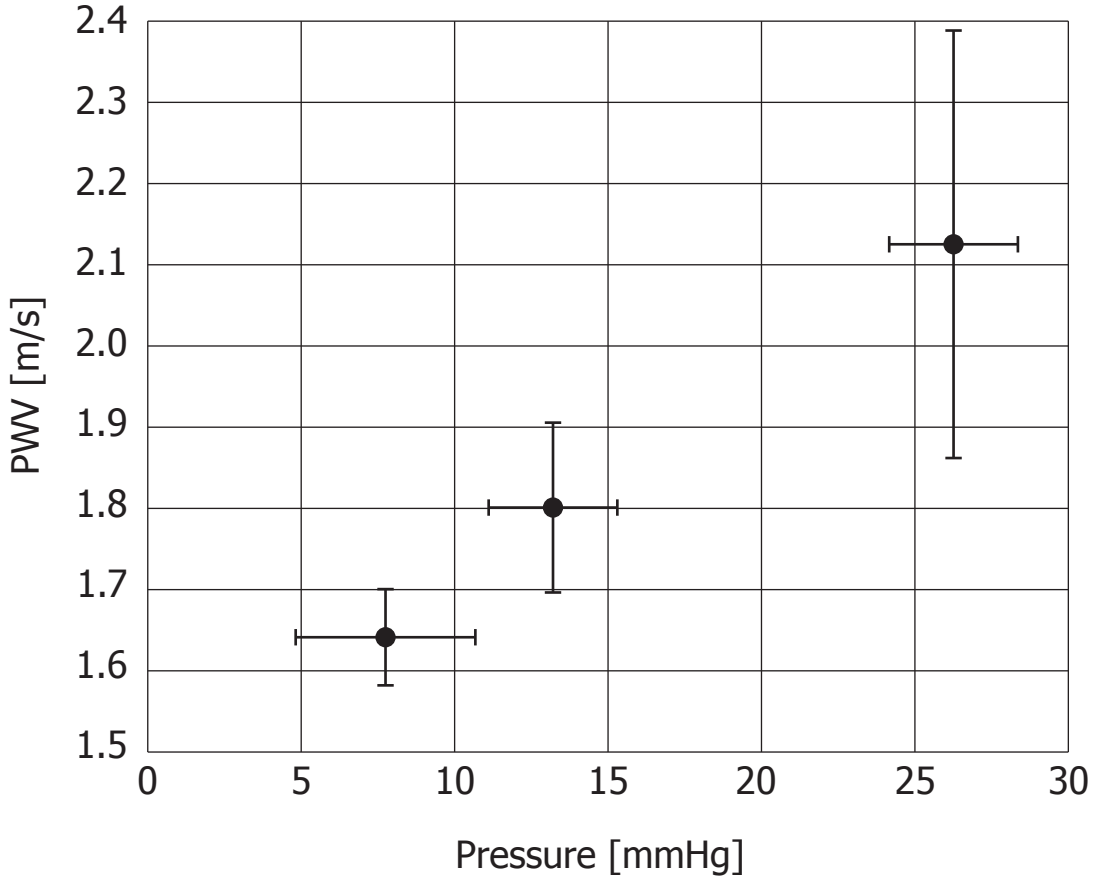
PWV [m/s]
2.4
2.3
2.2
2.1
2.0
1.9
1.8
1.7
1.6
1.5
0
5
10
15
20
25
30
Pressure [mmHg]

CLAIMS

1. Apparatus (10) for measuring the speed of a pressure wave propagating in the venous district of an individual (1), comprising:

- a pneumatic cuff (100) configured for being applied at an extremity of a limb of said individual (1),
- a pneumatic device (102) configured for inflating said pneumatic cuff (100) abruptly, and
- an electric control unit (104) coupled to said pneumatic device (102) and couplable to a sensing device (106), said sensing device (106) comprising a probe (108) configured for sensing a signal (*P*) indicative of pressure in a proximal vein (12) of the individual (1), said electric control unit (104) being configured for:
    - generating an activation signal (*A*) of said pneumatic device (102) for driving abrupt inflation of said pneumatic cuff (100) starting from a certain first time instant (t_1, t_3, t_4), and
    - sensing via said probe (108) said signal (*P*) indicative of pressure in a proximal vein (12) of the individual (1).

2. The apparatus (10) of claim 1, wherein:

- said sensing device (106) comprises a Doppler ecograph and said probe (108) comprises an echo-Doppler probe, and said signal (*P*) indicative of pressure in a proximal vein (12) of the individual (1) is a velocimetry signal indicative of the speed of blood in said proximal vein (12) of the individual (1); or
- said sensing device (106) comprises a tonometer, and said signal (*P*) indicative of pressure in a proximal vein

(12) of the individual (1) is a pressure signal sensed at the surface of the skin at said proximal vein (12) of the individual (1); or

- said sensing device (106) comprises an accelerometer, and said signal (*P*) indicative of pressure in a proximal vein (12) of the individual (1) is an acceleration signal sensed at the surface of the skin at said proximal vein (12) of the individual (1).

3. The apparatus (10) of claim 1 or claim 2, wherein said sensing device (106) comprises a display screen and is configured for displaying said activation signal (*A*) of said pneumatic device (102) and said signal (*P*) indicative of pressure in a proximal vein (12) of the individual (1) on said display screen.

4. The apparatus (10) of any of the previous claims, wherein said pneumatic cuff (100) comprises a pressure sensor (101) configured for sensing a signal indicative of an inflation pressure (*S*) of said pneumatic cuff (100).

5. The apparatus (10) of claim 4, wherein said sensing device (106) comprises a display screen and is configured for displaying said signal indicative of an inflation pressure (*S*) of said pneumatic cuff (100) and said signal (*P*) indicative of pressure in a proximal vein (12) of the individual (1) at said display screen.

6. The apparatus (10) of any of the previous claims, wherein said sensing device (106) is integrated in said electronic control unit (104), and said electronic control unit (104) is configured for:

- determining a certain second time instant (t_2) wherein said signal (*P*) indicative of pressure in a proximal vein (12) of the individual (1) comprises a rising edge indicative of a pressure wave sensed, and

- computing a value of the speed of said pressure wave sensed as a function of a time interval (Δt) elapsed between said first time instant (t_1, t_4) and said second time instant (t_2), and of a distance (Δx) between said pneumatic cuff (100) and said probe (108).

7. The apparatus (10) of claim 6, wherein said first time instant corresponds to a rising edge (t_1) of said activation signal (*A*) of said pneumatic device (102).

8. The apparatus (10) of claims 4 and 6, wherein said first time instant corresponds to a time instant (t_4) wherein said signal indicative of an inflation pressure (*S*) of said pneumatic cuff (100) exceeds a certain threshold.

9. The apparatus (10) of any of the previous claims, wherein said pneumatic device (102) and/or said electronic control unit (104) are configured for:

- inflating said pneumatic cuff (100) at an inflation speed comprised between 300 mmHg/s and 700 mmHg/s, preferably between 400 mmHg/s and 600 mmHg/s, more preferably between 450 mmHg/s and 550 mmHg/s;

- completing inflation of said pneumatic cuff (100) in a maximum time comprised between 100 ms and 300 ms, preferably between 150 ms and 250 ms; and

- keeping inflated said pneumatic cuff (100) for a time interval comprised between 0.5 s and 1.5 s, preferably between 0.8 s and 1.2 s.

10. The apparatus (10) of any of the previous claims, wherein said pneumatic cuff (100) comprises heating means configured for heating said pneumatic cuff (100), preferably at a temperature comprised between 37°C and 42°C.

11. The apparatus (10) of any of the previous claims, comprising at least one sensor (110) configured for sensing a signal (*B*) indicative of respiratory activity of the individual (1), wherein said electronic control unit (104) is configured for:

- detecting, in the signal (*B*) indicative of respiratory activity of the individual (1), a time instant (t_e) corresponding to the end of an exhalation act of the individual (1), and
- driving abrupt inflation of said pneumatic cuff (100) starting from said time instant (t_e) corresponding to the end of an exhalation act of the individual (1).

12. The apparatus (10) of claim 11, wherein said at least one sensor (110) configured for sensing a signal (*B*) indicative of respiratory activity of the individual (1) comprises an extensometric band (110) configured to be applied around the chest of the individual (1), said apparatus further comprising a set of electrodes (112) configured for sensing an electrocardiographic signal (*ECG*) of the individual (1),

wherein said electronic control unit (104) is configured for:

- detecting, in said electrocardiographic signal (*ECG*) of the individual (1), a first "R wave" following said time

instant (t_e) corresponding to the end of an exhalation act of the individual (1), and

- driving abrupt inflation of said pneumatic cuff (100) as a result of said first "R wave" being detected.

13. A method of measuring the speed of a pressure wave propagating in the venous district of an individual (1) by means of an apparatus (10) according to any of claim 1 to 12, the method comprising:

- applying said pneumatic cuff (100) of said apparatus (10) around an extremity of a limb of said individual (1),

- generating an activation signal (*A*) of said pneumatic device (102) of said apparatus (10) for driving abrupt inflation of said pneumatic cuff (100) starting from a certain first time instant (t_1, t_3, t_4), and

- sensing a signal (*P*) indicative of pressure in a proximal vein (12) of the individual (1) via said probe (108) of said apparatus (10).

14. The method of claim 13, comprising configuring said electronic control unit (104) of said apparatus (10) for:

- determining a certain second time instant (t_2) wherein said signal (*P*) indicative of pressure in a proximal vein (12) of the individual (1) comprises a rising edge indicative of a pressure wave sensed, and

- computing a value of the speed of said pressure wave sensed as a function of a time interval (Δt) elapsed between said first time instant (t_1, t_4) and said second time instant (t_2), and of a distance (Δx) between said pneumatic cuff (100) and said probe (108).